Mapping the dynamic immune landscape associated with therapeutic response in soft tissue sarcoma

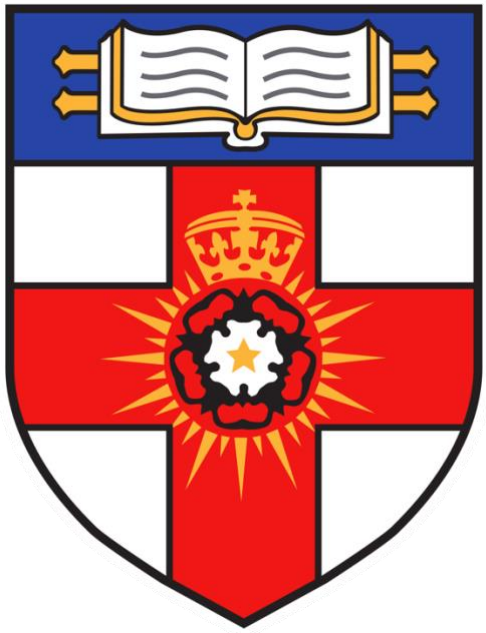

Christopher P. Wilding

A thesis submitted for the degree of

Doctor of Philosophy

The Institute of Cancer Research

University of London

Declaration

The work published in this thesis was completed under the supervision of Dr Paul Huang in the Molecular and Systems Oncology team at the Institute of Cancer Research, London, United Kingdom.

I, Christopher Wilding, confirm that the work presented within this thesis is my own. Information that has been derived from other sources is clearly indicated within the thesis.

Christopher Wilding

Abstract

Soft tissue sarcomas (STS) are a group of rare malignancies with over 150 different histological subtypes, each with different clinical behaviours and therapeutic responses. Following a diagnosis of advanced disease, the prognosis is poor, and following failure of first-line therapy, further-line treatments lack efficacy. The tyrosine kinase inhibitor (TKI) pazopanib showed promising results in early-stage clinical trials, however, failed to report a significant improvement in overall (OS) in the PALETTE phase III trial. Subsequent post-hoc analysis demonstrated a subset of patients experienced robust and durable responses to pazopanib, but at present there is no way to identify patients most likely to gain benefit.

To characterise the immune microenvironment and develop a clinically relevant survival model, two cohorts of patients were curated, the combined cohort which had received pazopanib and the comparator cohort which had received alternative second-line therapies. In these cohorts, the immune microenvironment was characterised by immunohistochemistry of tumour-infiltrating lymphocytes. Targeted immune gene expression was then undertaken on the pazopanib-treated cohort. Finally, a novel survival model in the pazopanib-treated cohort was developed, validated and refined.

In the combined cohort, there was a significant association between higher CD4+ count by IHC and inferior OS and progression-free survival (PFS). Conversely, in the comparator cohort, a higher CD4+ count was associated with improved PFS. Targeted immune gene expression identified three immune-based subgroups, with differential immune gene expression and immune cell infiltration. Subsequently, an immune gene signature was developed, and a prognostic model was built on the pazopanib-treated cohort which showed a significant association with both OS and PFS.

This body of work adds considerable knowledge towards the characterisation of the tumour immune microenvironment in STS. Furthermore, the development of

a prognostic survival model, including an immune gene signature, is exciting and with further validation may aid clinical decision-making in the future.

Acknowledgements

First and foremost, I would like to extend my heartfelt gratitude to my supervisory team of Dr Paul Huang, and Professor Robin Jones. Paul – thank you for providing the opportunity for me to undertake this research project and become a member of your lab. From your guidance and expertise I have learnt a huge amount during my time in the laboratory, and have developed a range of skills and experience I hadn't imagined when starting out. Your support has been unwavering. Prof Jones – thank you for your words of encouragement and support during the course of my time at the ICR.

My sinscere thanks must also go to Dr Maggie Cheang at the ICR Clinical Trials Unit, who has patiently supervised and aided my development and understanding of statistics and the use of R. Thank you for all of your advice and guidance. In addition, I would like to thank Richard Buus of the Breast Cancer Now Ralph Lauren Laboratory for his kindness and assistance with all things Nanostring assay related. In addition, I would like to thank Dr Khin Thway for her guidance and teaching of all things histopathology related. And thanks also to the members of the ICR's Histopathology Core Facility for always dealing with my IHC and sectioning requests as quickly as possible.

I would also like to thank all of my lab mates, past and present, within the Molecular and Systems Oncology team at the ICR. You have all shown incredible patience and kindness during my time within the lab, and always offered sage advice and support whenever I needed it. Particular thanks go to Nafia Guljar, who has worked tirelessly in supporting this work.

Last but by no means least, I am eternally grateful for the support and love of all of my family, especially my ever-supportive wife Lucy, and my wonderful daughter Olivia. Without the support I have received from those closest to me, both in the past and during the course of my PhD, I would not be where I am today. Thank you.

Table of Contents

List of figures

List of tables

5.1 Baseline clinicopathological variables for the discovery and validation cohorts.

5.2 Clinicopathological variables including response to therapy and survival in the discovery and validation cohorts.

5.3 Summary of the full and nested Cox multivariable regression models for overall survival in the discovery cohort.

5.4 Summary of the full and nested Cox multivariable regression models for progression-free survival in the discovery cohort.

5.5 Summary of the full and nested Cox multivariable regression models for overall survival in the combined cohort.

5.6 Summary of the full and nested Cox multivariable regression models for progression-free survival in the combined cohort.

5.7 Summary of the full and nested Cox multivariable regression models including soft tissue sarcoma subtype for overall survival and progression-free survival in the combined cohort.

Abbreviations and acronyms

AJCC	American Joint Committee on Cancer
Akt	Protein kinase B
AS	Angiosarcoma
ASPS	Alveolar soft part sarcoma
ASPS	Alveolar soft part sarcoma
C-index	Concordance index
c-KIT	Stem cell factor receptor
CAF	Circulating angiogenic factor
CBR	Clinical benefit rate
CI	Confidence Interval
CS	Chondrosarcoma
CT	Computerised tomography
CTLA	Cytotoxic T-lymphocyte associated antigen
CTLA-4	Cytotoxic T lymphocyte-associated protein-4
DCE-MRI	Dynamic contrast enhanced magnetic resonance imaging
DCs	Dendritic cells
DDLPS	De-differentiated liposarcoma
DFSP	Dermatofibrosarcoma protuberans
DSCRT	Desmoplastic small round cell tumour
DSS	Disease specific survival
ECs	Endothelial cells
EGFR	Epithelial growth factor receptor
EORTC	European Organisation for Research and Treatment of Cancer
ERK	Extracellular signal-related kinase
FAS	Fas cell surface death receptor
FFPE	Formalin-fixed, paraffin-embedded
FGFR	Fibroblast growth factor receptor
FISH	Fluorescence In Situ Hybridisation
FMS	Fibromyxoid sarcoma
FNCLCC	Fédération Nationale des Centres de Lutte Contre le Cancer
GEO	Gene expression omnibus
GIST	Gastrointestinal stromal tumour
HIF	Hypoxia-inducible factor
HR	Hazard ratio
ICI	Immune checkpoint inhibitor
IFN	Interferon

IHC	Immunohistochemistry
IL	Interleukin
ISS	Immune sarcoma subgroup
IV	Intravenous
LAG	Lymphocyte activation gene
LMS	Leiomyosarcoma
LPS	Liposarcoma
MAPK	Mitogen activated protein kinase
MDSCs	Myeloid derived suppressor cells
MDT	Multi-disciplinary team
MEK	Mitogen-activated protein kinase kinase
MFS	Myxofibrosarcoma
MHC	Major histocompatibility complex
MGES	Median gene enrichment signature
MHRA	Medicines and Healthcare products Regulatory Agency
MIC	MHC class I chain related
mOS	Median overall survival
mPFS	Median progression free survival
MPNST	Malignant peripheral nerve sheath tumour
MRI	Magnetic resonance imaging
NCT	National clinical trials identifier
NGS	Next Generation Sequencing
NICE	National Institute for Health and Care Excellence
NK	Natural killer
NLR	Neutrophil-to-lymphocyte
NPP	Named patient programme
ORR	Overall response rate
OS	Overall survival
PCA	Principle component analysis
PD	Progressive disease
PD-1	Programmed cell death receptor-1
PD-L1	Programmed death-ligand 1
PD-L1	Programmed cell death receptor-1 ligand
PDGFR	Platelet derived growth factor receptor
PFS	Progression-free survival
PI3	Phosphatidylinositol 3′-kinase
PIP_2	Phosphatidylinositol 4,5-bisphosphate
PIP_3	Phosphatidylinositol 3,4,5-triphosphate
PR	Partial response
PS	Performance status
PS	Performance status

RCC	Renal cell carcinoma
RFS	Recurrence-free survival
RNA	Ribonucleic acid
RT	Radiotherapy
RTK	Receptor tyrosine kinase
SARC	Sarcoma Alliance for Research through Collaboration
SD	Stable disease
SFT	Solitary fibrous tumour
SMA	Smooth muscle actin
SS	Synovial sarcoma
ssGSEA	Single sample gene set enrichment analysis
STAT3	Signal transducer and activator of transcription 3
STBSG	Soft Tissue and Bone Sarcoma Group
STS	Soft tissue sarcoma
TAMs	Tumour-associated macrophages
TCGA	The Cancer Genome Atlas
TGF-β	Transforming growth factor-β
Th1	T-helper1
Th2	T-helper2
TILs	Tumour infiltrating lymphocytes
TIM	T-cell immunoglobulin domain and mucin domain
TKI	Tyrosine kinase inhibitor
TLS	Tertiary lymphoid structure
TMA	Tissue microarray
TMB	Tumour mutational burden
TP53	Tumour protein 53
TRAIL	Tumour necrosis factor-related apoptosis-inducing ligand
Treg	Regulatory T-cell
TRK	Tropomyosin receptor kinase
UPS	Undifferentiated pleomorphic sarcoma
UPS	Undifferentiated pleomorphic sarcoma
VEGF	Vascular endothelial growth factor
WDLPS	Well-differentiated liposarcoma

Chapter 1 - Introduction

1.1 Soft tissue sarcomas are cancers of unmet need

Soft tissue sarcomas (STS) are a group of rare cancers of mesenchymal origin that display vast heterogeneity, comprising over 150 different histological subtypes with variable pathologies, genetic aberrations and therapeutic responses[1]. STS have an annual UK incidence of around 3,300 new cases per year, representing approximately 1% of adult cancer diagnoses, rising to approximately 10% in the paediatric population (**Figure 1.1.A**)[2]. Although when considering all STS this incidence is in a similar range to other malignancies such as testicular or thyroid cancer, given the large number of histological subtypes, the incidence of each distinct subtype is much lower. For example, the most common STS subtype leiomyosarcoma (LMS), representing approximately one fifth of all STS diagnoses, has an incidence of approximately 600 new cases per year, and an age-standardised incidence rate of around 8 cases per million of the population[2]. Given this rarity and the degree of heterogeneity, STS are inherently difficult to manage medically.

In general, rare cancers often receive less scientific interest than more frequently occurring malignancies, despite an average five-year relative survival of 47%, compared to 65% for more common malignancies[3]. Indeed, STS has an approximate 10-year overall survival (OS) rate from diagnosis of 43%, whilst the development of advanced disease has a dismal prognosis with a median OS of between 8.9 and 17.5 months (**Figure 1.1.B**)[4,5]. The cause of these worse patient outcomes in rare cancers is multifactorial; with their low prevalence associated with incorrect or late diagnosis, limited access to appropriate specialist care and less efficacious standard therapies. This is driven by a lack funding of pre-clinical and clinical studies and a paucity of clinical trials which impedes the approval of novel therapies[6]. Furthermore, randomised trials of rare cancers present challenges, including small cohorts of suitable patients leading to prohibitively slow accrual rates. In order to access sufficiently sized patient cohorts, international multi-centre collaborations are often necessary. However, this can also bring with it pitfalls, including complexities associated with international data and tissue sharing, and variability in management practises between regions,

impeding comparability of patient outcomes[7]. In recent years, organisations such as the International Rare Cancers Initiative have made progress in this regard and their ongoing success will be important to sustain progress in the management of rare cancers.

An additional consideration for clinical trials involving STS is that the inclusion of a broad range of STS subtypes in “all-comer” clinical trials risks dilution of subgroup-specific efficacy due to cohort heterogeneity[8]. Novel statistical methodologies and trial designs go some way to address this issue, for example, basket studies allow the exploration of inhibitors targeted at specific molecular aberrations across a range of tumour types. An example of this is the NAVIGATE phase II basket trial which demonstrated the activity of Larotrectinib (Vitraki®/LOXO-101/ARRY-470) in tumours harbouring TRK fusions (NCT02576431)[9,10].

However, despite increasing access to next-generation sequencing, and the approval of targeted therapies in a number of more common cancers, progress in STS is lagging and limited to a small subset of specific genomic aberrations or individual subtypes. For example, efforts to define molecular subtypes in gastrointestinal stromal tumours (GIST) have driven significant progress in the sequential management of advanced disease with tyrosine kinase inhibitors (TKI), with improved clinical outcomes the result[11]. Moving forward, subtype-agnostic identification of non-GIST STS patient subpopulations most likely to benefit from specific therapies could greatly improve both patient outcomes and ensure appropriate access to funding for specific therapies.

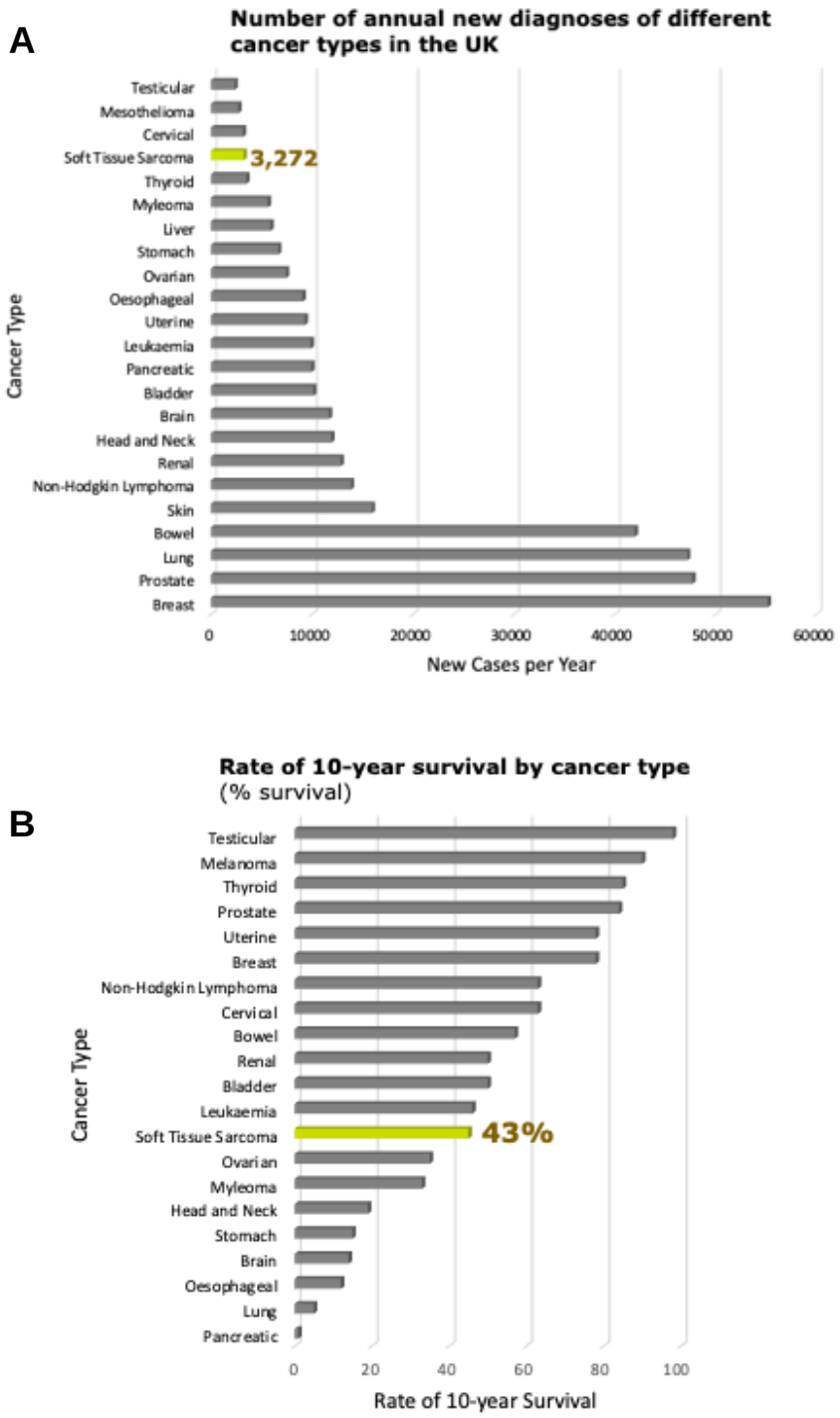

Figure 1.1 Incidence and survival of STS relative to other cancer types **(A)** Incidence in the UK of all subtypes of STS with other major cancer diagnoses also plotted. **(B)** Rate of 10-year survival from initial diagnosis of STS in UK with other major cancer types also plotted. Data for figures obtained from Cancer Research UK[2].

1.2 Diagnosing and classifying soft tissue sarcomas

1.2.1 Clinical diagnostic guidelines within the UK

Since the publication of guidance from the National Institute for Health and Clinical Excellence (NICE) bone and soft tissue sarcoma services have been centralised to 15 specialist centres in England and Wales, and this step has significantly improved disease-specific survival for patients with sarcoma[12,13]. Each specialist STS centre provides a multidisciplinary team (MDT) service comprising a number of medical specialties including histopathologists, radiologists, surgeons, medical and clinical oncologists, and specialist nurses to review referrals from external centres. Given the fact that on average general practitioners may only observe a single case of sarcoma in their careers, there has been a drive for clinical suspicion of sarcoma to be raised if any soft tissue lump is increasing in size, is greater than 5cm or is painful[14,15]. If any of these symptoms are present in the context of a soft tissue mass, then an urgent ultrasound or direct referral to the regional sarcoma treatment centre is indicated.

Given the lack of radiation exposure and low cost, an ultrasound is usually the imaging modality of choice as part of a triple assessment including history and examination. In those patients with features suspicious of STS, further cross-sectional imaging of the area is then usually undertaken, be it magnetic resonance imaging (MRI) or computerised tomography (CT). The final step of diagnosis is reliant on obtaining a tumour sample via percutaneous core needle or excisional biopsy for tissue-based diagnosis.

1.2.2 Tissue-based methods for subtype classification

1.2.2.1 Histological assessment of tissue

Histopathological assessment of tumour tissue obtained from biopsy remains the mainstay of diagnostic confirmation of STS subtype and, where feasible, tumour grade. Given the technical difficulty and variability in morphological appearances observed in STS, a specialist soft tissue histopathologist should be involved in the assessment of sarcoma tissue[16]. Indeed, numerous studies conducted at

specialist referral centres have demonstrated that the initial diagnosis made at referring centres was discordant with the expert second opinion in up to a third of cases[17–19]. In addition, the existence of less common morphological variants in STS, as well as the fact biopsies may not sufficiently capture representative tumour areas, can diminish accuracy in STS diagnosis and risks under-grading when purely based on assessment of haematoxylin and eosin (H&E) biopsy slides[20]. As sarcoma management moves towards histology-tailored therapy, accurate histotyping will become even more crucial to ensuring appropriate therapy is delivered.

1.2.2.2 Immunohistochemistry staining

Additional immunohistochemistry (IHC) stains can be undertaken in tumour specimens displaying uncertain morphological characteristics, and in some cases act as confirmation of diagnosis. Conventional IHC aims to identify cell lineage, which may yield insufficient information for a specific diagnosis, however, newer IHC stains are focused on specific genetic aberrations leading to higher specificity for particular STS subtypes (**Table 1.1**)[21–23].

1.2.2.3 Ancillary molecular tests

In addition to IHC testing, additional ancillary molecular tests are available to help confirm the subtype diagnosis in some STS. Broadly speaking, STS can be sub-categorised into two separate groups based upon their molecular complexity (**Figure 1.2**)[24,25]. These are;

- genetically “simple” STS, characterised by single pathognomonic, recurrent alterations and relatively simple karyotypes.
- genetically complex STS, characterised by unstable genomes, with numerous gains and losses, inconsistent genetic aberrations, often with multiple chromosomal abnormalities.

For the purposes of diagnosis, fluorescence in situ hybridisation (FISH) remains the most widely used technique of choice for detecting the presence of a suspected STS translocation. FISH is a cytogenetic method utilising fluorescent

probes specific to pre-determined sequences of the genome and in the presence of a chromosomal translocation, a fusion signal is observed under fluorescent microscopy. As such, FISH can be used in conjunction with morphological assessment and IHC to confirm a suspected diagnosis, or alternatively be used to rule out a subtype on the list of differential diagnoses. Indeed, an SS18-SSX fusion-specific antibody is employed in the United States of America for the diagnosis of synovial sarcoma (SS)[26]. Looking to the future, with technological advances leading to cheaper, quicker and more accessible next-generation sequencing (NGS) capabilities, it is likely that the majority of new patients with a diagnosis of STS will have some form of NGS undertaken on their tumour sample. This may be in the shape of an anchored multiplex polymerase chain reaction fusion detection platform, such as ArcherDx, targeted sequencing looking at specific regions of interest in the context of sarcoma, or more general whole exome/genome sequencing[27,28]. Not only will this potentially provide more confidence in the subtype diagnosis of the tumour, but it may also be used to identify mutations for which a targeted therapy with proven efficacy is available.

Table 1.1 Table of immunohistochemistry stains used in the diagnosis of common soft tissue sarcomas. SMA – smooth muscle actin; EMA – epithelial membrane antigen; ASPS – alveolar soft part sarcoma; WD/DDLPS – well-differentiated/dedifferentiated liposarcoma; MPNST – malignant peripheral nerve sheath tumour; SFT – solitary fibrous tumour.[21–23]

		Positive markers	Negative markers
Lineage based	Smooth muscle tumours	SMA, h-caldesmon, desmin	CD34, Myogenin, MyoD1, S100
	Straited muscle tumours	Desmin, myogenin, MyoD1, muscle specific actin	CD31, keratin, S100
	Neural tumours	S100, SOX-10, GFAP	-
	Vascular tumours	CD31, ERG, CAMTA1, TFE3, FOSB	-
	Osteogenic tumours	SATB2	-
Subtype specific	Dermatofibrosarcoma protuberans	CD34, vimentin	S100, CD31, desmin, SMA
	Ewing sarcoma	CD99, NKX2.2	ETV4, WT1, BCOR, CCNB3
	Synovial sarcoma	EMA, cytokeratin, TLE1, BCL2, S100	CD34, desmin, h-caldesmon, MyoD1, SOX10, INI1
	Epithelioid sarcoma	EMA, cytokeratin, CD34, vimentin	INI1, SMARCB1, CD31, CD68, S100
	PEComa	Cathepsin K, HMB45, SMA, cytokeratin, desmin, Melan-A	CD10, S100 (but both may be focally positive)
	ASPS	TFE3	-
	Low grade fibromyxoid sarcoma	MUC4, CD99, BCL2, EMA	S100, CD34, MDM2, desmin, keratin, SMA
	WD/DDLPS	MDM2, CDK4 (more positive in the more cellular DDLPS)	-
	MPNST	S100, SOX10 (but patchy and seen only in approx. 50%)	H3K27me3, INI1
	SFT	STAT6, CD34	S100, SOX10, CD31, desmin
	Epithelioid haemangioendothelioma	CAMTA1, CD31, ERG	S100, SOX10, desmin

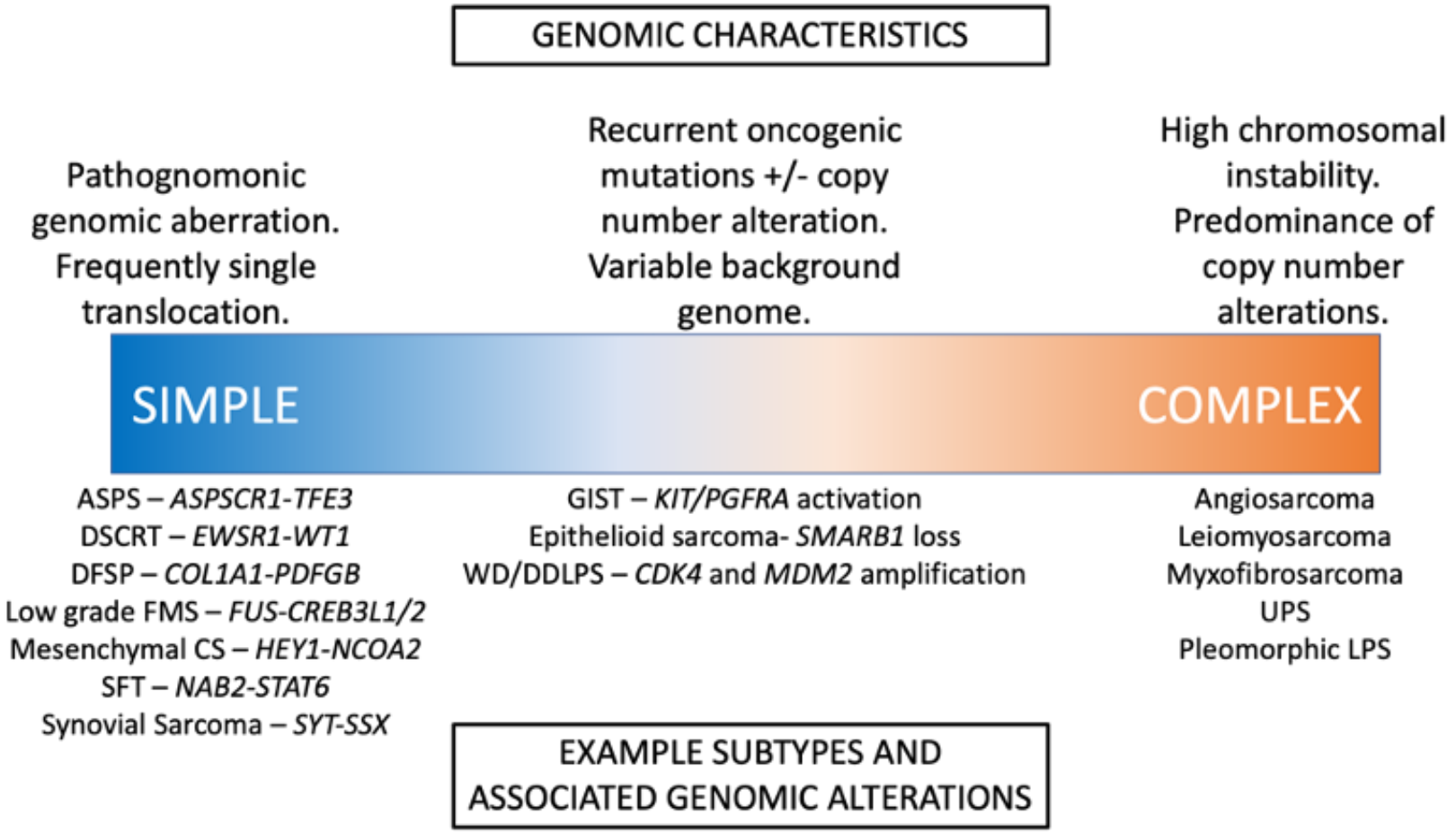

Figure 1.2 The spectrum of genomic characteristics in soft tissue sarcomas. ASPS – Alveolar soft part sarcoma; DSCRT – desmoplastic small round cell tumours; DFSP – dermatofibrosarcoma protuberans, FMS – fibromyxoid sarcoma; CS – chondrosarcoma; SFT – solitary fibrous tumour; WD/DD – well differentiated/dedifferentiated; LPS – liposarcoma; UPS – undifferentiated pleomorphic sarcoma.[24,25]

1.2.3 Grading and staging in soft tissue sarcomas

In addition to confirming the histological subtype in STS, acquisition of tumour samples as part of the diagnostic work-up allows the managing team to ascertain the grade of the tumour. Within Europe, the Fédération Nationale des Centres de Lutte Contre le Cancer (FNCLCC) is used to categorise tumours into one of three grades[14,29]. This grading system takes into account three factors discernible on histopathological assessment of tissues to assign a grading score:

- Degree of tumour differentiation is assigned a score from one to three based upon a classification of:
    - 1 point - well-differentiated
    - 2 points - moderately differentiated
    - 3 points - poorly differentiated/anaplastic.
- Degree of necrosis is assigned a score from zero to two:
    - 0 points - Absence of necrosis
    - 1 point - less than 50% necrosis
    - 2 points - greater than 50% necrosis
- Mitotic count per 10 high powered fields on microscopy is assigned a score from one to three:
    - 1 point - less than 10 mitoses
    - 2 points - 10-19 mitoses
    - 3 points - greater than or equal to 20 mitoses

The combined scores of these three factors contribute to the final grade assigned;

- Grade 1 – a combined score of 2 or 3
- Grade 2 – a combined score of 4 or 5
- Grade 3 – a combined score greater than 6.

Given the intra-tumour heterogeneity in STS, although biopsy samples are utilised for initial grading of tumours, further histological analysis of the full resection specimen may lead to modifications in the grade assigned.

Following confirmation of a diagnosis of STS, patients should undergo further radiological investigation to assess for the presence of distal metastases. The most common method for staging STS follows guidance laid out in the American Joint Committee on Cancer (AJCC) cancer staging manual[30]. This staging system draws upon the tumour grade based upon the FNCLCC system above, the primary tumour (T), presence or absence of regional lymph node metastases (N) and the presence or absence of distant metastases (M). Staging of STS is important as it is linked to disease prognosis and will direct clinicians to formulate the most appropriate management plan for each patient. For retroperitoneal, trunk and extremity STS, which make up the majority of STS, the TNM definitions are standardised. The tumour score is based on the greatest diameter:

- T1 – less than or equal to 5cm
- T2 – more than 5cm and less than or equal to 10cm
- T3 – more than 10cm and less than or equal to 15cm
- T4 – greater than 15cm

The scoring for lymph node and distance metastases is a binary measure, with the presence of lymph node or distance metastases classified as N1 or M1 respectively, compared to N0 or M0 if they are absent. For the formal staging score, anatomical site of the primary STS is considered, and there is a degree of variability based upon the TNM scores (**Table 1.2**)[30,31].

Table 1.2 Staging classification for STS based upon AJCC classification. Of note, primary STS located in the trunk or extremity are classified as stage IV in the presence of positive regional lymph nodes, whereas for retroperitoneal STS presence of local nodes in the absence of distal metastases is considered stage IIIB.[30,31]

	Stage	Primary tumor (T)	Regional lymph node (N)	Distant metastasis (M)	Histologic grade (G)
Trunk, extremity and retroperitoneum	IA	T1	N0	M0	G1, GX
	IB	T2, T3, T4	N0	M0	G1, GX
	II	T1	N0	M0	G2, G3
	IIIA	T2	N0	M0	G2, G3
Trunk and extremity	IIIB	T3, T4	N0	M0	G2, G3
	IV	Any T	N1	M0	Any G
		Any T	Any N	M1	Any G
Retroperitoneum	IIIB	T3, T4	N0	M0	G2, G3
		Any T	N1	M0	Any G
	IV	Any T	Any N	M1	Any G

Most notably, the presence of regional lymph node disease with or without distant metastatic disease is considered stage IV in trunk and extremity STS, whereas for retroperitoneal primary STS regional lymph node disease in the absence of distant metastatic disease is considered stage IIIB disease.

Although the AJCC system is the most widely accepted staging system in STS, one area of weakness is that it does not consider STS histological subtype in the risk stratification. Looking to the future, refinement of this system to be inclusive of histology could allow more robust stratification of patients most at risk[32].

1.3 Current treatment paradigms in soft tissue sarcomas

1.3.1 Surgical management of localised disease

Following appropriate staging and diagnostic investigations, cases of STS which have been confirmed to be locally confined should generally be offered surgery. In certain circumstances, surgery may not be appropriate, for example, for elderly and frail patients for whom the risk of surgery outweighs the potential benefits. However, for the general population surgical excision with clear margins remains the mainstay of treatment of curative intent. Tumour resectability is usually determined by the MDT and takes into account STS subtype, grade, patient comorbidities and the technical feasibility of removing the tumour with adequate margins[14,15]. The definition of what constitutes an adequate margin remains a contentious issue, although positive resection margins are recognised to be associated with an increased risk of local recurrence and worse OS[33–36]. In certain situations whereby anatomical constraints prevent resection with a wide margin, and balancing the risks of recurrence and the potential morbidity of a more radical procedure, it may be suitable to undertake a resection with planned positive margins after full consultation with the MDT and counselling of the patient[14,15].

For extremity STS, limb salvage is advantageous in terms of post-operative functionality, and in cases of lower limb sarcoma, anatomically higher amputation levels are associated with an increase in metabolic and oxygen demands upon ambulation[37]. However, in cases in which the STS involves the joint, is multi-focal, or in which the excision would be multicompartmental or risk significant neurovascular compromise, then amputation would be more appropriate. Indeed, a number of studies have shown that with judicial patient selection, amputations can lead to satisfactory functional outcomes, post-amputation quality of life and disease control and survival[38–40]. For truncal STS, similarly to extremity STS, contraindications for excision include unsuitability of the patient for major operative intervention, however more commonly unresectability is due to the inability to remove the tumour with a sufficiently adequate margin due to tumour proximity to major neurovascular or other important structures[41]. Given the

complex nature of the decisions and considerations associated with the surgical excision of STS, and the necessary pre-operative planning, the importance of MDT involvement is clear.

1.3.2 The management of advanced soft tissue sarcoma

Although surgical excision is the mainstay of treatment of curative intent, once STS becomes metastatic or locally advanced and unresectable, the disease is considered incurable. As such, the focus of management switches to palliation with the aim of improving symptoms, stabilising or reducing tumour burden and extending life[42]. Indeed, approximately 50% of patients presenting with a high-grade STS will develop advanced disease, with a diagnosis of disseminated disease associated with a dismal median overall survival (mOS) of between 8.9 and 17.5 months[4,5]. Although select patients may be suitable for individually tailored management involving targeted surgical resection or localised therapy, for the vast majority of patients with advanced STS systemic chemotherapy plays the most relevant role in the management of the disease.

1.3.3 Anthracycline-based chemotherapy remains the standard first-line systemic therapy in advanced soft tissue sarcoma

After the discovery of the anti-tumour activity of doxorubicin against STS in 1973, anthracycline-based chemotherapy has remained the cornerstone of first-line chemotherapeutic treatment in advanced STS for nearly 50 years[43]. Over this period of time, a number of trials have been conducted with the aim of identifying more efficacious regimens. These studies have explored combination strategies as well as alternative treatment regimens but as of yet have failed to provide robust evidence of prolongation of survival relative to doxorubicin alone. Furthermore, given the rarity of STS, the number of phase III trials is relatively small and often includes a heterogenous group of STS subtypes (**Table 1.3**).

Table 1.3 Select phase II and III trials of systemic cytotoxic chemotherapy comparing anthracycline-based regimens with alternative agents in advanced STS. *PFS and OS estimated from Kaplan-Meir plots, not formally reported in manuscript.[44–53]

	Trial Reference	Study Phase	Number of patients		Study arms	Response Rate (%)	Median PFS (months)	Median OS (months)
Olaratumab	Tap et al., *JAMA*, 2020	III	485	258	Doxorubicin 75mg/m2 day 1 plus olaratumab 15mg/kg day 1 + 8	14	5.4	19.7
				251	Doxorubicin 75mg/m2 day 1 + placebo	18.3	6.8	20.4
	Tap et al., *Lancet*, 2016	II	148	66	Doxorubicin 75mg/m2 day 1 plus olaratumab 15mg/kg day 1 + 8	18.2	6.6	26.5
				67	Doxorubicin 75mg/m2 day 1	11.9	4.1	14.7
Ifosfamide	Maurel, *J Clin Oncol.*, 2009	II	132	65	Doxorubicin 30mg/m2/day days 1-3 followed by ifosfamide 12.5g/m2 continuous IV for 5 days	24.1	6*	16*
				67	Doxorubicin 75mg/m2 day 1	23.4	6*	15*
	Lorigan, *J Clin Oncol.*, 2007	III	326	109	Ifosfamide 3g/m2/day over 3hr days 1-3	5.5	2.16	10.92
				107	Ifosfamide 3g/m2/day over 24hr days 1-3	8.4	3	10.92
				110	Doxorubicin 75mg/m2 day 1	11.8	2.52	12
	Judson et al., *Lancet Oncol.*, 2014	III	455	227	Doxorubicin 25mg/m2/day days 1-3 + ifosfamide 2.5mg/m2/day days 1-4	26	7.4	14.3
				228	Doxorubicin 75mg/m2 day 1	14	4.6	12.8
Gemcitabine	Seddon et al., *Clin Sarcoma Res.*, 2015	II	45	45	Gemcitabine 900mg/m2 days 1 and 8 + docetaxel 100mg/m2 day 8 (25% dose reduction if previous RT)	25	7.1	17.9
	Seddon et al., *Lancet Oncol*, 2017	III	257	129	Doxorubicin 75mg/m2 day 1	19	5.4	17.5
				128	Gemcitabine 675mg/m2 day 1 and 8 + docetaxel 75mg/m2 day 8	20	5.5	15.5
Trabectedin	Martin-Broto, *J Clin Oncol.*, 2016	II	115	54	Doxorubicin 75mg/m2 day 1 + Trabectedin 1.1mg/m2 day 1	17	5.7	13.3
				59	Doxorubicin 75mg/m2 day 1	17	5.5	13.7
	Bui-Nguyen, *Eur J Cancer*, 2015	IIB	133	47	Trabectedin 1.3mg/m2/3hr day 1	14.8	2.8	Not reached
				43	Trabectedin 1.5mg/m2/24hr day 1	4.7	3.1	Not reached
				43	Doxorubicin 75mg/m2 day 1	25.6	5.5	Not reached
	Blay et al., *Eur J Cancer*, 2014	III	121	61	Trabectedin 1.5mg/m2/24hr day 1	5.9	16.1	38.9
				60	Doxorubicin 75mg/m2 day 1 or Doxorubicin 60mg/m2 day 1 + ifosfamide 6-9g/m2 day 1	27	8.8	27.3

Of these studies, a number of the phase III trials stand-out as particularly notable, especially given the difficulty in undertaking large-scale trials in rare diseases such as STS. The first of these landmark trials is the EORTC sponsored, phase III, randomised, international trial of doxorubicin alone versus doxorubicin in combination with ifosfamide as first-line chemotherapy (EORTC 62012, NCT00061984)[48]. This trial recruited 455 patients with locally advanced, unresectable or metastatic high-grade STS and randomised them 1:1 to either doxorubicin alone or doxorubicin plus ifosfamide. The trial was uniquely powered to assess OS benefit as the primary outcome. This study reported no significant difference in OS, with median OS in the doxorubicin alone group 12.8 months compared to 14.3 months for the doxorubicin plus ifosfamide group (HR 0.83, 95.5% CI 0.67–1.03, p=0.076). However, secondary endpoint analysis did reveal a significant PFS advantage in the doxorubicin plus ifosfamide group (7.4 months versus 4.6 months; HR 0.74, 95.5% CI 0.60 – 0.90; p = 0.003) as well as a significantly higher overall response rate (ORR) in the combination therapy group (26%) compared to the doxorubicin alone group (14%)(p=0.0006). However, treatment-related toxicity was more problematic in the combination therapy group. Although this provided some evidence of an incremental improvement in tumour response to combination therapy, the lack of OS benefit, and the higher incidence of treatment-related toxicity, have limited the adoption of doxorubicin plus ifosfamide as the first-line standard of care. Instead, combination doxorubicin plus ifosfamide is often saved for certain patients in which tumour shrinkage might alleviate symptoms, or potentially facilitate alternative treatment options[14,15,54].

A more recent randomised, controlled, phase III trial looked to compare gemcitabine, a nucleoside anti-metabolite, plus docetaxel, a taxane with microtubule-inhibiting activity, versus doxorubicin in treatment-naïve advanced unresectable or metastatic high-grade STS (GeDDiS, International Standard Randomised Controlled Trial registry ISRCTN07742377)[50]. A total of 257 patients were randomised 1:1 to either doxorubicin or gemcitabine plus docetaxel. Assessment of the trial's primary end-point revealed no significant difference in PFS at 24 weeks; (46.3% in the doxorubicin group versus 46.4% in the

gemcitabine plus docetaxel group (HR 1.28, 95% CI 0.99–1.65; p=0.06)). As such, the trial did not show that gemcitabine plus docetaxel is a more appropriate standard of care for the first-line treatment of advanced STS, however gemcitabine alone might be an appropriate first-line agent in certain circumstances given the cardiotoxicity of both doxorubicin and docetaxel.

Finally, the most recent phase III trial of note involving doxorubicin was the double-blind, randomised, phase III trial of doxorubicin in combination with olaratumab vs doxorubicin plus placebo in anthracycline-naïve unresectable locally advanced or metastatic STS (ANNOUNCE, NCT02451943)[44]. A total of 509 patients were enrolled, all receiving doxorubicin, with 258 randomised to additionally receive olaratumab, and the remaining 251 patients receiving placebo. Olaratumab/placebo monotherapy continued until disease progression, toxicity, physician/patient decision or significant non-compliance. The study's primary end-point was OS from randomisation, and a planned analysis of the LMS subset was included. Analysis of these primary endpoints revealed no significant difference in median OS across all STS subtypes between the doxorubicin plus olaratumab cohort (20.4 months) versus the doxorubicin plus placebo group (19.7 months) (HR 1.05, 95% CI 0.84–1.30; p=0.69), nor in the LMS subgroup (median OS of 21.6 months in the olaratumab arm versus 21.9 months in those receiving placebo (HR 0.95, 95% CI 0.69–1.31; p=0.76)). This trial is interesting as the negative result reported was disappointing given the results of the phase Ib/II trial of olaratumab. In this preceding trial, a significant 11.8 month improvement in median OS was observed rising from 14.7 months in doxorubicin alone to 26.5 months in doxorubicin plus olaratumab (stratified HR 0.46, 95% CI 0.30–0.71; p=0.0003) (NCT01185964)[45]. The reasons behind the failure to observe a significant survival benefit in the phase III study, relative to the apparent and remarkable benefit observed in the phase II study remain unclear. However, it may be that a subset of patients do display differential treatment responses to olaratumab therapy, and given the heterogeneity of the STS cohorts enrolled and the lack of a biomarker predictive of response, this observable survival benefit is lost. Given the numerous trials to date,

anthracycline-based chemotherapy remains the standard first-line therapy in the majority of advanced STS subtypes.

1.3.4 Alternative and further-line systemic therapies in advanced soft tissue sarcoma

Although anthracycline-based chemotherapy shows some efficacy as first-line treatment in advanced STS, alternative other monotherapy and combination regimens have been trialled in the first- and further-line setting of advanced STS. However, the evidence remains less robust than for first-line therapies, with only a few showing meaningful efficacy, and as such following failure of first-line therapy the prognosis of these patients is generally poor. Indeed, the majority of patients with advanced STS are subjected to very similar treatment pathways, with the sequential stepwise use of a narrow array of therapies irrespective of tumour-specific factors. Commonly considered further-line systemic therapies include ifosfamide monotherapy, gemcitabine in combination either with docetaxel or dacarbazine, trabectedin, and additional and emerging therapies with varying levels of evidence available for their use (**Table 1.4**).

Table 1.4 Select studies of common alternate systemic cytotoxic chemotherapy agents in advanced STS. (AS – angiosarcoma; LMS – leiomyosarcoma; LPS – liposarcoma; OS – overall survival; PFS – progression-free survival).[55,56,65–67,57–64]

	Trial Reference	Study Type	Number of patients		Study arms	Response Rate (%)	Median PFS (months)	Median OS (months)	Most common toxicities
Ifosfamide	Nielsen et al., *Eur. J. Cancer.*, 2000	Phase II	114	89 first-line 25 second-line	Ifosfamide 12g/m2	17 16	3.4	12.7	Haematological (60%)
	Lee et al., Oncology, 2011	Retrospective review	30	21 second-line 9 third-line	Ifosfamide 14g/m2	25	2.9	8.7	Neutropenia (43%)
	Martin-Liberal et al., Sarcoma, 2013	Retrospective review	35	23 first-line 12 second-line	Ifosfamide 14g/m2	20	4.2	11.2	Encephalopathy (17.1%)
Gemcitabine	Okuno et al., Cancer, 2002	Phase II	29	10 first-line 19 second-line	Gemcitabine 1250mg/m2	3	2.1	Not reported	Haematological (32%)
	Švancárová et al., Eur. J. Cancer, 2002	Phase II	31	31 second-line	Gemcitabine 1250mg/m2	3	1.5	8.8	Neutropenia (12.9%)
Gemcitabine combination	Hensley et al., J. Clin. Oncol., 2002	Phase II in LMS	34	18 first-line 16 second-line	Gemcitabine 900mg/m2 plus docetaxel 100mg/m2	53	5.6	17.9	Thrombocytopenia (29%)
	Maki et al., J. Clin. Oncol., 2007	Phase II	122	73	Gemcitabine 900mg/m2 plus docetaxel 100mg/m2	16	6.2	17.9	Thrombocytopenia (40%)
				49	Gemcitabine 1200mg/m2 alone	8	3.0	11.5	Thrombocytopenia (35%)
	Pautier et al., Oncologist, 2012	Phase II in LMS	83	21 uterine 19 non-uterine	Gemcitabine 900mg/m2 plus docetaxel 100mg/m2	24 5	4.7 3.4	23.0 13.0	Thrombocytopenia (18%)
				21 uterine 22 non-uterine	Gemcitabine 1200mg/m2 alone	19 14	5.5 6.3	20.0 15.0	Leukopenia (25%)
	Losa et al., Cancer Cehmother. Pharmacol., 2007	Phase II	23	23 first-line	Gemcitabine 1,800mg/m2 plus dacarbazine 500mg/m2	4.3	1.2	8.5	Lymphopenia (52%)
	García-del-Muro et al., J. Clin. Oncol., 2011	Phase II	109	52 second-line	Dacarbazine 1,200mg/m2	4	2.0	8.2	Neutropenia (19%)
				57 second-line	Gemcitabine 1,800mg/m2 plus dacarbazine 500mg/m2	12	4.2	16.8	Neutropenia (16%)
Trabectedin	Demetri et al., J. Clin. Oncol., 2016	Phase III	518 LPS or LMS	345	Trabectedin 1.5mg/m2	9.9	4.2	12.4	Neutropenia (56%)
				173	Dacarbazine 1,000mg/m2	6.9	1.5	12.9	Neutropenia (15%)
	Takahashi et al., Oncologist, 2017	Pooled phase II results	66 trans-STS	66	Trabectedin 1.2mg/m2	12.1	5.6	17.5	Neutropenia (78%)
Others	Penel et al., J. Clin. Oncol., 2008	Phase II	30 AS	8 visceral AS 22 cutaneous AS	Paclitaxel 80mg/m2	18.5	4	8	Neutropenia (3%)
	Schöffski et al., Lancet, 2016	Phase III	452 LMS or LPS	228	Eribulin 1.4mg/m2	4	2.6	13.5	Neutropenia (15%)
				224	Dacarbazine 1,200mg/m2	5	2.6	11.5	Thrombocytopenia (8%)

Although an in-depth review of all of the trials included related to alternative and second/further-line therapies in the medical management of advanced STS is beyond the scope and relevance of this thesis, there are some interesting points to draw out in terms of the progress. In particular, the ability of trials to highlight potential efficacy in specific subtypes of STS.

For example, trials and retrospective reviews of ifosfamide in the management of STS identified particular sensitivity in patients with SS and liposarcoma, with a relative lack of activity in patients with LMS[56,57,68]. As such, high-dose ifosfamide is commonly used as second-line therapy, and particularly in patients with SS, LPS of the myxoid, well- and de-differentiated subtypes, whilst it is generally avoided in patients with LMS.

Additionally, gemcitabine is commonly used as standard second-line therapy in certain STS subtypes, and occasionally in the further line setting. Initially explored as monotherapy, two early phase II trials in advanced STS following failure of first-line therapy were disappointing, with only a single partial response observed in each study (ORR of 3%)[58,59]. As such, gemcitabine monotherapy is not frequently administered, but is commonly combined with additional synergistic anti-cancer agents such as docetaxel. The efficacy of gemcitabine plus docetaxel in patients with LMS was demonstrated in the first phase II trial of this combination[60]. This trial reported an ORR of 53% and the treatment regimen was generally well tolerated As such, although a small cohort, this trial suggested robust efficacy of gemcitabine plus docetaxel in patients with LMS. These results were supported by the Maki *et al*. a randomized open-label phase II study which utilised Bayesian adaptive randomisation to imbalance the cohorts in favour of the superior treatment (SARC002, NCT00142571)[61]. This confirmed superiority of combination gemcitabine plus docetaxel over gemcitabine monotherapy, with an ORR for gemcitabine plus docetaxel of 16% (12 of 73 patients) compared to 8% (4 of 49) in the gemcitabine monotherapy arm. This equated to a median PFS of 6.2 months and a median OS of 17.9 months in the combination therapy arm compared to a median PFS of 3 months and median OS of 11.5 months in the monotherapy arm. As such, this study concluded that gemcitabine plus docetaxel was superior to gemcitabine alone, with particular efficacy in LMS. Given the

apparent lack of efficacy of ifosfamide in LMS, the demonstrable activity of gemcitabine plus docetaxel this subtype allows tailoring of second-line therapy to specific STS subtypes.

Trabectedin is another therapy commonly used following the failure of first or further-line therapies with efforts made to demonstrate efficacy, particularly in the so-called L-sarcomas of LMS and LPS. This subtype-specific efficacy was demonstrated by Samuels et al. in their report from an expanded access program (NCT00210665)[69]. They presented results from 1803 patients and identified a clinical benefit rate (CBR) of 54% (258 of 476 patients) in the L-sarcoma cohort, compared to 38% (114 of 302 patients) in the non-L sarcoma cohort. Upon analysis of survival, this translated into a survival advantage for the L-sarcoma cohort (median OS 16.2 months; 95% CI 14.1-19.5) when compared to the non-L sarcoma cohort (median OS 8.4 months; 95% CI 7.1-10.7). This efficacy in L-sarcomas was further described in the multicentre, randomised, phase III trial comparing trabectedin with dacarbazine in patients with metastatic LPS or LMS following the failure of conventional chemotherapy (NCT01343277)[70]. A total of 518 heavily pre-treated patients were enrolled with the final analysis demonstrating trabectedin significantly reduced the risk of disease progression compared with dacarbazine (HR 0.55; 95% CI 0.44-0.70; $p<0.001$), translating into a notable improvement in median PFS (4.2 months vs. 1.5 months). As such, trabectedin is a viable option in the second and further line setting in advanced STS and in particular patients with LMS and LPS. Furthermore, a number of trials are planned or ongoing looking to expand the evidence base for trabectedin. For example, the Italian Sarcoma Group are undertaking a randomised phase II study comparing trabectedin with gemcitabine in advanced and pre-treated LMS, as well as a planned phase II study of trabectedin in advanced rearranged mesenchymal chondrosarcoma (NCT0438119 and NCT04305548 respectively)[71,72]. As such, the utilisation of trabectedin as a disease controlling agent in patients with advanced and pre-treated STS may continue to expand.

Further subtype-specific efficacy has been demonstrated for example with paclitaxel in advanced angiosarcoma in phase II trials (ANGIOTAX, European clinical trials database 2004-002841-12)[66] and eribulin in a phase II trial of heavily

pre-treated patients with LMS and LPS (NCT01327885)[67]. These trials are of particular importance given the limited treatment options available for patients with advanced disease in these subtypes which are refractory to conventional chemotherapy. As such, since the turn of the millennium, steady progress has been made in developing sequential treatment paradigms which are more patient-centric in the more targeted subtype-specific approach. However, further refinement through the identification of patient groups within subtype cohorts, and novel therapies, will further improve patient outcomes in these difficult to treat populations.

1.3.5 Summary

Despite numerous efforts to improve patient outcomes since the anti-tumour activity of doxorubicin in the early 1970s, anthracycline-based chemotherapy remains the standard of first-line care in subtype-agnostic advanced STS. The addition of ifosfamide is only occasionally used given the increased toxicity and is generally reserved for circumstances whereby tumour shrinkage might be directly beneficial by reducing symptoms or potentially allowing definitive treatment. In some circumstances whereby anthracyclines are contra-indicated due to their cumulative dose-dependent cardiotoxic effects alternative first-lines are necessary. In these cases, ifosfamide monotherapy or gemcitabine monotherapy may be suitable options and the most appropriate decided on a case-by-case basis. Looking forward, additional translational work may be beneficial in exploring patient stratification into specific molecular subgroups which may preferentially benefit from specific therapies. More recently, targeted therapies have been developed and the hope is these will go somewhere to avoid the treatment-related adverse events associated with systemic cytotoxic therapies as well as yield significant improvement in response rates and the survival of patients.

1.4 Pazopanib in the management of soft tissue sarcomas

Pazopanib is an oral multi-target tyrosine kinase inhibitor (TKI) with its anti-tumour effect postulated to be exerted by the anti-angiogenic effect of inhibiting multiple receptor tyrosine kinases (RTKs) such as VEGFR, platelet derived growth factor receptor (PDGFR), fibroblast growth factor receptors (FGFR) and stem cell factor receptor (c-KIT)[73]. It is known that angiogenesis is a key hallmark of cancer progression and dissemination, as sustained growth of tumours requires new blood vessels to deliver sufficient nutrients and oxygen[74]. Therefore, blockade of these angiogenic pathways represents an attractive target for therapeutic agents, such as TKIs.

1.4.1 Receptor tyrosine kinases as drivers of oncogenesis

Kinases have recently emerged as one of the most intensively examined targets in cancer research due to their vital role in cell signalling and behaviour, whilst TKIs represent the largest class of targeted therapies approved by the Food & Drug Administration[75].

RTKs are transmembrane structures and are essential for the transduction of extracellular signals into the cell[76]. Briefly, RTKs are made up of an extracellular domain able to bind specific ligands, a single transmembrane helix, and an intracellular domain made up of a juxtamembrane regulatory region, a tyrosine kinase domain and a carboxyl-terminal tail. Upon binding of a receptor-specific ligand to the extracellular domain, receptor dimerisation (and/or oligomerisation) is promoted with this change in conformation enabling trans-autophosphorylation of the tyrosine kinase domain and removal of cis-autoinhibition. The activated RTK then recruits signalling proteins, which themselves bind to specific phosphotyrosine residues within the receptor and are able to activate downstream mediators and trigger intra-cellular signalling cascades (**Figure 1.3.A**). In this way, the activation of signalling pathways results in cellular changes which can lead to proliferation, migration, survival and angiogenesis [77].

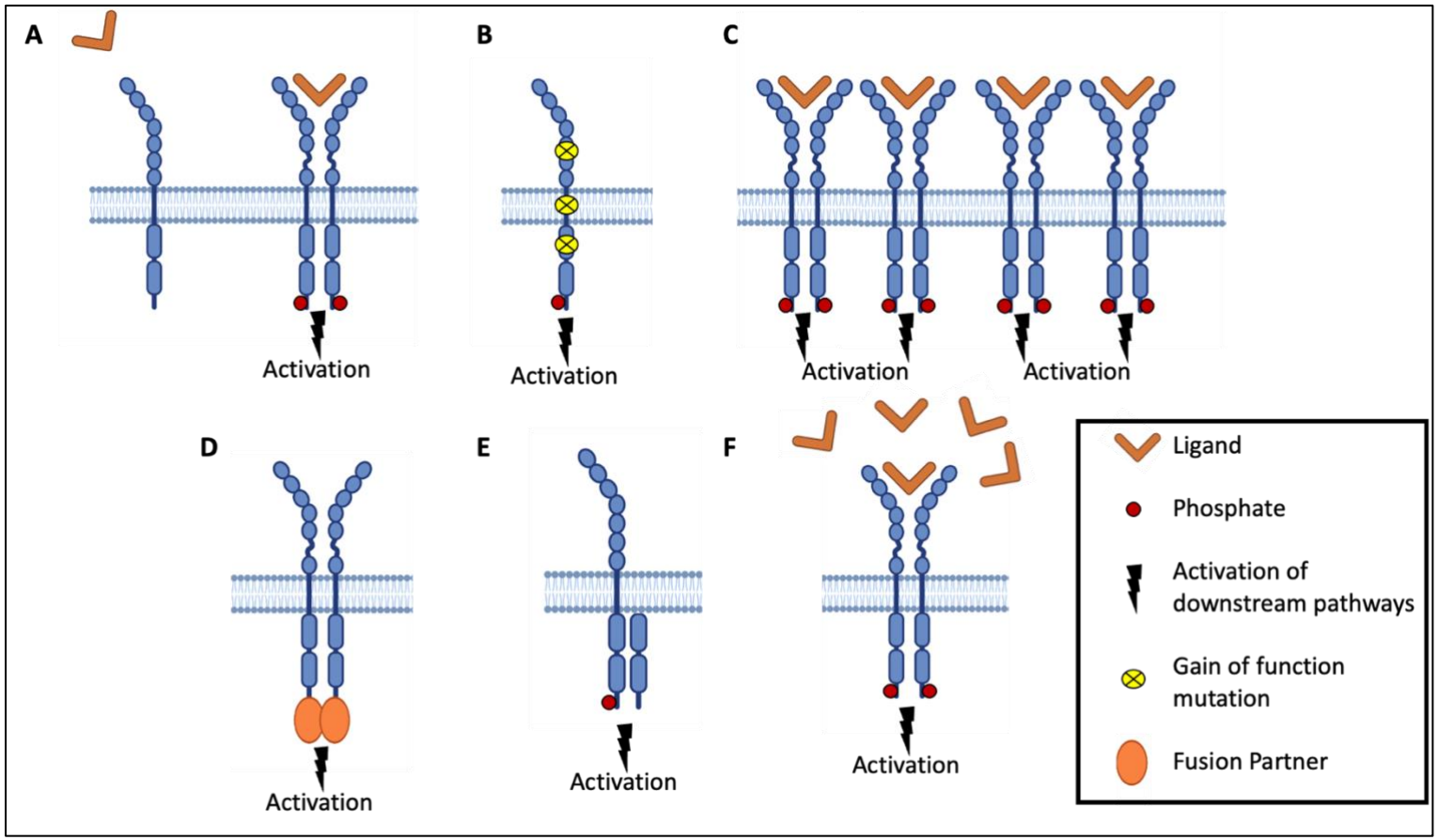

Figure 1.3. Schematic representation of RTK activation in health and in malignancies. **A**. Normal physiological response to ligand leading to receptor dimerization, autophosphorylation and activation of downstream signalling pathways. **B**. Gain of function mutations lead to ligand-independent receptor activation. **C**. RTK overexpression leads to increased local concentration of receptors overcoming antagonistic factors and over-activating intra-cellular pathways. **D**. Chromosomal translocation leads to generation of a fusion oncoprotein, part RTK and part fusion partner, leading to constitutive activation to the tyrosine kinase domain. **E.** Tyrosine kinase domain duplication leading to intra-cellular dimer formation and ligand-independent activation. **F**. Autocrine activation via increased concentration of ligands and subsequent RTK activation[77].

Under normal physiological conditions, RTK activity is tightly controlled. However, genomic aberrations can alter the behaviour of RTKs in a number of ways, ultimately leading to aberrant activation of downstream signalling pathways and dysregulation of normal cellular function.

The first of the mechanisms by which RTKs can drive tumourigenesis is through gain-of-function mutations which may occur at the extra-cellular domain, the intra-membranous single helix, or the intra-cellular domain (**Figure 1.3.B**). In the field of sarcomas, an example of this would be *KIT* gain-of-function mutations reported in gastrointestinal stromal tumours (GIST). These mutations are seen to cluster near the tyrosine kinase domain, the intracellular juxtamembrane regulatory region and the extra-cellular ligand binding region of the KIT protein[78,79]. Evidence suggests that mutations in the tyrosine kinase and juxtamembraneous domains lead to the removal of normal cis-inhibition in the tyrosine kinase domain, whilst in the extracellular regions mutations stabilise interreceptor interactions resulting in receptor-mediated dimerisation in the absence of ligand[78–80].

A second mechanism which may drive tumorigenesis is abnormal amplification of RTK genes leading to RTK overexpression. This results in a local overexpression of the receptor leading to elevated RTK signalling in the presence of the cognate ligand and overwhelms antagonizing regulatory effects (**Figure 1.3.C)**[77]. Well-differentiated and de-differentiated liposarcomas (WDLPS and DDLPS) are characterised by genomic amplifications, with one study analysing 56 samples reporting that, after *MDM2* and *CDK4* gene amplifications, the next most notable category of gene amplifications involved those encoding RTKs and was identified in 18 (36%) of the samples analysed[81].

A further genomic alteration which may lead to ligand-independent activation of RTKs is chromosomal re-arrangements. In these cases, a novel tyrosine kinase fusion oncoprotein is generated, with the tyrosine kinase oncoprotein under the control of the promoter of its fusion partner which also contributes a di/oligomerisation domain leading to constitutive activation of the RTK **(Figure 1.3.D)**. Within sarcoma, there are numerous examples of this, including *NTRK*

gene fusions resulting in tropomyosin receptor kinase (TRK) dysregulation which is pathognomonic of congenital infantile fibrosarcoma, and also sporadically observed in hemangiopericytomas, infiltrative spindle cell sarcomas and a subset of uterine LMS[10].

Kinase domain duplication is another genomic anomaly that may lead to aberrant RTK activity **(Figure 1.3.E)**. This phenomenon has been mostly widely characterised in the epithelial growth factor receptor (*EGFR*) gene, whereby the entire gene contains wild-type sequence but with a tandem in-frame duplication of exons 18-25 which encodes the entire tyrosine kinase domain. The forced proximity of the duplicated kinase domains leads to an intra-molecular asymmetric dimer and leads to constitutive activation of the receptor in a ligand-independent manner[82]. Although more commonly encountered in non-small cell lung cancer, glioma and breast cancer, there are reports of kinase domain duplication occurring in STS[82–84].

The final mechanism by which RTKs can drive oncogenesis is via autocrine activation, whereby the target cells of the ligand are also the cell secreting it, with this positive feedback loop driving clonal expansion and tumourigenesis (**Figure 1.3.F)**[85]. One such example is secretion of the cytokine autocrine motility factor which interacts with autocrine motility factor receptor, with a large cohort study showing both rhabdomyosarcoma and AS express higher levels of autocrine motility factor[86].

Given the critical role RTKs play in normal cellular function, and their ability to drive oncogenesis following aberrant activation, the rationale for the development of therapeutic agents directly targeting them is clear.

1.4.2 Angiogenesis is an important aspect of sarcoma development with pazopanib displaying anti-angiogenic activity

Induction of and sustained angiogenesis are key features of oncogenesis, and set-out in the Weinberg and Hanahan's series on the hallmarks of cancer[74,87]. As with all cells, supply of oxygen and nutrients is vital for cellular survival and function, and in order to sustain growth tumours require neovascularisation to fuel

their expansion. Indeed, evidence exists supporting the fact that sarcomas frequently have increased expression of angiogenic RTKs as part of their phenotype. Moreover, the fact that pazopanib inhibits these RTKs in the pre-clinical setting means it is an attractive potential agent in the management of STS[88].

1.4.2.1 Vascular endothelial growth factors and their receptors in angiogenesis, in the context of sarcoma and as a target for pazopanib

In health, the family of vascular-endothelial growth factors (VEGF) and their receptors (VEGFR) play a key role in vasculogenesis, the development of blood vessels from their precursor cells in the early stages of embryogenesis, as well as angiogenesis, the formation of blood vessels from pre-existing vessels in later life, for example in response to injury[89]. However, in the overexpressed state, VEGF overactivity can lead to pathological angiogenesis. In particular, the major pro-angiogenic signal is generated from VEGF-A activated VEGFR2 which triggers intra-cellular signalling via the mitogen activated protein kinase (MAPK) cascade[89].

Prior xenograft studies of pazopanib have quantified the IC_{50} of pazopanib against a range of RTK targets[88]. Of note, pazopanib had the greatest inhibitory effect on VEGFR1-3, in that order. Furthermore, within the same study, pazopanib was demonstrated to significantly inhibit VEGF-induced angiogenesis. This is relevant in the context of STS as numerous studies have indicated the potential role of VEGF and VEGFR in sarcoma development. For example, a number of studies have shown that circulating levels of VEGF are significantly higher when compared with normal controls[90]. And in addition, VEGF levels correlated with tumour grade as well as being prognostic for STS of the extremity and trunk[91–94]. As such, there is a rationale for extrapolating these findings to explore pazopanib in the clinical context of STS.

1.4.2.2 Platelet derived growth factors and their receptors in angiogenesis, in the context of sarcoma and as a target for pazopanib

Platelet derived growth factor (PDGF)-α and -β and their receptors (PDGFR) are a further key part of the angiogenic network. A major driver of growth, survival and motility of mesenchymal cells, as well as other cells, PDGF is usually synthesised in response to external stimuli including hypoxia, thrombin or through stimulation by other cytokines and growth factors[95–97]. In health, PDGF-α and -β have vital roles in embryogenesis and physiological control of tissue haemostasis[97]. Upon ligand binding, the PDGFR RTKs undergo dimerization and autophosphorylation, as previously described, allowing the triggering of intracellular signalling cascades including phosphatidylinositol 3′-kinase (PI3-kinase), phospholipase C (PLC)-γ, Src, and MAPK[98]. In terms of angiogenesis, PDGF and PDGFR are thought to support angiogenesis through the establishment of functional vessel walls via recruitment and stabilisation of perivascular cells[99]. Interestingly, VEGF-A has been shown to enhance endothelial PDGF-β expression, whereas fibroblast growth factor-2 leads to enhancement of perivascular PDGFR-β expression, with stimulation by VEGF and fibroblast growth factor (FGF)-2 leading to functional vessel formation *in vivo*[100].

In the context of sarcoma, given the role of PDGF as a driver of growth, survival and motility of predominantly mesenchymal cells, there is a rationale for considering PDGFs may have a role in the development of STS. Indeed, PDGFR overexpression has been documented in a number of histological STS subtypes, whilst high expression of PDGFR-β has been demonstrated to be significantly negatively prognostic[90,93,101]. In addition, PDGF-β expression per protein and mRNA quantification is significantly associated with STS tumour grade and cellular proliferation[102,103]. As with VEGFR, Kumar et al.'s study of pazopanib confirms pazopanib is potently active against both PDGFR-α and -β, with *in vitro* work confirming significant inhibition of PDGFR-β phosphorylation following pazopanib treatment[88]. Again, the rationale for assessing the clinical utility of pazopanib in STS is apparent based upon the link between PDGF, angiogenesis, sarcomagenesis and targeted pazopanib activity against PDGFR.

1.4.2.3 Fibroblast growth factors and their receptors in angiogenesis, in the context of sarcoma and as a target for pazopanib

The family of FGF, and their associated receptors (FGFR), play a role in angiogenesis, particularly in promoting the integrity of the endothelial cell barrier through the formation of tight junctions. Indeed, studies comparing VEGF-driven versus FGF-driven tumours demonstrated that the neovasculature was significantly more permeable when VEGF was the driving growth factor[104]. As with other RTKs, ligand activation leads to the activation of intra-cellular signalling cascades including MAPK, PI3K, PLC-γ and signal transducers and activators of transcription (STAT)[105]. In health, the role of FGF has been demonstrated in FGF-1/FGF-2 double knockout animal models, with the hosts demonstrating poor wound healing, indicative of FGFs role in tissue repair and neovascularisation post-trauma[106].

Compared to VEGF and PDGF, there is less evidence to suggest a prevalent upregulation of FGF in the context of sarcoma. Evidence does exist of a potential stimulatory effort of FGF in SS cell lines and high-grade LPS cell lines[107,108]. Furthermore, one study identified several activating FGFR tyrosine kinase domain mutations in 7.5% of primary human rhabdomyosarcoma samples[109]. In addition, circulating plasma levels of basic FGF were found to be 10-13 fold higher in patients with STS compared to healthy controls, particularly in those patients with fibrosarcoma and LMS[90]. Therefore, although the evidence demonstrating the role of FGF in sarcomagenesis is less compelling than for VEGF and PDGF, the fact that pazopanib has confirmed activity against FGFR, albeit with less affinity than against VEGFR and PDGFR, confirms the potential for clinical benefit.

1.4.3 Signalling pathways involved in soft tissue sarcoma development, and changes associated with pazopanib treatment

Following aberrant RTK activation, recruitment of intra-cellular signalling molecules to the activated carboxyl-terminal tail triggers the initiation of a variety of downstream signalling cascades[110]. A number of these cascades have been

implicated in the development and propagation of sarcomagenesis, whilst pre-clinical evidence exists of modulation of these pathways by pazopanib.

1.4.3.1 Mitogen activated protein kinase signalling

Dysregulation and activation of the MAPK pathway has been demonstrated to be integral in the development of numerous malignancies, including STS. In this pathway, aberrant sequential activation of RAS/RAF/mitogen-activated protein kinase kinase (MEK)/extracellular signal-regulated kinase (ERK) leads to upregulation of cellular processes involved in oncogenesis, including cell proliferation, survival, differentiation and migration[111]. Commonly, mutations in RAS and RAF are oncogenic drivers of the pathway, and although sources vary it is reported that around 20% of all human cancers harbour mutations in one of the three major forms of Ras[112]. Although common in cancers of epithelial origin, the role of the MAPK cascade in STS is less clearly defined. However, some pre-clinical studies have demonstrated activity in STS cell lines. For example, Sasaki et al. reported the expression of RAF1 and MAPK1/2 mRNA in sarcoma cell lines and clinical samples, with subsequent exposure of cell lines to a MEK inhibitor resulting in dose- and time-dependent inhibition of cell proliferation[113]. Furthermore, targeted modulation of the MAPK pathway in SS cell lines resulted in inhibition of the phosphorylation of MAPK and ERK, leading to G1 cell growth arrest and S phase decrease, and induction of apoptosis[114].

In relation to pazopanib activity, a number of studies have demonstrated that in addition to the antiangiogenic effects elicited, pazopanib also has an anti-oncogenic effect through modulation of the MAPK pathway. As mentioned above, pazopanib is known to potently inhibit VEGFR1-3, PDGFR-α and -β, c-KIT, and FGFR1, 3 and 4[88]. These RTKs activate the MAPK signalling pathway and can drive tumour progression through constituent activation of this axis[115–117]. Therefore, inhibition of VEGF, PDGFR-α and -β, c-KIT and FGFR receptors will have an anti-oncogenic effect, and this has been demonstrated in a number of studies.

1.4.3.2 Phosphatidylinositol 3'-kinase signalling pathway

The PI3K pathway is another major intracellular signalling cascade initiated by RTK activation and acts as a key regulator of survival during cellular stress. Following RTK activation through ligand binding, PI3K is recruited to the cellular membrane where it catalyses the phosphorylation of phosphatidylinositol 4,5-bisphosphate (PIP_2) to phosphatidylinositol 3,4,5-triphosphate (PIP_3)[118–120]. Activated PIP_3 then recruits signalling proteins with pleckstrin homolog domains, including protein kinase B (Akt), itself a key regulator of numerous cellular processes involved in cell survival[118]. Indeed, Akt is able to act on a number of pro-apoptotic factors including Bad and procaspase-9, as well as other regulators of survival factors such as NFκB. Furthermore, Akt also acts on several targets involved in cell cycle regulation, protein synthesis and glycogen metabolism including Raf (part of the MAPK pathway), the forkhead family of transcription factors, and importantly mammalian target of rapamycin (mTOR)[118]. Mammalian target of rapamycin activation results in the increased synthesis of numerous proteins which are implicated in oncogenesis, with particular involvement in the modulation of metabolic pathways vital for cell growth and proliferation[121].

Within the field of oncology, aberrant PI3K, Akt and mTOR activity have been demonstrated, driven by a diverse range of genomic alterations, leading to tumorigenesis, metastasis, and chemotherapy resistance[122]. Indeed, within STS numerous studies have confirmed activation of the PI3K pathway with PI3K overexpression in STS tumour tissue, evidence of active phosphorylated Akt, and an association between Akt-mTOR pathway activation and patient survival[123–125].

In addition to the anti-angiogenic action of pazopanib, activity against RTKs which utilise the PI3K pathway will likely have additional anti-oncogenic properties independent of any impact on the tumour vasculature. To this end, pre-clinical work has demonstrated that following pazopanib treatment of SS cell lines *in vitro*, they displayed significantly reduced phosphorylation of both Akt and mTOR[126]. The same study confirmed that the suppression of Akt was more significant following pazopanib therapy compared to anti-PDGFR inhibition alone.

Furthermore, Lanzi et al. demonstrated in xenograft models that sensitivity to pazopanib was diminished in cases with inefficient inhibition of Akt and ERK[127]. Thus, in addition to anti-angiogenic effects, activity against the PI3K pathway is a further mechanism by which pazopanib likely exerts its anti-tumour effects.

1.4.4 Early clinical development of pazopanib

Based upon promising pre-clinical evidence of the anti-tumour effects of pazopanib, a multicentre open-label, non-randomised, dose-finding phase I study of pazopanib in advanced solid tumours was undertaken (NCT00060151)[128]. A total of 63 patients were enrolled, 43 to the dose escalation arm, and a further 20 to the dose expansion arm, who had a histologically confirmed diagnosis of an advanced solid tumour refractory to standard therapy. The trial cohort was made up of a heterogeneous group of solid tumours, including 6 (10%) patients with STS. The documented treatment-related adverse events were in keeping with those associated with anti-angiogenic therapies, with grade 3-4 hypertension being the most commonly reported and seen in 16 (25%) patients. The median time to onset of hypertension was 7.5 days, and all episodes of hypertension were manageable with anti-hypertensive medications and resolved on treatment discontinuation. Pharmacokinetic analysis identified that steady-state exposure to pazopanib plateaued in the 800mg once-daily treatment group. Assessment of preliminary clinical activity in this trial reported 3 (4.8%) patients with a partial response to therapy, with 14 (22.2%) achieving a prolonged period (greater than 6 months) of disease stabilisation. Of note, prolonged disease stabilisation (range 7.6 months to 19.8 months) was reported in 4 out of 6 (66.6%) patients with sarcoma, made up of 2 patients with chondrosarcoma, 1 with LMS and 1 with a GIST. In addition, a subset of patients underwent dynamic contrast enhanced MRI (DCE-MRI) to visualise tumour blood flow following pazopanib. A greater than 50% reduction in tumour blood flow was observed in 58% (7 of 12) of patients at day 8 post-pazopanib initiation, and in 91% (10 of 11) of patients at day 22 post-pazopanib initiation. This suggested activity of pazopanib to target the tumour vasculature and diminish the supply of oxygen and nutrients vital for tumour growth. As such, and given the toxicity profile as well as preliminary

clinical efficacy, 800mg pazopanib once daily was the suggested dosing regimen to take forward in further clinical trials.

In addition, a further phase I study exploring the pharmacokinetic and pharmacodynamic activity of pazopanib in a paediatric population was undertaken (NCT00929903)[129]. A total of 51 patients between the ages of 2 and 22 years (median 12.9 years) with recurrent or refractory solid tumours, or primary central nervous system tumours, were enrolled and included for analysis, including 28 (55%) patients with STS. The maximum tolerable dose was determined to be 450mg/m2 for pazopanib tablets, and 160 mg/m2 for the suspension form, with dose-limiting toxicities including grade 3-4 biochemical abnormalities in lipase, amylase and transaminase, as well as proteinuria and hypertension. Of note, a patient with occult brain metastases experienced a grade 4 intracranial haemorrhage. Preliminary response evaluation for patients with STS confirmed a sustained partial response in a patient with desmoplastic small round cell tumour, who completed 24 weeks of protocol therapy, and a further 7 patients with durable stable disease of greater than 6 months (2 patients with alveolar soft part sarcoma, (ASPS) 1 osteosarcoma, 1 GIST, 1 alveolar rhabdomyosarcoma and 1 mesenchymal chondrosarcoma). Furthermore, 8 patients had evaluable DCE-MRI data available, and all 8 showed decreases in tumour blood volume and permeability consistent with the anti-angiogenic effects of pazopanib.

1.4.5 Clinical trials of pazopanib in soft tissue sarcomas

1.4.5.1 EORTC Phase II clinical trial of pazopanib in STS

Following the evidence of anti-tumour activity in phase I trials, a subsequent non-comparative phase II study of the anti-tumour activity of pazopanib in STS was undertaken (EORTC 62043, NCT00297258)[130]. They enrolled 142 patients with advanced intermediate- or high-grade STS, who were ineligible for chemotherapy or had received a maximum of two prior lines of chemotherapy prior to trial participation. Of note, the cohort was generally pre-treated, with only 2 (1.4%) patients out of the 142 enrolled having received no prior therapy. The trial utilised

PFS at 12 weeks as the primary end-point, and applied a Simon two-stage design to four histological strata, made up of adipocytic STS, LMS, SS, and “other” STS subtypes. This study design dictated that during the first stage of the trial, 17 patients would be recruited to each stratum, with at least 20% being progression-free at 12 weeks considered a success leading to the expansion of the cohort to a total of 37 patients per strata. A 12-week PFS rate of greater than 40% within the strata of 37 patients was deemed indicative that further investigation of pazopanib in this strata was warranted.

Each patient received 800mg pazopanib orally and continued on therapy until progression, toxicity or withdrawal of consent. In total, 136 patients were included in efficacy analyses. Based on the Simon two-stage design, accrual for the adipocytic sarcoma cohort was stopped after completion of the first stage as only 3 (17.6%) of the 17 patients were progression-free at 12 weeks, and as such this did not meet the pre-determined cut-off of 20%. The remaining three strata continued recruiting to the second stage of the trial, and had a 12-week PFS rate of 44% (18 of 41 patients) in the LMS strata, 49% (18 of 37 patients) in the SS strata and 39% (16 of 41 patients) in the “other” STS strata. At a cohort median follow-up of 677 days, median PFS rates were 80 days, 91 days, 161 days and 91 days, and median OS 197 days, 354 days, 310 days and 299 days in the adipocytic sarcoma, LMS, SS and “other” STS strata respectively. Of note, the median PFS and OS compared favourably to historical controls taken from the EORTC-STBSG database[131]. No complete responses were observed, but partial responses to therapy were seen in 9 (6.6%) patients, 1 (2.4%) with LMS, 5 (13.5%) with SS and 3 (7.3%) in the “other” STS strata. Pazopanib was well tolerated in this trial cohort, with the majority of adverse events grade 1 or 2, with the most frequent grade 3-4 toxicities being hypertension in 7.7% (11 of 142 patients), fatigue in 7.7% (11 of 142 patients) and hyperbilirubinemia in 6.3% (10 of 142 patients). Treatment interruptions were necessitated in 60% (85 of 142) of patients, and dose reductions in 23% (33 of 142 patients). These results confirmed the tolerability of pazopanib in a larger cohort of STS patients and demonstrated sufficient anti-tumour activity in non-adipocytic STS to warrant further investigation.

1.4.5.2 PALETTE phase III trial of pazopanib in metastatic non-adipocytic soft-tissue sarcoma

Building on the results of the phase II study, the EORTC-STBSG undertook the randomised, double-blind placebo-controlled phase III Pazopanib explored in Soft Tissue Sarcoma (PALETTE) trial, which represented the first placebo-controlled phase III trial undertaken in STS (EORTC 62072, NCT00753688)[132]. Between October 2008 and February 2010, a total of 372 patients were enrolled across 72 sites in 13 different countries, and included patients over the age of 18 with metastatic non-adipocytic STS demonstrating progression in the preceding 6 months, or 12 months following previous adjuvant therapy. Patients were required to have received at least one prior line of anthracycline-containing therapy, and up to a maximum of four prior lines of therapy. Enrolled patients were randomised 2:1 to receive either 800mg oral pazopanib daily or placebo, with the trial's primary end-point being PFS.

Across the cohort of 372 patients, the median age was 55 years, and they were heavily pre-treated with 207 (56%) patients having received 2 or more lines of systemic therapy, and 78 (21%) patients 3 or more lines. Three patients were lost prior to randomisation, therefore 369 patients were included in intention-to-treat analyses, 123 of which were randomised to receive placebo and the remaining 246 allocated to the pazopanib treatment arm. At median follow-up of 14.6 months in the placebo group and 14.9 months in the pazopanib group, there was a statistically significant improvement in PFS observed for the pazopanib group (4.6 months vs 1.6 months; HR 0.31, 95% CI 0.24-0.40; p<0.0001). Via external review of images, the CBR of pazopanib was 73% (14 partial responses and 164 with stable disease out of 246 patients) compared to 38% in the placebo group (47 stable disease out of 123 patients). However, despite the improved PFS associated with pazopanib therapy, disappointingly there was no significant difference in OS between the treatment arm and placebo arm (12.5 months vs 10.7 months; HR 0.86, 95% CI 0.67-1.11; p=0.2514). Generally pazopanib was well tolerated, with the most common grade 3-4 toxicities being fatigue in 13% (31 of 239 patients) compared to 5.7% (7 of 123 patients) in the placebo arm, and

hypertension reported in 7% (16 patients) in the pazopanib arm and 3% (4 patients) in the placebo arm.

Although this study demonstrated activity of pazopanib in a heterogenous group of STS patients as evidenced by the significant 3-month prolongation of PFS, the lack of significant benefit in OS was disappointing. Indeed, as some health services, including the UK, base funding for medications on quality of life years gained, the lack of OS benefit was detrimental to cost-effectiveness analyses undertaken in the wake of the PALETTE trial and indeed led to funding being withdrawn for the use of pazopanib in STS via the National Health Service (NHS) Cancer Drugs Fund[133,134]. It was noted that post-progression therapy was given frequently and varied substantially, and this may have impacted OS in both the placebo and treatment groups, although the nature of this potentially confounding factor was not qualified. In addition, the median OS of the placebo group was anticipated to be in the region of 8 months and was therefore much longer in the trial population (10.7 months). Indeed, the study power calculation was for 90% power at 5% significance level with 279 events to detect a 33% decrease in the hazard ratio of death, which corresponds to a median OS improvement from 8 months to 12 months. Given the unexpectedly long OS in the placebo group, the study may have been underpowered and a type II error may have occurred, whereby a false negative conclusion has been drawn. A further point to note is that in the preceding phase II trial two patients allocated to the “other” STS strata were later re-allocated to the adipocytic STS strata following central histopathology review. Both of these cases were progression-free at 12 weeks, resulting in a 12-week PFS rate of 26% (5 of 19 patients) for the adipocytic strata, and as such this cohort should have proceeded to the second stage of the trial.

Although the PALETTE trial had a negative result in the fact an OS benefit was not observed, a number of subsequent studies and analyses have confirmed that pazopanib may have considerable utility in certain STS subpopulations of patients[135–138].

1.4.6 Further evidence of pazopanib activity in soft tissue sarcoma

1.4.6.1 Post-hoc analyses from the PALETTE phase III trial

Following publication of the PALETTE trial results, a number of post-hoc analyses have been published undertaking subgroup and further analyses. One of the most important of these was by Kasper et al., who undertook a survival-based analysis of patients treated with pazopanib in both the phase II and phase III trials[135]. They excluded a total of 44 patients from this analysis, including those with adipocytic sarcomas, leaving a cohort for this retrospective analysis of 344 patients. At a median follow-up of 2.3 years, this cohort had a median PFS of 4.4 months, and a median OS of 11.7 months. What was interesting to note however, is that utilising a PFS of greater than 6 months as the definition for a long-term responder, and an OS of greater than 18 months to define a long-term survivor, from the combined cohorts 36% (124 patients) were deemed long-term responders, 34% (116 patients) were long-term survivors, and 22.1% (76 patients) were both long-term responders and survivors. These figures do support the fact that a substantial proportion of patients with advanced STS do gain benefit from treatment with pazopanib in the advanced setting. Indeed, 12 patients (3.5%) in this cohort remained on pazopanib therapy for over 2 years. Although small, this subgroup of 12 patients was not enriched for specific STS subtypes, and after a median time on therapy of 2.4 years, the median PFS was 2.3 years and median OS 2.8 years. Undertaking multivariate logistic regression across the whole pazopanib-treated cohort, worse performance status and low baseline haemoglobin were independently negatively associated with long-term response and survival, whilst bone metastases were negatively associated with long-term response, and higher tumour grade was associated with poor long-term survival. However, other factors such as STS subtype, patient sex, and site of primary were not significantly associated with pazopanib response. As such, and given that tumour grade and performance status are known prognostic factors in STS outcome, no additional factors were identified which were able to identify those patients most likely to gain clinical benefit from pazopanib[136].

A further retrospective study of the combined phase II and phase III study populations looked to explore differential response rates in uterine and non-uterine sarcomas[137]. The authors identified a total of 44 patients with uterine sarcomas in the pazopanib-treated arms, with 88.6% (39 patients) being uterine LMS, whilst this cohort also had a higher proportion of high-grade tumours relative to the non-uterine sarcoma cohort (84.1% vs 54.8%). Interestingly, when focusing solely on uterine sarcomas, patients randomised to pazopanib versus those treated with placebo have a significantly longer median PFS (3.0 months versus 0.8 months) and longer median OS (17.5 months vs 7.9 months; p=0.038). This indicated that in the subgroup of uterine sarcoma patients taken from the phase II and III studies, there was significant clinical benefit following the administration of pazopanib, and again highlights the fact that although the PALLETTE phase III trial has led to the withdrawal of funding for the general STS patient population, this is depriving some patients of an active and tolerable anti-cancer agent.

Finally, a more recent exploratory subgroup analysis utilising median PFS as the outcome of interest, compared the pazopanib-treated cohort with the placebo group from the PALETTE trial[138]. The only finding of note was that median PFS was higher in those patients who had received 1 prior line of therapy when compared with those who had received 2 or more lines of therapy (24.7 weeks versus 18.9 weeks). When split into over/under 65 years of age, median PFS was similar, and a reduction in median PFS was not seen in patients requiring dose interruptions of modifications in the management of toxicities.

Overall, these post-hoc analyses of the PALETTE study suggest that certain groups of patients do receive considerable benefit following treatment with pazopanib, but no particular clinicopathological variables are able to effectively stratify patients beyond those already known to be prognostic in STS.

1.4.6.2 Additional prospective and retrospective studies of pazopanib activity in soft tissue sarcomas

Following the results of the PALETTE study, there have been few prospective clinical trials exploring the role pazopanib may play in the management of variable STS subtypes. The most recent trial was led by a German group and was a randomised, open-label phase II non-inferiority study comparing pazopanib with doxorubicin as the first-line treatment of metastatic STS in those over 60 years of age[139]. A total of 120 patients with progressive advanced or metastatic STS were randomised 2:1, with 81 patients receiving pazopanib at a dose of 800mg daily until progression or intolerance, and the remaining 39 receiving doxorubicin 75m/m^2 once every 3 weeks for up to 6 cycles. The primary study end-point was non-inferiority, defined by the upper limit of the 95% CI for the HR for PFS being less than 1.8. The median age across the whole cohort was 71 years, and recruited all STS subtypes with LMS being the most common, followed by UPS and then LPS. At a median follow-up time of 11.8 months, the median PFS in the pazopanib arm was 4.4 months compared to 5.3 months in the doxorubicin arm (HR 1.00, 95% CI 0.65-1.53), which met the pre-defined criteria for non-inferiority in this study. Median OS in the pazopanib arm was 12.3 months compared to 14.3 months in the doxorubicin arm, and although interaction analyses revealed no significant parameters to be associated with OS, of note the LPS cohort (18 patients, 13 received pazopanib and 5 received doxorubicin) had a HR of 1.62 (95% CI 0.88 – 2.97). However, for this trial OS analyses are difficult to interpret due to a large amount of post-trial crossover, including cross-over to second-line pazopanib in 17.6% (6 of 39 patients) from the doxorubicin arm, and to second-line doxorubicin in 37.7% (29 patients) from the pazopanib arm. Tolerability of both regimens in this trial were as expected, especially considering the intentionally selected higher age of enrolled patients, with dose reductions necessary in 24.7% (20 patients) receiving pazopanib, and in 24.3% (9 patients) receiving doxorubicin. One of the secondary end-points of the study was the incidence of neutropenia in each cohort, with 0% of patients experiencing either grade 4 neutropenia or febrile neutropenia in the pazopanib arm, compared to 56.5% (22 of 39 patients) and 10.3% (4 patients) in the doxorubicin arm. As

such, the authors suggest that given certain considerations and given the risks associated with grade 4 neutropenia and febrile neutropenia in this elderly population, pazopanib represents a valid first-line treatment option in elderly patients presenting with advanced STS.

Further prospective studies have focused on the efficacy of pazopanib in specific STS subtypes, including traditionally chemoresistant tumours such as SFT, chondrosarcomas, and epithelioid sarcomas **(Table 1.5).**

Broadly speaking, these studies demonstrate pazopanib efficacy, although given the relatively small cohort sizes in a number of these studies, concrete assertions and comparisons with the OS and PFS data from the PALETTE study are difficult to make. Furthermore, a number of the STS subtypes, such as SFT and ASPS, tend to have a more unpredictable clinical course with occasional periods of indolence. As such, the surprisingly long periods of PFS and OS in these studies may not truly reflect pazopanib anti-tumour activity but rather might be part of the usual clinical course of that subtype.

Table 1.5 Select prospective trials published since the PALETTE trial of pazopanib monotherapy in STS subtype specific cohorts of patients. ASPS – alveolar soft part sarcoma; mOS – median OS; mPFS – median PFS; PD – progressive disease; PR – partial response; RECIST – response evaluation criteria in solid tumours; SD – stable disease; SFT – solitary fibrous tumour.[140–146]

Study	Subtypes	Study type	Number of patients	Number of line of systemic therapy	Patients evaluable for response	Best Response by RECIST	Survival (months)	Number of grade 3/4 adverse events
Urakawa et al., *Cancer Sci.*, 2020	ASPS (5) Epithelioid sarcoma (2) Clear cell sarcoma (1)	Japanese prospective single-arm multi-centre phase II trial	8	Treatment naive - 3 (37.5%) 1 prior line - 4 (50%) 2+ prior lines - 1 (12.5%)	8	PR - 1 (12.5%) SD - 6 (75%) PD - 2 (25%)	mPFS 15.7m mOS not reached	12
Kim et al., *Oncologist*, 2019	Metastatic ASPS	Korean single-arm, open-label, multi-centre phase II trial	6	Treatment naive - 4 (66.6%) 1 prior line - 1 (16.7%) 2+ prior lines - 1 (16.7%)	6	PR - 1 (16.7%) SD - 5 (83.3%)	mPFS 5.5m mOS 32.0m	1
Martin-Bronto et al., *Lancet Onc.*, 2020	Typical SFT	European multi-centre, single-arm phase II trial	34	Treatment naive - 7 (21%) 1+ prior line - 27 (79%)	31	PR - 2 (6%) SD - 29 (94%)	mPFS 11.2m mOS 49.8m	31
Martin-Bronto et al., *Lancet Onc.*, 2019	Advanced malignant and dedifferentiated SFT	European multi-centre, single-arm phase II trial	36	Treatment naive - 24 (66.6%) 1 prior line - 8 (22.2%) 2+ prior lines - 3 (5.6%)	35	PR - 2 (6%) SD - 21 (60%) PD - 12 (34%)	mPFS 5.57m mOS - not reached 24m OS - 73%	36
Maruzzo et al., *Clin. Sarc. Res.*, 2015	SFT	UK prospective single centre case series	13	Treatment naive - 13 (100%)	11	PR - 1 (7.7%) SD - 8 (61.5%) PD - 2 (15.4%)	mPFS 4.7m mOS 13.3m	6
Chow et al., *Cancer*, 2020	Unresectable or metastatic chondrosarcoma	American multi-centre, single-arm phase II trial	47	Treatment naive - 32 (68.1%) 1+ prior line - 15 (31.9%)	42	PR - 1 (2%) SD - 30 (64%) PD - 11 (23%)	mPFS 7.9m mOS 17.6m	51
Stacchiotti et al., *Lancet Oncol.*, 2019	Advanced extraskeletal myxoid chondrosarcoma	European multi-centre, single-arm phase II trial	26	Treatment naive - 21 (81%) 1 prior line - 2 (8%) 2+ prior lines - 3 (11%)	22	PR - 4 (18%) SD - 16 (73%) PD - 2 (9%)	mPFS 19m mOS not reached 24m OS 90%	27

Although lacking the confined parameters of clinical trials, retrospective reports also offer insights into the efficacy of pazopanib in mixed subtype cohorts, with real-world experience again supporting the notion that pazopanib has a place in the arsenal of STS systemic therapies. Gelderblom et al. published the results of a retrospective case notes review of patients who had received pazopanib as part of the named patient programme (NPP) allowing access to medications in the compassionate use setting[147]. The notes from a total of 211 patients with variable STS subtypes who had received at least one dose of pazopanib as part of the NPP were reviewed. The largest STS subtype represented was LMS making up 41% (87 out of 211 patients) of the cohort, followed by SS (11%, 24 patients) and UPS was the third most common subtype (9%, 19 patients). In general, the cohort was heavily pre-treated with only 6% (13 patients) receiving pazopanib in the first-line setting. Clinical benefit of pazopanib therapy at any time was observed in 46% (97 patients), with a median PFS of 3.0 months and median OS of 11.1 months from the start of pazopanib. In terms of differential responses by subtype, UPS had the highest percentage of partial responses (26%, 5 of 19 patients), whilst rate of clinical benefit was highest in SFT and SS (both 54%, 7 of 13 and 13 of 24 patients respectively). In terms of tolerability, the study confirmed a good level of dosing compliance with a relative dose intensity in this cohort of 92%, and only 27 patients (13%) discontinuing pazopanib due to adverse events. Furthermore, grade 3/4 adverse events were uncommon, with grade 3 nausea the most frequently reported and documented in only 6 (2.8%) patients. This study confirms the utility of pazopanib in the clinic, and in this advanced heavily pre-treated cohort the high rate of clinical benefit and tolerability across multiple subtypes is promising.

Oh et al.'s recently published multi-centre retrospective case series of Korean patients with advanced sarcoma treated with pazopanib is notable for the large cohort reported, with a total of 347 patients included[148]. The authors included all patients who had received pazopanib for the treatment of advanced sarcoma and who had failed at least one line of conventional systemic chemotherapy, with just under half having failed two or more lines of therapy (44.1%, 153 of 347 patients). The median age of the cohort was 51 years, and LMS was the most common

histological subtype represented (27.4%, 95 of 347 patients), with UPS (13.5%, 47 patients) and AS (12.7%, 44 patients) the next most common. Of the whole cohort, disease control was achieved in 60.1% (190 of 313 evaluable patients) with a median PFS of 5.3 months and median OS of 12 months. The authors note that patients with ASPS and SFT appeared to have excellent outcomes following pazopanib initiation, however as previously noted these results may be confounded by the occasionally indolent course of these tumours when compared to more aggressive subtypes such as LMS and UPS. As with previous studies, pazopanib was relatively well tolerated with a mean dose intensity of 83.4% and a daily average dose of 700mg. Indeed, although treatment-related adverse events were documented for 170 patients (49%), none were grade 4 or higher, and grade 3 toxicities were only observed in 8 (2.3%) patients. Although a retrospective study, this large cohort provides further evidence of the robust subtype-agnostic anti-tumour activity of pazopanib and its tolerability in the context of a heavily pre-treated cohort of patients. Numerous additional retrospective studies have been published demonstrating the real-world utility of pazopanib in both mixed and subtype-specific cohorts, and these are summarised in **Table 1.6**. From this selection of retrospective studies, what stands out in the mixed subtype studies is the relatively uniform median PFS and OS reported, and a combined PR and SD rate observed in most studies of above 40% and as high as 69% in Nakamura's cohort of 156 patients. This real-world evidence again supports the notion that a subgroup of patients, frequently heavily pre-treated and thus difficult to manage, gain significant benefit from pazopanib therapy.

Table 1.6 Select retrospective trials published since the PALETTE trial of pazopanib monotherapy in STS cohorts. AS – angiosarcoma; EHE – epithelial haemangioendothelioma; mOS – median OS; mPFS – median PFS; PD – progressive disease; PR – partial response; RECIST – response evaluation criteria in solid tumours; SD – stable disease.[147,148,157,149–156]

Study	Subtypes	Study type	Number of patients	Number of line of systemic therapy	Patients evaluable for response	Best Response by RECIST	Survival (months)	Number of grade 3+ adverse events
Alshamsan et al., *Cancer Manag Res*, 2021	Multiple subtypes	Saudia Arabian single-centre case series	45	1 prior line - 21 (46.7%) 2+ prior lines - 24 (53.3%)	45	PR - 9 (20%) SD - 16 (35.6%) PD - 20 (44.%)	mPFS 4.1m mOS 12.4m	13
Halim et al., *Cancer Treat Res Commun*, 2021	Multiple subtypes	Lebanese single-centre case series	15	1 prior line - 11 (73.3%) 2 prior lines - 4 (26.7%)	15	SD - 2 (32.4%) PD - 13 (86.7%)	mPFS 3.0m mOS not reached	Not reported
Karaağaç et al., *J Oncol Pharm Pract.*, 2020	Multiple subtypes	Turkish multi-centre case series	79	Treatment naive - 14 (17.7%) 1 prior line - 35 (44.3%) 2 prior lines - 24 (30.4%) 3+ prior lines - 6 (7.6%)	79	CR - 1 (1.3%) PR - 12 (15.2%) SD - 23 (29.1%) PD - 43 (54.4%)	mPFS 3.97m mOS 11.4m	23
Oh et al., *Targeted Oncol.*, 2020	Multiple subtypes	Korean multi-centre case series	347	1 prior line - 194 (55.9%) 2 prior lines - 92 (26.5%) 3+ prior lines - 61 (17.6%)	313	PR - 54 (17.3%) SD - 136 (43.5%) PD - 123 (39.3%)	mPFS 5.3m mOS 12.0m	8
Seto et al., *Med Sci (Basel)*, 2018	Multiple subtypes	American regional case series	123	1 prior line - 26 (21%) 2 prior lines - 28 (23%) 3+ prior lines - 69 (56%)	123	CR - 1 (0.8%) PR - 12 (9.8%) SD - 34 (27.6%) PD - 76 (61.8%)	mPFS 3.0m mOS not reported	Not reported
Gelderblom et al., *Acta Oncologica*, 2017	Multiple subtypes	Internaional multicentre case series	211	Treatment naive - 13 (6%) 1 prior line - 59 (28%) 2 prior lines - 60 (28%) 3+ prior lines - 80 (38%)	139	PR - 15 (10.8%) SD - 38 (27.3%) PD - 86 (61.9%)	mPFS 3.0m mOS 11.1m	15
Nakamura et al., *Cancer*, 2016	Multiple subtypes	Japanese multi-centre case series	156	Treatment naive - 30 (19.2%) 1 prior line - 57 (36.5%) 2+ prior lines - 69 (44.2%)	125	PR - 13 (10.4%) SD - 74 (59.2%) PD - 38 (30.4%)	mPFS 3.5m mOS 11.2m	44
Yoo et al, *BMC Cancer*, 2015	Multiple subtypes	Korean multi-centre case series	43	1 prior line - 9 (20.9%) 2 prior lines - 15 (34.9%) 3+ prior lines - 19 (44.2%)	41	PR - 7 (17.1%) SD - 18 (43.9%) PD - 16 (39%)	mPFS 5.0m mOS 8.2m	Not reported
Frezza et al., *JAMA Oncol.*, 2018	Epithelioid sarcoma	International multi-centre case series	18	Median number of prior lines - 2 (range 1-4)	18	SD - 9 (50%) PD - 9 (50%)	mPFS 3.0m mOS 14.0m	Not reported
Menegaz et al., *Oncologist*, 2018	DSRCT	American single-centre case series	29	1 prior line - 1 (3%) 2 prior lines - 6 (21%) 3+ prior lines - 22 (76%)	29	CR - 1 (3%) PR - 1 (3%) SD - 16 (55%) PD - 11 (38%)	mPFS 5.63m mOS 15.7m	Not reported
Kim et al., *J Gynecol Oncol*, 2017	Uterine sarcomas	Korean single-centre case series	35	1 prior line - 17 (49%) 2+ prior lines - 18 (51%)	34	CR - 1 (2.9%) PR - 9 (26.5%) SD - 11 (32.4%) PD - 13 (38.2%)	mPFS 5.8m mOS 20.0m	5
Kollar et al., *Acta Oncol.*, 2017	Vascular sarcomas	European multicentre case series	52	Treatment naive - 5 (9.6%) 1 prior line - 18 (34.6%) 2+ prior lines - 1 (55.8%)	49	CR - 1 (1.9%) PR - 11 (21.2%) SD - 11 (21.2%) PD - 26 (50%)	AS mPFS 3.0 m AS mOS 9.9m EHE mPFS 26.3m EHE mOS 26.3m	Not reported

1.4.6.3 Summative pazopanib effectiveness based on previous prospective and retrospective trials

Although the trials detailed above have a number of variables between them, given the potential use of pazopanib in a subtype agnostic manner it may be possible to combine the data to derive a pooled median overall and progression-free survival, as well as the proportions of patients obtaining clinical benefit from pazopanib treatment. In order to obtain a pooled median survival time, the use of an inverse weighted average is the most appropriate method, as it will give more weight to more precise trials[158,159]. In order for the data to be included, specific hazard ratio data for the OS and PFS from pazopanib initiation must be available from the published manuscript. Therefore, including all available data from the trials included above, the pooled median PFS from start of pazopanib therapy is 4.03 months, and pooled median OS is 11.4 months[132,142,156,157,160–162,144,145,147–149,151,153,154].

In terms of response rates per RECIST criteria, including all prospective and retrospective studies with complete data, a total of 1412 patients can be included for summative analysis[132,140,152–154,156,157,160–163,142,144–149,151]. In this combined cohort, best response upon radiological assessment was classified as complete response in 5 (0.4%) patients, partial response in 169 (12%), stable disease in 667 (47.2%), and progressive disease in 571 (40.4%).

1.4.7 Biomarkers for pazopanib response

Despite the promising evidence of pazopanib anti-tumour activity in both the clinical trial and real-world settings, what is apparent is that individual responses to therapy remain significantly variable. In the clinical setting, the challenge is then identifying those who might glean considerable advantage from being treated with pazopanib and those who might benefit from an alternative therapeutic regimen. This has ramifications on the management of the individual, in terms of optimising the care of each patient, but also at a healthcare system level, as the correct selection of patients most likely to gain benefit could drastically improve the cost-effectiveness of pazopanib therapy. As such,

biomarkers able to predict response to pazopanib in STS are highly sought after to improve patient outcomes and also to ensure funding for pazopanib is made available to those patients likely to respond.

1.4.7.1 The relationship between resistance, tumour progression and survival in the context of TKI therapy

Given the evidence of a statistically significant improvement in PFS compared to placebo in the PALETTE phase III trial and further real-world confirmation of activity, one challenge is exploring why this is not translated into an OS benefit[132].

One potential mechanism is that pazopanib exposure drives a phenotypic switch to a highly malignant, aggressive and invasive tumour, through the application of potent clonal selection pressure. Indeed, xenograft mouse modelling of pancreatic neuroendocrine tumour and glioblastoma has demonstrated that anti-angiogenic therapies drive tumour adaption[164]. In these models, VEGF blockade was associated with deficiency in tumour capsule, degree of invasiveness and progression to a form with greater malignant potential, with elevated invasiveness and greater propensity for metastasis. Given their observation of distinct regions of intense hypoxia in the VEGF targeted tumours, the authors suggested a role of the hypoxia response system as a key modulator of the shift to a more malignant and aggressive phenotype. As such, although pazopanib may be active as evidenced by a significant PFS advantage in the phase III trial, this may not have translated into an OS benefit due to this malignant transformation. In addition, VEGF inhibition has previously been shown to diminish tumour vasculature, however upon cessation of therapy it has been observed that there is a rebound rapid revascularisation response[165,166]. This would suggest that at evidence of progression, and subsequent treatment cessation, previously responsive tumours would demonstrate a rapid flare of disease activity resulting in rapid progression negating any anti-tumour activity during therapy and resulting in no observable survival benefit.

The idea of disease flare following withdrawal of therapy has been demonstrated across a range of neoplasms and various TKIs. In a study of patients with EGFR-

mutant lung cancer, after a period of initial benefit and subsequent progression, after cessation of the TKIs erlotinib or gefitinib, 23% experienced a disease flare after TKI discontinuation[167]. Similarly, in patients with thyroid cancer treated with lenvatinib, upon treatment cessation 14.3% of patients experienced a flare of disease[168]. Indeed, although only a small number of patients, 37.5% (3 of 8 patients) who experienced a disease flare had died within a month of treatment cessation. In addition, a case report has demonstrated the phenomenon of disease flare in the context of STS and pazopanib[169]. In this report, a patient with uterine LMS was treated with pazopanib with good effect, with stable disease after 3 months of therapy. However, upon treatment cessation she experienced rapid disease progression, with a 55% increase in the size of the lung metastases 2 weeks following pazopanib withdrawal, and the patient died one month after treatment cessation.

Therefore, there is evidence that treatment with TKIs, as with other therapies, is responsible for the application of significant selective pressures generating a more aggressive subclonal population. In addition, in a subset of patients, withdrawal of TKI therapy may lead to rapid tumour progression and early death. This may all contribute to the results observed in the PALETTE study, whereby a significant PFS advantage was reported versus placebo, but with no apparent OS benefit. Furthermore, the rebound rapid progression following treatment cessation in a subset of patient may have contributed to this finding, and being able to identify those at risk and combatting this phenomenon may help personalise and target therapy for improved patient outcomes.

1.4.7.2 The development and use of predictors of response in oncology

With the development of therapies targeted at specific vulnerabilities harboured by cancer, biomarkers are becoming a promising avenue to help tailor therapy to individual patients. Broadly, prognostic biomarkers are able to stratify patients based on disease outcome, whilst predictive biomarkers are more specific to a drug of interest. As such, prognostic biomarkers are able to stratify a cohort of patients based upon the prognosis of their disease based upon the marker(s) of interest in the absence of treatment, or following standard of care. Conversely,

predictive biomarkers are able to stratify patients based on the marker(s) of interest with respect to their outcome following a particular specific treatment[170].

In order for a biomarker to be acceptable to be adopted into routine clinical usage it should fulfil certain criteria;

It should be robust and reliable;

It should reliably trigger a clinical decision that results in patient benefit;

The clinical community has to be convinced of the need for the biomarker and the benefit it affords, weighed against the cost and burden of undertaking the test[171].

Failure to fulfil any of these three criteria would result in a biomarker which would not have utility in the clinical setting. In order to develop biomarkers a number of critical steps need to be undertaken[171–173]. Foremost, a cohort of samples must be available to be analysed to test or discover a new potential biomarker. Subsequent testing of an independent cohort of samples is then necessitated to validate the original biomarkers findings from the hypothesis-generating analysis, and confirm that the biomarker will provide additional information in the clinical setting to help drive decision-making for patient benefit.

1.4.7.2.1 Analytical validity

An important prerequisite in the process of developing a new biomarker is an assessment of the robustness and reliability of the analytical process involved in determining the result of any biomarker testing[174]. This step also involves pre-analytic validity, whereby factors involved in the handling and processing of tissues may negatively influence the reliability of the assessment of the biomarker. Analytical validity involves an assessment of the specificity, sensitivity and robustness of a chosen assay, as well as considering inter-user reliability such that results from different laboratories do not display excessive variability[175].

1.4.7.2.2 Clinical validity

Once a technically sound analysis pathway has been settled upon, the question of clinical validity is then approached. Following discovery of a potential

biomarker which is apparently able to stratify a cohort into those more or less likely to respond, it must then be validated on a separate cohort of samples[172]. Important considerations of this stage include the sensitivity/specificity of the test, reproducibility, analyte stability and the cut-off used for the biomarker result[176]. After training and validation, the next stage to confirm clinical validity would involve obtaining high-level evidence of robustness. The original guidance from the American Society of Clinical Oncology (ASCO) stated that a prospective randomised trial was the only means to formulate level I evidence of biomarker validity[177]. However, more recent updated guidance opened additional routes whereby sufficient validity could be obtained via less costly and time-consuming means. Indeed, the use of samples from a previously completed prospective trial can be utilised in this regard, in a “prospective-retrospective“ biomarker study[177]. The benefits of such an approach include the fact that previously obtained and archived samples are made use of, with careful curation of clinical data, patient recruitment practices and standard sampling procedures all followed as part of the original prospective clinical trial. Furthermore, a pre-determined biomarker analysis operating procedure and statistical analysis plan ensure unbiased validity of subsequent biomarker results.

A number of challenges can be faced during the clinical validity stage of biomarker development. For example, a single analyte biomarker, such as an aberration of a single gene, should have a relatively straight forward analysis process. However, in cases of a multianalyte biomarker, for example utilising high-dimensionality data will often require a degree of computational processing in order to derive a useable result. As such, the computational pipeline and analytical framework involved in processing the data to derive the biomarker result should be “locked in” prior to assessment of validation on the validation cohort[176]. Statistical “over-fitting” is another potential pitfall in biomarker development, in which a large number of potential predictors are applied to a small number of outcome variables. However, the inclusion of a validation set of samples which are independent of the original discovery set of samples can go some way to act as an internal validation of the biomarker validity. During development, it is vital that the validation set remains independent and analysis

is not undertaken upon it which may influence the design of the biomarker algorithm[176,178].

1.4.7.2.3 Clinical utility

Finally, the biomarker should have clinical utility. One aspect of this is there should be clear and well-communicated guidance on how to interpret and act on results from a biomarker used in the clinic[177]. Indeed, a lack of clarity following the introduction of a new biomarker can be highly detrimental to patient care and result in incorrect clinical decisions being made. In addition, the steps of analytical and clinical validity must have been completed to generate robust high-level evidence to ensure the correct patients are receiving the correct treatments[172].

1.4.7.2.4 Clinical biomarkers - treatment stratification and methods used

Clinically relevant biomarkers able to stratify and select for patients most likely to respond to a specific therapy, or family of therapies, are becoming more commonplace. Generally, the methodologies utilised for identification of the biomarker of interest are variable, and depend on the type of biomarker being assessed, as well as implications related to availability, cost and feasibility of the test involved.

In its most simple format, biomarkers predictive of treatment response might be a particular drug target protein expressed in cancer cells which is detectable via IHC testing. IHC has the advantage of being inexpensive, making it feasible for large-scale biomarker testing, whilst also not requiring high-cost equipment, as is the case with genomic assays. Furthermore, it is relatively simple to perform, once an optimised protocol for staining and scoring which is repeatable and robust is established. One example of a clinically relevant, drug target detectable by IHC and able to predict treatment response is Human epidermal growth factor receptor 2 (HER2). Overexpression of HER2 is found in approximately 20% of cases of invasive breast cancer, and as well as being associated with worse prognosis, it is the sole predictor of sensitivity to HER2 targeted therapies, such as trastuzumab (Herceptin)[179]. Indeed, numerous large-scale clinical trials have confirmed a significant survival benefit associated with trastuzumab therapy in

patients with HER2 positive breast cancer[180]. Detection of HER2 positivity, and therefore stratification of patients to receive HER2 targeted therapy, is usually via IHC, with in situ hybridization utilised to classify cases deemed equivocal by IHC[179]. Another clinically relevant biomarker that is usually determined by IHC testing is PD-L1. The landmark phase III KEYNOTE-024 trial demonstrated a significant OS and PFS advantage for patients with non-small cell lunger cancer (NSCLC) treated with the anti-PD-L1 drug pembrolizumab when compared to standard platinum-based chemotherapy, in a cohort of 305 patients in which greater than 50% of cancer cells expressed PD-L1[181]. As a result of this work, pembrolizumab is approved by NICE in the first-line treatment of NSCLC with greater than 50% positive staining of tumour cells for PD-L1[182].

Aside from IHC staining of particular drug target proteins of interest, specific genomic aberrations, such as translocations, may also act as biomarkers which are effectively able to stratify patients into those most likely to gain clinical benefit from treatment. Indeed, identification of the reciprocal chromosomal translocation between chromosomes 9 and 22, forming the “Philadelphia chromosome”, was a landmark discovery in the field of oncology. The *BCR-ABL1* fusion gene resulting from the translocation leads to abnormal tyrosine kinase activity, driving dysregulated proliferation of immune precursors[183]. This disease process can then drive the development of haematological malignancies, including the majority of cases of chronic myeloid leukaemia, and up to 30% of acute lymphoblastic leukaemia[184]. Identification of the driver *BCR-ABL1* fusion gene paved the way for the development and eventual clinical use of targeted TKI therapies, with a number of TKIs approved for first line use in chronic myeloid leukaemia. As the driver mutation, and key vulnerability targeted by the first-line TKIs in the management of these malignancies, identification of the *BCR-ABL1* fusion gene is crucial at diagnosis. Historically this was done by FISH, with fluorescent probes binding to the *BCR* and *ALB1* genes able to confirm the rearrangement. However, more recently guidance suggests the use of polymerase chain reaction (PCR) techniques to establish the presence of quantifiable *BCR-ABL1* mRNA transcripts and subsequent monitoring of these levels during treatment[185,186].

Another example of translocation-driven cancers not amenable to IHC characterisation are cancers resulting from tropomyosin receptor kinase (TRK) fusion proteins, postulated to occur in 1% of solid tumours[9,10]. Indeed, although recurrent rearrangement of *ETV6-NTRK3* in congenital infantile fibrosarcoma was the first described *NTRK* fusion gene driving sarcomagenesis, subsequent work has also described sporadic *NTRK* fusions in a number of other sarcomas, including spindle cell sarcomas and uterine LMS[187–189]. Given the development of the anti-TRK inhibitors larotrectinib, entrectinib, and ongoing development and testing of second-generation inhibitors, there is a need to identify cancers harbouring *NTRK* fusions which could be targeted. Although pan-TRK IHC protocols exist, high levels of false-positive expression has been reported in tumours of neuronal and smooth-muscle differentiation, limiting IHC's role in STS *NTRK* fusion screening. Furthermore, application of FISH is not a robust approach due to variable partner genes in *NTRK* fusions, leading to an inability to identify the 5' fusion partner and limiting clinically vital information. In addition, complex genomic rearrangement patterns, or deletion of genomic regions, leads to failure of the FISH probes to bind and can result in false-negative results[190]. As such, screening of tumours known to harbour *NTRK* fusions is reliant on nucleic acid based assays, for example, whole exome/genome sequencing, or anchored multiplex PCR in which only one of the fusion partners is targeted, in this case *NTRK1-3*, but which allows characterisation of novel or variable fusion sequences[27]. Given the sequencing options and lack of clarity as to the best approach, a recent European Society of Medical Oncology released a consensus approach for detecting TRK fusions[191]. In specific histological tumours types in which *NTRK* fusions are recurrently rearranged with specific fusion partners, any confirmatory method is valid, including FISH, reverse transcription PCR, and increasingly commonly targeted RNA sequencing. For histology-agnostic screening, RNA sequencing remains the gold standard, assuming RNA quality is sufficient, with subsequent IHC confirmation of protein kinase expression advisable given this is the pharmacological target.

In addition to specific genomic aberrations, more complex genomic analyses have also been deployed to act as biomarkers for therapy response. One such

example is the role of tumour mutational burden (TMB) to act as a biomarker for therapy response to immune checkpoint inhibitors (ICIs) and other immunotherapies. Although showing promising results, ICIs do show variable response between patients, and as such a biomarker predictive of response helps select patients for which treatment is most effective. The rationale behind the association between TMB and immunotherapy response lies in the fact that mutations will lead to the formation of neoantigens present on the cancer cell surface[192]. Of these, some may be immunogenic, thus driving an anti-tumour immune response and leading to the accumulation of immune cells within the tumour microenvironment. Upon initiation of immunotherapy, these immune cells are then able to act directly against the tumour cells leading to a treatment response. Indeed, TMB has been demonstrated to predict response to a number of immunotherapies in the clinical setting. The first association between TMB and response to ICIs was in melanoma, with mutational load demonstrated to be significantly associated with clinical benefit to anti-CTLA-4 therapy[193]. This led to the exploration of TMB and ICI response across a number of different cancers, with Goodman et al. showing that across a diverse range of tumour types, high TMB was an independent predictive factor of clinical response to PD-1/PD-L1 blockade[194]. A subsequent prospective, non-randomised phase II trial, KEYNOTE-158, was then undertaken to investigate the role of TMB as a biomarker for objective response to pembrolizumab in a range of solid tumours (NCT02628067)[195]. Of 790 patients evaluable for TMB quantification and clinical response, 102 (13%) were considered TMB-high, and of these patients an objective response to pembrolizumab was seen in 29% (30 patients), compared to just 6% in the TMB-low cohort. Historically, next-generation whole exome sequencing (WES) was deployed to give a measure of TMB, reported as the number of mutations per megabase. However, given the complexity and cost of undertaking WES, a number of targeted representative panels have been designed and approved for use in the clinical setting, Indeed, the KEYNOTE-158 trial utilised the FoundationOne assay of 324 genes to determine TMB in their cohort, and following the trial this assay was approved in the United States of America for TMB quantification for use as a biomarker for anti-PD-1 therapy following failure of prior lines of therapy[196,197]. Of note, the FoundationOne assay

includes analysis of the *NTRK1-3* genes, allowing determination of *NTRK* gene fusions which may be amenable to anti-TRK therapy.

Finally, complex molecular signatures have also been developed with the aim of guiding targeted therapy in the era of precision medicine. One example is in breast cancer where variation in gene expression patterns in breast tumour tissue from 42 patients using DNA microarrays covering 8,102 genes was observed[198]. Selection of a subset of 496 'intrinsic', genes with significantly greater variation in expression between different tumours than between paired samples, was able to identify 4 intrinsic breast cancer subtypes. Since this initial work, the gene list has been refined to 50 genes (PAM50) and the Prosigna score based upon the classification derived from this gene signature is licensed and approved by the Medicines and Healthcare Products Regulatory Agency (MHRA) to help guide adjuvant chemotherapy decisions in early stage breast cancer[199–201]. Indeed, prospective studies examining the use of the Prosigna score in the real-world setting have confirmed its clinical utility, with one study showing that Prosigna classification and risk stratification led to a change in adjuvant therapy indicated in 39% of patients[202]. Although the Prosigna platform in breast cancer represents the most developed molecular classification system, work has also been done in a number of other solid tumours, including colorectal, pancreatic and bladder cancer, in pursuit of a clinically relevant molecular classification system[203–205].

1.4.7.3 Clinical predictors of pazopanib response in STS

Through a number of analyses, both pre-planned and ad-hoc analyses have been undertaken on the PALETTE phase III trial cohort with the aim of identifying predictive clinicopathological biomarkers able to stratify patients most likely to gain benefit from pazopanib. As expected, good performance status and tumours being of low or intermediate grade were deemed favourable prognostic factors based upon multivariable modelling, but these are known prognostic factors in STS and not specific to pazopanib response[132]. Further post-hoc analysis by the authors looked to explore additional baseline characteristics with the aim of identifying additional factors predictive of OS following pazopanib, but none of age, gender, ethnicity, histology or the number of prior lines of therapy were

associated with OS in this cohort[206]. In addition, when the PALETTE pazopanib-treated cohort was combined with the preceding phase II trial cohort, Kasper et al. reported that multivariate logistic regression identified low baseline haemoglobin as negatively impacting PFS and OS, whilst bone metastases were associated with worse PFS alone[135]. However, low haemoglobin has also been shown to be a poor prognostic factor in STS, whilst the presence of bone metastases may be associated with more aggressive primary disease[207,208]. From the numerous retrospective studies including various STS subtypes, as discussed above, clinical benefit was not specific to a histological subtype, and responses and prolongation of survival following pazopanib therapy were independent of any specific and clinically relevant factor.

Given the fact a number of toxicities associated with pazopanib are driven by the on-target effect of VEGF-receptor (VEGFR) inhibition, the development of toxicities as predictive markers of pazopanib efficacy has been explored. Duffaud et al. drew on the pazopanib-treated cohorts enrolled in the PALETTE phase III trial and preceding phase II trial to assess the association of pazopanib-induced hypertension with antitumour efficacy[209]. Of the 337 patients included in analysis, 130 (38.6%) previously normotensive patients developed hypertension, with the majority doing so within 5 weeks of pazopanib initiation. At this cut-off, on both multivariate analysis including other important prognostic factors, and univariate analysis, there was no significant association between hypertension and OS or PFS. Vos et al. undertook a similar study on the same cohort, however analysed pazopanib-induced proteinuria, hypothyroidism and grade 3/4 cardiotoxicity[210]. However, as with the Duffaud study, no significant association was identified between pazopanib-induced toxicities and OS or PFS.

As such, this evidence suggests that pazopanib-induced toxicities are not able to identify those patients experiencing an anti-tumour effect of pazopanib. Alternative avenues are required to explore potential serological or molecular biomarkers which may be able to stratify patients into those most likely to respond, and shed some light on the biology driving sensitivity and resistance.

1.4.7.4 Serological predictors of response to pazopanib

Given the activity of pazopanib against mediators of angiogenesis, and the rise of multiplex antibody-based platforms to quantify a number of proteins in blood utilising a relatively small volume of plasma as input material, there have been a number of studies exploring circulating cytokines and angiogenic factors in response to pazopanib therapy. Although not in STS, the work by Tran et al. which retrospectively explored circulating factors in patients with metastatic renal cell cancer (RCC) treated with pazopanib is of interest. The authors initially screened 17 circulating angiogenic factors (CAF) in 129 patients who had the largest or smallest change in tumour size in an open label phase II of 215 patients with metastatic RCC treated with pazopanib. These candidate CAFs were then confirmed to be associated with tumour response and PFS on assessment of the entire 215 patient cohort from this phase II trial via an independent analytical platform. Finally, the findings were then validated on a cohort of 344 patients enrolled on a placebo-controlled phase III trial of pazopanib. Of the candidate circulating candidate biomarkers taken to the validation stage, interleukin (IL)-6, IL-8 and osteopontin were all associated with poorer PFS following pazopanib therapy. However, both IL-8 and osteopontin were also prognostic markers in the placebo group, and only IL-6 was a significant predictive marker for PFS benefit from pazopanib treatment compared to placebo. Interestingly, high baseline levels of IL-6 were associated with worse PFS, but this negative prognostic effect appeared to be attenuated by pazopanib when compared to placebo. Indeed, a more recent meta-analysis has confirmed the negative prognostic effect of high IL-6 levels in RCC[211]. However, despite this finding, IL-6 as a biomarker is yet to make an impact in the clinical setting and may be due to limitations related to the analytical reproducibility of IL-6 assays on a wider scale.

Focusing on an STS-specific study of CAFs in a pazopanib-treated cohort, Sleijfer et al. quantified the baseline levels of 23 CAFs from 85 patients enrolled in the phase II trial of pazopanib in advanced STS utilising PFS at 12 weeks as their primary end-point for prediction of pazopanib response[130,212]. Based on a univariate logistic regression model, low levels of both IL-12 p40 subunit and monocyte chemotactic protein-3 were significantly associated with improved PFS

at 12 weeks. However, because of repeat statistical testing the false discovery rate was around 50%, limiting the reliability of these results, and this is further confounded by a lack of validation of these results in an independent cohort.

In addition, studies of peripheral blood for markers predictive of pazopanib response have shown that a low pre-treatment neutrophil-to-lymphocyte ratio (NLR), and a decrease in the ratio following treatment, are both predictive of favourable outcomes following pazopanib therapy[213,214]. However, a high NLR ratio has consistently been demonstrated to be a poor prognostic factor across a range of solid tumours[215]. Furthermore, analysis of the NLR for 333 pazopanib-treated patients from the phase II and phase III trials of pazopanib in advanced STS demonstrated that although the negative prognostic impact of a high pre-treatment NLR was confirmed, there was no difference in outcome observed with a drop in the NLR following therapy[216]. As such, although the NLR is a widely available and simple measure to quantify, its role as a predictive biomarker for pazopanib response does not appear particularly encouraging at this time.

1.4.7.5 Molecular predictors of response to pazopanib

An alternative strategy employed in the search for biomarkers predictive of pazopanib responses has involved the interrogation of tissue samples in the hope of identifying molecular characteristics which might allow stratification of patients most likely to respond. Earlier pre-clinical work in STS cell lines demonstrated that loss of function tumour protein 53 (*TP53*) mutant cells produced significantly more VEGF, contributing directly to angiogenesis and metastasis[217]. As such, given pazopanib's activity against VEGFR there is a rationale for exploring *TP53* mutational status as a potential predictive biomarker for response. Koehler et al. reported results of 18 patients with advanced mixed-subtype sarcoma treated with pazopanib and whose tumours had undergone pre-treatment next generation sequencing[218]. Of this cohort of 19 patients, 9 (53%) harboured *TP53* mutations predicting loss of function in p53. Utilising PFS as the primary clinical outcome of interest, those patients identified as having a tumour classified as *TP53* mutant had a significantly improved PFS relative to cases considered wild-type *TP53* (HR 0.38, 95% CI 0.09–0.83; p=0.036). A similar finding was reported

in a phase I study of combination pazopanib and vorinostat, a histone deacetylase inhibitor, therapy in a range of advanced malignancies (NCT01339871)[219]. A total of 78 patients were enrolled, of which 23 (30%) had a diagnosis of STS, and of which 36 were tested for *TP53* mutations. Of these 36 patients, *TP53* mutations were detected in 11 (31%) and compared to those considered wild-type, this mutant *TP53* cohort had a significantly longer median PFS (3.5 months versus 2.0 months; p=0.042) and a favourable improvement in median OS (12.7 months vs 7.4 months; p=0.1). Although potentially promising as a biomarker predictive of response to pazopanib, more recent research, although not validated, has demonstrated that *TP53* mutation is also associated with response to anthracycline based chemotherapy[220]. As such, although potentially promising, *TP53* mutational status as a clinical aid for stratifying patients for pazopanib response has not yet been adopted into the clinic, and is currently lacking proven clinical utility.

More recently, a survival-driven genome-wide approach to biomarker discovery has been explored by Suehara et al., in which 13 patients with advanced STS and treated with pazopanib were followed up, and genomic alterations associated with clinical response retrospectively identified. The discovery phase of this study involved whole-exome sequencing, transcriptome sequencing, and RTK phosphorylation profiling of pre-pazopanib tumour tissue from a single case of high-grade axillary UPS which was observed to have a complete response to pazopanib, in order to characterise genetic alterations in this case. These findings were then validated via targeted sequencing utilising tissue from a further 5 patients, 3 of which experienced long-term stable disease and 2 who experienced progressive disease on pazopanib, and a further validation of comparative expression levels compared to 27 other high grade STS. From this molecular profiling, glioma-associated oncogene homolog-1 (*GLI1*) amplification and elevated PDGFRB phosphorylation were both associated with high antitumour activity of pazopanib. However, this study did have limitations in only having one patient with a complete response to analyse, and only included 5 pazopanib treated patients in the validation phase of this study. As such, although methodologically interesting the findings lack robustness, and a larger cohort of

patients and further independent validation would be necessary to confirm the role of *GLI1* amplification and PDGFRB phosphorylation as clinically relevant biomarkers.

1.4.8 Summary

Despite promising early-stage clinical trial results, as well as real-world and retrospective experience, a lack of OS benefit in the PALETTE phase III trial has had serious ramifications for the regular use of pazopanib in advanced STS. Although, numerous studies have demonstrated that a subpopulation of patients gain significant and robust benefit from pazopanib treatment, there is currently no clinically relevant marker which is able to stratify and predict which patients are most likely to gain benefit from treatment with pazopanib. With technological advances, the ability to undertake molecular characterisation of tumours has led to advances in a number of solid tumours, and this route could yield similar progress in identifying biomarkers for pazopanib response in STS.

1.5 The tumour immune microenvironment in cancer development and responses to pazopanib

1.5.1 Immune evasion as a hallmark of cancer

1.5.1.1 The immunosurveillance hypothesis of cancer development

Although the concept that the host immune system is a key factor in the development of malignancy has existed for over 100 years, the field of cancer immunology has developed significantly in recent years as technological advances have enhanced our ability to understand the cellular and molecular basis of this immunity. Indeed, it is now well recognised that elements of the host immune system are able to recognise neo-antigens present on tumour cells that develop as a result of an accumulation of genetic aberrations required for tumourigenesis. The original hypothesis behind host anti-tumour immunity was one of cancer immunosurveillance, whereby an ever-alert immune system is constantly surveying tissues and cells of the host, and upon detection of cancer-specific antigens the immune system is directed to launch a cytotoxic response thus eliminating incipient cancer cells and nascent tumours[74]. This theory leads to the logic that tumours that are able to thrive do so due to some mechanism which has allowed them to avoid this usual detection, and as such avoid eradication. Indeed, the observation that immunodeficient mice have a higher incidence of malignancies, as well reports indicating higher rates of cancers of non-viral aetiology in patients with both acquired or innate immunodeficiencies, indicates that immunosurveillance is at least in part involved in anti-tumour immune responses[221,222].

1.5.1.2 The immunoediting hypothesis of cancer development

More recently, however, there has been a general acceptance that immunosurveillance is actually part of a more complex tumourigenesis facilitating process termed cancer immunoediting. Initially described by Dunn et al. in the early 2000s, the cancer immunoediting hypothesis was founded on early experiments which demonstrated that the host immune system exerts control not

only on tumour quantity but also on tumour quality in terms of the degree of immunogenicity displayed by the tumour (**Figure 1.4**)[223,224].

As such, the host immune system has dual functionality, both protecting against tumour formation but also shaping the phenotype and genotype of the subsequently formed tumour via the selective immune pressure applied. The hypothesised process of cancer immunoediting follows three phases (**Figure 1.4**), elimination, equilibrium and escape, however this is over-simplistic and tumour cells may enter equilibrium or escape and bypass early stages. Furthermore, external factors may influence the flow of tumour cells through the phases, and may explain the influence of external factors of tumour growth in patients.

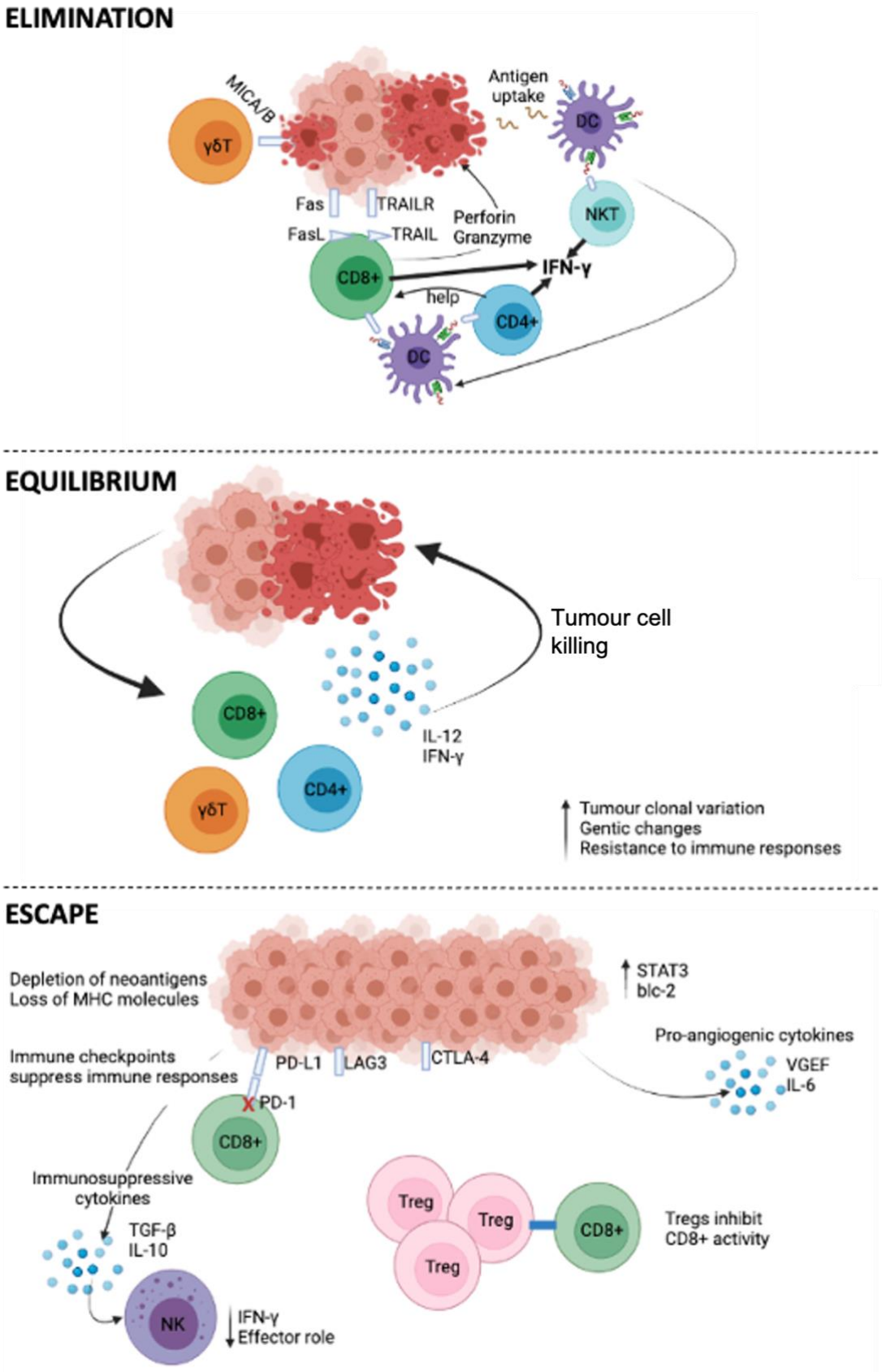
ELIMINATION
MICA/B
γδT
Antigen uptake
DC
Fas
TRAILR
FasL
TRAIL
Perforin
Granzyme
NKT
CD8+
IFN-γ
help
CD4+
DC
EQUILIBRIUM
Tumour cell killing
CD8+
IL-12
IFN-γ
γδT
CD4+
Tumour clonal variation
Gentic changes
Resistance to immune responses
ESCAPE
Depletion of neoantigens
Loss of MHC molecules
STAT3
blc-2
Pro-angiogenic cytokines
Immune checkpoints
suppress immune responses
PD-L1
LAG3
CTLA-4
VGEF
IL-6
PD-1
CD8+
Immunosuppressive
cytokines
Treg
Treg
Treg
CD8+
Tregs inhibit
CD8+ activity
TGF-β
IL-10
NK
IFN-γ
Effector role

Figure 1.4.A-C: Schematic representation of the three phases of the immunoediting hypothesis. (A) Initial elimination of the most immunogenic tumour cells. Tumour neoantigens present as a result of genomic mutations are detected by cells of the innate and adaptive immune system. The release of immune stimulatory chemical signalling proteins recruits additional immune cells to the microenvironment. Effector cells of the innate and adaptive immune work in synergy to launch an anti-tumour immune response. (B) A phase of equilibrium whereby cells which evaded the initial elimination phase enter a period of dynamic equilibrium with the immune system. This moulds the tumour cells through selective pressures to preferentially develop a population of tumour cells immune to anti-cancer immune influences. (C) Tumour outgrowth and occult cancerous growth occurs in the escape phase. The selective pressures and subsequent evolution of resistant tumour cells eventually leads to a state of occult tumour growth through evasion of host immune responses driven by a number of potential escape mechanisms. Figure created by myself using the Biorender figure design software, and based upon figures included in previously published peer-review articles[224–226].CTLA – cytotoxic T-lymphocyte associated antigen; DC – dendritic cell; FAS – Fas cell surface death receptor; IFN – interferon; IL – interleukin; LAG – Leukocyte activation gene; NKT – Natural killer T-cell; NK – Natural killer cell; PD-1 ; programmed cell-death receptor-1; PD-L1 – programmed cell-death ligand receptor-1; STAT – Signal transducer and activator of transcription; TGF - Tissue growth factor; TRAIL – Tumour necrosis factor-related apoptosis-inducing ligand; Treg – regulatory T-cell.

1.5.1.2.1 Elimination phase of cancer immunoediting

The elimination phase of the immunoediting hypothesis represents an updated form of the immunosurveillance hypothesis, whereby aspects of both the innate and adaptive host immune system work synergistically to detect and destroy developing tumour cells before they are able to flourish and become clinically apparent (**Figure.1.4.A**). The transformation of normal cells into tumour cells by genetic aberrations and failure of intrinsic tumour suppressor mechanisms results in expression of tumour specific neoantigens and other stress-induced cell surface markers. The exact mechanism for the initiation of tumour cell elimination is unclear, however most accept there is interplay between cells of the innate and adaptive immune system, with cell surface markers recognised by effector CD8+ cells, natural killer (NK) cells, γδT cells, and antigen presentation by dendritic cells (DCs) to CD4+ and CD8+ T-cells. Ultimately, the key outcome from the first stages of elimination is believed to be the release of interferon (IFN)-γ from the activated effector cells, which acts as a central orchestrator of the elimination phase[227]. Indeed, IFN-γ directly regulates the differentiation and activation of T-helper1 (Th1) cells, inhibits the development of T-helper2 (Th2) cells, promotes NK cell activity, and via induction of several other cytokines recruits specific effector cells of the immune system to the microenvironment. Effector CD8+ T-cells are able to cause tumour cell apoptosis by interacting with Fas and TRAIL receptors on tumour cells, or by secreting perforin and granzymes, whilst γδT cells are able to kill tumour cells expressing major histocompatibility complex (MHC) class I chain-related (MIC) proteins[228–230]. The destruction of tumour cells then causes the release of tumour antigens which are further presented by activated DCs, whilst cell death leads to a pro-inflammatory state further increasing the influx of immune cells to the microenvironment. The elimination phase may be wholly successful with complete removal of tumour cells and eradication prior to progression to the next stages. If not totally cleared, then it is thought a subset of rarer variant tumour cells which have avoided elimination enter the immune-mediated tumour dormancy phase.

1.5.1.2.2 Equilibrium phase of cancer immunoediting

The cancer immune equilibrium phase is defined as a period during which those tumour variants which escaped elimination enter into a phase of dynamic equilibrium with the immune system (**Figure.1.4.B**)[223]. Evidence behind the equilibrium phase of immunoediting is predominantly generated from murine models. An example of this was the work by Koebel et al., in which immunocompetent mice were treated with the carcinogen 3'-methylchloranthrene and were found to harbour cancerous cells without developing occult tumours[231]. However, upon ablation of their immune systems via monoclonal antibodies targeted against T-cells and IFN-γ, sarcomas rapidly appeared and enlarged at the carcinogen injection site, suggesting a crucial role of the adaptive immune system in maintaining cancerous cells in the state of equilibrium. Indeed, this was confirmed in further mouse studies in which the comparative analysis of the immune microenvironments of tumours in equilibrium versus escape was undertaken[232]. In this study, higher proportions of CD8+ T-cells, NK cells and γδT-cells and lower proportions of FOXP3+ regulatory T-cells (Treg) and myeloid derived suppressor cells (MDSCs) were associated with maintaining occult cancerous cells in a state of immune-mediated equilibrium. As such, although the elimination phase is reliant on both the innate and adaptive immune systems to function, the current belief is that equilibrium is maintained predominantly by cells of the adaptive immune system.

Of the three phases, equilibrium is thought to be the longest phase, and may occur over many years in humans[224]. Of the variant clones that manage to survive the elimination phase, heterogeneity and inherent genetic instability allow these tumour cells to resist the host immune responses, whilst subsequently produced variants with decreased immunogenicity will have the capacity to grow unabated by host immune influences.

1.5.1.2.3 Escape phase of cancer immunoediting

Following the often drawn-out process of immune-mediated equilibrium, the clones of cancerous cells that remain, via immune pressures, have been selected

to be immune-resistant largely owing to the activation of immunosuppressive and/or immunoevasive pathways (**Figure.1.4.C**). Recently, there has been a focus on identifying mechanisms of immune escape and then developing therapies which target these mechanisms with the hope of re-activating the host immune system against the cancerous cells. A prime example of this is the immunoevasive action of tumour cells presenting immune checkpoint proteins such as programmed death-ligand 1 (PD-L1) on their cell surface. In physiological conditions, PD-L1 interacts with programmed cell death-1 (PD-1) on T-cells to prevent immune system hyperactivity and is used to maintain immune haemostasis in healthy individuals. However, when hijacked by cancer cells the PD-1/PD-L1 axis is able to counter the T-cell receptor signalling cascade, resulting in impaired T-cell activation and cancer cell escape from immune influences[233]. However, a number of monoclonal antibodies have been developed which target this immune checkpoint axes, and with removal of the inhibitory effect of tumour cell PD-L1, CD8+ T-cells are induced to kill cancer cells. Indeed, the management of a number of cancers have been revolutionised by the introduction of ICIs into the clinic, for example advanced melanoma is particularly sensitive to ICI therapy and long-term durable disease control for up to 6 years is now possible in up to 50% of patients compared to less than 10% in the pre-ICI era[234].

There are numerous other mechanisms which allow unrestricted tumour outgrowth and they can be broadly classed into;

- Evasion of tumour cell recognition; for example cancer neoantigen depletion, and loss of MHC class I surface antigens[235,236]
- Increased resistance to the cytotoxic effect of the immune system; for example hyperactivation of signal transducer and activator of transcription 3 (STAT3), and overexpression of anti-apoptotic bcl-2 proteins[237,238]
- Expression of immunosuppressive molecules; for example PD-L1, cytotoxic T-lymphocyte associated antigen (CTLA)-4, and lymphocyte activation gene (LAG)-3[239]

- Secretion of cytokines which promote an immunosuppressive environment; for example VEGF, transforming growth factor-β (TGF-β), and IL-6[240,241]

Ultimately, the escape phase of the tumour immunoediting model results in unrestricted outgrowth by a subset of tumour cells which, through over-exposure and Darwinian selection exerted by host immune factors, have become resistant to immune attack.

1.5.2 Tumour evolution and clonal selection as a further hallmark of cancer driving sarcomagenesis and treatment responses

In addition to the selection of immune-resistant clones of cells, during their development populations of cancerous cells also undergo molecular and phenotypic evolution and preferential proliferation. From a linear perspective, the progression and evolution goes from normal tissue, through localised treatment-naïve tumour, to metastatic and therapy-resistant disease. Along this timeline, variable environmental selective pressures are exerted on the tissues to select for clonal molecular variants within the primary tumour cell mass[242,243]. Indeed, microenvironmental pressures including hypoxia, restricted nutrient availability and restricted space for expansion encourage proliferation of an invasive and migratory phenotype[244–246]. Furthermore, initiation of therapy acts as an intense selection pressure for the most drug-resistant clones leading to eventual treatment failure and tumour progression whilst on therapy[247].

1.5.2.1 Heterogeneity drives evolution

One of the key facets of cancer which allows their evolution is tumour heterogeneity whereby a single tumorous mass is made up of a diverse population of phenotypically and genetically variable cells. As a result, different cells will survive selective pressures in a variable manner leading to the expansion of clones, groups of tumour cells with highly similar genotypes, and subclones, the differentiation of several tumour cells from one single cell following the acquisition of new mutations[248]. Indeed, a higher number of subclonal

populations within a single tumour has been shown to correlate with invasiveness, metastasis, and poorer prognosis[249].

1.5.2.2 Genomic and epigenomic evolution leads to phenotypically variable cell populations

Inherent tumour heterogeneity is driven by a number of factors. Firstly, genomic instability is one of the characteristics of cancer, increasing the probability of new mutations at each cellular replication[248,250]. Furthermore, driven by higher levels of apoptosis and cell turnover, the number of cell generations per unit time in tumours is increased, and as such the number of mutations per unit time will also be higher[251].

In addition to genomic alterations, the phenotype of individual cancer cells is also driven by epigenetic factors. Components of the epigenome play a role in regulating gene expression, without intrinsic changes in the DNA sequence, therefore the epigenome also acts as a driver of intratumoural heterogeneity and neoplastic evolution[252]. Indeed, epigenetic variation in tumour cells of origin may drive increased phenotypic flexibility and intercellular heterogeneity before the emergence of genomic mutations, and as such be selected for in the tumour tissue upon progression[253]. In addition, aberrant epigenetic changes, predominantly DNA hypermethylation and histone modification, have been identified in many of the major components of cancer-related signalling pathways[252]. These include components of cell cycle regulation, DNA damage repair and tumour suppressor pathways, such as p53. In this way, the epigenome, in response to environmental factors, is able to influence the genomic evolution of tumour cells.

Interestingly, genetic and epigenetic mechanisms are inter-linked whereby not only do epigenetic factors influence expression of DNA sequences, but also mutations in epigenetic regulators can occur altering the function of the epigenome[254]. As such, both the genome and epigenome are vital for cancer cell evolution and progression towards a phenotype able to survive and proliferate. Importantly, the process of tumour evolution and clonal/subclonal selection

results in a tumour which is able to evade immune elimination, respond to hostile microenvironmental changes, be locally invasive, metastasise, and be resistant to therapeutic interventions[255–257].

1.5.2.3 Evidence of evolution in soft tissue sarcoma

Within the field of STS, numerous studies have demonstrated the importance of tumour evolution and clonal selection in clinical course and treatment responses.

A pre-clinical study involving mouse models of sarcoma was able to trace clonal dynamics throughout the natural progression of sarcoma development[258]. Harvesting tumours at the early stages of sarcomagenesis and comparing them to sarcomas at later stages of progression demonstrated a significantly higher degree of clonal heterogeneity early in the process of sarcomagenesis, suggesting primary tumour progression is associated with the selective expansion of a dominant clone. Interestingly, when assessing the clonal heterogeneity in these models, lesions from a local recurrence were polyclonal, whereas advanced metastatic lesions were driven by the clonal selection of a single metastatic clone. Crucially, to model metastasis, the tumours were excised early in their progression at a point characterised by intratumoural heterogeneity, indicating that the metastatic clone was selected prior to the reduction in clonal numbers as the primary tumour progressed. This could guide future studies targeting the specific metastatic clones to better guide treatments and prolong patient survival.

A different study looked to explore clonal evolution in sarcomas arising through variable mechanisms, namely amplicon-driven well-differentiated LPS, translocation-driven myxoid LPS and STS characterised by complex genome rearrangements[259]. For the amplicon driven LPS, only a small number of mutations were observed with few known to be oncogenic, suggesting well-differentiated LPS either develops early in life or has undergone far fewer cell cycles prior to the development of the progenitor cell. In a similar way, the translocation-driven myxoid LPS showed slow clonal evolution at the chromosome level, with only 5% of cells showing non-clonal aberrations.

Furthermore, following local recurrence the myxoid LPS samples showed less complexity compared to the primary lesion, highlighting the importance of the driver translocation as the key mediator of sarcomagenesis. In contrast, the complex karyotype STS samples displayed nucleotide and chromosome level mutations in a similar fashion to carcinomas. The importance of this study highlights that within the field of STS, between subtype differences in natural history and behaviour at the genomic level are important considerations and will direct therapy.

Finally, Anderson et al. has undertaken two studies assessing at the role and context of evolution in sarcomas. The first of these undertook genomic and transcriptomic analysis of LMS samples, including multi-regional sampling and paired metastatic samples[260]. Interestingly, within their cohort of LMS, they were able to define three distinct molecular subtypes via principle component analysis. Furthermore, analysis of temporal samples confirmed that stability of the subtype classification suggesting early acquisition of canonical mutations with subsequent acquisition of additional mutations occurring in parallel following divergence from the progenitor clone. This study supports the notion of "catch-all" histological subtypes of STS actually being formed of distinct molecular subgroups with variable biological behaviour and treatment responses, and the potentially value in defining these further for more targeted therapies. Further supporting the idea of early canonical mutations as a driver for sarcomagenesis, Anderson et al. have also explored the evolution of gene-fusion sarcomas[261]. They identified that chromoplectic rearrangements led to the formation of canonical driver gene fusions, and furthermore this chromoplexy likely occurs as a singular burst event as one of the primary, clonal mutations in translocation-driven sarcomagenesis.

1.5.3 The relationship between neoangiogenesis and the tumour immune microenvironment

As previously mentioned, the growth of tumour cells requires the formation of an expanding network of blood vessels to provide sufficient oxygen and nutrients for growth, and to remove waste products of metabolism. In health, aside from

following trauma and in the female reproductive cycle, normal vasculature is largely quiescent. However, during tumour progression, an angiogenic switch is almost always activated and remains active to help sustain growing occult tumours[74].

1.5.3.1 The impact of elevated angiogenic factors on anti-tumour immune responses

The interplay between the host immune system and angiogenesis is complex, as a number of cells of the immune system display versatility in their effect on blood vessel formation[262]. In addition, increases in levels of pro-angiogenic factors including VEGF, PDGFR and FGFR, as well as cytokines such as TGF-β, in the tumour microenvironment contribute to polarization of immune cells towards a pro-tumour and pro-angiogenic phenotype[263].

Macrophages are thought to play a key role in orchestrating the immune systems influence of tumour angiogenesis. Macrophages are recruited from the peripheral circulation by angiogenic growth factors, including VEGF, and chemokines, such as CCL2, which are present in the tumour microenvironment. Furthermore, macrophages are then able to produce additional CCL2, recruiting further macrophages to the microenvironment[264]. Macrophages typically undergo activation to a polarized state dependant on the surrounding environment and are considered to polarize to;

- M1 macrophages associated with high quantities of pro-inflammatory cytokines, mediating pathogen and tumour cell killing. They are typically associated with high levels of IL-23 and IL-12 and help drive Th1 and T-helper 17 (Th17) cell pro-immunogenic responses.
- M2 macrophages associated with a more anti-inflammatory phenotype and are associated with high levels of IL-10 which acts to promote Th2 cells and their anti-immunogenic profile[265].

Tumour-associated macrophages (TAMs) themselves display plasticity, responding to stimuli within the tumour microenvironment and behaving along the spectrum of M1- and M2-like phenotypes[266]. However, hypoxia-primed cancer

cells tend to polarize TAMs to a pro-angiogenic M2-like state via eotaxin and oncostatin M[267]. In this state, M2-like TAMs secrete a number of pro-angiogenic factors, including growth factors such as VEGF, PDGF, FGF, and EGF, angiogenic CXC-family chemokines, and other immune inhibitory cytokines, such as TGF-β. In addition, release of matrix metalloproteases act to degrade components of the extracellular matrix and basement membrane, leading to destabilisation of the vasculature and facilitating sprouting of new blood vessels[263]. Within the tumour microenvironment, the interplay between various aspects of the immune system is complex, driven by a number of cytokines and cellular interactions (**Figure 1.5**).

In addition to macrophages, DCs are another cell of the innate immune system which undergoes polarization to an immunosuppressive subtype driven by tumour cell signalling and hypoxia-induced factors. In health, mature DCs act as key antigen presenting cells, taking in foreign antigen and then presenting the captured antigen in the form of peptide-MHC complexes to T-cells. Upon interaction with DCs, naïve CD4+ cells can differentiate into Th1, Th2, Th17 or follicular T-helper cells, with their main function being communication with B-cells to differentiate into specific antibody-secreting cells. Whilst naïve CD8+ T-cells frequently give rise to effector cytotoxic T-cells[268]. In relation to cancerous cells, DCs have the ability to capture tumour neoantigens and present them to T-cells, either through the capture of antigen following apoptosis or through 'nibbling' of live tumour cells[269]. However, in order to evade anti-tumour immune responses, tumours are able to preferentially recruit and maintain DCs in their immature state through high levels of TGF-β and, via the receptor neurolipin-1, VEGF[270,271]. In this immature state, DCs predominantly act to stimulate and encourage proliferation of Treg cells which act to inhibit cytotoxic cells. The suppression of effector T-cell responses and proliferation of Tregs to enforce their immunosuppressive actions tends to be an indirect result of the effects of angiogenic factors on cells of the innate immune system. However, some recent studies have demonstrated that sub-populations of Tregs in cancer express VEGFR2, and therefore are able to undergo VEGF-A-dependent proliferation[272]. In addition, evidence suggests that VEGF-A present in the tumour

microenvironment enhances the expression of the inhibitory molecules PD-1, CTLA-4 and LAG3 on VEGFR-expressing intratumoural CD8+ T-cells[273].

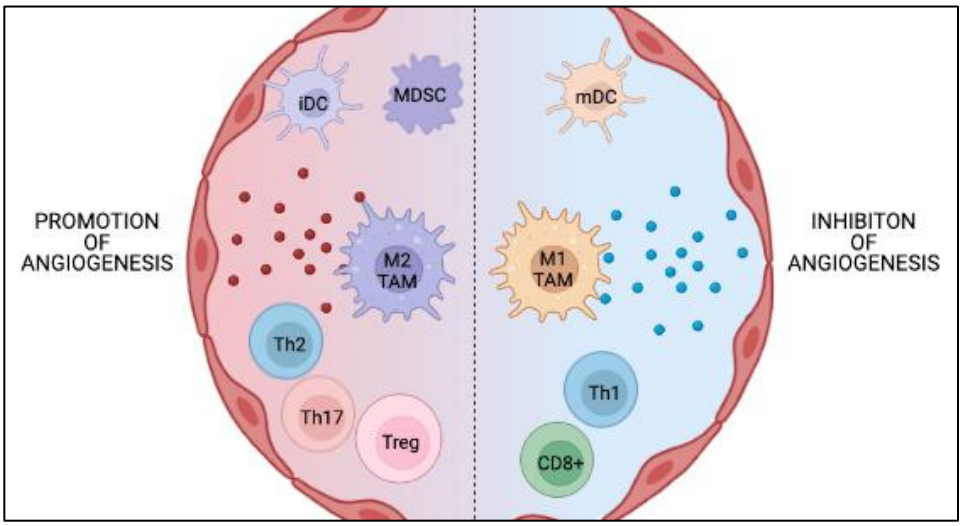

Figure 1.5: Interplay between pro and anti-angiogenic immune factors. M2-type tumour-associated macrophages (TMAs), immature dendritic cells (iDC) and myeloid derived suppressor cells (MDSC), secrete pro-angiogenic cytokines including VEGF, IL-10 and matrix metalloproteases 1,2 ,3, 9 and 12, whilst Th2, Th17 and Tregs secrete VEGF and interleukins to stimulate angiogenesis. In terms of inhibitors of angiogenesis, M1 polarized macrophages and mature dendritic cells produce cytokines including TNFα, IL-12 and tumour necrosis factor (TNF) and chemokines, such as CCL21, which act to suppress angiogenesis. In addition, MDSCs and Tregs can interact with TAMs and promote polarization towards the M2-like phenotype. Figure generated in Biorender based upon information in the literature[266].

1.5.3.2 Abnormal tumour vasculature facilitates immune suppression in the tumour microenvironment

The process of neoangiogenesis in tumours is typically reliant on sprouting from pre-existing blood vessels promoted by the imbalance of pro- and anti-angiogenic factors as discussed above. The abundance of these pro-angiogenic signals leads to chaotic blood vessel formation, and relative to normal vasculature, the neovasculature supplying tumour beds is characterised by slow and irregular blood flow, variable and often oversized luminal diameters, erratic and tortuous branching, high compression levels due to raised interstitial pressure, and the basement membrane may be lacking or unusually thick[274]. This immature and chaotic network of blood vessels generates a hypoxic and acidic tumour microenvironment, and in itself also contributes to suppression of the antitumour immune response.

In order to mount an anti-tumour immune response, effector cells of the host immune system must pass from the circulation into the microenvironment through the endothelium of adjacent blood vessels. However, the endothelial cells (ECs) of tumour neovasculature act themselves as a barrier for this influx of anti-tumour effectors. For example, the high levels of VEGF in the vicinity of tumour vasculature has been shown to induce defects in intercellular adhesion molecule-12 and vascular cell adhesion protein-1 clustering at the EC surface[275]. This leads to dramatic inhibition of lymphocyte adhesion on activated ECs and acts as a physical barrier preventing the influx of immune cells into the tumour microenvironment. In addition, high levels of VEGF, IL-10 and prostaglandin E_2 in the tumour microenvironment induce the expression of Fas ligands on the ECs of tumour vasculature, which upon binding of Fas expressed on T-cells leads to immune cell apoptosis[276]. Furthermore, this T-cell killing was predominantly of effector CD8+ T-cells, whilst Treg cells were preserved due to higher levels of c-FLIP cell surface expression. Finally, another study demonstrated that tumour-related ECs showed increased expression of stabilin-1, which acts to support T-cell transendothelial migration but with strong preferential activity of Treg cells[277]. As such, this suggests that the endothelial cells themselves are supporting the generation of an immunosuppressive environment through being less penetrable

to immune cells, and via the preferential transport of immunomodulating Treg cells in the tumour microenvironment at the expense of CD8+ effector T-cells.

1.5.4 The immune microenvironment as a source for prognostic and predictive biomarkers in sarcoma

Relative to other more common solid tumours, the immune microenvironment STS remains incompletely characterised and immune influences on prognosis and treatment responses are lacking. More recent efforts have gone some way to address this with a number of studies looking at the prognostic impact of immune cell numbers quantified by IHC. In addition, the emerging potential for gene-signature based immune subgroups to stratify patients has been explored in STS. However, there is little in the way of immune-based biomarkers predictive of response to pazopanib and other anti-angiogenic therapies.

1.5.4.1 Tumour infiltrating immune cells and checkpoint inhibitors as soft tissue sarcoma biomarkers

A number of relatively small variable STS subtype studies have been published exploring the potential for quantification by IHC of tumour infiltrating to act as a prognostic tool. The largest of these was published by Dancsok et al., in which they generated formalin-fixed, paraffin-embedded (FFPE) tissue microarrays (TMAs) containing tissue from 1072 STS samples covering 22 different subtypes, with complete matched clinical and outcome data available for 660 (61.6%)[278]. IHC assessment was carried out on serial TMA sections, with sections stained for CD4, CD8, CD56, FOXP3, PD-1, LAG3 and T-cell immunoglobulin domain and mucin domain (TIM)-3. Of the 660 specimens with matched data, all were primary surgical resections, and 58% (380 patients) were treatment-naïve. As translocation-associated sarcomas are believed to have a lower mutational burden and be less immunogenic, the authors looked to compare translocation and non-translocation driven sarcomas. Upon multivariate analysis, non-translocation-associated sarcomas had significantly increased tumour infiltrating lymphocytes (TILs) ($p=0.002$), with increased CD8+ ($p=0.03$) and CD4+ ($p<0.001$) tumour-infiltrating lymphocytes. To explore the prognostic role of

immune cell IHC, multivariate Cox proportional hazards modelling was undertaken, taking into account age, grade and diagnosis, and among the non-translocation-associated sarcomas, increasing lymphocytic infiltration was significantly associated with marginally superior OS (HR 0.996, 95% CI 0.992-0.999; p=0.02) and PFS (HR 0.996, 95% CI 0.992-0.999; p=0.012). In addition, increasing CD56+ TILs (HR 1.059, 95% CI 1.005-1.116; p=0.032) and PD-1+ TILs (HR 1.047, 95% CI 1.001-1.096; p=0.046) were associated with a significantly inferior on OS, but no difference in PFS. It should be noted however, that CD56+ TILs were rare across the entire sample set, as such it may be a few tumours that did attract NK cells were a particularly aggressive subset of STS. In separate survival analysis of the translocation-associated sarcoma subgroup, no significant associations between TILs nor immune checkpoint expression and OS or PFS were reported. Taken in isolation this study suggests that, at least in non-translocation-associated sarcomas, given the association between both higher levels of CD8+ and lower levels of PD-1 and improved OS, that a tumour microenvironment which is conducive to anti-tumour immune activity correlates with a positive prognosis. Indeed a number of additional IHC-based studies have explored the relationship between levels of TILs, PD-1/PD-L1 expression and clinical outcome (**Table 1.7**). The results of these individual studies are somewhat difficult to interpret in a combined fashion given the variable histological subtypes included, combination of primary, metastatic and recurrent lesions, and variable exposure to prior treatments. Furthermore, despite the numerous studies often exploring multiple immune cells of interest, the majority showed no significant association with immune cell infiltration and clinical outcome. Of note, all of these studies were aiming to define prognostic biomarkers, and none were designed to explore the role of immune cell infiltrate to predict response to specific therapy.

Regarding expression of the immune checkpoint molecule PD-L1, given recent advances in anti-PD-L1 therapies, more studies have explored this expression in STS, and subsequently a recently published systematic review was undertaken by Wang et al., to comprehensively review the role of PD-L1 expression as a prognostic biomarker in bone and soft tissue sarcoma. In total, 31 publications were included to assess the prognostic significance of PD-L1 expression, with 30

containing sufficient data to allow pooled HR quantification for OS. Of note, 11 of the articles were related to osteosarcoma, and 2 to chondrosarcoma, with the remainder made up of STS subtypes. Across the studies, PD-L1 expression was quantified by either IHC, quantitative polymerase chain reaction or RNA sequencing. A random-effect model was utilised for analysis, and showed that elevated PD-L1 expression was significantly correlated with poor OS (HR 1.445, 95% CI 1.11-1.90; $p<0.001$), with neither sarcoma subtype nor assay method responsible for the observed effect. In addition, elevated PD-L1 expression also predicted poor metastasis-free survival and event-free survival. These results appear to confirm that given the activity of elevated PD-L1 to create an immunosuppressive environment, that patients with STS considered immune "hot" have superior clinical outcomes.

Table 1.7: Select trials assessing the prognostic effect of tumour infiltrating immune cells by immunohistochemistry analysis, with or without immune checkpoint analysis. ARMS – alveolar rhabdomyosarcoma; AYA – children, adolescent and young adult; CS – chondrosarcoma; DFS – disease free survival; DSS – disease specific survival; LMS – leiomyosarcoma; MFS – metastasis free survival; MPNST – malignant peripheral nerve sheath tumour; OS – overall survival; PFS – progression free survival; RFS – recurrence free survival; SS – synovial sarcoma; TC – tumour cell; TMA – tissue microarray; UPS – undifferentiated pleomorphic sarcoma.[279,280,289,281–288]

Study	N	Subtypes	Methods	T-cell markers	Prognostic association with high immune cells	Immune checkpoint markers	Prognostic association with high checkpoint markers
Boxberg et al., 2017	37	Primary UPS	TMA	CD3, CD8	CD3+ and CD8+ : improved OS and DFS	PD-1, PD-L1, PD-L2	TC PD-L1 : improved OS and DFS
Shurell et al., 2016	35	Primary MPNST	TMA	CD8	No association	PD-L1	No association
van Erp et al., 2017	208	Primary mixed-subtype AYA sarcomas	TMA and sections	CD8	CD8+ : worse MFS in SS	PD-1, PD-L1	PD-L1 : improved OS in ARMS
Simard et al., 2016	26	Primary conventional CS	Sections	CD3, CD4, CD8, CD163	CD3+, CD4+, CD8+ : improved OS		
D'Angelo et al., 2015	50	Primary mixed subtype	Sections	CD3, CD4, CD8, FOXP3	CD3+, CD4+ : worse OS	PD-1, PD-L1	No association
Nowicki et al., 2017	29	Mixed-time point SS	Sections	CD8	No association	PD-1, PD-L1	PD-1 at invasive margin - worse PFS
Kostine et al., 2018	100	Mixed-time point LMS	Sections	CD3, CD163	CD163+ : worse OS and DSS	PD-L1, PD-L2	No association
Sorbye et al., 2012	80	Primary mixed subtype	TMA	Peritumoural CD3, CD4, CD8, CD20	Peritumoural CD20 - worse DSS		
Oike et al., 2018	36	Primary SS	Sections	CD4, CD8, FOXP3, CD163	CD163+ : worse OS and PFS	PD-L1, PD-L2	No association
Smolle et al., 2021	192	Primary mixed subtype	TMA	CD3, CD4, CD8, FOXP3	FOXP3+ : worse RFS	PD-1, PD-L1	No association
Sorbye et al., 2011	249	Primary mixed subtype	TMA	CD3, CD4, CD8, CD20, CD45	CD20+ - improved DSS CD3+ worse DSS in none-wide resection margin		

1.5.4.2 Emerging potential for immune subtypes as a biomarker

Moving forward from individual immune cells and markers as biomarkers in STS, there is a growing body of evidence exploring the potential for immune gene based signatures as a source of biomarkers in STS, and to further our understanding of STS biology and therapeutic responses. The Cancer Genome Atlas (TCGA) 2017 publication is one such comprehensive body of work which included immune-based analysis[290]. A total of 206 sarcomas were included for analysis and included five subtypes of interest, but was predominantly made up of LMS, DDLPS and UPS. The authors report that generally, adult STS harbour frequent copy number alterations, but have a relatively low mutational burden when compared to other solid tumours. From the pan-sarcoma RNA analysis, 206 of the 2038 most variably expressed genes were considered immune-related and/or inflammatory-related. When assessing these differentially expressed genes, immune-related ontologies significantly upregulated included inflammatory responses, positive regulation of immune system processes, regulation of lymphocytes, cell and leukocyte activation and chemotaxis. The authors then assigned each sample an immune infiltration score for various immune cells of interest based upon the gene expression data. Unsupervised clustering identified three distinct clusters, with a subset of DDLPS, UPS, LMS and myxofibrosarcoma (MFS) reported to have high immune infiltrates. The authors then compared disease specific survival (DSS) with tumours in the top third versus the bottom third based on immune infiltrate scores. Of note, a higher NK cell infiltration score was significantly associated with improved DSS across different sarcoma subtypes, whilst a higher CD8+ infiltration score was associated with better survival in uterine LMS, and higher DC infiltration scores were associated with superior DSS in the UPS/MFS subgroup. Conversely, higher Th2 infiltration scores were associated with poorer DSS in DDLPS. These findings suggest that a pro-immune microenvironment are generally associated with better survival. However, this work was based on primary tumour samples only, and no treatment effect was considered in the analysis. As such, although these findings might be useful in prognostication for patients with STS, potentially highlighting patients who would most benefit from more aggressive therapy, they

are not predictive of response to specific therapies. This work does however highlight the value of exploring immune gene expression analysis to add granularity to immune subtyping.

In addition to the above study, a number of more recent studies have also utilised the TCGA STS dataset to generate immune-based prognostic signatures. The first of these reported by Hu et al., identified differentially expressed immune related genes when comparing the data from 259 tumour tissues from the TCGA STS dataset with RNA sequencing data obtained from 911 non-diseased muscle and adipose tissue samples from the Genotype-Tissue Expression dataset[291]. A total of 364 differentially expressed immune related genes were identified, and based upon consensus clustering the cohort of 259 STS samples was separated into 4 clusters. Interestingly, the C3 cluster was significantly associated with worse OS relative to the remainder of the cohort, and was noted to be enriched for immune checkpoints and had the lowest immune scores of the four clusters. The study subsequently generated a prognostic predictor score based upon the weighted expression of 11 immune-related genes. Again, as the tissue samples are primary tumours and treatment was not taken into consideration, this risk score is prognostic in nature as opposed to being predictive in nature. However, this study represents further evidence of the value of exploring immune-related gene expression to elucidate potentially meaningful signatures in STS. An additional study reported by Shen et al. adopted a slightly different methodology to develop an immune-based prognostic signature[292]. Clinical and RNA sequencing data was obtained from the TGCA dataset, and the samples were randomly allocated to either the training set (170 of 255 included samples) or the validation set (85 of 255 samples). From the immune related gene set covering 2498 genes, univariate cox proportional hazard modelling selected 105 genes to be related to OS, with further analysis generating a 19 gene signature which was able to stratify patients into high and low risk in the training set, and this result replicated in the validation set. Interestingly, utilising the CIBERSORT package, the study found that the infiltration level of resting and activated NK cells, monocytes and pro-immune M1 macrophages were all significantly higher in the low risk group. As previously discussed, these are all primary samples and

therefore as a prognostic signature the utility of the derived nomogram would be in the pre-treatment setting to stratify patients most at risk of adverse outcomes. In addition, although the risk score was validated, both the training and validation set are effectively from the same cohort and an external validation utilising an independent cohort would be necessary to prove replicability.

Although the articles discussed above all focused solely on generating prognostic signatures based upon the TCGA cohort, a recent paper from Petitprez et al. includes additional cohorts to derive immune signatures, and then applied these to a real world cohort to demonstrate the signature's utility as a predictor or clinical response to immune checkpoint blockade[293]. In order to generate an immune-based classification of STS, the publicly available gene expression data from the TCGA (n=213) dataset as well as from Gene Expression Omnibus (GEO) accessions GSE21050 (n=283), GSE21122 (n=72) and GSE30929 (n=40) were analysed for a total discovery cohort of 608 samples. From this cohort, 5 sarcoma immune classes (SIC) A-E were identified with significantly variable immune microenvironments described. Of note, 3 SICs showed homogenous profiles; SIC A being characterised as having the lowest expression of immune cell gene signatures and considered an 'immune desert', SIC C being dominated by high expression of endothelial cell genes and considered 'vascularised', and SIC E which was categorised as 'immune and tertiary lymphoid structure (TLS) high' and demonstrated the highest expression of T cells, NK cells, CD8+ cells and most differentially high expression of B lineage signature. Utilising the two cohorts for which survival data was available, namely the TCGA cohort and GSE21050 (496 patients), the authors reported that the 'immune desert' SIC A cohort exhibited the shortest overall survival, with significantly poorer outcomes when compared to SIC D and E (p=0.048 and 0.025 respectively). The validity of these molecular SIC profiles were confirmed by IHC in an independent cohort of 73 samples from the National Taiwan University Hospital. Characterisation of these immune subgroups identified that the 'immune desert' SIC A was observed to have very low densities of CD3+, CD8+ and CD20+ TILs, whereas SIC E tumours had significantly higher densities of these cells. Finally, the authors obtained 47 pre-treatment metastatic samples

from the SARC028 phase II clinical trial of the anti-PD1 antibody pembrolizumab in patients with advanced STS (NCT02301039)[294]. These pre-treatment tumour samples were classified into SICs based upon gene expression data, and it was observed that SIC E tumours were associated with the highest response rate to pembrolizumab relative to other SIC groups, and exhibited significantly improved PFS compared to SIC A and B tumours. As such, this study added value to the exploration of the immune contexture as a potential biomarker for response. Relative to the previously discussed studies in this section, inclusion of data from the GEO created a larger discovery cohort from which the subgroups were generated. In addition, inclusion of the independent cohort from Taiwan and IHC data goes some way to validate the gene expression based classifications. And as well as demonstrating the prognostic impact of the immune classifications, with the immune cold SIC A having the worst outcome, the study was also able to demonstrate the SIC classification was able to predict response to pembrolizumab, with the immune hot SIC E patients gaining the most benefit.

1.5.4.3 Evidence exists confirming immune-modulatory effect of tyrosine kinase inhibitors, including pazopanib

Given the evidence presented previously (**section 1.5.2)** which demonstrates a complex but interwoven relationship between angiogenic factors and host immune responses, there is a rationale to explore the potential for anti-angiogenic therapies to confer off-target immunomodulating effects as part of their mechanism of action. Indeed, a number of pre-clinical studies have demonstrated immunological effects of anti-angiogenic TKIs (including pazopanib), and although there is a paucity of clinical studies in STS patients treated with pazopanib, a number of studies exist from cohorts of RCC patients.

1.5.4.3.1 Pre-clinical evidence of immune modulating effects of anti-VEGF TKIs

Zizzari et al. undertook *in vitro* work exploring the impact of pazopanib on a number of immune cells and demonstrated activity which acts to promote anti-tumour immunity[295]. Human monocyte derived DCs were obtained from the blood

of healthy donors, and these cells were cultured in the presence of pazopanib. Relative to untreated controls, pazopanib led to a significant increases in both immature and mature DC activation, evidenced by increased expression of HLA-DR and CD40 by immature DCs, and increased expression of CCR7 and CD40 by mature DCs. In addition, during the activation of immature DCs, exposure to pazopanib resulted in a decrease in PD-L1 expression compared to untreated DCs. And finally, treatment with pazopanib significantly reduced the production of IL-10 by DCs which favours immune activation. The pro-immunogenic impact of these changes was then confirmed, as DCs differentiated in the presence of pazopanib had a greater capacity to stimulate T-cells when compared with untreated DCs and DCs which underwent differentiation in the presence of an alternate anti-angiogenic therapy sunitinib. As such, this work suggests that as well as the anti-angiogenic RTK activity, pazopanib also exerts an effect on the immune contexture creating an environment which promotes anti-tumour immunity through the activation of DCs and subsequent stimulation of effector T-cells.

Further pazopanib-specific *in vitro* work is limited, however alternative anti-VGEF therapies have also been shown to modulate immune cell differentiation. For example, the anti-VGEF TKI sunitinib has been shown *in vitro* to increase the population of IFN-γ producing cells leading to diminished Treg function, whilst the peripheral blood from 28 patients with metastatic RCC treated with sunitinib demonstrated a reduction in the number of Treg cells which was also associated with improved OS[296,297]. Sorafenib, another multi-target TKI with anti-VGEF activity, has also demonstrated similar off-target immunomodulating effects, with *in vivo* mouse models of hepatocellular carcinoma demonstrating that sorafenib induces a reversal of the accumulation of immune suppressive MDSCs and Tregs as well as decreasing the proportion of PD-1 expressing cytotoxic CD8+ T-cells[298,299]. Indeed, blood taken before and after sorafenib therapy from 30 patients with advanced hepatocellular carcinoma demonstrated a sustained reduction in circulating Tregs and MDSCs as well as enhancement of IFN-γ producing effector CD4+ and CD8+ T-cells which was seen to correlate with improved survival[300]. Finally, assessment of the immune microenvironment in

tumour-bearing mice treated with the anti-VEGF TKI axitinib, demonstrated an increase in the number of CD8+ T-cells, and via downregulation of STAT3 expression, a reduction in the number of MDSCs[301,302]. As such, although pre-clinical this evidence from a number of TKIs targeting the VEGF axis suggests that there is off-target immune modulating effects which acts to diminish immune suppressive cells and create a microenvironment which is conducive to anti-tumour immune activity.

1.5.4.3.2 Clinical evidence of the immune modulating impact of pazopanib

Given the rarity of STS, there is minimal evidence exploring the impact of the immune microenvironment in STS and changes to the immune microenvironment following pazopanib therapy. As such, to gain some potential insights in the immune modulating effects of pazopanib in the clinical setting, we are reliant on studies involving patients with RCC who have received pazopanib as part of their management.

Looking solely at serial peripheral blood samples taken from 21 patients with metastatic RCC treated with pazopanib, Khurana et al. reported that pazopanib led to a significant increase over time in the proportion of IFN-γ producing effector T-cells present in the peripheral blood mononuclear cells collected[303]. Although no changes were reported in various subsets of MDSCs, the increase in effector T-cells provides initial evidence of an *in vivo* shift promoting anti-tumour immunity. In addition, Rinchai et al. recently published their transcriptional analysis of serial blood samples at baseline and 3 and 6 months following treatment initiation in 8 patients with metastatic RCC treated with pazopanib as the first-line agent[304]. As with Khurana et al., the predominantly differentially upregulated genes from pre- to post-treatment blood samples were associated with cytotoxic functionality and IFN signalling, consistent with an increase in the activity of NK cells and effector T-cells. Of note, although attenuated, these changes were consistent at both 3 and 6 months following treatment initiation. Further analysis comparing baseline and post-treatment samples by single sample Gene Set Enrichment Analysis (ssGSEA) demonstrated enriched scores for NK^{dim}, NK cells, cytotoxic cells, CD8+ cells and γδT-cells, whilst Tregs and

MDSCs showed diminished expression scores. These results again suggest that administration of pazopanib induces synergistic modulation of the immune system, enhancing anti-tumour immunity whilst diminishing cells associated with suppressive mechanisms. However, both of these studies are in small patient populations with no confirmatory external validation reported, and it should be noted that analysing populations of peripherally circulating immune cells may not reflect the tumour microenvironment effectively.

1.5.4.4 Evidence supporting an association between baseline tumour immune microenvironment and response-benefit to pazopanib

In addition to modulating the tumour immune microenvironment, there is a body of evidence that baseline immune contexture is associated with variable responses to pazopanib. Although robust immune-based biomarkers predictive of pazopanib response in patients with STS are lacking, these reports are suggestive of a mechanistic link between the immune microenvironment and response benefit.

1.5.4.4.1 Immunohistochemistry of PD-L1

Given the role PD-L1 has in acting as an immune checkpoint, and dampening anti-tumour immune responses, there is rationale for investigating levels of expression as an indicator for the immune contexture. A previous study undertook retrospective analysis of pre-treatment tumour tissue of a cohort of patients with unresectable or metastatic STS who went on to receive pazopanib therapy[305]. In a cohort of 67 patients, they performed PD-L1 IHC staining, as well as scoring the number of TILs, quantified by counting the number of mononuclear cells (excluding neutrophils) in each tumour specimen. Of the 67 patients, 13 (19.4%) stained positively for PD-L1, and survival analysis showed a significantly inferior PFS in the PD-L1 positive strata compared to the PD-L1 negative (median PFS 2.8 months versus 5.0 months; $p = 0.003$) and a non-significant inferior OS (median PFS 7.9 months versus 12.6 months; $p= 0.11$). Indeed, multivariable Cox regression analysis demonstrated that only PD-L1 status was an independent factor for determining inferior response to pazopanib after adjusting

for confounding variables. Interestingly, in additional analysis PD-L1 and TIL status were combined to form three strata namely PD-L1 and TIL positive, PD-L1 and TIL negative, and either PD-L1 or TIL negative. The study then identified that specimens classified as both PD-L1 and TIL positive were significantly associated with the shortest PFS when compared with specimens classed as PD-L1 and TIL negative, or either PD-L1 or TIL negative (median PFS 2.7 months, 5.1 months and 4.3 months respectively; p = 0.035). This would suggest that an immune-cold microenvironment is associated with inferior clinical response to pazopanib treatment.

Further evidence of an association between baseline tumour immune features and pazopanib response in STS is limited, however two additional studies have reported a similar observation where increased pre-treatment PD-L1 expression is associated with an inferior clinical response to other anti-VEGF therapies. The first of these studies leveraged on clinical samples obtained from the phase III COMPRAZ trial of first-line pazopanib versus sunitinib in metastatic renal cell carcinoma (NCT 00720941)[306,307]. Of the 1,110 patients enrolled onto the trial, IHC data for PD-L1 and intra-tumoural CD8+ TILs was available for 453 patients. Combining the number of tumour cells staining positively for PD-L1 and the intensity of this staining, the authors generated a semi-quantitative score and reported an association between higher PD-L1 scores (greater than 55) and inferior OS in the pazopanib cohort (median OS 15.1 months versus 35.6 months). Furthermore, when additionally considering the intra-tumoural CD8+ T-cell count, specimens with a PD-L1 score of greater than 55 and a CD8+ TIL count of greater than 300 were associated with the shortest OS when compared with PD-L1 high and TIL low, and PD-L1 low cases (median OS 9.6 months).

A similar but smaller study also investigated PD-L1 expression in metastatic renal cell carcinoma, also undertaking IHC analysis of pre-treatment samples in patients who went on to receive anti-VEGF TKI therapy[308]. Pre-treatment tissue was available for 91 patients, with 16 (17.6%) specimens identified as being PD-L1 positive. As with the above studies, PD-L1 positivity was significantly associated with an inferior response rate to anti-VEGF TKI therapy, with 87.5% of PD-L1 positive cases being non-responders compared to 53.3% in the PD-L1

negative cases (p = 0.012). Of note, this study only included 3 patients treated with pazopanib, with the majority being treated with sunitinib, and a further cohort treated with sorafenib. Although a smaller study, in conjunction with the abovementioned studies, there is evidence that the pre-treatment immune contexture impacts subsequent treatment response upon initiation of anti-VEGF TKI therapy.

1.5.4.4.2 Gene expression based immune subtypes

In addition to IHC based studies of the immune checkpoint PD-L1, additional work exists investigating pre-treatment gene expression-based immune subtypes and the impact these may have on response benefit to pazopanib and other anti-VEGF TKIs. Although specific studies exploring the potential for gene-based immune scores predictive of anti-VEGF TKIs in STS are limited, the associations identified in other tumour types do suggest a mechanistic role the immune microenvironment may play in clinical responses to pazopanib and other anti-VEGF TKIs.

The first example is drawn from a study where transcriptomic profiles of pre-treatment FFPE tissue samples obtained from patients with metastatic clear cell RCC who were subsequently treated with first-line pazopanib versus sunitinib as part of the phase III COMPRAZ trial (NCT00720941) were analysed[307,309]. The translational study included a total of 409 patients of which 212 received sunitinib and the remaining 197 pazopanib, and identified 4 clusters of patients based on gene expression data. Survival analysis identified cluster 4 as having the poorest OS and PFS, and subsequent analysis of immune related gene expression categorised this cluster as having the highest immune score using the estimation of stromal immune cells in malignant tumours using expression data (ESTIMATE) method[310]. In addition, cluster 4 also had a significantly higher tumour cell PD-L1 expression (60% vs 34%, p<0.001). Immune deconvolution via ssGSEA demonstrated that macrophages were the most differentially enriched cell type, with higher macrophage scores in cluster 4 compared to clusters 1-3, and when assessing the whole cohort irrespective of cluster, patients with high immunosuppressive M2 macrophage infiltration had worse OS. Of note, when

assessing the cohorts by TKI received, only in the pazopanib treated group was having a high level of macrophage infiltration associated with inferior OS and PFS. Although one of the limitations of this study is the lumping together of sunitinib and pazopanib treated patients, it represents one of the few studies which has characterised pre-treatment immune gene signatures and their relation to response to pazopanib. Given the fact the study was in clear cell RCC, there is evidence here to support the rationale for investigating the immune microenvironment in STS will not only shed light on the biology of STS but may be fruitful in the pursuit of biomarkers for pazopanib response.

Also of interest is the work reported by Beuselinck et al., who developed a molecular classifier for metastatic clear cell RCC predictive of response to the anti-VEGF TKI sunitinib[311]. A total of 121 patients were retrospectively identified who had undergone nephrectomy, had developed synchronous or metachronic metastases and had received sunitinib as first-line chemotherapy. The pre-TKI tissue was then interrogated via a multi-omic pipeline including genomic and transcriptomic analyses. Unsupervised consensus clustering identified four robust subgroups of tumours, named ccrcc 1-4, with distinct immune profiles and variable response to sunitinib. Indeed, pre-treatment specimens classified as ccrcc1 and ccrcc4 were associated with significantly inferior PFS when compared to ccrcc2 and ccrcc3 (13, 8, 19 and 24 months respectively; $p = 0.0003$) and significantly inferior OS (24, 14, 35 and 50 months respectively; $p = 0.001$). Subsequent analyses demonstrated that ccrcc4 was characterised by high expression of markers of pro-immunogenic inflammation, and contained high amounts of B, T and cytotoxic cells-specific transcripts. However, ccrcc4 was also found to highly express immune suppressive IL-10, FOXP3+ regulatory T-cells, and the inhibitory receptors PD-1 and LAG3 and their cognate ligands. This study suggests of a link between the baseline immune microenvironment and patient benefit in response to the anti-VEGF TKI sunitinib.

The team then looked to investigate the utility of the same classifier in a retrospective cohort of patients treated with pazopanib[312]. A total of 28 patients who presented with clear cell RCC with synchronous or metachronous metastases and who were treated with pazopanib in the first-line setting were

included for analysis. Extracted ribonucleic acid (RNA) was analysed and the tumour classified into one of the four molecular subgroups based upon the 35-gene classifier previously determined. Due to the small number of patients classified as ccrcc3, these were pooled with the ccrcc2 samples, as both subgroups had previously been associated with improved response to sunitinib. Of the 28 patients, 6 (21%) were assigned to ccrcc1, 4 to ccrcc4 (14%) and the remaining 18 (60%) to the pooled ccrcc2&3 subgroup. Across the whole cohort median PFS was 7 months and median OS was 28 months, however both median PFS and OS were significantly different between subgroups. Median PFS was 9 months in ccrcc2&3 compared to 5 months for the ccrcc1 subgroup and 3 months for ccrcc4 (p=0.011), whilst ccrcc2&3 subgroup median OS was 69 months compared to 19 months for ccrcc1 patients and 5 months for ccrcc4 patients (p=0.003). Furthermore, mean change in tumour size was -34% in the ccrcc2&3 group, -6% in the ccrcc1 subgroup and -2% in the ccrcc4 subgroup.

Although retrospective and a relatively small cohort size, these results are promising and act to validate the robustness of the signature as previously demonstrated in the sunitinib-treated cohort. As a result of this work, a biomarker-driven phase II has recently completed recruitment, and follow-up is ongoing (NCT02960906)[313]. The study was designed to test the utility of the ccrcc classification to improve patient outcomes by assigning treatment based on classification. In the study, given the previous immune-based characterisation of ccrcc1 or 4, these patients were randomised to immune checkpoint inhibitor (ICI) monotherapy, nivolumab, or ICI combination therapy, nivolumab plus ipilimumab, whilst patients classed as ccrcc2 or 3 were randomised to receive either combination ICI therapy or to either pazopanib or sunitinib based upon clinician's choice. Provisional results with a median follow-up time of 16 months were presented at the European Society of Medical Oncology 2020 virtual congress, and interestingly for the ccrcc2 cohort, the median PFS for the immune checkpoint inhibitor arm was 10.4 months but was yet to be reached at 16 months of follow-up in the TKI arm[314]. The data regarding OS was not yet mature as there had only been 16% of necessary events at the time of the presentation. Although the full trial results are awaited, this is a very promising example of the

development of a molecular classification which is able to stratify patients and allow a more patient-specific treatment algorithm. Furthermore, given the link between immune contexture and response to anti-VEGF TKIs, it utilises this knowledge to target specific vulnerabilities in a patient's tumour. At present, no such work has been carried out in the field of sarcoma, but such an endeavour could prove equally promising, resulting in patients receiving the most optimal management for their tumour, but also potentially leading to the re-approval for pazopanib funding for STS via the NHS Cancer Drugs Fund.

1.5.5 Summary

In recent times there has been a growing appreciation of the importance of the role the immune system plays in the development of cancer, and great progress has been made harnessing the host immune system to improve outcomes in a number of solid tumours. For now, the immune microenvironment is incompletely characterised, but evidence exists that anti-angiogenic therapies have off-target immuno-modulating effects which reverse immune suppressive influences whilst empowering effector cells. As such, there is a rationale to further characterise the immune microenvironment in STS, and assess how the immune contexture may influence responses to anti-angiogenic TKIs.

1.6 Thesis overview

Soft tissue sarcomas are rare cancers of unmet clinical need, and the term STS covers a wide range of different histologies with vastly different behaviours and responses to therapies. Despite efforts within the STS community, across many subtypes anthracycline-based chemotherapy remains the first-line treatment of choice in the advanced setting. Upon failure of first-line treatment, patients have limited further-line therapies available and each subsequent line has diminishing returns in terms of tangible clinical benefit.

Encouragingly, the recent development of therapies which target the vulnerabilities harboured by cancers has shown promising results, and in certain cancer types these therapies have led to drastic improvements in outcomes for patients. The multi-target TKI pazopanib is one such targeted therapy, with activity demonstrated against VEGF, PDGFR and FGFR. Although showing promising results in early stage clinical trials, the PALETTE phase III study comparing pazopanib with placebo in non-adipocytic STS was disappointing, in that although a PFS benefit was shown, a lack of OS benefit has impacted cost-effectiveness analyses, and in the UK led to the withdrawal of funding via the NHS cancer drugs fund. Despite this, subsequent post-hoc analyses and additional studies have demonstrated that a proportion of patients with STS do derive robust and meaningful benefit from treatment with pazopanib. The clinical challenge however, is being able to identify which patients are most likely to gain benefit from treatment. Identification and validation of a biomarker which is predictive of response to pazopanib would not only benefit the individual patients by ensuring the correct individuals receives the most appropriate treatment, but may also improve the perceived benefit and thus ensure cost-effectiveness and therefore funding is made available once more.

In recent times, there has been a growing appreciation of the role the host immune system plays, not only in cancer development, but also as a tool in the armoury in the treatment of cancer. However, the immune microenvironment in STS is incompletely characterised, and there are gaps in the science community’s knowledge about the immune-based biology which may be driving

STS. Furthermore, it is known that the process of neoangiogenesis and the various signalling factors which drive this process are inexorably linked to creating an immune suppressive environment and hindering anti-tumour immune responses. As such, there is a rationale to explore the impact of the tumour immune microenvironment and how it may influence responses to therapies which target the mechanisms involved in driving neoangiogenesis.

1.6.1 Hypothesis

The overarching hypothesis of this thesis is that the characterisation of the tumour immune microenvironment in patients treated with pazopanib or alternate systemic therapies will identify if immune signatures are associated with clinical outcomes.

1.6.2 Aims

1. Generate the cohorts of patients required to explore the immune microenvironment in STS and undertake IHC of TILs to identify immune based profiles associated with clinical outcomes following pazopanib therapy
2. Undertake targeted gene expression analysis of immune related genes to characterise the immune microenvironment in STS, and identify any associations between STS subtype, tumour grade and patient age with differential immune gene expression
3. Build prognostic models incorporating an immune gene signature which is associated with differential survival in a pazopanib-treated cohort of patients

Chapter 2 - Materials and Methods

2.1 Study design and overall strategy

The overall study design was based on undertaking comprehensive profiling of the immune microenvironment of soft tissue sarcoma (STS) samples integrated with clinicopathological features and mature survival data. The research strategy involved profiling of formalin-fixed paraffin-embedded (FFPE) pre-treatment tissue samples in a combined cohort of patients treated with pazopanib utilising immunohistochemistry (IHC) of tumour infiltrating lymphocytes (TILs) and targeted immune gene sequencing through the nCounter immune profiling panel. Data generated were correlated with a well-annotated database of clinicopathological features and survival outcomes curated for this work. An in-depth analysis of this data was then undertaken to identify differential survival outcomes based on TIL counts determined via IHC, and distinct immune-gene based subgroups within the combined cohort. These immune subgroups were further analysed to describe differential immune-gene expression and contrasting enrichment of specific immune cells, to shed light on the immune-based biology of STS. Furthermore, the association between STS subtype, patient age, and tumour grade with immune-gene expression was assessed. Finally, survival models were built employing Cox proportional hazards regression modelling with the ultimate goal of generating a prognostic model which included information gleaned from immune-gene expression analysis.

In terms of the overall strategy, given the relative scarcity of patients meeting the criteria for inclusion, the quality and volume of tumour tissue available for analysis was limited and it was necessary to prioritise work packages. Indeed, a number of FFPE samples had been stored for a number of years leading to significant challenges associated with degradation of the ribonucleic acid (RNA). Furthermore, for some cases, only physically small biopsy samples were available. As such, the decision was made that extraction of RNA would be the priority, as the data yield from the targeted gene expression profile would be highest. In order to maximise the number of patients included, the degree of RNA degradation sometimes necessitated a number of RNA extractions. As such, some cases initially planned to be included for both gene sequencing and IHC

workflows had insufficient material for either tissue microarray (TMA) construction or single section staining for TILs. This was due to the exhaustion of the tissue blocks available for analysis and no further tissue samples available for inclusion.

2.2 Patient selection and cohort generation

2.2.1 Combined cohort

Sixty-five patients for inclusion in the combined cohort were identified either from the Royal Marsden (RM) or from external collaborators. For the RM patients, these were retrospectively identified from the prospectively-maintained Royal Marsden (RM) STS patient database. All patients who had received pazopanib as part of the management of their STS at the RM were assessed and screened for inclusion. To expand the number of patients available for inclusion, suitable cases were also obtained from collaborators at the Beaston West of Scotland Cancer Centre (Glasgow, Scotland) and the National Cancer Centre Singapore (Singapore). For inclusion in the study, both RM and external cases were screened for the following inclusion and exclusion criteria;

Inclusion criteria for the combined cohort

- Confirmed diagnosis of STS, as per contemporaneous histopathology record
- Received at least one dose of pazopanib in the treatment of advanced STS
- In absence of patient death, a minimum of 18 months follow-up from first dose of pazopanib
- Presence of metastatic disease and/or localised/locally recurrent disease not amenable to radical resection at time of pazopanib initiation, as per contemporaneous medical records
- Retrievable FFPE tumour material sampled prior to initiation of pazopanib
- Where recorded, Eastern Cooperative Oncology Group (ECOG) performance status ≤2

Exclusion criteria for the combined cohort

- Diagnosis of fibromatosis, desmoid tumour, lymphangiomatosis, GIST
- Insufficient period of documented follow-up

In cases identified from the RM, pre-treatment FFPE tumour material was requested from the archival tissue bank maintained at the RM. Baseline clinicopathological characteristics and survival data were collected via a retrospective review of contemporaneous electronic patient medical records held by the RM. For the purposes of outcome analysis overall survival (OS) was defined as the period of time from the date of the first dose of pazopanib until the date of death or the date of most recent evidence of survival if still alive at the time of data censoring. For progression-free survival (PFS), this was defined as the length of time from the date of the first dose of pazopanib until the date of progression as demonstrated on cross-sectional imaging and reported by a specialist radiologist using response evaluation criteria in solid tumours (RECIST).

For cases supplied by external collaborators, tissue blocks or curls were transferred from their centre to ours under a tissue transfer agreement. In order to comply with data transfer responsibilities, patients included from collaborators were assigned a study-specific code and all clinical data were obtained at the collaborating site by inputting it into a data template and transferring it in a pseudonymised format. All clinical data for the combined cohort was censored at 18 months.

2.2.2 Comparator cohort

The comparator cohort was designed to closely resemble the combined cohort, aside from the fact these patients had not received pazopanib as they were managed after the withdrawal of NHS funding for pazopanib. The comparator cohort (n=28) was assembled from patients managed at the RM with the same inclusion and exclusion criteria as the combined cohort apart from;

Inclusion criteria for comparator cohort

- Commenced 2nd line clinician's choice systemic treatment for advanced STS no earlier than April 2015 (after withdrawal of pazopanib availability through NHS Cancer Drugs Fund funding)

Exclusion criteria for comparator cohort

- Patients must never have received one or more doses of pazopanib

As such, the comparator cohort was designed to identify a cohort of patients who may have been suitable for pazopanib therapy, but this was unavailable due to the central decision to withdraw NHS funding. In order to identify these patients, the prospectively maintained RM STS database was searched for all patients who had received at least two lines of systemic therapy since April 2015. Patients with available pre-second line FFPE tissue were identified and tissue blocks were requested from the RM STS archival tissue bank. Clinical data were acquired from the RM electronic patient record system, with the definitions for OS and PFS the same for the combined cohort, but calculated from the date of the first dose of the alternative second-line systemic therapy used.

2.2.3 Power calculation

This study is a retrospective biomarker data study, as opposed to a prospective clinical trial, thus the conventional sample size methodology developed for prospective clinical studies was not applicable. The appropriate method for power calculation is based on the study population and modelled against their associated survival outcome. Using the Riley *et al*[315,316]. sample size calculator methodology, based on the observed clinical data of the combined cohort (n = 65) in this study, it was indicated as follows:

(i) Overall survival:

To develop a prediction model for overall survival probability at 18 months that minimised overfitting and allowed up to 8 parameters*, with a median follow-up of 0.60 in years, a sample size of 540 patients will be needed assuming an outcome event rate of 0.914 corresponding to 324 person-time of follow-up with 297 outcome events.

A sample size of 68 patients is needed to develop a model with 1 parameter** assuming an outcome event rate of 0.914, corresponding to 40.8 person-time of follow-up with 38 outcome events.

(ii) Progression-free survival:

To develop a prediction model for progression-free survival probability at 18 months that minimised overfitting and allowed up to 8 parameters*, with a median follow-up of 0.60 in years, a sample size of 515 patients will be needed assuming an outcome event rate of 1.731 corresponding to 309 person-time of follow-up with 535 outcome events.

A sample size of 65 patients is needed to develop a model with 1 parameter** assuming an outcome event rate of 1.731, corresponding to 39 person-time of follow-up with 64 outcome events.

*8 parameters = gene signature (1 parameter, continuous variable) + Age (1 parameter, continuous variable) + performance status (3 parameters, categorical variable – 4 level) + grade (3 parameters, categorical variable – 4 level)

*1 parameter = gene signature (1 parameter, continuous variable)

It will be extremely challenging to assemble a cohort of hundreds of pre-treatment sarcoma samples exposed to the same therapy, however, as it will be of interest to adjust for confounding factors, we took a pragmatic approach to estimate the clinical value of a biomarker of interest in both univariable and multi-variable analyses. Within chapter 5, the aim was to determine the potential clinical applicability of an immune signature as a predictor for patient survival, therefore the strategy was to first determine whether there is a consistent association of increased or reduced survival risk within the training and validation cohort. Given the small sample size, if there is a consistent direction of signal, this would suggest the immune biomarker could be a useful marker. Then the final survival models of the immune biomarker with other clinicopathological variables would be estimated in the combined cohort of 65 patients.

2.3 Tissue processing procedures

2.3.1 Sample processing

All blocks received from the RM archival tissue bank were formally logged onto FreezerPro, (Azenta Life Sciences, Massachusetts, USA) a laboratory information management system in order to comply with legislation laid out in the Humans Tissue Act 2004 and to allow tracking of samples. Each individual patient for which tissue was received was allocated a laboratory-specific 5-digit identifier, and each FFPE block and histopathology slide assigned a laboratory-specific code. Following receipt of the FFPE block within the lab, a single haematoxylin and eosin (H&E) slide was then generated. The slide was then marked to show which areas of the section harboured tumour tissue. Additionally, three dots were marked to identify representative tumour area for subsequent tissue microarray (TMA) generation.

2.3.2 Tissue microarray generation

Following marking up of H&Es slides, all cases with sufficient tumour area were identified. For each cohort, a TMA was designed and manually created to include

1mm cores from each case in triplicate distributed randomly across the design[317]. Aside from tissue cores, the TMA also included;

Blank areas to aid subsequent TMA orientations

Positive control for immune stains in the form of tonsillar and lymph node tissue

Negative controls in the form of normal adipose tissue.

Utilising the manual TMA machine, a 1mm core was removed from the recipient FFPE block. For each case to be included, the FFPE block and H&E slide were compared, and the position of one of the marked TMA sample points noted for the FFPE block. A 1mm core of tumour tissue was then taken from this position and deposited into the vacant slot in the recipient block. A minimum of 0.5mm gap was allowed between cores in all directions, whilst occasional blank channels allowed for TMA orientation as well as providing structural integrity. Following completion of TMA creation, the recipient block was placed in an oven at 60^{o}C for 15 minutes topped with a glass slide to ensure adequate embedding of the cores within the paraffin and to provide integrity for subsequent sectioning.

2.4 Immunohistochemistry workflow and analysis

The methods detailed in this section relate to experiments for which the results are discussed in **Chapter 3**.

2.4.1 Immunohistochemistry for tumour infiltrating lymphocytes

To undertake IHC staining of TMA slides, sequential 4 µm sections were taken and utilised as input for the IHC protocol. For cases where there was insufficient tumour tissue to obtain TMA cores, single whole sections were used instead. Immunohistochemistry experiments were performed on the Dako Link Autostainer (Agilent, California, USA) and carried out by the Institute of Cancer Research (ICR) core facility. Tissue sections underwent deparaffinisation with

xylene, and then rehydrated down an ethanol gradient (100%, 95%, then 70%) to water. Antigen retrieval was then undertaken, with the method selected based on previous antibody optimisation and detailed below. Slides were then incubated with the primary antibody of investigation, as detailed below, for 60 minutes at room temperature, followed by the application of 3,3'-diaminobenzidine (DAB) resulting in a dark brown staining of positively labelled cells. Finally, haematoxylin counter-staining of the nuclei was undertaken. prior to the application of a cover slip.

CD3 IHC method

Staining for CD3 was performed using rabbit polyclonal anti-human CD3 antibody (Agilent product A0452) at a dilution of 1/600. Epitope retrieval was carried out using Dako Target low pH retrieval solution using the pressure cooker module.

CD4 IHC method

Staining for CD4 was performed using mouse monoclonal anti-human CD4 antibody(clone 4B12, Agilent product M7310) at a dilution of 1/80. Epitope retrieval was carried out utilising Dako Target high pH retrieval solution in the PT link tank.

CD8 IHC method

Staining for CD8 was carried out using mouse monoclonal anti-human CD8 antibody (clone C8/144B, Agilent product M7103) at a dilution of 1/100. Epitope retrieval was carried out with Dako Target low pH retrieval solution in the PT link tank.

For all IHC experiments, technical controls were included in the form of; positive control was normal tonsillar tissue, negative control omitting the primary antibody, and isotype control using mouse/rabbit immunoglobulin G.

2.4.2 Automated cell counting of immunohistochemistry stained immune cells

Following staining, the TMA slides were converted to digital images using the Nanozoomer 2.0HT digital slide scanner (Hamamatsu, Japan). The number of TILs per 1mm core was then quantified by automated cell counting.

2.4.2.1 ImageJ automated cell counting

The first method for automated cell counting utilised the ImageJ software with the Fiji image processing package[318]. Each core was isolated at 10x magnification, exported as a .tif file and cropped to a uniform 1mm diameter (0.785mm^2 area) using ImageJ, and saved as a new image. With all of the files for analysis in a single folder the code detailed (**Table 2.1**) was utilised to sequentially open the image file of the single TMA core, undertake colour deconvolution resulting in a black and white image (**Figure 2.1**), and then count the positively stained cells using the ImageJ 'Analyze Particles' function utilising optimised conditions taking into account circularity, particle size and pixel intensity;

Table 2.1: Macro code used for automated cell counting on the ImageJ platform.

//gets filename and directory	*selectWindow("Colour Deconvolution");*
dir=getDirectory("image");	*run("Close");*
name=getTitle;	*selectWindow(name+"-(Colour_1)");*
path=dir+name+"result195-18-25.txt";	*run("Close");*
colour2=name+"-(Colour_2)";	*selectWindow(name+"-(Colour_3)");*
run("Colour Deconvolution", "vectors=[H DAB]");	*run("Close");*
selectWindow(colour2);	*run("Watershed");*
run("8-bit");	*run("Analyze Particles...", "size=18-Infinity circularity=0.25-1.00 display exclude clear");*
setAutoThreshold("Default");	*//saves to defined path and closes windows down to original image*
run("Threshold...");	*saveAs("Results", path);*
setThreshold(0, 195);	*selectWindow("Results");*
setOption("BlackBackground", false);	*run("Close");*
run("Convert to Mask");	*selectWindow(name+"-(Colour_2)");*
run("Close");	*run("Close");*

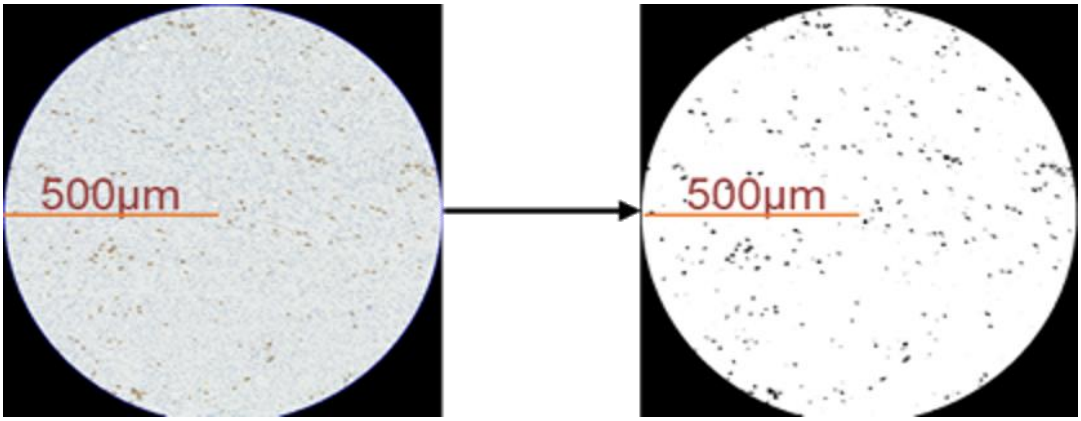

Figure 2.1: Example of the ImageJ processing of a single CD8 stained TMA core. The image on the left represents a single core isolated from the digital image of the whole TMA section. Following colour deconvolution the resultant image is shown on the right, which is then processed using the 'Analyze Particles' function in ImageJ to quantify the number of cells present.

2.4.1.2 QuPath automated cell counting

The second method for automated cell counting utilised QuPath, an open-source software platform for bioimage analysis and able to quantify TILs in TMA cores[319]. The digitally stored TMA slide images were opened in the QuPath software and the image type set to Brightfield (H-DAB). The 'TMA Dearrayer' function was then used with the expected number of rows and columns added, the core diameter set to 1.2mm, the density threshold set to 1 and the bounds scale set to 100. This then generated a grid over the scanned TMA, and any cores which were intentionally left blank for orientation, or whereby a core has dropped out during sectioning were classified as "missing" cores and not included in further automation steps. All cores were then selected and the simple tissue detection function was utilised with the threshold set to 250 and the pixel size to 2. In order to optimise the parameters for the cell detection functionality available on QuPath, a small number of cores were selected, the parameters modified and the resulting automated positive cell allocation checked until optimal detection of positively stained cells was achieved. For example, for CD8 staining the optimal conditions were pixel size 0.4, minimum area 20, threshold 0.05, maximum background intensity 2, single threshold of 0.2 and nucleus DAB optical density mean. Once optimised, the positive cell detection programme was run on the whole TMA slide, and the data was exported for further analysis.

2.4.3 Statistical analysis of immunohistochemistry data

2.4.3.1 Bland-Altman plots

In order to identify the most reproducible method of automated cell counting, a pilot study was undertaken in which a selection of cores (n=120) from CD8 stained TMA slides were selected and the CD8+ cells were counted manually. Independently, both the ImageJ platform and the QuPath platform were used to quantify the number of CD8+ cells present in the same cores[319,320]. The agreement between the manual counts and the two methods for automated cell counting were then compared using a Bland-Altman agreement plot[321]. This scatter graph plots the difference between the two paired measurements, manual

cell count versus automated count, against the mean of the paired measurements. On the same figure, lines are plotted for the mean difference between the values, and 1.96 standard deviations above and below the mean. The interval between the two standard deviation lines represents the limits of agreement between the two methods, and 95% of values are expected to fall within this interval if the two methods are felt to be comparable. Based on the results of this pilot study, and the subsequently generated Bland-Altman plots, the most appropriate automated counting method was subsequently taken forward.

2.4.3.2 Outcome analysis based on IHC results

In order to analyse the association between IHC-derived TIL counts and OS and PFS, following automated cell counting of the TMA cores the average TIL value from the three cores included per-sample in the TMA was calculated. For the combined cohort, the median cohort TIL value for each stain was determined, and this cut-off was used to stratify the cohort into TIL high and low subgroups. Based upon this stratification, Kaplan-Meier plots were generated, and Cox univariable analysis was employed to assess if TIL count was significantly associated with OS and PFS, with a p-value <0.05 considered significant[322,323]. In addition, Cox multivariable proportional hazards regression models were used to analyse the association between TIL and survival, with the routine clinicopathological variables including age, performance status and tumour grade added as co-variables[324]. Subsequently, the same CD3+, CD4+ and CD8+ median value determined in the combined cohort was used to stratify the comparator cohort into high and low TIL subgroups. Kaplan-Meier plots were then generated for OS and PFS to identify any association between subgroup classification and survival. Additional Cox multivariable models were also built for the comparator cohort, incorporating the same clinicopathological features as co-variables.

2.4.3.3 Correlation of CD3 count with CD4 and CD8

As a method of checking the reliability of the IHC counts generated, correlation

analysis was undertaken to compare the TMA core CD3+ raw count with the summation of the raw CD4+ and CD8+ counts for the same core. Correlation plots were generated utilising the $\log_2$ raw TIL counts, and a correlation coefficient of greater than 0.65 was considered “good”, and greater than 0.75 was considered “strong” correlation.

2.5 Nanostring data generation and analysis

The methods detailed in this section relate to experiments for which the results are discussed in **Chapter 4**.

2.5.1 Nucleic acid extraction

Samples selected for inclusion for targeted gene expression analysis underwent standard processing, whereby 4x20 µm sections were cut by microtomy, and where necessary macrodissected to enrich for a minimum of 75% tumour content. Tumour RNA was then extracted from the tissue sections utilising the All Prep DNA/RNA FFPE kit (Qiagen, Hiden, Germany) following the standard procedures dictated by the vendor. The concentration of RNA was quantified using both the Qubit and Nanodrop fluorometer (both Thermo Fisher Scientific, Massachusetts, USA), and the RNA integrity number and proportion of total RNA between 50 and 300 base pairs was measured using the 2100 Bioanalyzer and associated software (Agilent, California, USA). Based on the RNA quality and concentrations, a total of 150 ng RNA, or up to 300 ng in particularly degraded samples, was aliquoted and used as input material for targeted immune gene expression analysis using the nCounter PanCancer Immune Profiling Panel (Nanostring Technologies, Washington, USA).

2.5.2 Raw data normalisation

Data output from the Nanostring platform was in the form of .RCC files. In order to normalise the data, all .RCC files for the combined cohort were normalised utilising the “NanostringNorm” R package[325], through;

Subtraction of the geometric mean of the negative control probes

Normalisation by the positive control normalisation factor calculated as the geometric mean of the positive control probes

Normalisation as a factor of the housekeeping gene probes

Data was then $\log_2$ transformed and the normalised data matrix was then subjected to gene-based median centring.

2.5.3 Principle component analysis

With the aim of reducing dimensionality whilst minimising data loss, principle component analysis (PCA) is a method for transforming potentially correlated variables into a smaller number of uncorrelated variables[326]. As such, PCA was undertaken at various stages of data analysis utilising the PCAtools R package[327].

Initially, PCA was undertaken on the combined cohort with a PCA plot used to visualise if 2 principle components were sufficient to cluster different groups of samples together. Overlaying the gene loadings as a biplot was also used to identify which specific genes were driving the separation of samples. A scree plot was also generated, with both the horn and the elbow method added to the plot, to identify the ideal number of principal components required to explain the variance within the dataset[328,329]. A pairs plot was also generated to visualise the variance explained by each paired sets of principle component. Finally, a loadings plot was used to visualise which genes were driving each principle component.

2.5.4 Heatmap generation

In order to observe more complex patterns in the data not diminishable by PCA, heatmaps were generated utilising the ComplexHeatmap package in R[330]. A heatmap of the immune gene expression for the combined cohort was plotted using unsupervised hierarchical clustering to group samples together based on the similarity in expression profiles. Any obvious subgroups following this

clustering were then taken forward and investigated further to better describe the immune-based biology underpinning STS.

2.5.5 Identifying differentially expressed genes between subgroups

Significance analysis of microarray (SAM) was undertaken to identify any differentially expressed genes between subgroups of interest. In order to undertake this, the "samR" package was employed[331]. An appropriately formatted .xsls data sheet was uploaded to samR console launched through R studio. The data type was set at array, and for all SAM analyses, two-class unpaired was the response type selected. For analyses involving more than two subgroups, serial SAM analyses were undertaken to compare the subgroup of interest with the rest of the cohort, and the genes in which differential expression was unique for that subgroup were taken forward for discussion. After running the SAM analysis, a robust delta value was selected which generated the maximum number of significant genes, whilst keeping the false discovery rate to a minimum, and no greater than 5%[332].

2.5.6 Single samples gene set enrichment analysis

In order to define specific phenotypic characteristics of the immune gene expression data, single sample gene set enrichment analysis (ssGSEA) was undertaken. ssGSEA is an analytical method which derives its power by focusing on pre-defined sets of genes which share a common biological function[333]. The gene annotations as supplied by Nanostring were used to generate gene sets for specific immune cells of interest (**Table 2.2**). In order to undertake ssGSEA, a .gct data file was created using the desired normalised, log2 transformed, median-centred data set. In addition, a .gmt file of the gene set of interest was also created. Both files were uploaded to the Gene Pattern website (www.genepattern.org) and the gene set enrichment function used. The subsequent .gct data file was then read into R, and used to generate heatmaps and boxplots of the ssGSEA results.

Table 2.2: Gene set for specific immune cells.

Immune cell	Genes included in gene set								
Activated dendritic cells	*CCL1*	*EBI3*	*IDO1*	*LAMP3*	*OAS3*				
Dendritic cells	*CCL13*	*CCL17*	*CCL22*	*CD209*	*HSD11B1*				
Immature dendritic cells	*CD1A*	*CD1B*	*CD1E*	*F13A1*	*SYT17*				
Plasmacytoid dendritic cell	*IL3RA*								
B-cell	*BLK*	*CD19*	*CR2*	*HLA-DOB*	*MS4A1*	*TNFRSF17*			
Cytotoxic cells	*GNLY*	*GZMA*	*GZMH*	*KLRD1*	*KLRF1*				
Eosinophils	*CCR3*	*IL5RA*	*PTGDR2*	*SMPD3*	*THBS1*				
Macrophages	*APOE*	*CCL7*	*CD68*	*CHIT1*	*CXCL5*	*MARCO*	*MSR1*		
Mast cells	*CMA1*	*CTSG*	*KIT*	*MS4A2*	*PRG2*	*TPSAB1*			
Neutrophils	*CSF3R*	*FPR2*	*MME*						
Natural killer bright	*FOXJ1*	*MPPED1*	*PLA2G6*	*RRAD*					
Natural killer dim	*GTF3C1*	*GZMB*	*IL21R*						
Natural killer	*BCL2*	*FUT5*	*NCR1*	*ZNF205*					
T-cell	*CD2*	*CD3E*	*CD3G*	*CD6*					
CD8 T-cell	*CD8A*	*CD8B*	*FLT3LG*	*GZMM*	*PRF1*				
T-helper cells	*ANP32B*	*BATF*	*NUP107*	*CD28*	*ICOS*				
T-helper1 cells	*CD38*	*CSF2*	*IFNG*	*IL12RB2*	*LTA*	*STAT4*	*TBX21*	*CTLA4*	
T-helper2 cells	*CXCR6*	*GATA3*	*IL26*	*LAIR2*	*PMCH*	*SMAD2*	*STAT6*		
T-helper17 cells	*IL17A*	*IL17RA*	*RORC*						
Follilcular helper T-cells	*BCL6*	*CXCL13*	*MAF*	*PDCD1*					
Memory T-cell	*ATM*	*DOCK9*	*NEFL*	*REPS1*	*USP9Y*				
Effector T-cells	*AKT3*	*CCR2*	*EWSR1*	*LTK*	*NFATC4*				
Gamma delta T cells	*CD160*	*FEZ1*	*TARP*						
T-reg cell	*FOXP3*								
Immune checkpoint	*ADORA2A*	*BTLA*	*CD27*	*CD40LG*	*HAVCR2*	*KIR3DL1*	*LAG3*	*TNFRSF4*	*TNFRSF9*

2.6 Building survival models

The methods detailed in this section relate to experiments for which the results are discussed in **Chapter 5**.

2.6.1 Strategy to analyse the combined cohort

For this workflow, after considering the desire to generate a prognostic model and validate it on an independent cohort, as well as the small cohort size, the strategy employed was to split the combined cohort into distinct discovery and validation cohorts. This would allow a prognostic model to be built on the discovery cohort, and for any significant findings to be tested and validated on the independent validation cohort. However, due to the small sample size, the decision was made to then combine the discovery and validation cohorts together to build the final model.

2.6.2 Building prognostic models using the discovery cohort

To address this work package, the immune gene expression data for discovery cohort (n = 37) was normalised using the “NanostringNorm” R package. Following this normalisation, a gene-filtering process was performed in which genes for which 25% or greater of the samples had a value of 0 were removed for subsequent analysis. Following normalisation and filtering, the median immune gene value of the remaining genes for each sample was identified, termed the median immune score (MIS). Subsequently, six different Cox regression models incorporating different variables for both OS and PFS were built using the discovery cohort;

A univariate Cox regression model for both OS and PFS built using the MIS for each sample,

A Cox multivariable regression model for OS and PFS built incorporating the clinicopathological features of patient age at the start of pazopanib, patient performance status (PS), at the start of pazopanib therapy, and tumour grade,

A multivariable Cox regression model for OS and PFS built using tumour grade, patient age, patient PS, and MIS.

This strategy would allow the association of MIS and differences in survival through univariate analysis, whilst comparing the multivariable clinicopathological model with the model which also includes the MIS has the aim of identifying if MIS adds additional prognostic information compared to standard clinicopathological variables alone.

2.6.3 Building prognostic models on the validation cohort

To build prognostic models using the validation cohort (n=28) immune gene data, the data set was first normalised with normalisation factors for the geometric means of positive control and housekeeping genes of the discovery cohort used to dictate a normalisation target[334]. Genes which were filtered out of the discovery cohort analysis were then also excluded from the validation cohort analysis. From this gene list, the median gene score, the MIS, was calculated for each sample. The same six Cox regression models were then built using the validation cohort, with the aim of validating any findings previously reported during analysis of the discovery cohort.

2.6.4 Building prognostic models on the combined cohort

Finally, the discovery and validation cohorts were merged into the combined cohort (n=65) and the final models were built on this larger cohort. The same six Cox models as previously detailed were built, but in addition on the combined cohort Cox multivariable models for OS and PFS were built incorporating clinicopathological features, MIS and STS subtype as co-variables. The aim of including STS subtype was to assess if the histological subtype had an impact on the prognostic value of the model, or if it could be used across a range of STS subtypes.

2.7 Ethical approval

The collection and analysis of pseudonymised archival FFPE tissue and the associated clinical data obtained from the RM electronic patient records was approved under the RM-sponsored Elucidation of a Molecular signature of Pazopanib Response in Advanced STS including SFT (EMPRASS) study denoted by NHS Research Ethic Committee reference 14/WA/0164 and RM Committee for Clinical Research reference 4107.

Chapter 3 - Generating cohorts and immunohistochemistry assessment of immune associations with clinical outcomes following pazopanib treatment

3.1 Background and objectives

Soft tissue sarcomas (STS) are rare cancers with limited treatment options in the advanced setting following failure of first-line therapies[4,5]. Although newer targeted therapies have led to advances in a number of other solid tumours, in STS this progress is lacking. Pazopanib is a multi-target, anti-angiogenic tyrosine kinase inhibitor (TKI) which although showed promise in early-stage clinic trials, disappointingly showed no overall survival (OS) advantage in the PALETTE phase III clinical trial[132]. Although post-hoc analysis demonstrated that a subgroup of patients did gain robust progression-free survival (PFS) and OS benefit from treatment with pazopanib, at present there is no way of stratifying patients into those most likely to respond[135]. Given the relationship between neoangiogenesis and the creation of an immune-suppressive tumour microenvironment[274–277], the reported potential for the immune contexture to provide prognostic biomarkers in STS[290,291,293] and existing evidence of immune modulation by anti-angiogenic therapy[303,304,307,309], there is a rationale for exploring the immune tumour microenvironment and its association with clinical benefit from pazopanib.

Given the rarity of STS, there currently exist no published studies looking to define immune-based biomarkers for clinical outcomes following pazopanib therapy in this patient group. Furthermore, studies undertaking immune-based genomic analyses in STS are infrequent, and the immune microenvironment of STS is incompletely characterised. As such, the aims of this chapter are to;

1. design and generate cohorts of patients with adequate tissue samples and clinical data available to characterise the tumour immune microenvironment. These cohorts include a population of patients with a diagnosis of advanced STS, including a range of STS subtypes, who received pazopanib in their treatment.
2. undertake immunohistochemistry (IHC)-based analysis of pre-pazopanib STS samples to explore the immune contexture of a cohort including a range of STS subtypes. This looks to address the discordant published reports of IHC-based biomarkers in STS (**Table 1.6**)[279,280,289,281–288], whilst additionally, there

remains a lack of IHC-based work concerning STS treated with pazopanib. Tissue microarrays (TMAs) permit high-throughput histological studies of multiple samples simultaneously and were therefore chosen as the most effective and tissue-efficient method for this analysis[335].

3. correlate IHC-based immune profiles with clinical outcomes in relation to pazopanib therapy.

3.1.1 Contributions

Work of the candidate include;

- Study conception and design in conjunction with the supervisory team.
- Review and modification of the pre-existing Royal Marsden cohort generated by Dr Alex Lee, and updating of the associated clinical data.
- Identification, collection and curation of archival formalin-fixed paraffin-embedded (FFPE) material and associated clinical data for additional Royal Marsden (RM) cases for the validation cohort and all cases in the comparator cohort.
- Co-ordination and processing of samples and incoming clinical data from external collaborating centres.
- Tissue mark-up for tumour area and tissue microarray (TMA) cores under the training of Dr Khin Thway, consultant histopathologist, RM.
- TMA design and creation.
- Digital microscopy image capture and processing, and quantification of IHC stained immune cells.
- Figure generation and data analysis.

Cases included in the validation cohort were identified and provided by collaborators in Glasgow and Singapore, who also transferred pseudonymised clinical data in a pre-designed database form designed by the candidate.

FFPE slide cutting, IHC optimisation, and IHC staining were performed by staff of the ICR's histopathology core facility.

3.2 Results

3.2.1 Patient selection

To address the first aim of this chapter, namely generating cohorts on which to describe the immune microenvironment in STS, and subsequently to assess immune associations with clinical outcomes following pazopanib therapy, I curated a cohort of patients who received treatment with pazopanib (named the combined cohort), and an additional cohort of patients who were treated with an alternative second-line therapy (named the comparator cohort)(**Figure 3.1**). These two cohorts were designed to allow in-depth characterisation of the immune microenvironment of pre-pazopanib tissue, with the aim of determining biomarkers associated with differential clinical outcomes. The two cohorts are:

1. The combined cohort is made up of pre-pazopanib tissue from patients who received pazopanib as part of the management of advanced STS from the Royal Marsden, Beatson Cancer Centre in Glasgow and National Cancer Centre in Singapore.
2. The comparator cohort is made up of patients treated with clinician's choice alternative second-line therapies from the Royal Marsden, and the pre-second line tumour tissue was analysed.

3.2.1.1 Combined cohort

Between October 2009 and September 2016, a total of 42 patients were identified to have been treated with pazopanib at the RM, who met the inclusion and exclusion criteria as detailed previously (**section 2.2.1**) and who on review had retrievable pre-pazopanib FFPE material which was of adequate quality for downstream analysis. In addition, 23 cases from collaborating centres (Glasgow and Singapore) were added. In total, there were 65 cases with sufficient tissue in the combined cohort (**Figure 3.1**).

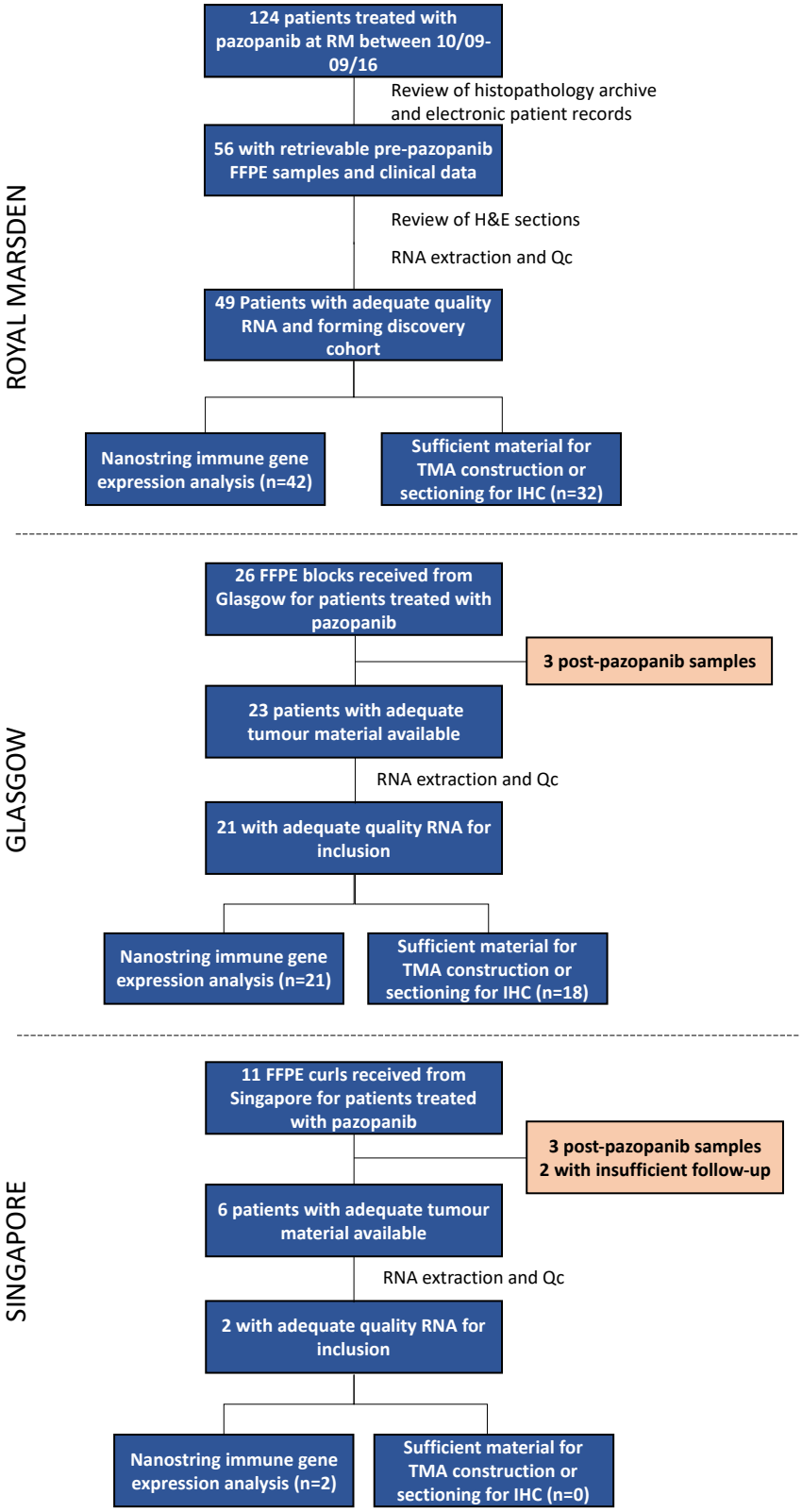

Figure 3.1: Consort diagram showing patient selection for cases from the Royal Marsden (RM) as well as from external collaborators for the combined cohort. A total of 65 cases were included for Nanostring immune gene expression analysis (42 from the RM, 21 from Glasgow and 2 from Singapore) with 50 of these cases having sufficient tissue for TMA construction or sectioning for immunohistochemistry (IHC) experiments.

3.2.1.2 Comparator cohort

For the comparator cohort, all patients identified on the RM STS prospectively maintained database who had received a minimum of two lines of systemic therapy but never received a dose of pazopanib, between April 2015 and January 2019 were assessed. For those with archival tissue available, this was requested. Following extraction and assessment of RNA quality, a total of 28 patients were suitable for inclusion in the comparator cohort (**Figure 3.2**).

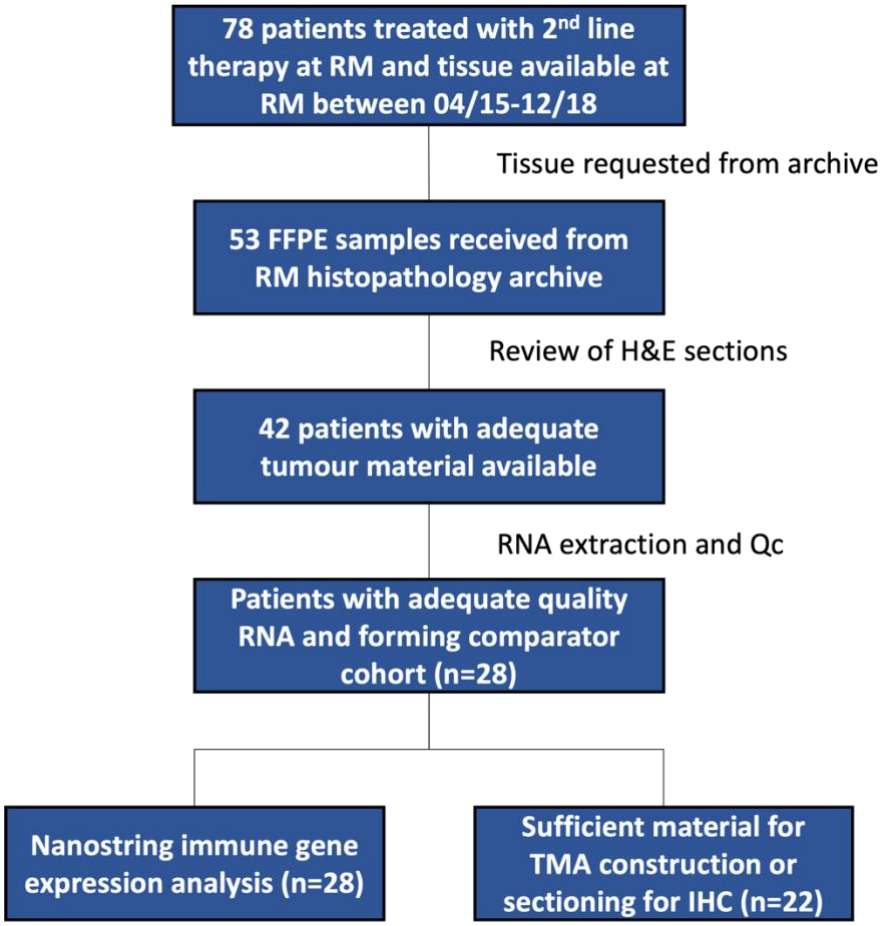

Figure 3.2: Consort diagram for patient inclusion for the comparator cohort.

3.2.2 Baseline clinicopathological characteristics

Baseline clinicopathological variables of the pazopanib-treated combined cohort and the comparator cohort are summarised in **Tables 3.1** and **3.2).** The median age at the start of pazopanib therapy was 55 years in the combined cohort (range 18 – 81.2 years), whilst for the comparator cohort the median age at the start of second-line therapy was 54.3 years (range 29 to 79.9 years).

Tumour grade is a known prognostic factor, and where retrievable was documented. The majority of tumours across the cohorts were grade 2 or 3 (**Figure 3.3.A**). To assess for any statistically significant differences between the cohorts in relation to clinicopathological variables, Chi-squared statistical testing was employed which showed no significant difference in the proportion of cases being classified as low, medium or high grade.

All patients had an Eastern Cooperative Oncology Group (ECOG) performance status (PS) of between 0 and 2. The majority of cases in these cohorts were PS 0 or 1, with only a small minority PS 2, and there was no significant difference in PS when comparing the cohorts (**Figure 3.3.B**).

The best response to treatment was also recorded for each patient, and determined by cross-sectional imaging and per Response Evaluation Criteria in Solid Tumours (RECIST). Across the cohorts, there were no complete responses (CR), and statistical analysis did not show any significant differences in the best responses to treatment between the cohorts (**Figure 3.3.C**).

A range of STS subtypes were included, as the intention of the study was to investigate the immune microenvironment of STS across multiple histological subtypes (**Figure 3.4**). For the combined cohort and the comparator cohort, the most common STS subtype was leiomyosarcoma (LMS), and these made up a similar proportion of the cases across both cohorts. The most noticeable difference between the cohorts in terms of subtype distribution was the relative enrichment for solitary fibrous tumours (SFTs) in the combined cohort compared to the comparator cohort. Otherwise, the subtype breakdown between cohorts is

comparable, and around 15% of each cohort is made up of subtypes with a single case included.

Table 3.1: Baseline clinicopathological variables for the combined and comparator cohorts generated for this study. Prior lines of therapy for the combined cohort refers to systemic therapies prior to pazopanib. For the comparator cohort, all cases were second-line, therefore all had received 1 line of prior systemic therapy. LMS – leiomyosarcoma; LPS - liposarcoma; MPNST – malignant peripheral nerve sheath tumour; NOS – not otherwise specified; SFT – solitary fibrous tumour; UPS – undifferentiated pleomorphic sarcoma.

Cohort	Combined	Comparator	p value
n	65	28	
Sex			
M	26	12	
F	39	16	0.797
Age (years)			
Median	55	54.3	
Range	18 - 81.2	29 - 79.9	0.503
Grade			
1	4	0	
2	21	8	
3	35	16	
UNK	5	4	0.435
Performance Status			
0	19	8	
1	32	14	
2	7	3	
UNK	7	3	0.999
Sarcoma Subtype			
LMS	18	9	
SFT	9	0	
UPS	3	4	
Angiosarcoma	1	3	
Chondrosarcoma	2	0	
MPNST	1	2	
Myxofibrosarcoma	2	1	
Myxoid LPS	2	0	
Synovial Sarcoma	5	4	
Sarcoma NOS	5	0	
Spindle Cell Sarcoma	7	1	
Other*	10	4	0.078
Prior lines systemic therapy			
0	12	0	
1	24	28	
2	15	0	
3+	14	0	<0.001

* other cases include; in the discovery cohort, single cases of alvolear soft part sarcoma, clear cell sarcoma, fibromyxoid sarcoma, fibrosarcoma, granular cell tumour, malignant haemangioendothelioma, and PEComa; in the validation cohort atypical Ewings, dedifferentiatied liposarcoma and fibromyxoid sarcoma; and in the comparator cohort two cases of adenosarcoma, and single cases of endometrial sarcoma and pleomorphic rhabdomyosarcoma.

Table 3.2: Clinicopathological variables of the combined and comparator cohorts including response to therapy and survival data at 18-month censor. Response to therapy was assessed on cross-sectional imaging by response evaluation criteria in solid tumours (RECIST 1.1)[336]. For some patients best response is unknown, either as a scan wasn't performed due to the patient's medical condition, or the scan was not available for review. CR – complete response; IQR – interquartile range; OS – overall survival; PD – progressive disease; PFS – progression-free survival; PR – partial response; SD – stable disease; UNK – unknown.

Cohort	Combined	Comparator	p value
n	65	28	
Sample Type			
Primary	35	20	
Metastasis	17	4	
Local Recurrence	10	4	
UNK	3	0	0.314
Best Response			
PD	14	14	
SD	26	8	
PR	12	6	
CR	0	0	
UNK	13	0	0.093
PFS (months)			
Median	3.7	3.43	
Range	0.27 - 18	1.1 - 18	
IQR	1.93 - 8.65	1.4 - 7.0	0.556
OS (months)			
Median	8.9	10.7	
Range	0.27 - 18	2.27 - 18	
IQR	3.67 - 15.58	4.54 - 15.68	0.599

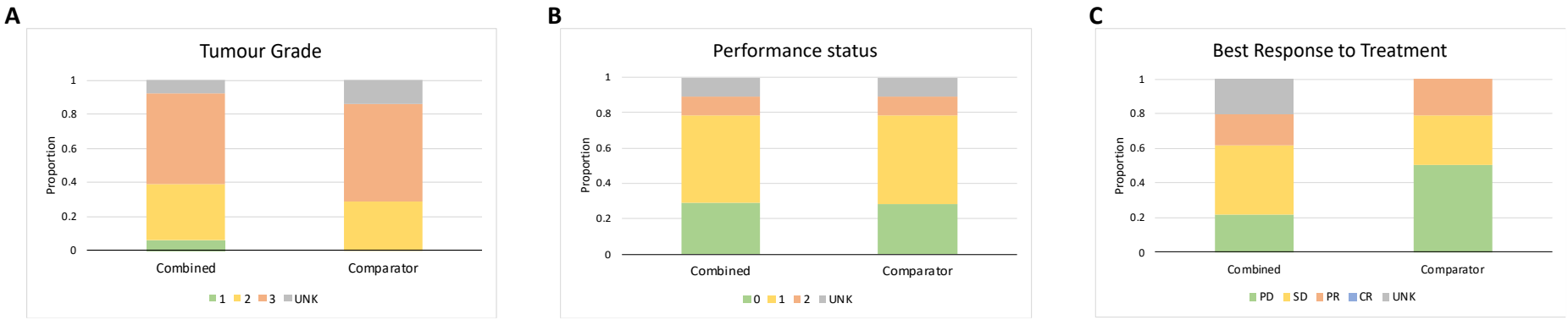

Figure 3.3: Stacked bar charts showing the proportional make-up of the combined and comparator cohorts by **A** tumour grade, **B** performance status, and **C** best response to treatment. PD – progressive disease; PR – partial response; SD – stable disease; UNK – unknown.

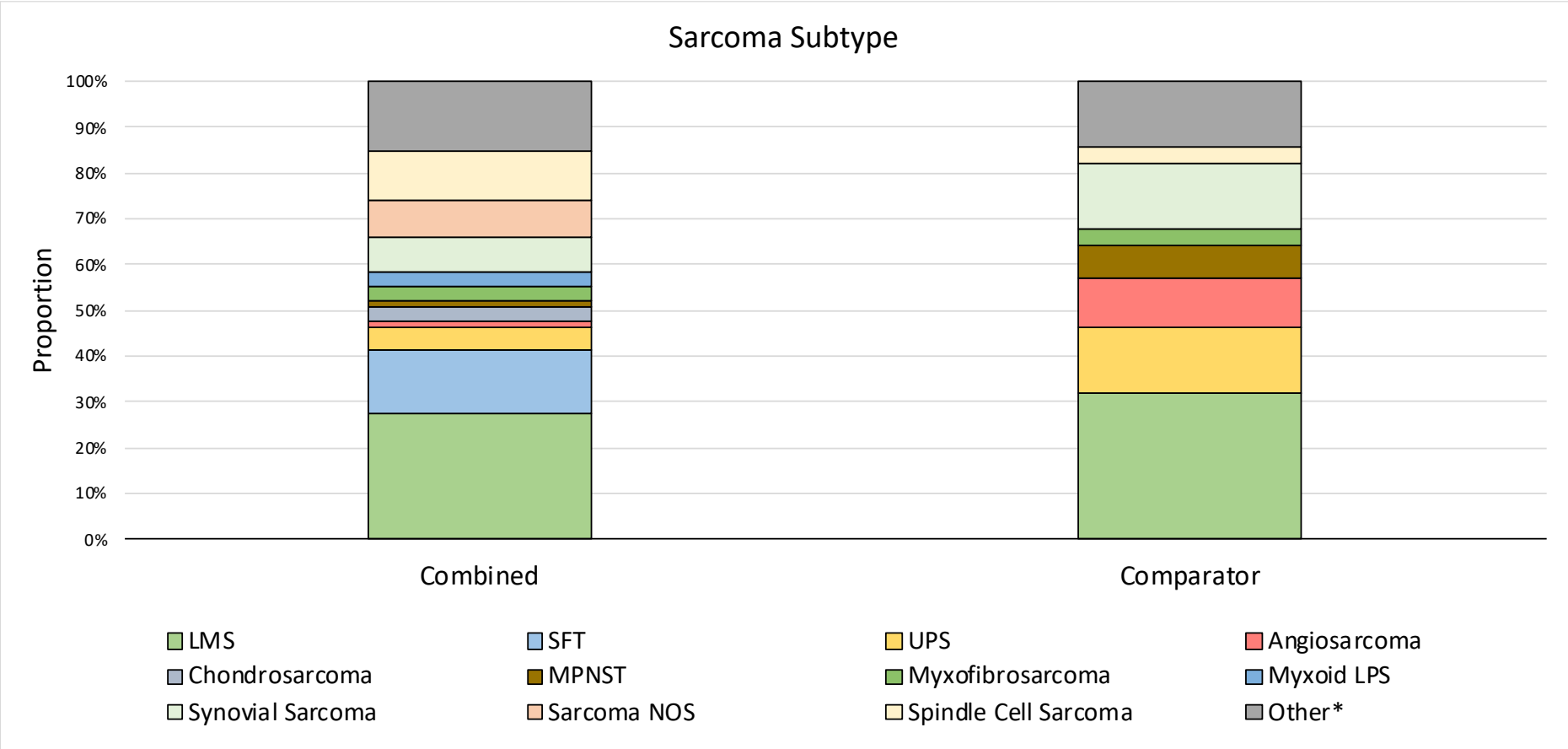

Figure 3.4: Breakdown of STS subtypes in the combined and comparator cohorts. Of note, leiomyosarcoma (LMS) is the most common subtype included across both cohorts; LPS - liposarcoma; MPNST – malignant peripheral nerve sheath tumour; NOS – not otherwise specified; SFT – solitary fibrous tumour; UPS – undifferentiated pleomorphic sarcoma.

For all cases included in this study, based upon the PALETTE phase III trial median OS (mOS) from pazopanib of 12.5 months[132], and real-world experiences in STS reporting a mOS from pazopanib of between 8.2 months and 12.4 months[147–149,151,153], all survival data were censored after 18 months. At this 18-month cut-off, for the combined cohort, 59 of the 65 (90.1%) patients had experienced disease progression and 50 of 65 (84.6%) had died. For the comparator cohort, 25 out of the cohort of 28 (89.3%) patients had experienced disease progression following second-line therapy, and 20 out of 28 (71.4%) patients had died.

To undertake comparative survival analysis between the cohorts, Kaplan-Meier plots were generated showing the OS and PFS of the combined cohort and the comparator cohort over time. Univariable survival analysis based on cohort assignment showed no significant difference in OS between the cohorts (mOS combined cohort 8.9 months vs 10.7 months in comparator; p=0.556)(**Figure 3.5**). Additionally, no significant difference in PFS was observed, with a median PFS (mPFS) of 3.9 months in the comparator cohort compared to 3.7 months in the combined cohort (p=0.599)(**Figure 3.6**).

The importance of confirming comparable OS and PFS between the cohorts is that the patients included in the combined cohort, and treated with pazopanib, have not been selected based on clinical outcomes. As such, the aim of biomarker discovery was to identify a subset of these patients with superior clinical outcomes following pazopanib treatment. In order to then compare this biomarker with the comparator cohort, it was important to confirm the two cohorts had similar baseline survival risks. Therefore, having no significant difference in OS and PFS between the combined cohort and the comparator cohort provides confidence that they are comparable in terms of their survival profiles, and will allow comparison of the impact of a biomarker on clinical outcomes.

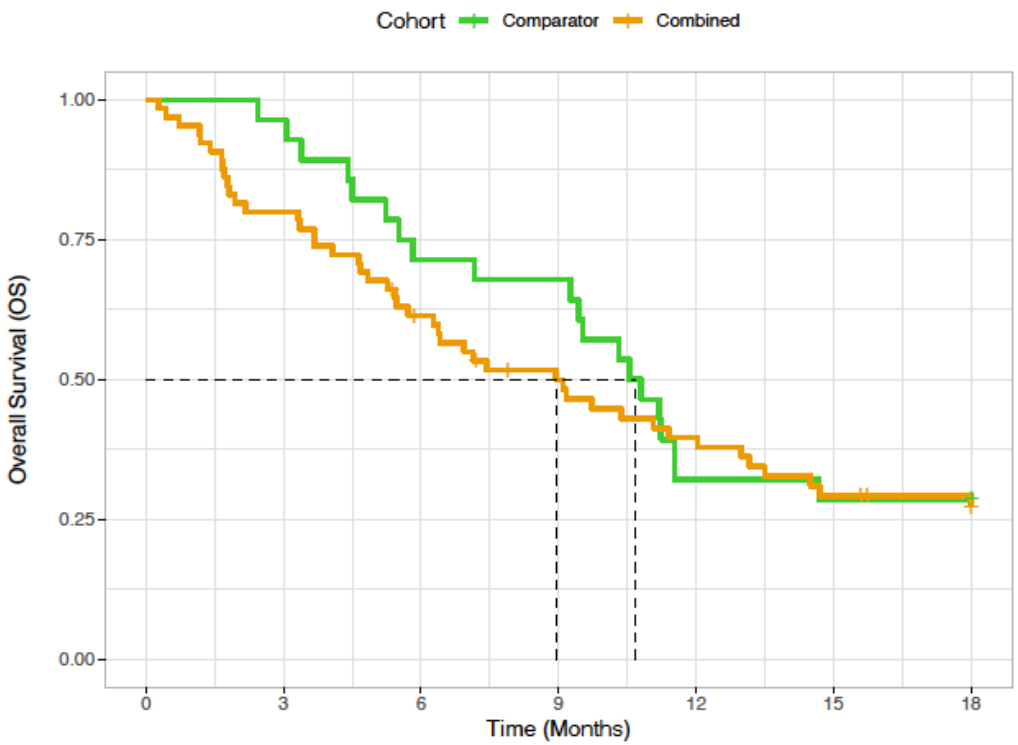

Number at risk								Median OS (months)	HR (95% CI)	p value
Cohort										
	28	27	20	19	9	8	8	10.7	1.00	
	65	52	38	29	23	17	15	8.9	1.17 (0.69 – 1.99)	0.556

Figure 3.5. Kaplan-Meier plots for overall survival (OS) comparing the pazopanib-treated combined cohort with the alternative second-line therapy comparator cohort, with the comparator cohort the reference for hazard ratio (HR) analysis. 95% CI – 95% confidence interval.

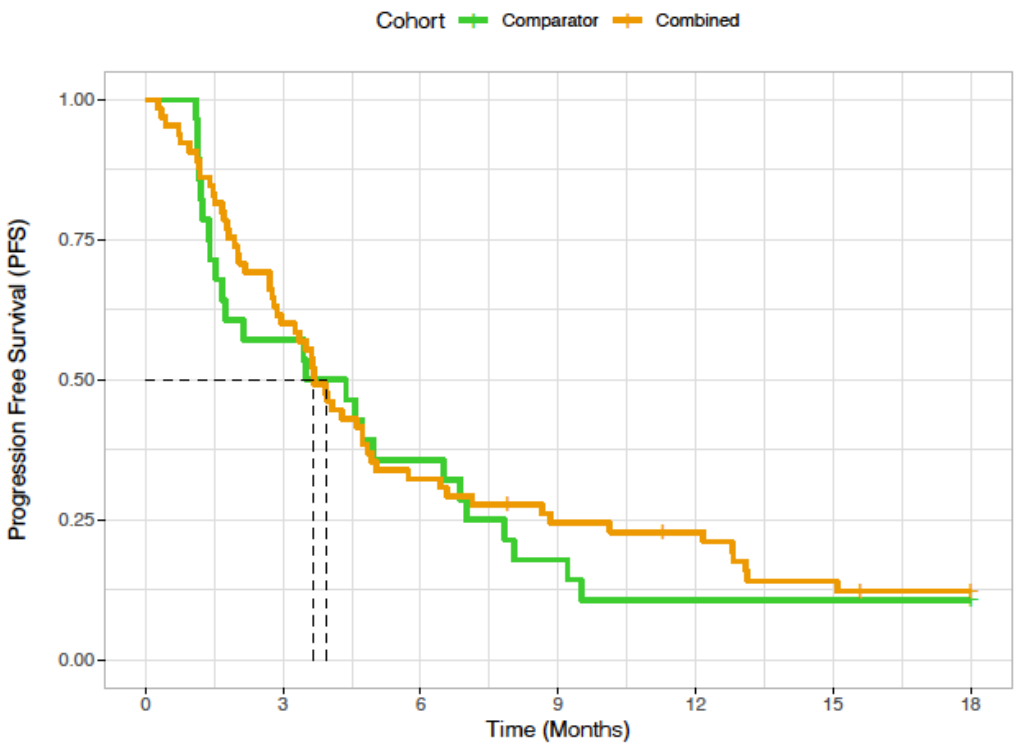

Number at risk								Median OS (months)	HR (95% CI)	p value
Cohort	28	16	10	5	3	3	3	3.9	1.00	
	65	39	21	15	13	8	6	3.7	0.88 (0.55 – 1.41)	0.599

Figure 3.6: Kaplan-Meier plot showing progression-free survival (PFS) comparing the pazopanib-treated combined cohort with the alternative second-line therapy comparator cohort, with the comparator cohort acting as the reference for hazard ratio (HR) comparisons. 95% CI – 95% confidence interval.

3.2.3 Comparing ImageJ and QuPath for automated cell counting

Having curated clinical cohorts and acquired tumour tissue on which to assess the tumour immune microenvironment, I then looked to quantify tumour infiltrating lymphocytes (TILs) in these samples. This looks to address aims 2 and 3 of this chapter;

- undertake IHC-based analysis of pre-pazopanib STS samples to analyse the immune contexture of a cohort including a range of STS subtypes.
- correlate IHC-based immune profiles with clinical outcomes in relation to pazopanib.

The rationale for undertaking this work is multi-factorial, including evidence that;

- Elevated levels of angiogenic factors in the tumour microenvironment contribute to the polarization of immune cells into their immune-suppressive subtypes[267,272,273].
- Tumour-induced neoangiogenesis facilitates immunosuppression via the formation of chaotic blood vessels, and the preferential transendothelial migration of immunosuppressive regulatory T-cells and apoptosis of effector CD8+ T-cells[274,276,277].
- Evidence of immune-modulation by pazopanib to promote anti-tumour immunity *in vitro*, and *in vivo* in patients with renal cell carcinoma treated with pazopanib[295,303,304].

However, there remains a lack of work assessing the immune microenvironment in STS and how it may be associated with clinical outcomes in patients who have received pazopanib. As such, I aim to address this initially by undertaking IHC for TILs and correlating these findings with clinical outcomes in relation to pazopanib.

In view of the different available software to facilitate automated IHC cell counting, a pilot study was undertaken on a selection of cores stained for CD8, a cell surface co-receptor of the T-cell receptor, with CD8+ cells involved in T-cell signalling and cytotoxic activities. The number of CD8+ cells for each core were counted manually, and then also quantified using two widely available automated

counting platforms. The first of these platforms was ImageJ, a free-to-use image processing software suite, which previous studies have used to quantify tumour infiltrating immune cells[318,337,338]. The second software assessed was QuPath, an open-source platform for bioimage analysis which has also been used by previously published studies for immune cell quantification in tumour samples[319,339,340].

For this pilot study, a total of 120 individual cores were selected from the combined and comparator cohorts, and the number of infiltrating CD8+ cells was quantified. Bland-Altman plots were then generated to identify the automated cell counting method which correlates most closely with manual cell counting (**Figure 3.7.A and B**). Bland-Altman plots map the difference in score between the two methods against the mean of the combined scores. Also shown on the plot is the interval of agreement, defined as the mean score +/- 1.96 standard deviations. An acceptable degree of concordance between two methods is visualised on a Bland-Altman agreement plot when 95% of the points lie within this interval of agreement[321]. From **Figure 3.7.A**, when comparing the manually counted CD8+ scores with the value quantified on ImageJ, all but 2 of the 120 scores lie outside the interval of agreement, with the remaining 118 (98.3%) within the interval. In comparison, from **Figure 3.7.B**, a total of 8 points lie outside the interval of agreement when comparing manual counting with QuPath automated counting, with 112 of the 120 (93.3%) within the acceptable range. As such, this suggests that ImageJ is the preferable method for undertaking automated cell counting as the scores are most closely aligned to manual counting.

However, Bland-Altman plots are subjective in the sense they allow a visual assessment of agreeability between tests but not a statistical assessment. Therefore, the intraclass correlation coefficient (ICC), an index to measure reproducibility and reliability, for both methods was determined[341]. The ICC for ImageJ was 0.767 compared to 0.629 for QuPath, confirming not only that ImageJ is the superior method but that there is strong agreement between ImageJ and manual counting. Although from **Figure 3.7.A** two outliers are noted, these represented a small proportion of cases. In addition, as one if high and one is low, there is no clear bias for under or over-estimation of either method. As

such, and given the comparatively superior results relative to QuPath, the most acceptable method for automated immune cell quantification was deemed to be ImageJ.

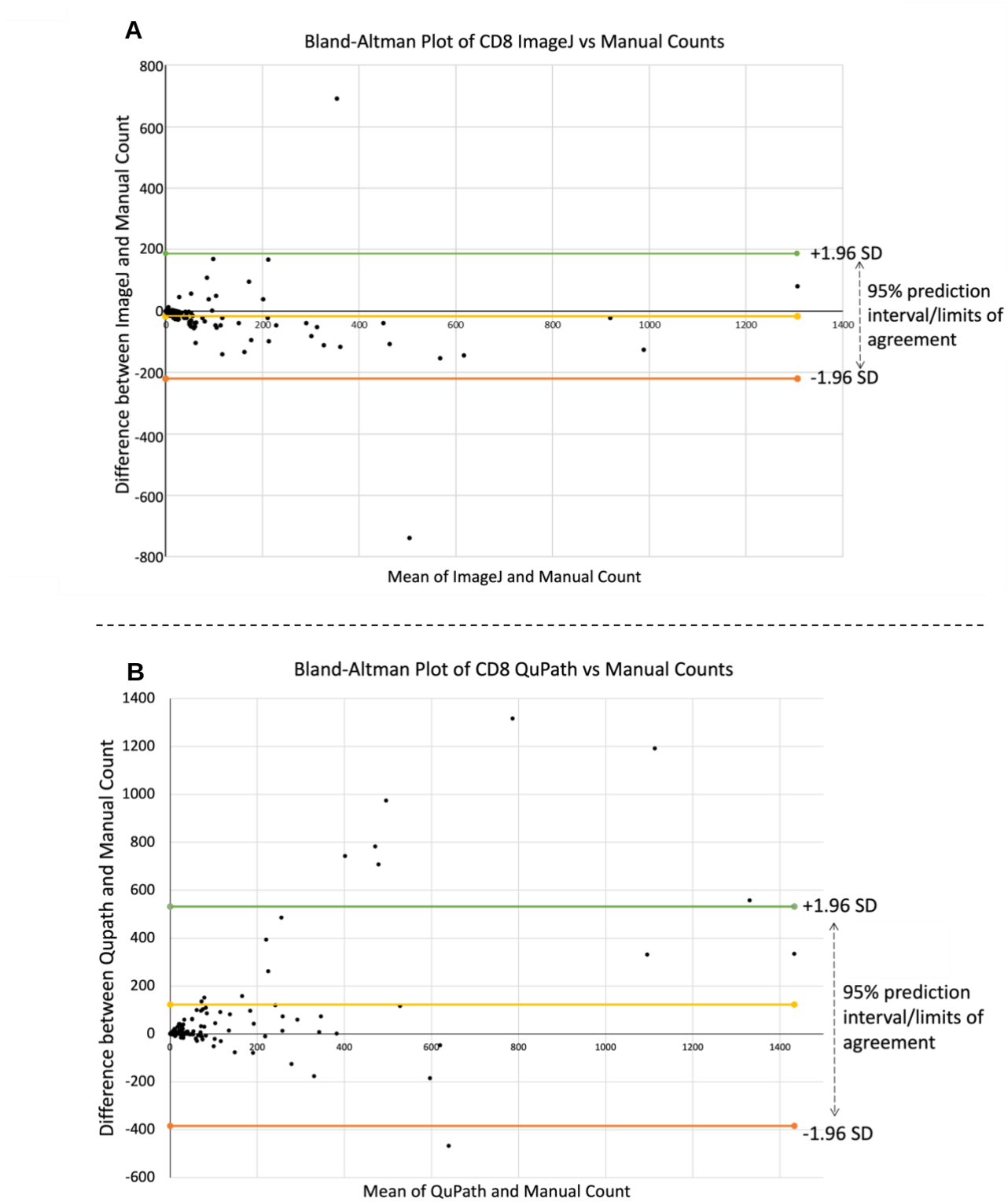

Figure 3.7: Bland-Altman plot of CD8+ count comparing manual scoring with automated scoring by **A** Image J and **B** QuPath.

3.2.4 Immunohistochemistry of tumour infiltrating lymphocytes

As discussed above, evidence exists that there may be value in exploring the tumour immune microenvironment as a potential source of biomarkers associated with outcomes following pazopanib treatment. However, at present, there is a paucity of published work exploring this line of research. In addition, the immune microenvironment in STS is incompletely characterised, and therefore there is value in further exploring the immune contexture in cohorts of a range of STS subtypes.

In order to analyse the immune microenvironment in our STS cohorts, I undertook a study workflow as outlined in **Figure 3.8**. IHC was undertaken initially as it is a widely available and cheap method for allowing the characterisation of TILs. Furthermore, tissue microarrays (TMAs) permit high-throughput histological studies of multiple samples simultaneously and was therefore chosen as the most effective and tissue-efficient method for this analysis[335].

To assess tumour infiltrating lymphocytes (TILs) in our cohort, TMAs were generated (per **Section 2.3.2**) for each cohort for those cases with sufficient tissue. If the tumour available was unsuitable for TMA generation, whole sections were cut and stained. The TMAs were designed such that each tumour block was represented in triplicate, with additional positive and negative controls added to the TMA. Consecutive sections were then cut from the TMA and IHC staining for TILs was carried out (per **Section 2.4.1**) with stains undertaken for CD3, CD4 and CD8. CD3 is a pan-lymphocyte marker, whilst CD4 and CD8 are T-cell co-receptors commonly associated with T-helper cells and cytotoxic T-cells respectively. As such the stains were selected as markers of the T-cell infiltrate in the tumour microenvironment. Stained slides were then converted to digital images, with individual cores isolated as digital images to be used as input for subsequent immune cell quantification. For IHC-stained whole sections, digitally annotated 0.5mm radius cores were applied to the scanned slide images.

Following our pilot study, ImageJ was deemed the most effective and reliable automated cell counting software to quantify the number of positively stained TILs

(per **Section 2.4.2**). Therefore, ImageJ was employed to quantify the raw TIL count for each core, and the average for the three cores was taken as the TIL count for each patient.

As outlined in **Figure 3.8**, the average IHC result for each case was determined, and survival analysis undertaken as a categorical variable following stratification of the combined cohort based on the median IHC value. Survival analysis was carried out for OS and PFS, with Kaplan-Meier plots generated to visualise any differences in survival. Further survival analysis was then undertaken utilising the IHC as continuous data employing univariable and multivariable Cox regression analysis.

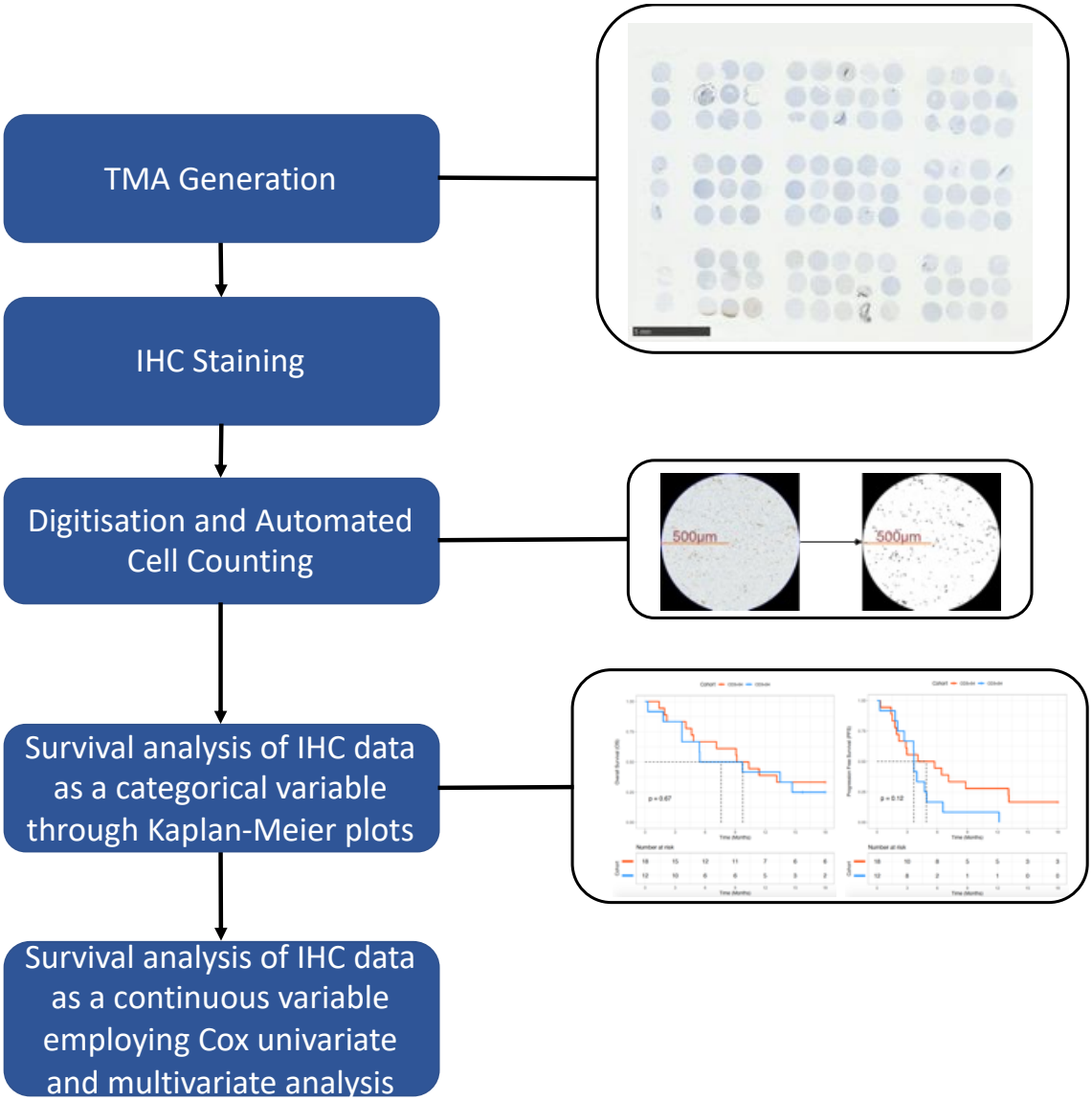

Figure 3.8: Workflow for assessment of tumour infiltrating lymphocytes (TILs), stratification of the cohorts and survival analysis. Tissue microarrays were generated and IHC was employed to stain for TILs. Slides were then digitised, individual cores isolated and then interrogated by automated cell count using ImageJ software resulting in a raw TIL count per core. Each sample was represented on the TMA in triplicate, and these individual core scores were averaged to give a per-sample TIL count. These average IHC scores then underwent survival analysis, initially as categorical data after stratification based on the median IHC value. The data was then further analysed as a continuous variable employing Cox univariable and multivariable analysis. IHC – immunohistochemistry; TMA – tissue microarray.

3.2.4.1 CD3+ lymphocytes

The first TIL marker assessed on the two cohorts previously discussed was the pan-lymphocyte marker CD3. This was selected on the basis that all lymphocytes will express CD3 on their cell surface and would provide information on the global level of infiltrating lymphocytes in my cohorts. Each sample was represented on a TMA in triplicate, with the CD3 positively stained TILs quantified for each 0.7854mm^2 circular core. The average score from the three cores was taken as the TIL count for analysis. The CD3+ IHC data for the combined pazopanib-treated cohort (n=50) was first analysed as a categorical variable, by splitting the cohort into two equally sized subgroups based on the median IHC value for the cohort. For the combined cohort, the median IHC score for CD3+ was 44.8 cells per 0.7854mm^2 core, the interquartile range (IQR) was 12.5 to 96.5, and the cohort range was 1 to 613.5. Following stratification into CD3+ high and CD3+ low subgroups, Kaplan-Meier plots were generated for OS and PFS, with univariable Cox regression analysis employed with CD3+ count the variable of interest (**Figure 3.9.A** and **B**). For OS, there was no significant difference when comparing CD3+ high and low groups (mOS CD3.Hi 9.1 months versus CD3.Lo 9.7 months; p=0.821). For PFS, again there was no statistically significant difference reported (mPFS CD3.Hi 4.7 months versus 3.7 months CD3.Lo; p=0.820).

To assess if any survival difference was observed in a cohort of STS treated with an alternative second-line therapy, the comparator cohort (n=22) was then analysed. The comparator had a median CD3+ IHC score of 44.7 cells per core, the IQR was 20.2 to 103.2, and a cohort range of 1 to 1249. Using the same cut-off score as was applied to the combined cohort, the comparator was stratified into CD3+ high and CD3+ low groups, each containing 11 cases. Kaplan-Meier survival curves for OS and PFS were plotted, and Cox univariable regression based on high or low subgrouping was employed for statistical analysis (**Figure 3.10.A** and **B**). The CD3+ high group had a mOS of 11.2 months and a mPFS of 4.7 months. For the CD3+ low group, the mOS was 11.2 months and mPFS was 3.4 months. For both OS and PFS, there was no significant difference reported between the CD3+ high and low subgroups (p=0.789 and p=0.188 respectively).

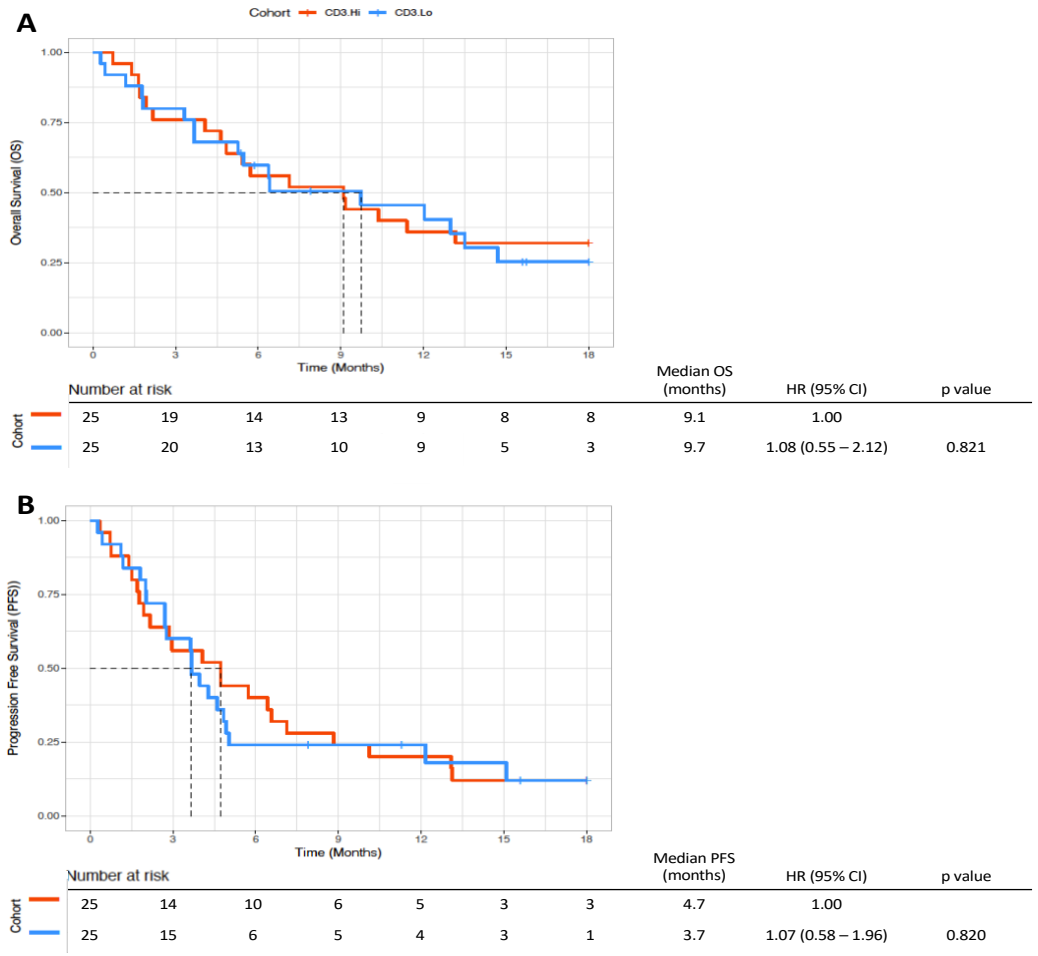

Figure 3.9: Kaplan-Meier survival plots for **A** overall survival and **B** progression-free survival for the combined cohort stratified based on the median CD3+ count into high and low subgroups.

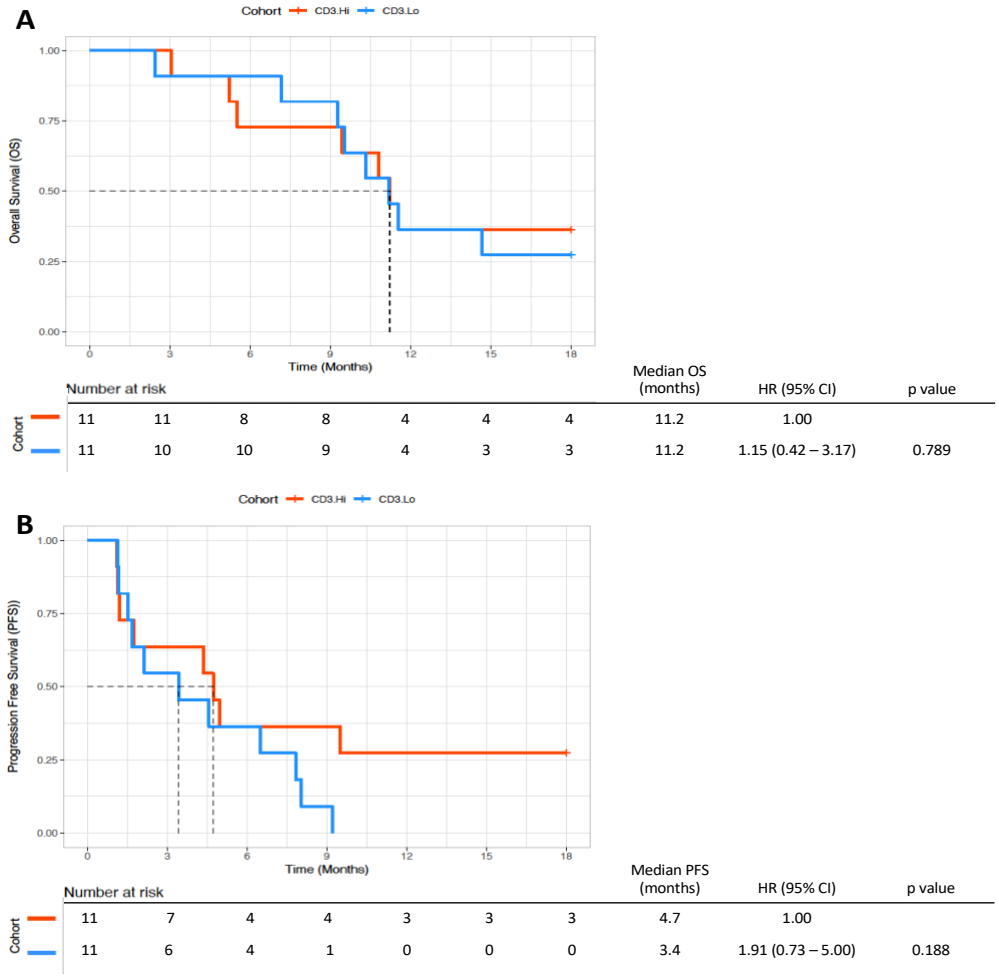

Figure 3.10: Kaplan-Meier survival plots for **A** overall survival and **B** progression-free survival for the comparator cohort stratified based on the median CD3+ count (44.8) previously reported in the combined cohort, into high and low subgroups.

The CD3+ IHC data were then analysed as a continuous variable, employing Cox univariable and multivariable analysis. For multivariable analysis, patient age, tumour grade, performance status and STS subtype were included as co-variables along with the CD3+ count. For the combined cohort, Cox univariable analysis did not show any statistically significant association between CD3+ count and either OS or PFS (OS – HR 1.002 (95% CI 0.99 – 1.01), p = 0.222; PFS – HR 1.00 (95% CI 0.99 – 1.00), p = 0.602). For the multivariable analysis of the combined cohort, both performance status and tumour grade were significantly associated with OS, however, the other co-variables including CD3+ count did not have a significant association with OS (**Figure 3.11.A**). Multivariable analysis for PFS only revealed a significant association between performance status and PFS, with all the other co-variables not demonstrating any significant differences (**Figure 3.11.B**).

The comparator cohort was then analysed utilising the same methods. Univariable analysis of CD3+ count showed no significant association with either OS or PFS (OS – HR 1.00 (95% CI 0.99 – 1.00), p = 0.694; PFS – HR 1.00 (95% CI 1.00 – 1.00), p = 0.336). Furthermore, following multivariable analysis, CD3+ demonstrated no significant association with either OS or PFS (**Figure 3.12.A** and **B**). Indeed, the only variable associated with significant differences in either OS or PFS was tumour grade which was significantly associated with PFS.

A

Overall Survival

OS	HR	95% CI	p value
CD3	1.001	1.00 - 1.00	0.603
Age	1.006	0.98 - 1.04	0.627
PS	2.131	1.29 - 3.52	0.003
Grade	3.145	1.47 - 6.72	0.003
Subtype	1.256	1.00 - 1.58	0.052

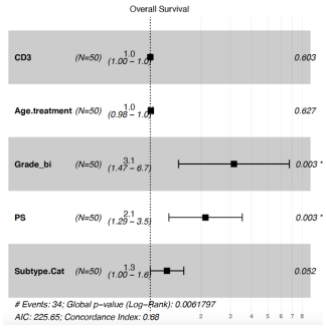

B

Progression Free Survival

PFS	HR	95% CI	p value
CD3	1.000	1.00 - 1.00	0.832
Age	1.001	0.98 - 1.02	0.955
PS	1.551	1.02 - 2.36	0.041
Grade	1.825	0.94 - 3.53	0.074
Subtype	1.065	0.87 - 1.31	0.551

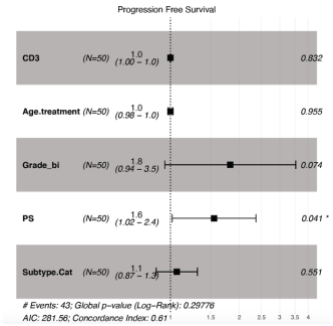

Figure 3.11: Table of results and equivalent forest plot demonstrating results of multivariable Cox analysis of the combined cohort for **A** overall survival and **B** progression-free survival.

A

Overall Survival

OS	HR	95% CI	p value
CD3	1.001	1.00 - 1.00	0.599
Age	1.036	0.98 - 1.10	0.207
PS	1.285	0.53 - 3.10	0.577
Grade	0.395	0.12 - 1.35	0.139
Subtype	1.243	0.89 - 1.74	0.207

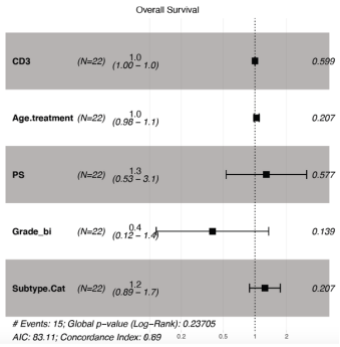

B

Progression Free Survival

PFS	HR	95% CI	p value
CD3	1.000	1.00 - 1.00	0.738
Age	1.023	0.98 - 1.07	0.330
PS	1.388	0.61 - 3.14	0.431
Grade	0.313	0.11 - 0.91	0.033
Subtype	0.864	0.65 - 1.16	0.324

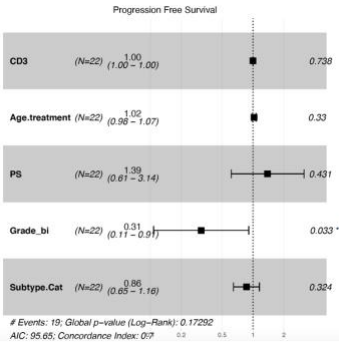

Figure 3.12: Table of results and equivalent forest plot demonstrating results of multivariable Cox analysis of the comparator cohort for **A** overall survival and **B** progression-free survival.

3.2.4.2 CD4+ lymphocytes

The CD4 cell surface glycoprotein serves as a co-receptor for T-cell receptors and is expressed on several immune cells, including helper class T-cells. Given the interaction between CD4+ T-cells and B-cell driven antibody production, as well as the interaction with cytotoxic T-cells, CD4+ cells play a key role in immune responses. As such, there is a rationale for exploring these as potentially important biomarkers associated with clinical outcomes following treatment with pazopanib.

The CD4+ IHC data for the combined cohort (n=50) was first analysed as a categorical variable, with stratification using the cohort median CD4+ value of 14.2 cells per 0.7854mm^2 core to categorise the cohort into CD4+ high and low subgroups. For the combined cohort, the IQR was 2.8 to 28.8 positively stained cells per core, whilst the cohort minimum CD4+ cell count was 0, and the maximum was 168.7. Survival differences between the CD4+ high and low subgroups of the combined cohort were then analysed by plotting Kaplan-Meier survival curves for both OS and PFS, with univariable Cox analysis with CD4+ positive cell counts the variable of interest (**Figure 3.13.A** and **B**). In terms of OS, the CD4+ high subgroup had a mOS of 6.4 months compared to 9.1 months in the CD4+ low subgroup, and this was not a significant difference (p=0.544). For PFS, the CD4+ high subgroup mPFS was 2.7 months compared to 4.8 months in the CD4+ low subgroup, and again this was not a significant difference (p=0.155).

The association between CD4+ count and survival was then analysed for the comparator cohort (n=21). For the comparator cohort, the median CD4+ score was 35 cells per core, with a cohort interquartile range of 5.3 to 35 positive cells, and a cohort minimum value of 0 and maximum value of 689.7. In order to stratify the cohort, the same cut-off that was applied to the combined cohort, an average score of 14.2 positive CD4+ cells per core, to determine CD4+ high and low subgroups in the comparator cohort. This resulted in a CD4+ high subgroup containing 14 cases, and a CD4+ low subgroup containing 7. Kaplan-Meier OS and PFS survival plots were generated, and Cox univariable analysis was

employed to assess for any between-subgroup significant differences in survival (**Figure 3.14.A** and **B**). From these analyses, the CD4+ low subgroup mOS was 14.7 months compared to 10.2 months in the CD4+ high subgroup, and this was not significantly different (p=0.188). However, the CD4+ low subgroup had a shorter mPFS than the CD4+ high subgroup (1.7 months versus 5.7 months), and Cox univariable analysis demonstrated that the difference in PFS between the two subgroups was statistically significant, with the CD4+ low subgroup having a higher risk of progression (HR 3.0, 95% confidence interval (CI) 1.06-8.58); p=0.039).

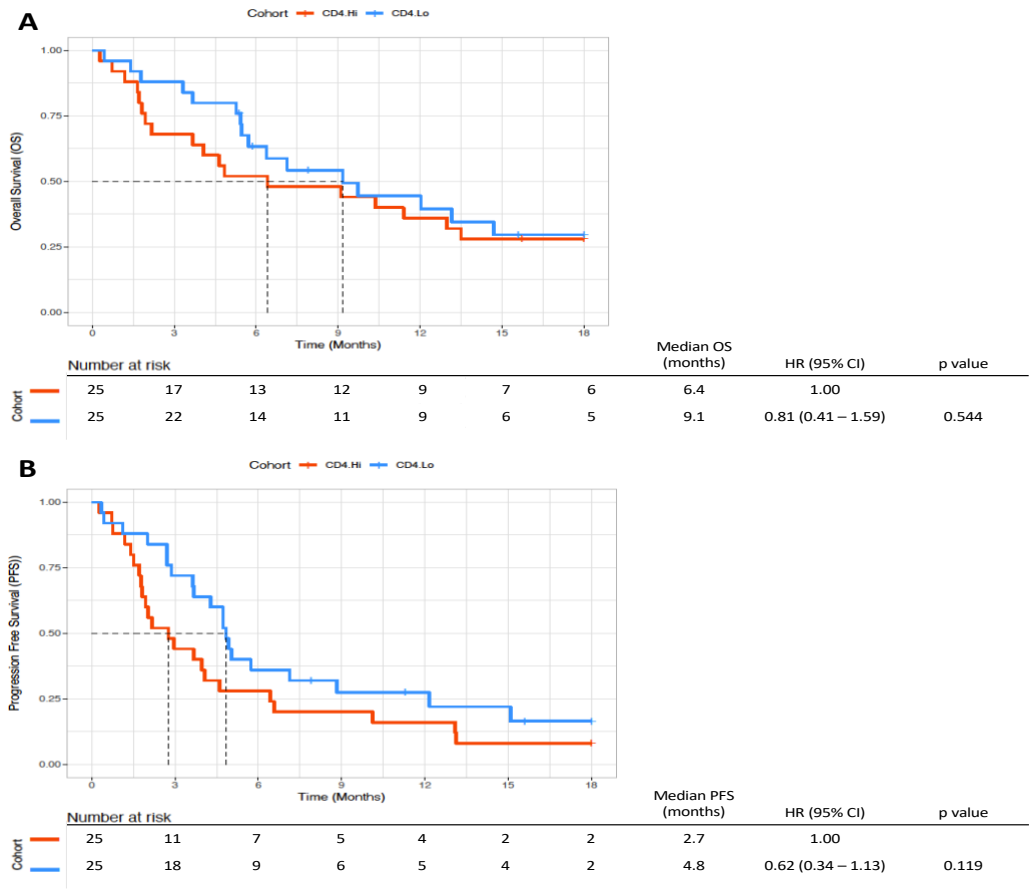

Figure 3.13: Kaplan-Meier survival plots for **A** overall survival and **B** progression-free survival for the combined cohort stratified based on the median CD4+ count into high and low subgroups.

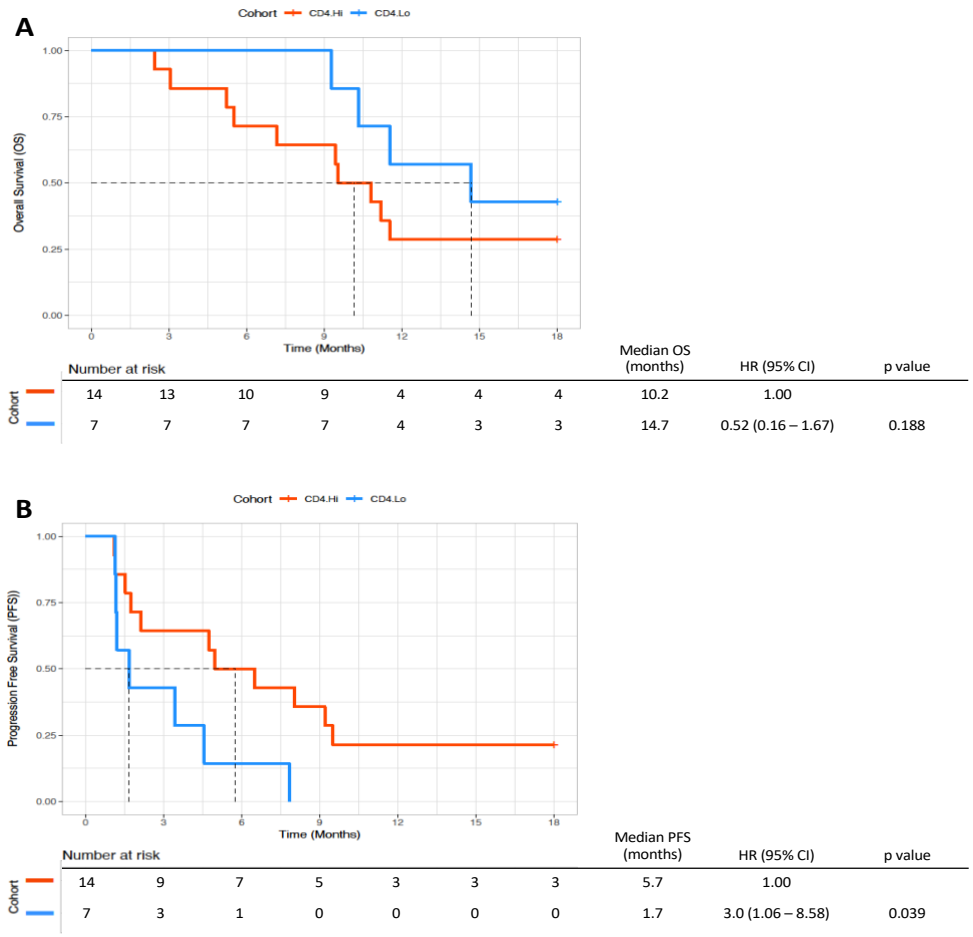

Figure 3.14: Kaplan-Meier survival plots for **A** overall survival and **B** progression-free survival for the comparator cohort stratified based on the median CD4+ count (14.2) previously reported in the combined cohort, into high and low subgroups.

To further investigate the CD4+ data, it was then analysed as a continuous variable and Cox univariable and multivariable analysis was employed. As with the CD3+ analysis, for the multivariable analysis, patient age, tumour grade, performance status and STS subtype were included as co-variables along with the CD4+ count.

In the combined cohort, from univariable analysis, there was a significant association between CD4+ count and OS (HR 1.02 (95% CI 1.01 – 1.03); p = 0.0026). In addition, there was a significant association between CD4+ count and PFS (HR 1.02 (95% CI 1.004 – 1.03); p = 0.0048). In both cases, increased CD4+ count was associated with a higher hazard ratio and therefore shorter OS and PFS. When including the clinicopathological variables described above as part of the multivariable analysis, again both OS and PFS showed a significant association with CD4+ count (OS p=0.0007; PFS p=0.002) **(Figure 3.15.A** and **B**). As with the univariable analysis, for multivariable analysis increasing CD4+ count was associated with an increase in the hazard ratio, and therefore a shorter OS and PFS time. In addition, tumour grade and patient performance status were significantly associated with inferior OS (p=0.006 and p=0.0004 respectively), whilst for PFS only tumour grade, as well as CD4+ count, were associated with inferior PFS (p=0.012).

The comparator cohort was then analysed utilising the same methods. Univariable analysis of CD4+ count showed no significant association with either OS or PFS (OS - HR 1.00 (95% CI 0.99 – 1.00), p = 0.478; PFS - HR 0.992 (95% CI 0.98 – 1.00; p = 0.051). In addition, multivariable analysis did not show any significant associations between any of the variables included and OS (**Figure 3.16.A**). However, multivariable analysis for PFS showed a significant association between CD4+ count and PFS, with increased CD4+ count associated with a reduced hazard ratio, and thus a longer time to progression (p=0.049)(**Figure 3.16.B**). For the comparator cohort, tumour grade was also shown to be significantly associated with PFS.

A

Overall Survival

OS	HR	95% CI	p value
CD4	1.022	1.01 - 1.04	0.0007
Age	1.006	0.98 - 1.04	0.703
PS	2.383	1.48 - 3.84	0.0004
Grade	2.839	1.34 - 6.01	0.006
Subtype	1.319	1.06 - 1.65	0.015

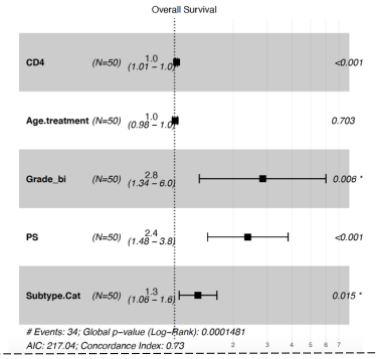

B

Progression Free Survival

PFS	HR	95% CI	p value
CD4	1.020	1.01 - 1.03	0.002
Age	0.998	0.97 - 1.02	0.864
PS	1.658	0.84 - 3.12	0.148
Grade	1.621	1.12 - 2.46	0.012
Subtype	1.100	0.90 - 1.34	0.348

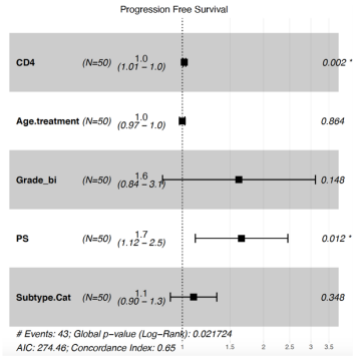

Figure 3.15: Table of results and equivalent forest plot demonstrating results of multivariable Cox analysis of the combined cohort for **A** overall survival and **B** progression-free survival.

A

Overall Survival

OS	HR	95% CI	p value
CD4	0.998	0.99 - 1.00	0.477
Age	1.030	0.98 - 1.08	0.307
PS	1.335	0.58 - 3.08	0.498
Grade	0.487	0.15 - 1.62	0.240
Subtype	1.278	0.89 - 1.83	0.178

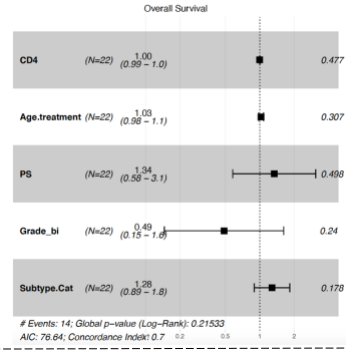

B

Progression Free Survival

PFS	HR	95% CI	p value
CD4	0.990	0.98 - 1.00	0.049
Age	1.004	1.055	0.862
PS	1.844	0.77 - 4.40	0.168
Grade	0.259	0.08 - 0.82	0.022
Subtype	0.847	0.62 - 1.15	0.290

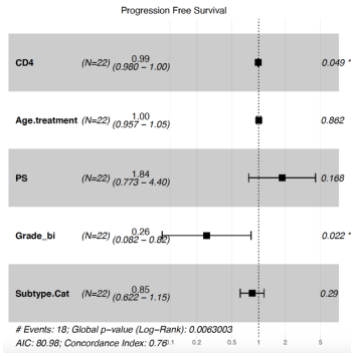

Figure 3.16: Table of results and equivalent forest plot demonstrating results of multivariable Cox analysis of the comparator cohort for **A** overall survival and **B** progression-free survival.

3.2.4.2 CD8+ lymphocytes

The final IHC stain considered was CD8, another T-cell co-receptor expressed most frequently by cytotoxic effector T-cells. As such, a high CD8+ cell count was hypothesised to be a marker for an immune microenvironment with strong anti-tumour immune activity.

Following the same workflow as previous, the combined cohort was stratified into CD8+ high and low around the median cohort CD8+ value of 26.7 positively stained cells per 0.7854mm^2 core. The cohort CD8+ cell count IQR was 5.7 to 59.1 per core, with the minimum count being 0 and the maximum count 469.3 CD8 positively stained cells. Kaplan-Meier plots for OS and PFS were generated, with statistical analysis by Cox univariable analysis based on CD8+ high or low subgroups (**Figure 3.17.A** and **B**). For OS, the CD8+ low subgroup mOS was 13.2 months compared to 6.4 months for the CD8+ high subgroup, but this difference was not significant (p=0.201). For PFS, the CD8+ low subgroup mPFS was 3.7 months compared to 4.6 months for the CD8+ high subgroup, and again this difference was not significant (p=0.683).

The comparator cohort was then analysed in the same fashion, being divided into high and low subgroups based on the combined cohort CD8+ median score of an average of 26.7 CD8+ positive cells per core. For the comparator cohort, the cohort median CD8+ count was 36.7 per core, with a cohort IQR of 13 to 93.3 positively stained cells, a maximum count of 1365.5 and a minimum count of 0.3. For the comparator cohort, the CD8+ high subgroup had a mOS of 11.5 months compared to 10.7 months for the CD8+ low subgroup, and no significant difference was observed (p=0.273) (**Figure 3.18.A**). For PFS, the CD8+ high subgroup mPFS was 4.7 months compared to 4.0 months for the CD8+ low subgroup, with no significant difference in PFS reported (p=0.364)(**Figure 3.18.B**).

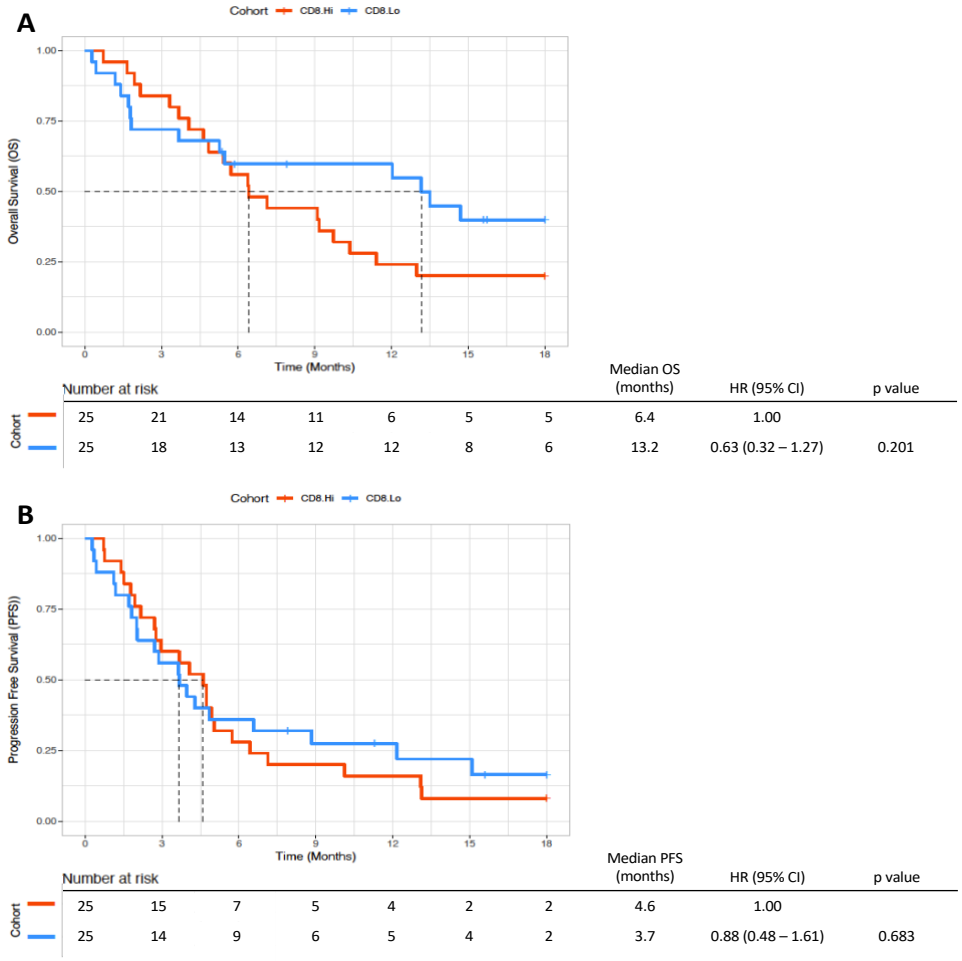

Figure 3.17: Kaplan-Meier survival plots for **A** overall survival and **B** progression-free survival for the combined cohort stratified based on the median CD8+ count into high and low subgroups.

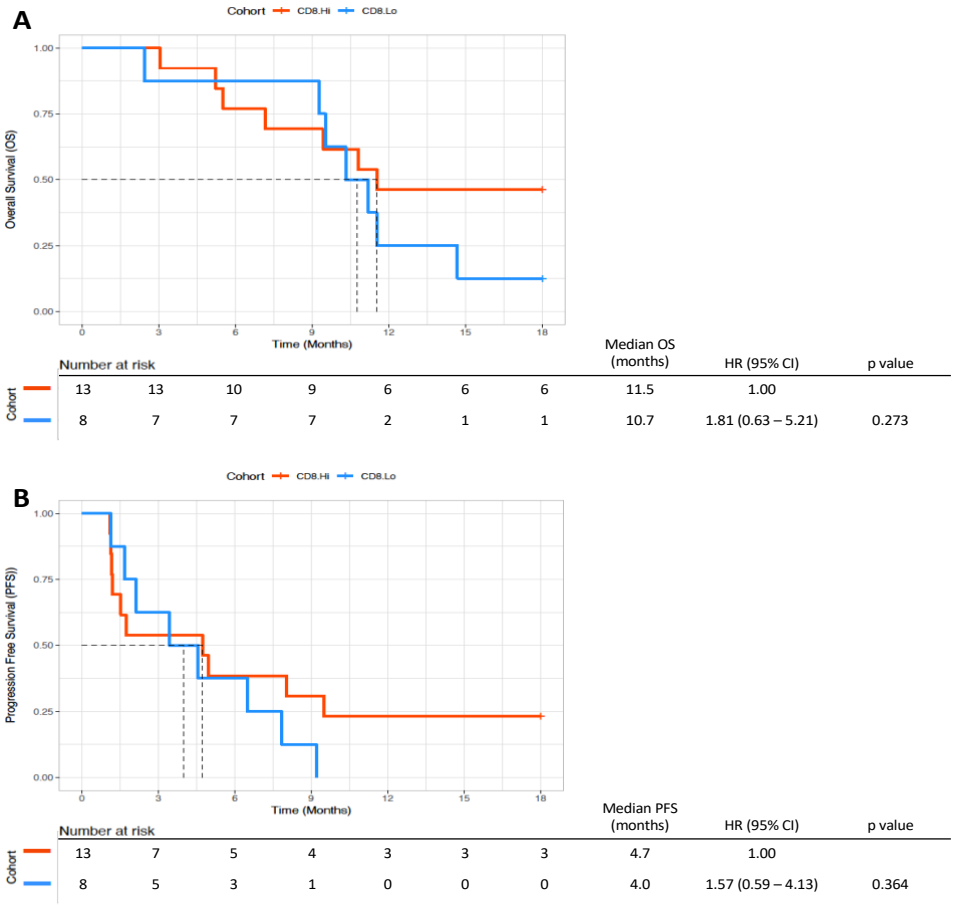

Figure 3.18: Kaplan-Meier survival plots for **A** overall survival and **B** progression-free survival for the comparator cohort stratified based on the median CD8+ count (26.7) previously reported in the combined cohort, into high and low subgroups.

The CD8+ data was then analysed as a continuous variable, employing Cox univariable and multivariable analysis to assess for associations between CD8+ count and variable OS and PFS. For the multivariable analysis, patient age, tumour grade, performance status and STS subtype were included with CD8+ count as co-variables for analysis.

In the combined cohort, the univariable analysis did not show any significant association between CD8+ and either OS (HR 1.002 (95% CI 0.99 – 1.01), p = 0.280) or PFS (HR 0.999 (95% CI 0.99 – 1.00), p = 0.860). Following multivariable analysis for OS, both performance status (p=0.005) and tumour grade (p=0.002) were both significantly associated with OS (**Figure 3.19**). However, the CD8+ count was not significantly associated with OS. Following multivariable analysis for PFS, only performance status was significantly associated with PFS (p=0.033), with none of the other co-variables, including CD8+ count, significantly associated with PFS.

Subsequent analysis of the comparator cohort CD8+ results was also undertaken, and again there was no significant association between CD8+ count and either OS or PFS on univariable analysis (OS - HR 1.00 (95% CI 1.00 – 1.00), p = 0.857; PFS - HR 0.999 (95% CI 0.997 – 1.001), p = 0.290). Multivariable analysis did not show any of the co-variables to be significantly associated with OS, whilst only tumour grade was found to be significantly associated with PFS (**Figure 3.20**).

A

Overall Survival

OS	HR	95% CI	p value
CD8	1.002	1.00 - 1.01	0.403
Age	1.006	0.98 - 1.03	0.673
PS	2.049	1.24 - 3.39	0.005
Grade	3.341	1.54 - 7.24	0.002
Subtype	1.246	0.99 - 1.56	0.056

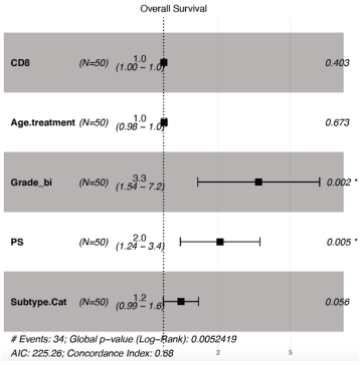

B

Progression Free Survival

PFS	HR	95% CI	p value
CD8	0.999	0.99 - 1.00	0.621
Age	1.002	0.98 - 1.03	0.883
PS	1.628	1.04 - 2.55	0.033
Grade	1.776	0.91 - 3.47	0.093
Subtype	1.090	0.89 - 1.34	0.412

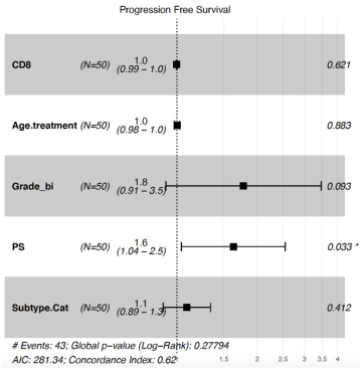

Figure 3.19: Table of results and equivalent forest plot demonstrating results of multivariable Cox analysis of the combined cohort for **A** overall survival and **B** progression-free survival.

A

Overall Survival

OS	HR	95% CI	p value
CD8	1.000	1.00 - 1.00	0.819
Age	1.035	0.98 - 1.10	0.226
PS	1.374	0.55 - 3.41	0.493
Grade	0.409	0.11 - 1.46	0.168
Subtype	1.205	0.85 - 1.70	0.291

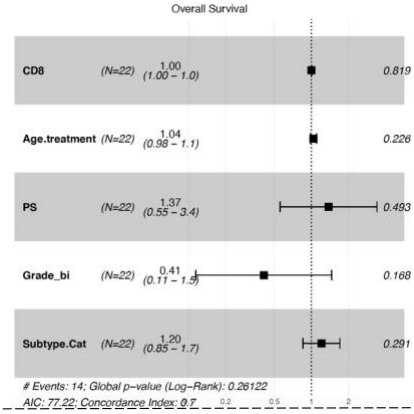

B

Progression Free Survival

PFS	HR	95% CI	p value
CD8	1.000	1.00 - 1.00	0.681
Age	1.027	0.98 - 1.08	0.291
PS	1.504	0.63 - 3.59	0.358
Grade	0.281	0.09 - 0.89	0.030
Subtype	0.833	0.61 - 1.13	0.236

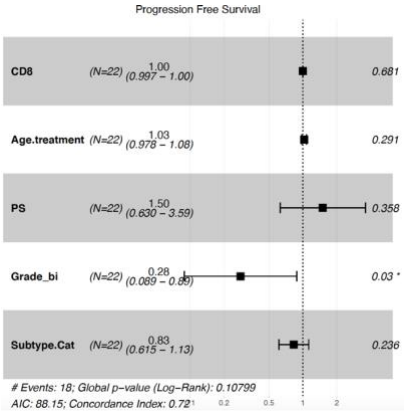

Figure 3.20: Table of results and equivalent forest plot demonstrating results of multivariable Cox analysis of the comparator cohort for **A** overall survival and **B** progression-free survival.

3.2.4.3 Correlation of immune markers

In order to confirm the robustness of our results, correlation plots were generated to examine the relationship between CD3+ cells and the sum of CD4+ and CD8+ cells per 0.7854mm^2 TMA core (**Figure 3.21**). The rationale for this being that as a pan-lymphocyte marker, CD4+ and CD8+ lymphocytes would also express CD3. Therefore, as the sum of the CD4+ and CD8+ counts increase, so should the CD3+ counts. From the correlation plot, a Spearman coefficient of 0.79 confirms, as expected, a strong positive correlation between the two IHC measures.

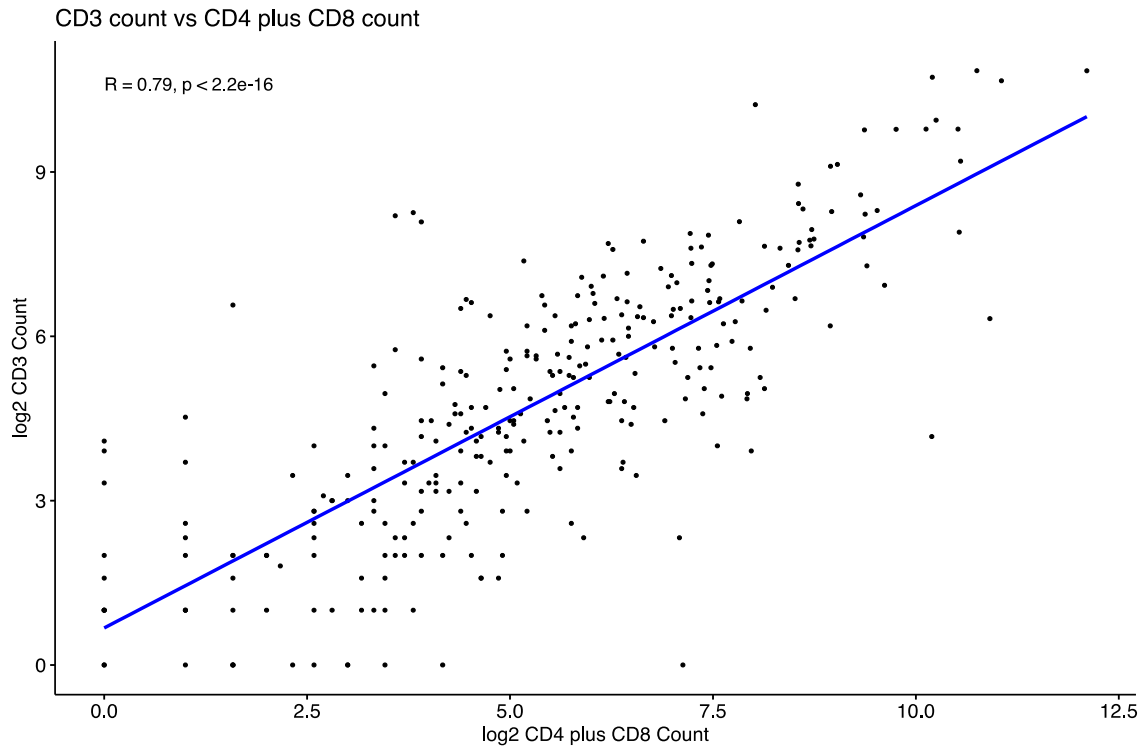

Figure 3.21: Correlation plot of the log2CD3+ cell count per 0.7854mm^2 circular core, plotted against the log2 of the sum of the CD4+ plus CD8+ cell count per 0.7854mm^2 core.

3.2.4.5 Summary of results

From my analysis of the IHC data for the combined cohort and comparator cohort, I observed that for the pazopanib-treated combined cohort on both univariable analysis, and multivariable analysis including clinicopathological features, increased CD4+ count was significantly associated with inferior OS and PFS. Conversely, for the non-pazopanib treated cohort, the data showed that following both stratification into CD4+ high and low subgroups, and from multivariable analysis as a continuous variable, lower CD4+ count was significantly associated with inferior PFS. For CD3+ and CD8+ IHC, there were no significant associations between IHC count and either OS or PFS in both the combined cohort and comparator cohort.

3.3 Discussion

3.3.1 Cohort generation and curation

Given the rarity of STS, and the scarcity of pre-pazopanib tissue available for these patients, one of the key steps for this thesis was to generate robust cohorts of patients. This would allow us to undertake work characterising the immune microenvironment and its association with clinical outcomes following pazopanib treatment in patients with advanced STS. To my knowledge, this body of work represents the largest effort to date to analyse the immune-based biology associated with clinical outcomes following pazopanib treatment in STS and identify immune-based biomarkers.

Initial analysis of the cohort clinicopathological variables shows the cohorts to be well balanced. Indeed, given the associations between both tumour grade and performance status and clinical outcomes, the lack of significant difference between the cohorts was an important observation to ensure comparability[342,343]. In addition, analysis of the Kaplan-Meier survival plots for OS and PFS comparing the combined and comparator cohorts showed no significant difference in survival by Cox univariable analysis. As the ultimate aim of this thesis is to identify immune-based biomarkers able to identify a subset of patients with superior clinical outcomes following pazopanib therapy, it was desirable to have cohorts with comparable survival data. The reason being that the pazopanib-treated combined cohort has not been selected based on clinical outcomes, but rather the combined cohort represents an unselected group of patients a clinician would encounter in the clinical setting. Thus, via description and characterisation of the tumour immune microenvironment, the study aims to determine a biomarker which is able to identify a subset of patients more likely to gain clinical benefit from pazopanib therapy.

The range of subtypes generated is also noted (**Figure 3.4**). Given the stated aim of generating an immune-based biomarker that can be utilised across multiple STS subtypes, and the use of pazopanib in the management of all non-adipocytic STS in the real-world setting, this variety of subtypes is a strength of these

cohorts. Furthermore, I chose to include tissue from a range of time points during the clinical course of disease, including primary tumour tissue, local recurrence tissue and metastatic tissue. As mentioned, there was only limited availability of primary tumour tissue available in patients with advanced STS treated with pazopanib. Therefore, in order to generate cohorts of sufficient size, the study was not limited to only include primary tissue. In addition, adopting this pragmatic approach would be more clinically relevant in the real-world setting for any future biomarkers as it would not limit applicability only to patients for whom primary tissue is readily available for analysis. Comparative analysis of the tissue timepoint between the cohorts also showed no significant difference in the proportion of primary, recurrence or metastatic tissue.

3.3.2 Association between tumour infiltrating lymphocytes and clinical outcome

Having confirmed the relative comparability of our cohorts in terms of clinicopathological variables, I then evaluated associations between levels of TIL and survival outcomes. My analysis showed a limited number of statistically significant results when utilising IHC TIL count to assess the association with OS and PFS. Comparing the results obtained here to the previously published literature is challenging because, as mentioned (**Section 1.5.3.1**), previously published results are relatively discordant. Indeed, from **Table 1.6**, it appears that in general, quantification of CD3+, CD4+ and CD8+ cells has rarely yielded statistically significant prognostic value, save for a small number of studies[282,283,344].

The most interesting results from the analysis of TILs in this chapter relate to the CD4+ results. For the combined cohort, multivariable analysis demonstrated a significant association between CD4+ count and inferior OS and PFS. Conversely, for the comparator cohort, CD4+ count was significantly associated with superior PFS, but not with OS. The results in the comparator cohort are concordant with the previous work by Schroeder et al., which demonstrated that for dedifferentiated liposarcoma, higher levels of CD4+ cells were significantly associated with longer recurrence-free survival[345]. As a generic marker for T-

helper cells, the association between CD4+ and variable clinical outcome is interesting, as it highlights the potential for characterisation of the immune microenvironment to offer potential clinically relevant biomarkers for variable clinical outcomes. Furthermore, the fact higher CD4+ levels are associated with superior outcomes in the pazopanib-treated cohort, whilst in the cohort which received alternative second-line therapy higher CD4+ counts were associated with inferior PFS, suggests there may be an association with pazopanib treatment. This would be more valuable in the clinical setting as it would allow patient stratification and identification of patients who would most likely gain clinical benefit from pazopanib, thus leading to patient-specific treatment. This has benefits in terms of the specific patient being targeted with the most efficacious treatment, gaining clinical benefit whilst also limiting exposure to the morbidity of less effective therapy. And on a wider health economics perspective, the cost of treating patients would be focused on those most likely to benefit from it.

The consensus from previous molecular studies is that STS which are considered immune hot and have higher levels of infiltrating effector cells of the immune system tend to be associated with superior clinical outcomes[290,291,293]. It is hypothesised that an immune-infiltrated tumour microenvironment is indicative of an active anti-tumour immune response. Conversely, in an “immune desert” tumour which is poorly infiltrated by immune cells, this provides a niche for tumour cells to grow without exposure to the effects of anti-tumour immune cells[293]. Immunohistochemistry only characterises single immune cells, and therefore may not capture nuanced interactions between various immune cells as well as other microenvironment factors. Nonetheless, in our combined cohort I reported a trend for higher levels of CD4+ cells to be associated with inferior clinical outcomes. Although not possible to imply causation from these associations, our data can be used as a hypothesis-generating exercise. Based on the fact that the more immune infiltrated tumours, in terms of CD4+ cells, have a trend towards inferior PFS and OS following pazopanib therapy, we could hypothesise that fewer immunosuppressive CD4+ regulatory or helper2 T-cells present in the microenvironment heightens the anti-tumour immunity of additional effector cells

recruited into the microenvironment following pazopanib therapy. However, in order to confirm this hypothesis, a comparison of pre- and post-pazopanib immune profiles would be necessary. Alternatively, it could be that a regulated immune tumour microenvironment in some way protects STS from the anti-tumour effects of pazopanib. The observed trends in this chapter do indicate that there is value in looking at the immune microenvironment in more detail. Firstly to gain a deeper knowledge of the immune biology in STS, but also as a potential source for biomarkers predictive of clinical outcomes following pazopanib treatment.

3.3.3 Critical assessment of methods and potential alternatives

One of the key considerations when designing the cohorts and planning the flow of experiments was the scarcity and quality of tumour tissue available for a small subset of patients with rare cancers. As such, the choices made reflect a need to maximise the information acquired from each tissue sample. Indeed, a sizeable portion of the samples available were tumour biopsies rather than excisional samples, and therefore only provided a small volume of tumour tissue for analysis. In these cases, taking three cores for TMA generation would exhaust the tissue sample, whilst taking whole sections would only allow a small number of IHC stains before the tissue block was exhausted. Thus, the decision was made to prioritise nucleic acid extraction for downstream analysis over IHC studies. The rationale being that the planned immune gene expression analysis would offer more insight and granularity to the immune microenvironment, including immune cell infiltration through deconvolution techniques. Furthermore, surplus nucleic acids could be stored for future experiments outside the remit of this present study. Given this decision, some cases were available for immune gene analysis but the number available for IHC analysis was smaller (**Figures 3.1** and **3.2**).

As well as focusing on nucleic acid extraction, the decision to employ TMAs as input for the IHC experiments was again based on the limited volume of tissue required for TMA construction. An alternative approach would have been to take whole sections and stain each for the marker in question, however, such an

approach would be more consumptive of the precious tumour tissue. In addition, studies have previously demonstrated TMAs to be a reliable method for immune cell characterisation, robustly accounting for intra-tumoural heterogeneity[317].

If a greater supply of tissue were to become available, a potentially interesting extension of this IHC work could become feasible. For example, an assessment of the immune microenvironment in different spatial areas of the tumour might be an interesting study to undertake given evidence that immune cells, including regulatory T-cells, demonstrate significant spatial intratumoural heterogeneity[346]. Therefore, exploring the spatial variability in the immune contexture could highlight variable clinical outcomes based on enrichment of immune cells in different tumoural areas. An alternate body of work could employ recent advances in multiplex IHC or immunofluorescence techniques to undertake the staining of multiple immune cells on the same single section of tumour tissue. This has the advantage of allowing the description of the spatial relationships between different immune cells. Both of these techniques require multiple sections of tumour tissue, and assessing spatial intratumoural heterogeneity requires multiple well-curated tissue blocks. As such, given the limited tissue available these were not feasible in this study, but would represent interesting future studies if more tissue becomes available.

Having decided on the approach to proceed with, this arm of the project did have some limitations. Firstly, by only examining the IHC stains CD3, CD4 and CD8, these markers are relatively generic in their expression across a range of immune cells involved in both anti- and pro-immunogenic responses. For example, CD4 is expressed on both T-helper1 cells which promote the cytotoxic anti-tumour effects of CD8+ cells, but also on T-helper2 cells and regulatory T-cells, which suppress effector cells of the immune system and help promote tumour growth. As such, it is difficult to confidently imply the biology driving the trends identified in OS and PFS differences between the high and low subgroups. Indeed, genomic analyses may yield more granularity into the nature of the immune microenvironment and the immune-related biology within our cohorts.

In terms of the markers selected for IHC analysis, additional immune cells of interest could have been assessed to add further information to the microenvironment in these samples. Indeed, a number of additional stains were explored as part of the experimental work associated with this chapter. For example, tumour-associated macrophages have previously been identified as potentially associated with clinical outcomes in STS[264,347]. However, previous attempts within the lab had difficulty in accurately quantifying the number of positively stained macrophages given the amorphous structure macrophages adopt. As such, past experience with the assistance of a consultant histopathologist (Dr Khin Thway) deemed it not feasible to include macrophage stains due to the lack of robust and reliable quantification methods. Additionally, the TMA slides were stained for CD20, a marker for antibody-producing B-cells. However, it was observed there was minimal positive staining across the whole cohort. Subsequently, a paper was published which identified that within STS, B-cells tend to be focused within B-cell rich tertiary lymphoid structures, and as such are more likely to be identified, if at all, on whole sections rather than TMAs[293]. Given the generally minimal staining observed, and the high risk of not sampling B-cell rich tertiary lymphoid structures as part of the TMA core, the decision was made not to include this stain within the data. Finally, the marker for the anti-immunogenic regulatory T-cells, FOXP3, was explored as a potential interesting marker to quantify. However, the facility which undertook these IHC staining experiments did not have an optimised protocol to undertake the staining. Despite efforts to acquire robust antibodies and determine an optimal protocol, this was ultimately unsuccessful.

A further limitation to note is that these cohorts were generated retrospectively, and do represent a heterogeneous cohort, making them susceptible to a range of biases. Indeed, factors such as variable time from sampling to treatment initiation, STS subtype heterogeneity, and the inclusion of primary, recurrence and metastatic tissue, need to be considered as potential sources of uncontrollable variability. However, as discussed this heterogeneity is more aligned to real-world clinical experience, and could allow greater unrestricted utility for any putative biomarkers for improved outcomes following pazopanib

treatment that I develop. Furthermore, for the combined cohort, the OS and PFS from pazopanib are similar to those reported in the literature supporting the generalisability of results garnered from analysis of these cohort[130,132].

3.3.4 Summary

In summary, given the finding that higher CD4+ levels are significantly associated with OS and PFS in the combined cohort following initiation of pazopanib, and the lack of granularity provided by these IHC experiments, there is a rationale for pursuing more in-depth characterisation of the immune contexture through gene expression analyses which will be described in subsequent chapters.

Chapter 4 - Immune gene expression in soft tissue sarcomas and the association with clinical benefit from pazopanib therapy

4.1 Background and objectives

In order to characterise the tumour immune microenvironment of a cohort of patients with advanced soft tissue sarcoma (STS) treated with the tyrosine kinase inhibitor (TKI) pazopanib, targeted immune-related gene expression analysis was undertaken. As discussed in **Section 1.5.3.2**, there is an increasing appreciation of the potential of molecular immune genotypes to play a role as biomarkers in STS, including evidence of value in predicting response to immune checkpoint inhibitors[291,293]. Furthermore, in **Section 1.5.3.3**, published reports have demonstrated an immune-modulating effect of anti-vascular endothelial growth factor receptor (VEGFR) TKIs including pazopanib[303304]. In **Chapter 3** I showed a statistically significant association between increased CD4+ tumour infiltrating lymphocyte (TIL) count and inferior overall survival (OS) and progression-free survival (PFS) in the pazopanib-treated combined cohort. Conversely, in the comparator cohort treated with alternative second-line therapies, increased CD4+ TIL count was associated with superior PFS.

At present, the tumour immune microenvironment in STS is incompletely characterised. As such, the work in this chapter looks to address the hypothesis that molecular characterisation of the tumour immune microenvironment will identify immune-based biological subgroups which are characterised by differential immune gene expression and enrichment for different immune cells.

In order to address this hypothesis, the aims of this chapter were to;

1. Undertake immune gene expression analysis of pre-pazopanib formalin-fixed paraffin-embedded (FFPE) tumour samples from patients who received pazopanib in the management of advanced STS.
2. Identify immune-gene based subgroups, and assess these subgroups for differential enrichment for different immune cells.
3. Characterise differences in the tumour immune microenvironment in STS based on histological subtype, patient age and tumour grade.

4.1.1 Contributions

Work of the candidate included;

- Study conception and design in conjunction with the supervisory team
- Data normalisation
- Principle component analysis
- Complex heatmap generation
- Curation of gene sets for immune cells from gene annotations supplied by Nanostring
- Single sample gene set enrichment analysis
- Generation of box plots based on immune cell and immune function gene signatures

Advanced statistical analysis was undertaken under the supervision of Dr Maggie Cheang, team leader at the Institute of Cancer Research's (ICR) Clinical Trials and Statistics Unit.

The original Royal Marsden cases for the combined cohort were identified by Dr Alex Lee. This cohort was checked and modified by the candidate, and the clinical data was updated.

RNA extraction, quality control and aliquoting of RNA for subsequent Nanostring analysis were performed by higher scientific officer Nafia Guljar.

Running of the Nanostring assay was performed by Richard Buus, senior scientific officer at the ICR's Ralph Lauren centre.

4.2 Results

4.2.1 Comprehensive immune gene expression analysis employing the Nanostring nCounter platform

In order to generate robust immune gene expression profiles of pre-pazopanib tissue in the combined cohort, I chose to employ the nCounter PanCancer immune profiling panel (Nanostring Technologies, Washington, USA). Nanostring nCounter is a high-throughput, multiplex, fluorescence-based digital hybridisation technology which allows the profiling of individual molecular targets[348]. This is achieved by assigning fluorescently labelled probes to genes of interest. Each assay consists of two probes of 50 base pairs (bp) in length, constituting a biotin-labelled capture probe and a reporter probe labelled with 7 fluorescent tags. The fluorescent tags are then read by a computerised camera and microscope, with the order of the tags acting as a barcode to indicate which gene target the probs have bound to. In this manner, up to 800 genes can be assessed per sample, and up to 12 samples can be analysed on a single cartridge.

The Nanostring platform has a number of advantages over other technologies available for gene expression analysis. One of the greatest considerations for this study was the quality and quantity of tumour material available for analysis. All of the samples included in my cohort were obtained from archival storage, and had been processed via formalin fixation and generally had been stored for long periods in paraffin. FFPE tissue has the advantage of preserving morphological features of the tumour, however, the process is known to lead to the degradation of ribonucleic acid (RNA) into low molecular weight species, limiting its use as input material for other gene expression technologies[349]. In addition, in my cohorts, for a number of cases, the only available tissue for analysis was a biopsy sample and therefore was of low tissue volume. As such, although utilising an optimised RNA extraction protocol, the key challenges faced were in terms of RNA integrity and quantity which was extractable from a limited supply of precious tumour material. However, Nanostring technology is able to reliably

detect fragmented RNA, whilst the direct measurement of target molecules and the absence of an amplification step help reduce bias. Indeed, a number of studies have confirmed that Nanostring is able to generated high-quality data from degraded RNA samples, including from clinical biopsy samples[350–353].

There are alternative methods for gene expression analysis but some lack this flexibility when handling low-quality RNA samples. There are optimised protocols for next generation sequencing platforms, such as total RNA-Seq, that would allow characterisation of many thousands of transcripts. However, given the primary focus of this work is the immune microenvironment, the decision was made to proceed with Nanostring, having balanced the cost and need for roubst data–In addition, techniques such as reverse transcription polymerase chain reaction (RT-PCR) are only able to measure the expression of small panels of genes at a time. As such, they lack the multiplex capability of the Nanostring technology. Therefore, Nanostring was selected as the most suitable methodology to employ for immune-gene profiling of my cohorts.

The PanCancer immune profiling panel is a targeted 770-plex gene expression panel designed to allow comprehensive profiling of immune-related genes that fall into one of four functional categories[354];

- Infiltrating immune cells, including cells of the innate and adaptive immune systems
- Assessment of immunological functions including signalling pathways
- Identification of tumour-specific antigens
- Housekeeping genes for normalisation of data

As such, the PanCancer immune profiling panel provides an annotated set of genes encompassing the spectrum of immune influences on cancer development.

In order to optimise results obtained from the Nanostring experiments, a standardised workflow was adopted for the extraction of RNA and subsequent data analysis (**Section 2.5.1**). To assess tumour-related immune gene expression, haematoxylin and eosin (H&E) slides were marked for tumour area,

and where necessary macrodissection was performed to ensure a minimum of 75% tumour content. A total of four 4x20 µm sections were cut by microtomy for each case, and RNA extracted utilising the All Prep DNA/RNA FFPE kit (Qiagen, Hiden, Germany) as per the vendors procedures. Quality control (Qc) of the extracted RNA was then undertaken;

- The concentration of RNA was quantified using both the Qubit and Nanodrop fluorometer (both Thermo Fisher Scientific, Massachusetts, USA)
- The RNA integrity number (RIN) and proportion of total RNA between 50 and 300 bp was measured using the 2100 Bioanalyzer and associated software (Agilent, California, USA).

Based on prior experience within the team, a total of 150 ng of RNA, or up to 300 ng in particularly degraded samples, was aliquoted and was the input material for targeted immune gene expression analysis on the Nanostring platform. The raw data files were then processed and subsequent downstream analysis performed (**Figure 4.1**).

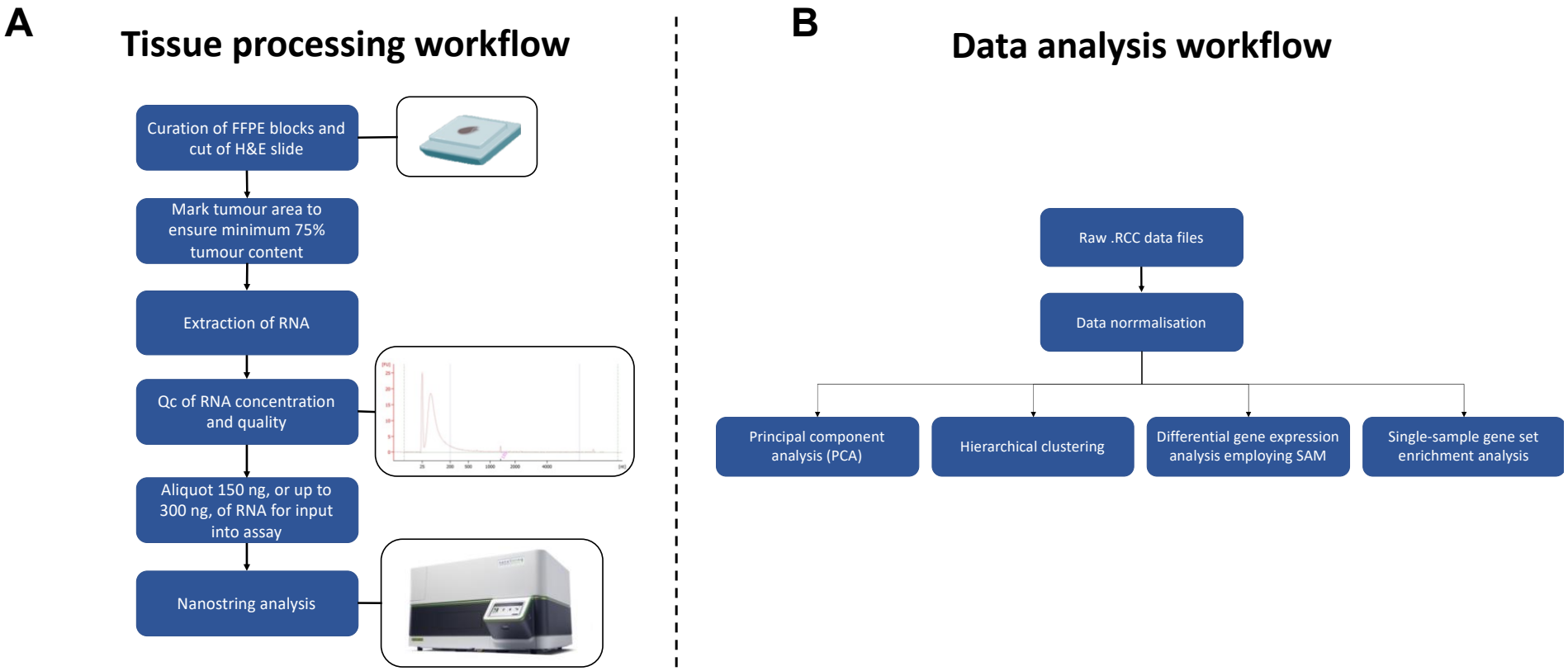

Figure 4.1.A and B: Planned workflows for **A** Tissue processing from formalin-fixed paraffin-embedded (FFPE) blocks, through RNA extraction and quality control (QC) to final aliquot to be used as input for Nanostring analysis **B** Data analysis work plan. RNA – ribonucleic acid.

4.2.2 Data normalisation

A total of 65 patients treated with pazopanib for the management of advanced STS met the inclusion and exclusion criteria for this study. In addition, adequate tumour material was available and extracted RNA was of sufficient quality to be included in Nanostring immune gene codeset analysis. Raw .RCC data files were log2 transformed, normalised in relation to positive and negative controls, and housekeeping genes, and finally median-centred (**Figure 1.A-E**).

For the combined cohort, **Figure 1.A** demonstrates that the distribution of the raw data, as expected, is skewed by the overexpression of a small number of genes in a few samples, but following log2 transformation, this effect is diminished (**Figure 1.B**). Background technical variability is corrected by normalisation (**Figures 1.C and D**) before the final standardised data set is visualised in **Figure 1.E** with the gene expression ranges centred around the median value.

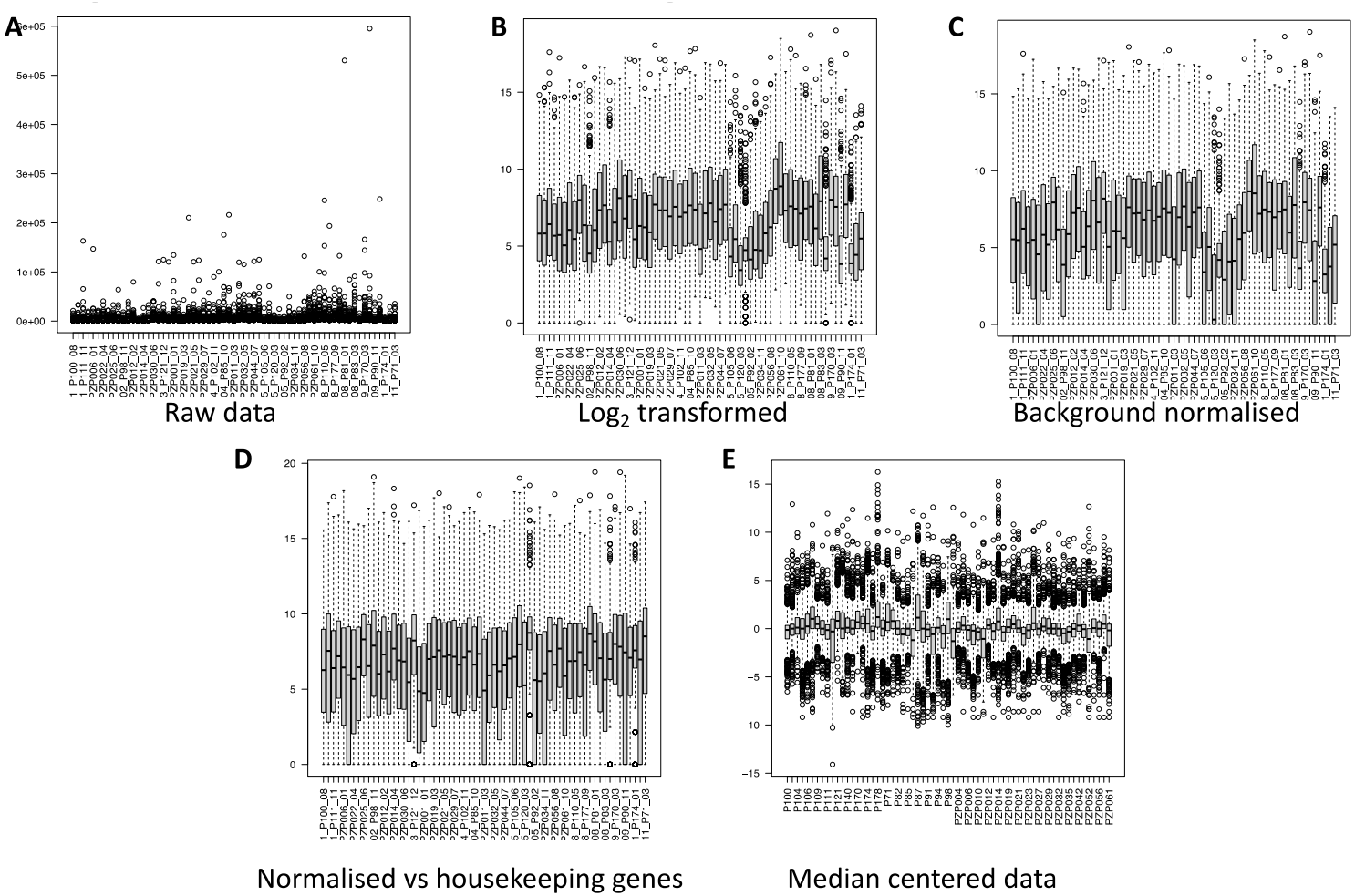

Figure 4.2.A-E: Dot and Box plots generated from the individual gene expression scores for each sample, and demonstrating the data normalisations processes for the discovery cohort. **A**. Raw gene expression data. **B** log_2 transformation of the data. **C** Normalised against positive controls to remove background noise. **D** Normalised against housekeeping genes. **E** The final data set for downstream analysis following median centring.

4.2.3 Principal component analysis

Following normalisation of the combined cohort immune gene expression dataset, I then proceeded to undertake exploratory analysis, starting with principal component analysis (PCA). The role of PCA is to act as a dimensionality-reduction approach, whereby a large set of variables is transformed into a smaller set of variables contributing to the highest variance for each principle component[326]. The ultimate goal is to reduce the large gene expression data set into a small number of principal components, retaining only the most important variables which can be used to explain the between-sample variations observed in the data.

From **Figure 2.A**, it can be observed that the samples do not cluster together when taking into account principal components 1 and 2. This suggests that reducing the dimensionality of the data to 2 principal components is not suitable for the dataset, as too much granularity is lost. Indeed, the variance explained by principal components 1 and 2 should be greater than 60%[355]. If less than 60% of variance is explained, then any assessment of between-sample differences would not be robust as not all of the available information is taken into account. Therefore, for these data in which the first 2 principal components only explain 30.0% of variance, reducing the data to principal components is not robust for subsequent analysis. To assess if alternative principle components might cluster the samples more effectively, a pairs plot (**Figure 2.B**) was generated. However, for all of the combinations up to five principal components, no clear clustering of samples is observed. Finally, the scree plot shown in **Figure 2.C** demonstrates that the optimal number of principal components is 10 by Horn's method or 11 by the elbow method. However, this degree of dimensionality is not suitable for data visualisation and analysis, and therefore for robust downstream analysis, reduction of these data to principle components was not considered the best method for this dataset.

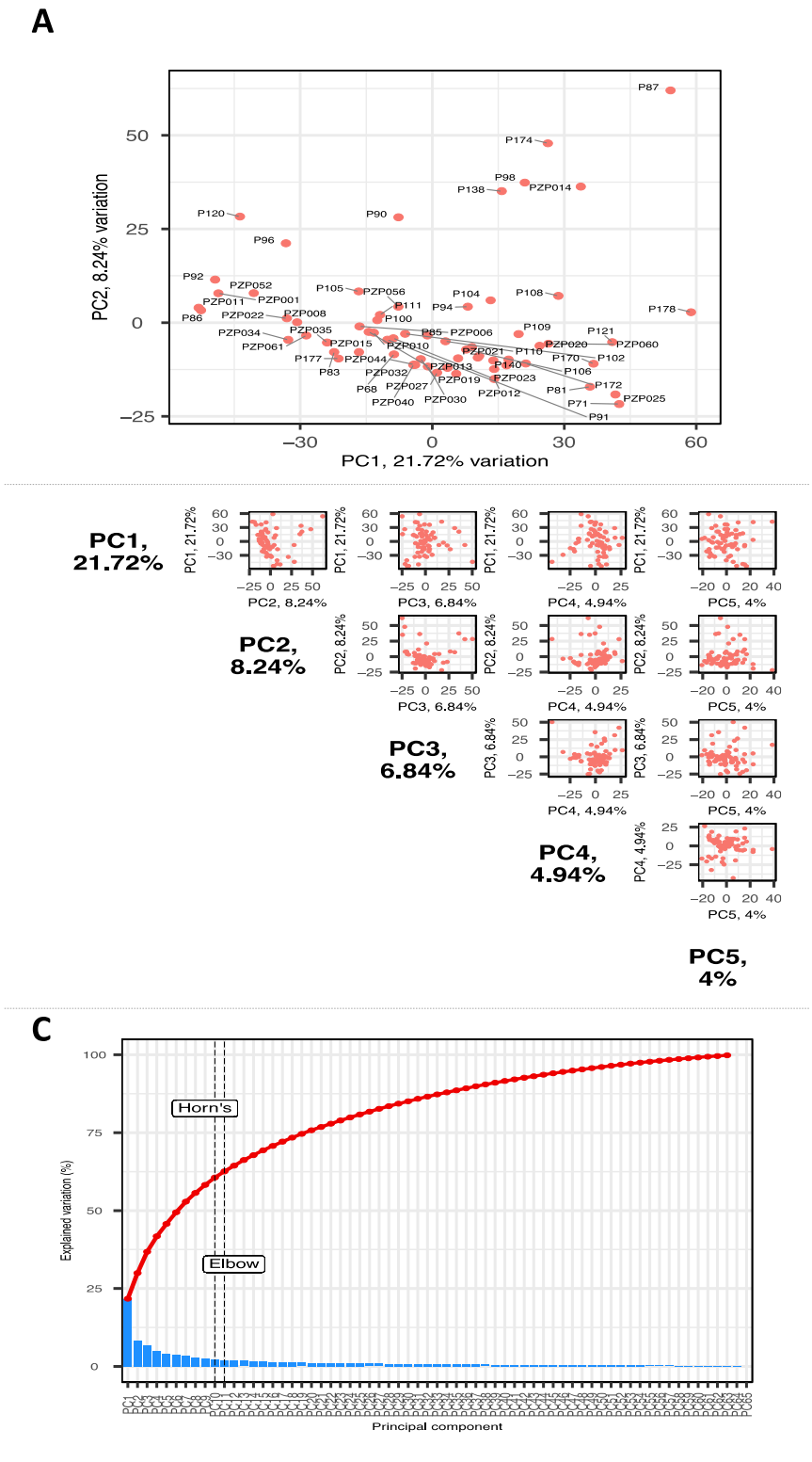

Figure 4.3.A-C: Principle component analysis of the combined cohort (n=65) data set. **A** PCA plot showing the distribution of samples based on the first two principal components. **B** Pairs plot showing sample distribution based upon different combinations up to the fifth principal component. **C** Scree plot demonstrating the degree of variance explained by each principal component, with Horn's and the elbow method labelled showing the optimal number of principal components.

4.2.4 Hierarchical clustering identifies three distinct immune-based subgroups

I next looked to analyse the gene expression patterns through hierarchical clustering. A heatmap of the 65 samples based on the 730 genes captured by the entire Nanostring immune codeset was generated using unsupervised hierarchical clustering (**Figure 4.4**). Based on this heatmap there is differential expression of these immune genes across the samples. Furthermore, three immune-based sarcoma subgroups (ISS) are apparent, with one subgroup appearing to be characterised by generally elevated expression of immune-related genes (ISS1), one by average immune-gene expression (ISS2), and the third by low expression of immune-related genes (ISS3). In addition, STS subtypes do not appear to fall specifically into any of the three subgroups and there is substantial heterogeneity in immune subtype within groups of the same STS subtype. Indeed, cases of leiomyosarcoma (LMS), synovial sarcoma (SS), and spindle cell sarcoma are present in each of the 3 immune-based subgroups. Of note, the cases of solitary fibrous tumour (SFT) are only identified in immune subgroups 2 and 3, suggesting they tend towards an immune-based profile characterised by lower expression of immune genes.

A table comparing the clinicopathological features of each of the ISS groups was generated (**Table 4.1**). Statistical analysis for differences between ISS groups was performed by one-way analysis of variation (ANOVA) for age, and by chi-square analysis for the remaining clinicopathological variables. From this table, there are no statistically significant differences between the three ISS groups in terms of the patient age, tumour grade, performance status or STS subtype.

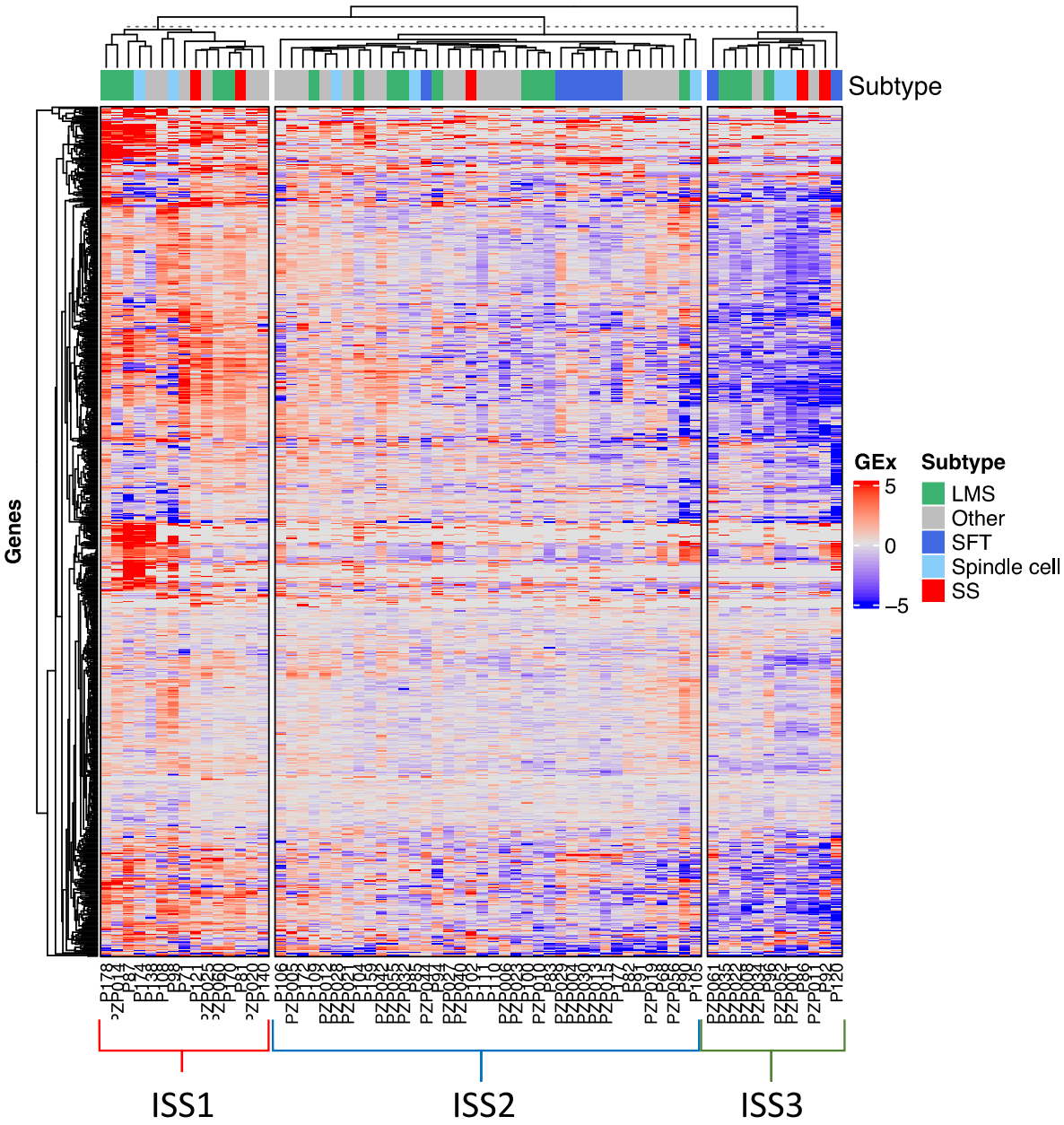

Figure 4.4: Heatmap displaying unsupervised hierarchical clustering of the full gene expression data set of the combined cohort (n=65). GEx – gene expression; LMS – leiomyosarcoma (n=18), SFT – solitary fibrous tumour (n=9), spindle cell sarcoma (n=7), SS- synovial sarcoma (n=5).

Table 4.1: Clinicopathological features of the combined cohort (n=65) when split into the three immune sarcoma subgroups (ISS). Statistical analysis was performed with one-way ANOVA for age, and with chi-square for the other variables, and revealed no significant differences between the three ISS subgroups. LMS – leiomyosarcoma, LPS – liposarcoma, NOS – not otherwise specified, SFT – solitary fibrous tumour, spindle cell sarcoma, SS-synovial sarcoma, UNK – unknown.

Cohort	Combined cohort split into			p value
	ISS1	ISS2	ISS3	
n	15	38	12	
Age (years)				
Median	53	57.2	51.3	
Range	43.1 - 68.4	18 - 77	30 - 81.2	0.565
Grade				
1	1 (6.5%)	3 (8%)	0	
2	4 (27%)	13 (34%)	4 (33.3%)	
3	9 (60%)	19 (50%)	7 (58.3%)	
UNK	1 (6.5%)	3 (8%)	1 (8.3%)	0.965
Performance Status				
0	5 (33%)	10 (26%)	4 (33%)	
1	7 (47%)	20 (53%)	5 (42%)	
2	2 (13%)	4 (10.5%)	1 (8%)	
UNK	1 (7%)	4 (10.5%)	2 (17%)	0.972
Sarcoma Subtype				
LMS	5 (33%)	9 (24%)	4 (33%)	
SFT	0	7 (18%)	2 (17%)	
UPS	0	3 (8%)	0	
Chondrosarcoma	0	1 (2.5%)	1 (8%)	
Myxofibrosarcoma	0	2 (5%)	0	
Myxoid LPS	1 (7%)	1 (2.5%)	0	
Synovial Sarcoma	2 (13%)	1 (2.5%)	2 (17%)	
Sarcoma NOS	1 (7%)	4 (11%)	0	
Spindle Cell Sarcoma	2 (13%)	3 (8%)	2 (17%)	
Other*	4 (27%)	7 (18.5%)	1 (8%)	0.108

* other cases include single cases; in ISS1 of angiosarcoma, fibromyxoid sarcoma, fibrosarcoma,and dedifferentiated liposarcoma; in ISS2 of alveolar soft part sarcoma, atypical Ewing, clear cell sarcoma, fibromyxoid sarcoma, granular cell sarcoma, haemangioendothelioma, and malignant peripheral nerve sheath tumour; and in ISS3 one case of PEComa.

SAM analysis was then undertaken to identify the immune genes statistically significantly differentially expressed between the three ISS subgroups. For this purpose, two-class unpaired SAM analysis was performed, comparing ISS1 with ISS2 and ISS3, ISS2 versus ISS1 and 3, and ISS3 versus ISS1 and 2. Differentially expressed genes which were unique to each subgroup were thus identified. Via this method, 204 differentially expressed genes were identified, 102 genes with comparatively high expression in ISS1, 3 genes with comparatively low gene expression in ISS2, and 99 with comparatively low expression in ISS3. A heatmap and table of these 204 genes were then generated, visually demonstrating the differential expression of the genes within each immune subgroup (**Figure 4.5, Table 4.2**). As expected based on the heatmap of the entire 730 gene set, the SAM results outputs were driven by high and low expression of two gene clusters (ISS1 and ISS3).

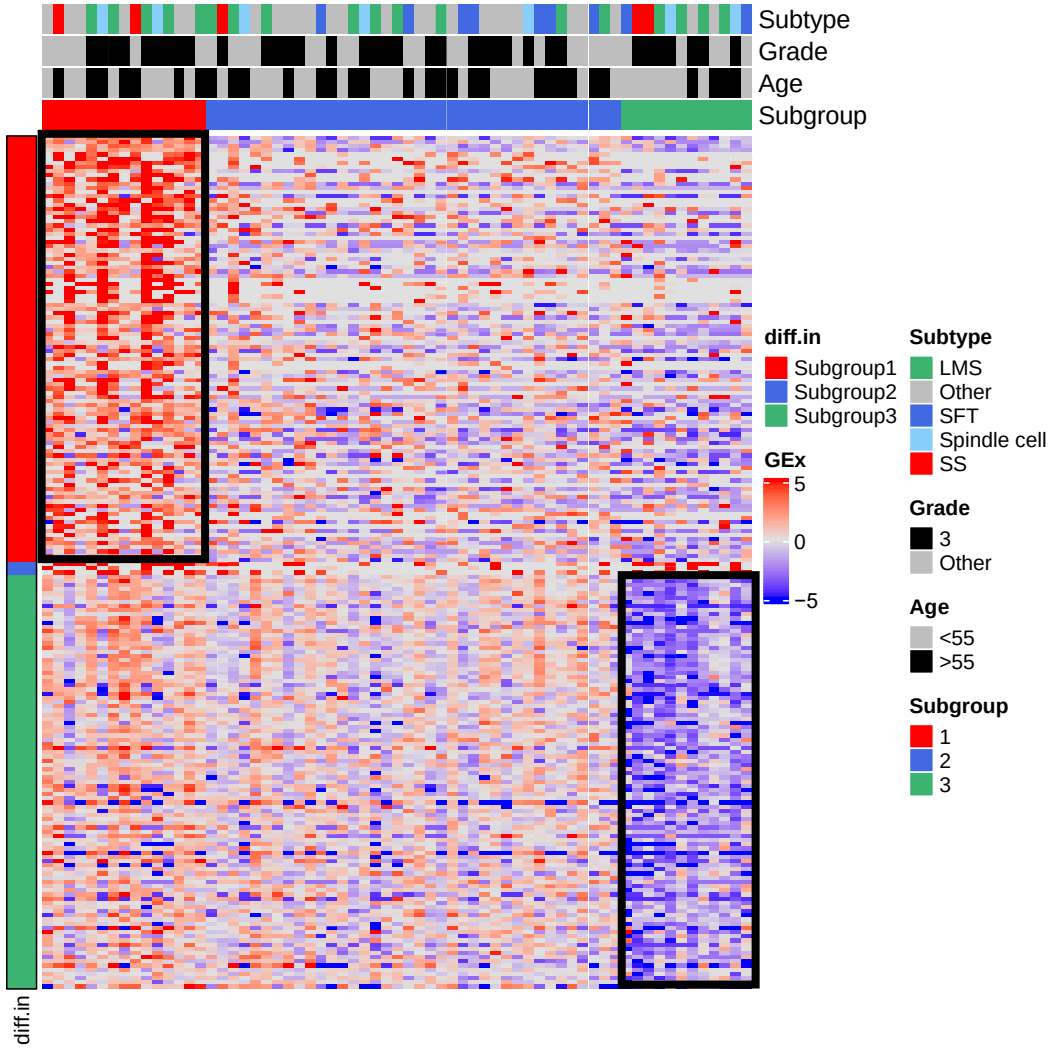

Figure 4.5: Heatmap of 204 genes identified as being differentially expressed between immune subgroups 1-3 in the combined cohort (n=65). Diff.in – differentially expressed in, GEx – gene expression; LMS – leiomyosarcoma, SFT – solitary fibrous tumour, SS-synovial sarcoma.

Table 4.2: List of genes with differential expression based on SAM comparing immune sarcoma subgroup (ISS)1 with ISS2 and 3, ISS2 compared to ISS1 and 3, and ISS3 compared to ISS1 and 2. Genes with differential gene expression, and which were unique for a particular ISS are included.

Immune Subgroup1						Immune Subgroup2		Immune Subgroup3					
Gene	d score	Gene	d score	Gene	d score	Gene	d score	Gene	d score	Gene	d score	Gene	d score
LY9	5.83	IFNA8	3.73	PTGDR2	3.15	PRAME	-3.31	LYN	-6.42	IFITM2	-3.89	CD33	-3.24
FLT3	5.38	SSX1	3.71	IFNB1	3.10	MAGEA12	-2.73	FCGR3A	-6.12	TNFRSF11A	-3.88	NOD1	-3.23
CCL4	5.09	IFNA17	3.69	FLT3LG	3.09	F12	-2.65	SYK	-5.36	ITGA4	-3.88	ITGB3	-3.21
CCL3	5.06	MAGEB2	3.67	CCL26	3.04			C3AR1	-5.28	CD53	-3.84	OAS3	-3.19
SLAMF1	5.02	C8A	3.64	IL1RL1	3.03			TLR4	-5.11	CMKLR1	-3.83	NCR1	-3.18
MS4A1	4.96	SSX4	3.62	IL12RB2	3.00			HLA-DPA1	-5.01	IFITM1	-3.83	LGALS3	-3.15
CD160	4.80	CR2	3.62	FOS	3.00			CX3CR1	-4.86	FCGR2A	-3.81	BST1	-3.12
IRGM	4.73	NLRC5	3.61	CLEC4C	2.99			GZMB	-4.78	CXCL13	-3.79	TNFRSF9	-3.10
TLR10	4.62	CD83	3.59	PYCARD	2.99			HAVCR2	-4.74	ICAM1	-3.74	IL6	-3.04
MBL2	4.52	LCN2	3.58	CD79A	2.99			ANXA1	-4.67	ISG20	-3.74	NRP1	-3.03
CCL16	4.49	IFNA7	3.57	TLR5	2.98			TNFSF13B	-4.64	VEGFC	-3.71	IRF1	-3.03
FPR2	4.42	CAMP	3.52	CCL18	2.97			CXCL10	-4.52	IL6R	-3.70	THY1	-3.03
IL5RA	4.40	KLRC1	3.48	IFNL2	2.94			IFI27	-4.50	HLA-DMA	-3.69	CCL14	-3.01
CCL1	4.36	CD1A	3.44	ATM	2.92			IL10	-4.50	INPP5D	-3.68	STAT1	-2.99
CTSG	4.35	IL4	3.42	PRM1	2.92			CTSS	-4.49	GNLY	-3.65	TICAM2	-2.96
LILRA4	4.32	DEFB1	3.38	C4B	2.91			HLA-DRA	-4.43	CSF1	-3.62	C3	-2.96
CLEC6A	4.30	NFKB2	3.34	IL22	2.89			MRC1	-4.36	CD5	-3.62	CD44	-2.94
PAX5	4.26	CCL22	3.33	IRF4	2.89			FCGR2B	-4.23	CD96	-3.61	FN1	-2.93
IFNG	4.23	CD8B	3.33	LAMP3	2.88			TAP1	-4.21	F13A1	-3.59	HLA-C	-2.90
S100A12	4.10	CEACAM6	3.33	TCF7	2.86			LILRB1	-4.21	C1R	-3.53	EGR2	-2.89
IL27	4.09	CXCL1	3.31	IL24	2.86			MSR1	-4.21	HLA-DQA1	-3.47	CD28	-2.88
MS4A2	3.98	IL12B	3.30	FCER2	2.84			HLA-DMB	-4.21	ICOSLG	-3.43	CD58	-2.87
AMBP	3.96	IL5	3.29	IL1A	2.84			HLA-DPB1	-4.16	IL1R1	-3.43	PLAU	-2.87
CHIT1	3.92	OSM	3.29	IL25	2.81			ITGAM	-4.15	IFIH1	-3.40	IL23A	-2.86
IL17F	3.91	APOE	3.28	C7	2.80			CCR1	-4.07	IFI16	-3.39	COL3A1	-2.84
CXCL6	3.90	CXCR2	3.28	IL23R	2.80			IRF5	-4.07	TLR6	-3.38	IL8	-2.82
C9	3.88	IL21	3.27	CCL11	2.80			EBI3	-4.06	KLRG1	-3.37	PSMB8	-2.82
IKBKE	3.87	AIRE	3.26	IL2	2.76			JAK3	-4.06	S100B	-3.34	LTBR	-2.81
IFNA2	3.86	CCR3	3.24	TNFRSF18	2.75			KLRK1	-4.04	IFNGR1	-3.32	IL4R	-2.81
FOXP3	3.85	RORC	3.24	CLU	2.75			IL2RB	-4.03	PDCD1LG2	-3.31	RIPK2	-2.80
KIR3DL2	3.82	CLEC4A	3.22	MX1	2.72			MICB	-3.99	THBD	-3.27	CXCL14	-2.74
HLA-DOB	3.81	EGR1	3.21	C8B	2.70			C1S	-3.97	HLA-DQB1	-3.27		
S100A7	3.75	PRG2	3.20	CD68	2.70			PDGFRB	-3.97	CD163	-3.25		
PMCH	3.74	PTGS2	3.16	BID	2.67			ITGAX	-3.93	LTF	-3.25		

From the list of differentially expressed genes, a number of interesting observations can be made regarding the immune microenvironment of the tumours in each subgroup. For example, ISS1 has comparatively high expression of *C4B*, *C7*, *C8A* and *B* and *C9*, genes associated with components of the complement cascade. In addition, several immune-stimulating cytokine and chemokine genes have comparatively high levels of expression in ISS1, including a number of C-C motif chemokine ligand (*CCLK*), interferon (*IFN*) and interleukin (*IL*) genes. Individual genes may also suggest an increased presence of particular immune cells based upon the proteins and markers they encode for, and indicate a potentially immune infiltrated phenotype. For instance, *CD83* encodes a protein associated with antigen-presenting cell activation and maturation, *CD8B* encodes a subunit of the CD8 cell surface glycoprotein found on cytotoxic T-cells, CD79A protein expression is a marker for mature B-cells, and CD68 protein expression is a marker for cells of monocyte/macrophage lineage[356–358]. Conversely, the increased gene expression of *FOXP3*, a marker for regulatory T-cells, and *CD160*, an immune-inhibitory molecule leading to the inhibition of CD4+ T-cells, suggest the potential for suppression of anti-tumourigenic immune activity even if infiltrated by populations of immune cells[359,360].

In contrast, the genes differentially expressed in ISS3 all had low relative expression. As such, the immune genotype demonstrated by the immune gene list suggests an immune cold phenotype. For example, elements of the complement cascade have decreased expression (*C1R*, *C1S* and *C3*), and the same is true for the C-X-C motif chemokine ligand (*CXCL*) family of genes associated with pro-inflammatory chemokine activity, as well genes associated with the anti-tumourigenic cytokines IL-6 and IL10, and tumour necrosis factor (*TNF*) genes. Strikingly, a number of human leukocyte antibody (*HLA*) genes have decreased expression in ISS3. As key components of the adaptive immune system through neo-antigen presentation, their comparatively low expression in ISS3 would suggest the STS in this group have an immune cold phenotype. A number of genes associated with specific immune cells also have comparatively low expression, including *CD163* a marker for monocyte/macrophage lineage

cells, *CD28* a major costimulatory marker essential for activation of naïve T-cells, and the leukocyte surface antigen *CD53*[361–363]. In addition, *CD96* a known stimulatory modulator of both NK and T-cells has decreased gene expression in ISS3[364].

4.2.5 Single sample gene set enrichment analysis identifies immune cells enriched in different immune subgroups

Given the findings of differential immune gene expression between the different immune subgroup previously described, I wished to characterise in more detail the immune-based biology underpinning the different subgroups. Based on the published evidence that;

- specific classes of immune cells behave in a way that can be either pro- or anti-tumourigenic[227–230,232,233]
- certain immune cells are impacted by cancer-driven neoangiogenesis[263,267,270–273]
- anti-angiogenic therapies may influence the activity of various cells of the immune system[295,298–300,303,304]

I looked to describe the immune cell infiltrate within the tumour microenvironment employing single-sample gene set enrichment analysis (ssGSEA). Prior to analysis, genes associated with a specific immune cell type are curated into specific gene sets[333]. ssGSEA was then employed to calculate the enrichment scores for each sample and gene set. Each enrichment score represents the degree to which the genes which make up that specific gene set have concordantly elevated or reduced expression levels. This results in an enrichment score for each gene set of interest for each individual sample. Statistical differences between immune subgroups was assessed employing pairwise t-tests with the Bonferroni correction applied to correct for multiple statistical testing.

I curated gene sets for 22 immune cells of interests based upon Nanostring supplied gene annotations for the PanCancer immune profiling panel. The

immune cells included for analysis were selected to provide cells from both the adaptive immune system, including B-cells and a range of T-cells, as well as the innate immune system, including macrophages, mast cells and natural killer (NK) cells. In addition, antigen-presenting cells, such as dendritic cells and neutrophils, were also included for analysis. Furthermore, immune cells encompassing both anti-tumourigenic activity, such as CD8+ T-cells and T-helper1 (Th1) cells, and pro-tumourigenic activity, such as T-helper2 cells (Th2), were included. The immune cells included along with their categorisation as being part of the innate or adaptive immune systems, and their functions are included below (**Table 4.3**). Having conducted ssGSEA utilising the immune cell gene sets, the enrichment scores generated were then plotted as a heatmap supervised by the immune subgroup categorisation (**Figure 4.6**).

Table 4.3: Summary of the 22 immune cells included in gene sets used for ssGSEA. Categorisation of an immune cell type as being part of the innate or adaptive immune system is included, in addition to a description of their role within the immune system.

Immune cell gene set	Adaptive or Innate?	Function and activity related to cancer
Activated dendritic cells	Innate	Antigen presenting cells. Activity involves capture, processing and presentation of of antigens, including tumour antigens. Play a role in polarization of cells of the adaptive immune cells into effector subtypes.
Dendritic cells		
Immature dendritic cells		
B-cell	Adaptive	Respond to foreign/cancer antigens by secreting specific antibodies into the microenvironment.
Cytotoxic cells	Both	Non-specific term used to describe immune cells able to directly lyse tumour cells.
Eosinophils	Innate	Effector cells which play a role in killing cells as well as stimulating inflammation.
Macrophages	Innate	Act to phagocytose and destroy foreign material, and present antigens to cells of the adaptive immune system.
Mast cells	Innate	Act to stimulate inflammation throught the secretion of histamine via degranulation.
Neutrophils	Innate	Able to phagocytose foreign material and present antigen to cells of the adaptive immune system.
Natural killer bright	Innate	Effector cells which are able to lyse cells under stress, including tumour cells. The NKdim class tends towards a more cytolytic subgroup, whilst NKbright are more secretory and involved in cytokine secretion.
Natural killer dim		
Natural killer		
T-cell	Adaptive	The term T-cell covers both effector cells of the adaptive immune system, but also those involved in regulation of immune responses.
CD8 T-cell	Adaptive	Key effector cell with cytotoxic activity against tumour cells.
T-helper cells	Adaptive	T-helper class of cells includes cells which have activity which stimulate anti-tumour immune activity, but also can inhibit anti-tumour immunity.
T-helper1 cells	Adaptive	Involved in anti-tumour immune responses through stimulation of CD8+ cells.
T-helper2 cells	Adaptive	Immune modulating class of T-helper cells, with activity to inhibit anti-tumour immune responses.
T-helper17 cells	Adaptive	Can act in both a pro- and anti-immune stimulating capacity, given their varied cytokine profile.
Follilcular helper T-cells	Adaptive	Specialised T-helper cell, commonly located in secondary lymphoid tissue and involved in B cell activation.
Memory T-cell	Adaptive	Antigen-specific T-cells which contribute to triggering adaptive immune responses upon re-exposure to a known antigen.
Effector T-cells	Adaptive	Non-specific term covering adaptive immune cells involved in pro-inflammatory and anti-tumour immune responses.
Gamma delta T cells	Both	Considered innate immune cells as they do not require antigen presentation to activate, but do posses T-cell receptors. Have a role in lysis of tumour cells, but also immune regulation through cytokien release.

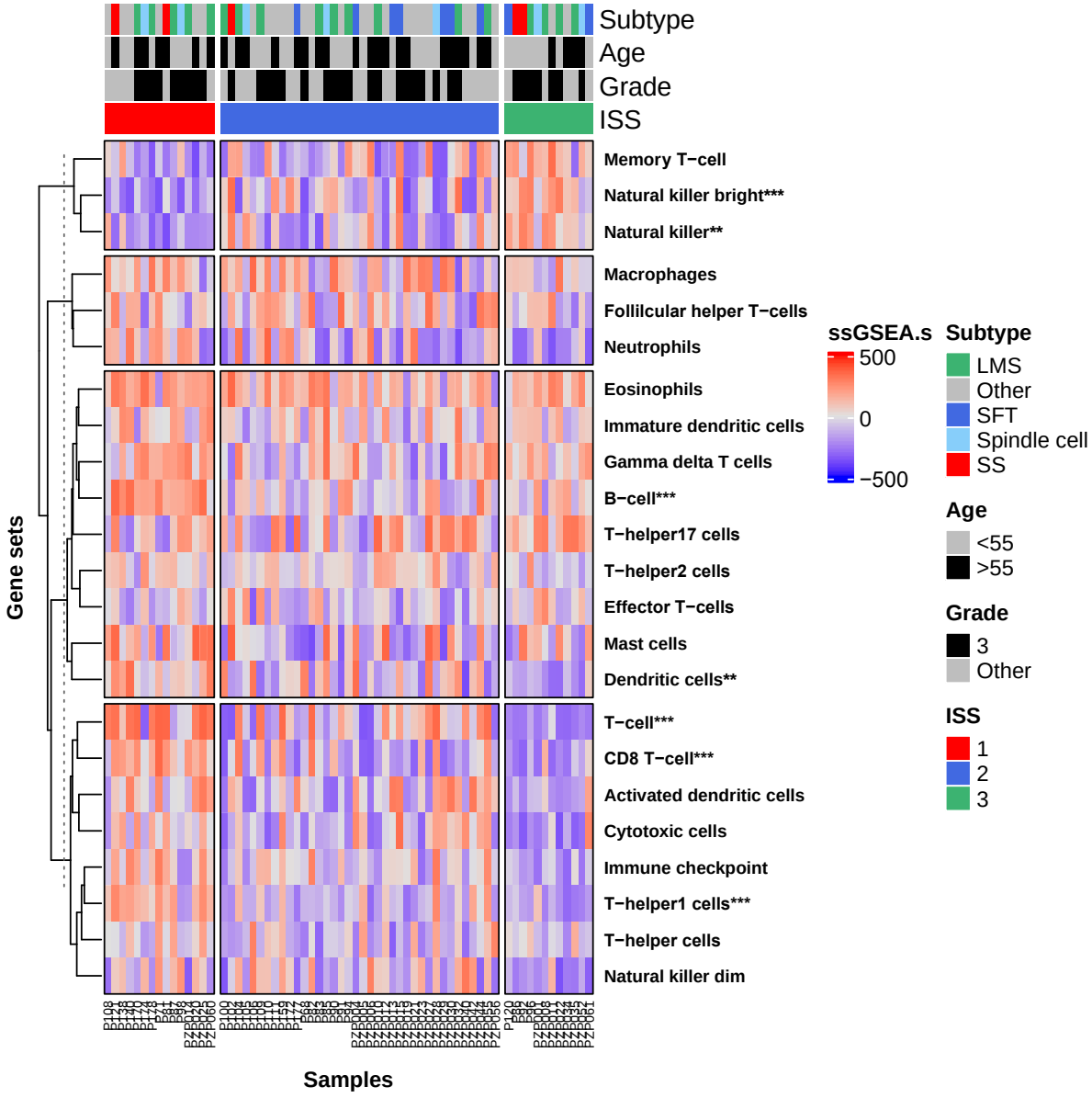

Figure 4.6: Heatmap of single-sample gene set enrichment analysis (ssGSEA) immune cell gene set scores for the combined cohort (n=65), supervised by immune sarcoma subgroup (ISS). LMS – leiomyosarcoma; SFT – solitary fibrous tumour; SS – synovial sarcoma; ssGSEA.s – single sample gene set enrichment analysis score.

Assessing the heatmap, as would be expected ISS1 has generally higher ssGSEA enrichment scores for a proportion of the immune cells analysed. For example, the anti-tumourigenic CD8+ cells, T-helper1 cells, cytotoxic cells and activated dendritic cells all appear to be enriched for in ISS1 compared to the rest of the cohort, and especially ISS3. The immune checkpoint gene set also appears to have higher enrichment scores for ISS1, again suggesting an infiltrated but suppressed immune phenotype. Also of note, ISS3, which was characterised as being immune cold when assessing the 730 gene dataset, upon ssGSEA can be seen to be enriched for memory T-cells, natural killer (NK) and NK^{bright} cells. This finding supports the fact that ssGSEA adds important complementary granularity to analysis relative to single-gene approaches. To better visualise the comparative immune cell enrichment between the three immune subgroups, box and dot plots were generated for gene sets identified as having significantly different enrichment scores by multiple t-tests, with the Bonferroni correction employed to account for multiple testing.

Looking first at cells of the adaptive immune system which were identified as showing significant variation, a number of observations can be made. Firstly, ISS1 is significantly enriched for T-cells of all subsets compared to ISS3 (p=0.0001 respectively), and ISS2 is significantly enriched compared to ISS3 (p=0.0001)(**Figure 4.7.A**). Although a general class of immune cells, covering both pro- and anti-tumourigenic cells, this suggests significantly lower T-cell infiltration within the microenvironment of tumours classed as ISS3 compared to the rest of the cohort. Furthermore, assessing different subsets of T-cells allows the identification of particular subsets which may be driving this result. And indeed, when analysing the ssGSEA enrichment scores for CD8+ cells, ISS1 has significantly higher enrichment scores than both ISS2 (p=0.001) and ISS3 (p=0.0006)(**Figure 4.7.B**). This would suggest an immune microenvironment in cases classed as ISS1 with higher levels of anti-tumour and pro-inflammatory cytotoxic T-cells when compared to both ISS2 and ISS3. Although there was no significant differences in the global T-helper ssGSEA enrichment scores, it can be seen that ISS1 is significantly enriched for T-helper1 cells compared to both ISS2 and ISS3 (p=0.008 and p=0.0003 respectively)(**Figure 4.7.C**). The

importance of this result is that T-helper1 cells are considered pro-immunogenic and interact with and facilitate the activity of cytotoxic CD8+ T-cells. Finally, a further key adaptive immune system effector cell, antibody-producing B-cells, also demonstrated significantly different enrichment scores between the ISS subgroups, with ISS1 having significantly higher scores compared to ISS2 (p=0.0002)(**Figure 4.7.D**). Taken as a whole, these results suggest ISS1 appears to have significant enrichment for anti-tumour cells of the adaptive immune system compared to both ISS2 and ISS3.

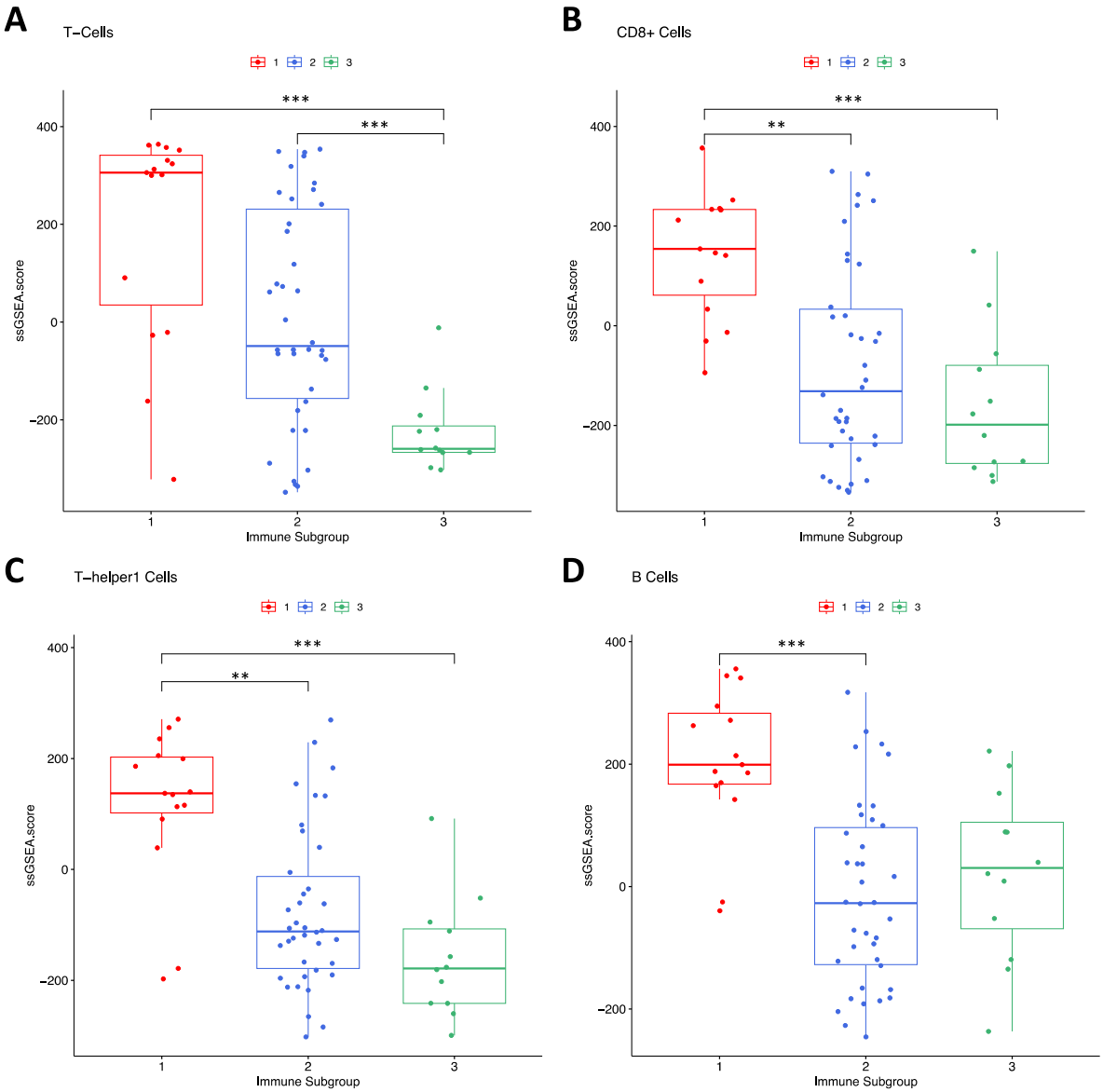

Figure 4.7: Box and dot plots categorised by immune subgroup for **A** T-cells **B** CD8+ cells **C** T-helper1 cells **D** B-cells. ** p<0.01, *** p<0.001.

Although considered part of the innate immune system, dendritic cells play a key role in antigen presentation and activation of effector cells of the adaptive immune system, including cytotoxic T-cells and antibody-producing B-cells. Assessing the ssGSEA enrichment scores for dendritic cells in general, it can be seen that ISS1 has significantly higher enrichment scores compared to ISS3 (p=0.001)(**Figure 4.8.A**). Looking more closely at the innate immune system, general and bright and dim NK cells were assessed via ssGSEA. When looking solely at the global NK cell ssGSEA scores, these are significantly higher for ISS3 compared to ISS1 (p=0.002)(**Figure 4.8.B**). However, with the added granularity of distinguishing NK^{dim} and NK^{bright} cells, it appears this significant difference in global NK cell ssGSEA score is driven by higher scores for NK^{bright} cells in ISS3 compared to ISS1 (p=0.0006)(**Figure 4.8.C**). For NK^{dim} cells, there were no significant differences in enrichment between the subgroups. Previous research has demonstrated that NK^{bright} cells can produce abundant cytokines and act in an immunoregulatory capacity, whereas NK^{dim} cells play a key role in natural and antibody-mediated cytotoxicity and contain greater levels of perforin and granzyme A[365]. As such, and in conjunction with significantly higher CD8+, T-helper1, B-cell, and dendritic cell gene set scores for ISS1, these results suggest that ISS1 is characterised by a more pro-immunogenic phenotype, whereas ISS3 is more characterised by an immune-modulating phenotype.

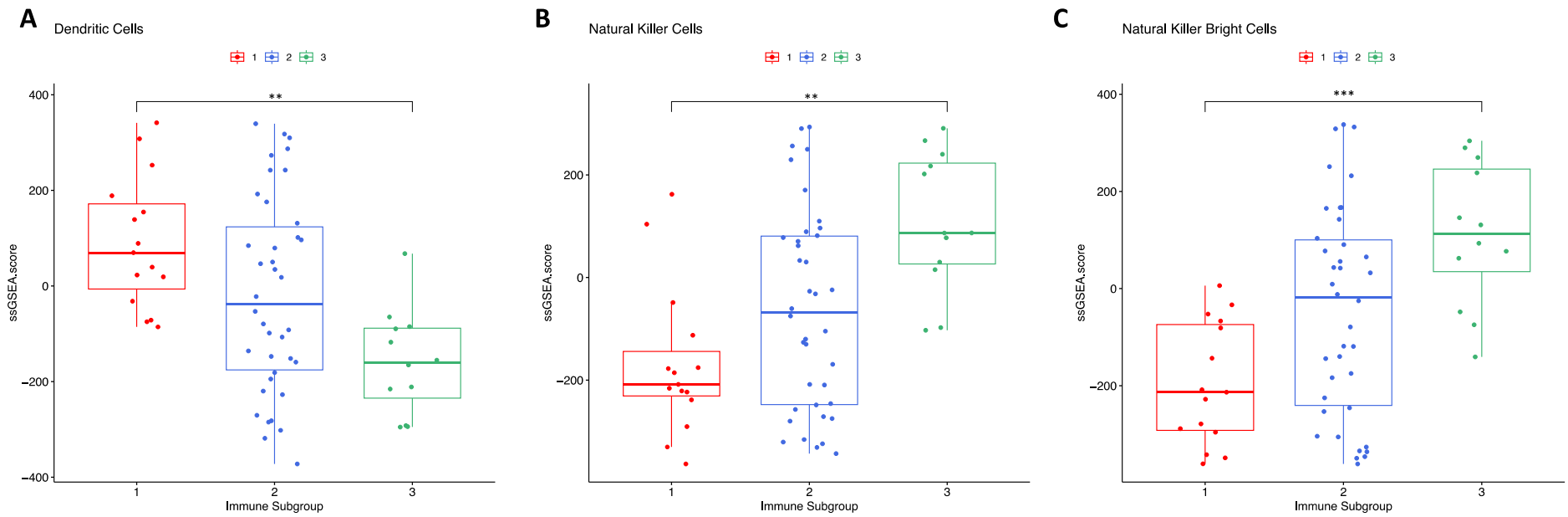

Figure 4.8: Box and dot plots for **A** dendritic cells **B** natural killer cells **C** natural killer bright cells

4.2.6 Characterising the differences in the immune microenvironment based on sarcoma subtype

In addition to describing immune-based gene profiles identified independently from histological subtypes, given the range of STS subtypes within this combined cohort, describing differences in the tumour microenvironment between subtypes was then undertaken. Initially, a heatmap of the 730 genes captured by the entire Nanostring immune codeset was generated, supervised by STS subtype (**Figure 4.9**). Assessing this heatmap, no obvious patterns of differential gene expression was observed between the different STS subtype categories. As such, SAM analysis was undertaken to define genes which were statistically significantly differentially expressed between the different subtypes. Two-class unpaired SAM was employed comparing each subtype-specific subgroup with the remainder of the cohort to identify uniquely differentially expressed genes for that subtype. This generated a list of 64 differentially expressed genes; 11 differentially expressed in leiomyosarcoma (LMS), 38 in solitary fibrous tumours (SFT), 2 in spindle cell sarcomas, 4 in synovial sarcoma (SS) and 9 in “other” STS subtypes (**Figure 4.10 and Table 4.4**).

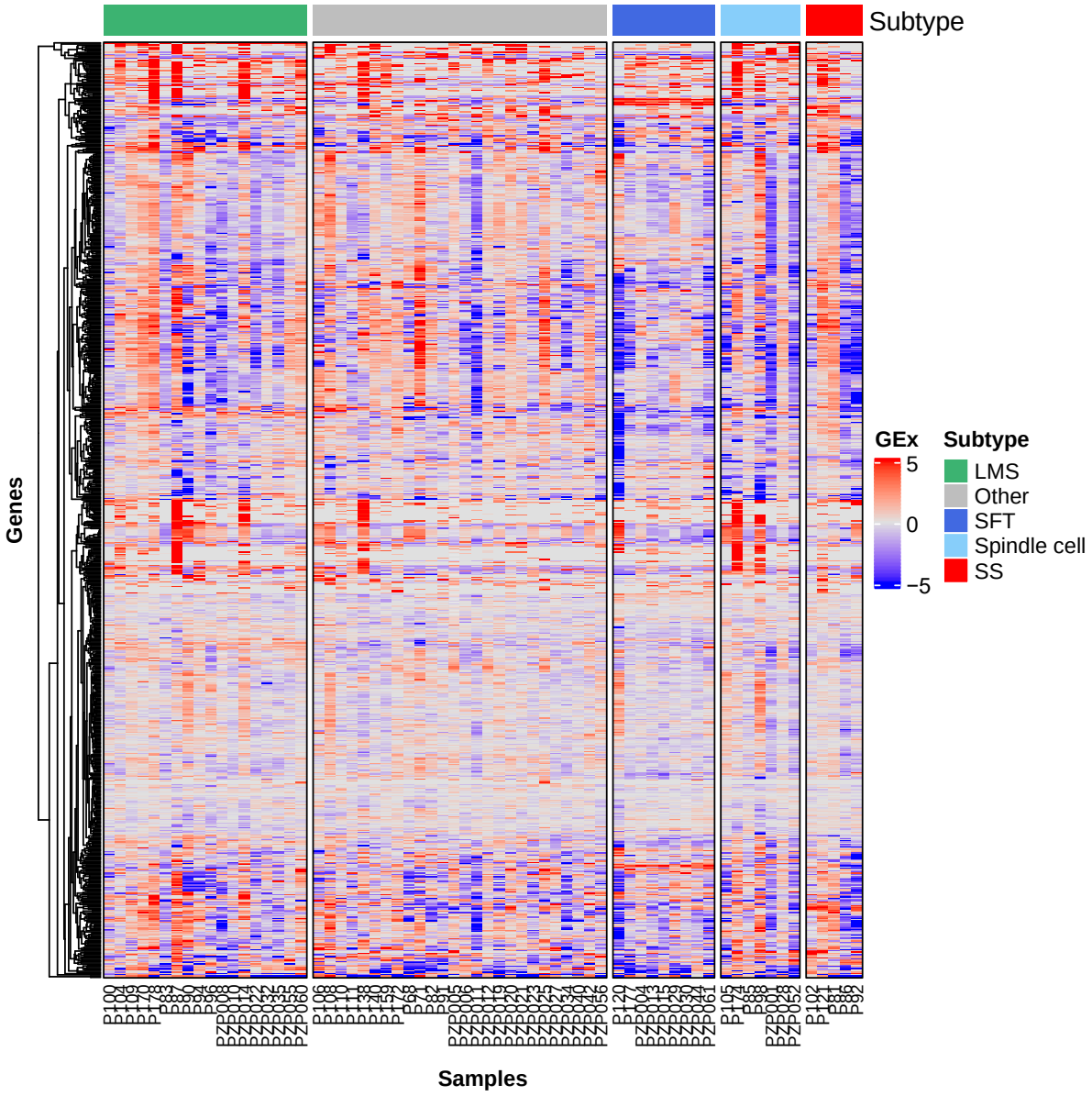

Figure 4.9: Heatmap of the gene expression data for the full 730 immune gene Nanostring codeset of the combined cohort (n=65), supervised by histological subtype. LMS – leiomyosarcoma; SFT – solitary fibrous tumour; SS – synovial sarcoma.

Table 4.4: List of differentially expressed genes by STS subtype identified by a series of two-class unpaired SAM analyses, with subtype-specific groups compared to the rest of the cohort. This identified a total of 64 genes, represented in this table along with the T-statistic output from SAM showing the direction and degree of differential expression.

LMS		Others		SFT				Spindle		SS	
Gene	d score	Gene	d score	Gene	d score	Gene	d score	Gene	d score	Gene	d score
CDH1	3.95	APP	3.94	CD207	8.84	CD79B	-2.98	MAGEA1	3.62	PSMB9	-2.82
LBP	3.45	LYN	3.39	HSD11B1	6.55	IL4R	-3.12	ITGAE	-3.43	PSMB8	-2.83
CXCL2	3.21	IL2RB	3.34	LAG3	6.20	ST6GAL1	-3.13			MICB	-3.12
RRAD	3.12	CXCL13	3.22	VCAM1	5.68	TNFSF15	-3.16			PBK	-3.59
A2M	3.09	IL21R	3.20	STAT6	5.11	IL6R	-3.16				
ALCAM	3.02	CXCR4	2.97	IL11RA	4.43	IRAK1	-3.20				
IL24	2.98	FCGR3A	2.97	CD40	3.88	CREB5	-3.24				
MFGE8	2.81	PPARG	2.83	SAA1	3.85	CD276	-3.28				
ROPN1	2.51	NFATC4	-3.20	PRKCD	3.82	ITGA4	-3.30				
CD97	2.44			CD1D	3.67	CD24	-3.38				
C5	2.39			CFI	3.55	PNMA1	-3.61				
				LRP1	3.53	LTK	-3.62				
				IL1RL2	3.50	FN1	-3.74				
				CEACAM1	3.39	COL3A1	-3.86				
				KLRD1	3.34	ITGB4	-4.21				
				SPA17	3.26	THBD	-4.34				
				KLRF1	3.16	PDGFC	-4.66				
				ADORA2A	-2.94	THBS1	-4.71				
				CCL20	-2.95	RORA	-5.19				

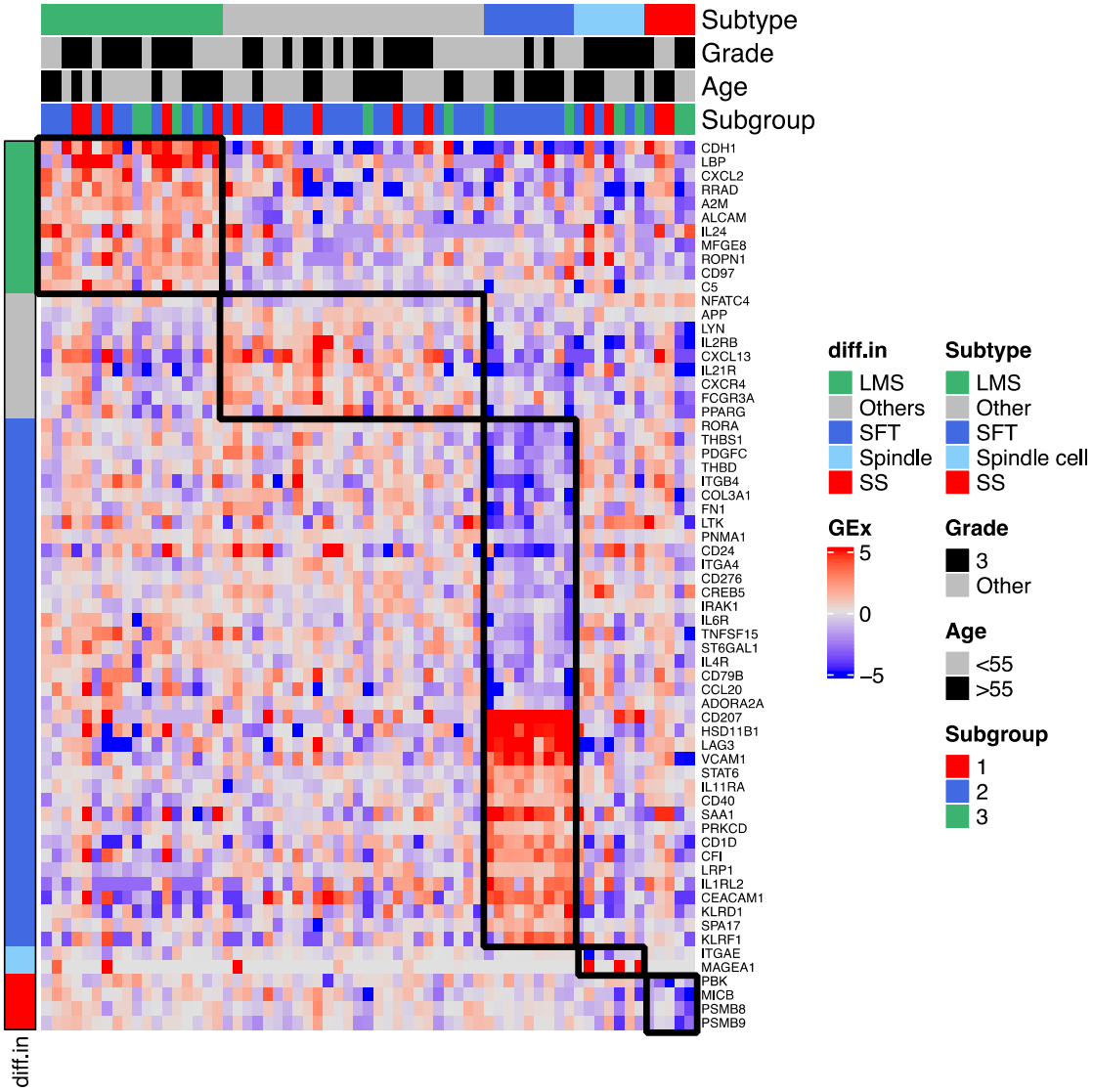

Figure 4.10: Heatmap of differentially expressed genes in the combined cohort (n=65) based on STS subtype. A series of two-class unpaired SAM analyses were performed with subtype-specific groups compared to the rest of the cohort. This identified a total of 64 genes, represented in this heatmap supervised by the sarcoma subtype and ordered by the subtype the genes are differentially expressed in.

From the heatmap and results of SAM, for the LMS cases, all of the 11 differentially expressed genes have higher gene expression relative to the rest of the cohort. The genes are predominantly associated with increased immune activity and include pro-inflammatory chemokines and cytokines (*CXCL2*, *A2M* and *IL24*) and a component of the complement cascade (*C5*). In addition, *CD97* has been associated with the stabilisation of immunological connections between dendritic cells and T-cells. Conversely, *MFG-E8* has previously been shown to be involved in reprogramming macrophages from the pro-inflammatory M1 subtype to the anti-inflammatory M2 subtype[366]. And furthermore, higher expression of cadherin-1 (*CDH1*), as seen in the LMS subgroup, has previously been shown to inversely correlate with immune infiltration in other cancer types[367]. As such, the genes overexpressed in LMS have both anti and pro-inflammatory facets.

For the subgroup of SFTs, of the 38 differentially expressed genes, 17 had increased relative expression compared to the rest of the cohort, with the remaining 21 having decreased expression. Of those which have higher levels of expression, some interesting observations can be made. For example, both *CD40* and *CD207* both encode proteins identified on antigen-presenting cells and may help drive anti-tumour immune responses through antigen presentation and activation of effector immune cells. Indeed, based on SAM, *CD207* is the most strongly differentially expressed gene in SFTs compared to the rest of the combined cohort. Furthermore, *IL-11* encodes a cytokine released by tumour-associated macrophages and T-cells. In addition, high expression of protein kinase C delta (*PRKCD*) has previously been correlated with TIL infiltration[368]. These findings are suggestive of SFTs harbouring an immune microenvironment characterised by T-cell infiltration, with enrichment for antigen-presenting cells driving activation of these cells. Conversely, higher expression of *LAG3*, a described immune checkpoint, in this the subgroup of SFTs might indicate that despite infiltration with effector immune cells, their anti-tumourigenic activity may be suppressed. Furthermore, serum amyloid A1 (*SAA1*) has been associated with the induction of suppressive neutrophil subtypes, giving further evidence of a suppressed immune microenvironment.

In the SS subgroup, 4 genes were differentially expressed relative to the rest of the cohort, with all 4 showing comparatively low levels of expression. Notably, proteasome subunit beta (*PSMB*)8 and 9, key components of the immunoproteasome and correlated with immune infiltration and immune checkpoint inhibitor response, were both found to have decreased expression in SS[369,370]. In addition, PDZ binding kinase (*PBK*) is classed as a cancer antigen, being involved in the regulation of mitosis and tumorigenesis, but was found to have reduced expression in this SS subgroup. Previously, *PBK* expression has been shown to correlate with tumour mutational burden as well as infiltration of M0 and M1 macrophages, follicular helper T-cells and memory T-cells[371]. Finally, MHC class I chain-related polypeptide B (*MICB*) also had decreased expression in SS, but is known to play a role in NK cell-mediated cell death[372].

Finally assessing the “other” subtype group, 9 genes were found to have differential expression, with nuclear factor of activated T-cells (*NFATC4*) showing decreased expression, and the remaining 8 showing higher levels of expression. Of the genes with increased expression, these include genes involved in pro-inflammatory chemokine signalling (*CXCL13* and *CXCR4*) and cytokine signalling (*IL21R* and *IL2RB*). In addition, expression of Fc gamma receptor 3A (*FCGR3A*) has been found to positively correlate to the infiltration of numerous immune cells across various cancer types[373]. This would suggest a generally pro-immunogenic microenvironment, but given the wide range of subtypes included in the ”other” category, it may be difficult to extrapolate these findings.

4.2.7 Characterisation of subtype specific immune cell populations

Given the differential expression of individual genes as identified via SAM and presented above, ssGSEA was then undertaken to identify any significant differences in specific immune cell enrichment scores based on STS subtype. The same gene set list was used as previously described. Looking at the whole immune cell ssGSEA heatmap, supervised by STS subtype, there are no obvious clear patterns of expression scores (**Figure 4.11**). However, by analysing individual immune cells there does appear to be differences in enrichment scores

between different STS subtypes. For example, SFTs appear to have higher expression scores for activated dendritic cells compared to the rest of the cohort, but lower natural killer dim cells, especially relative to the “other” STS subtype subgroup. Given these observations, multiple t-tests, with the Bonferroni correction employed to account for repeat testing, were performed to identify gene sets with statistically significant differences based on STS subtype. Only NK^{dim} cells were found to have significantly different enrichment scores between subtypes, with a box and dot plot generated to visualise this difference (**Figure 4.12**). Indeed, the “other” STS subtype group, made up of subtypes with fewer than 5 cases in the combined cohort, has significantly higher NK^{dim} enrichment scores relative to the SFT subgroup ($p=0.0009$).

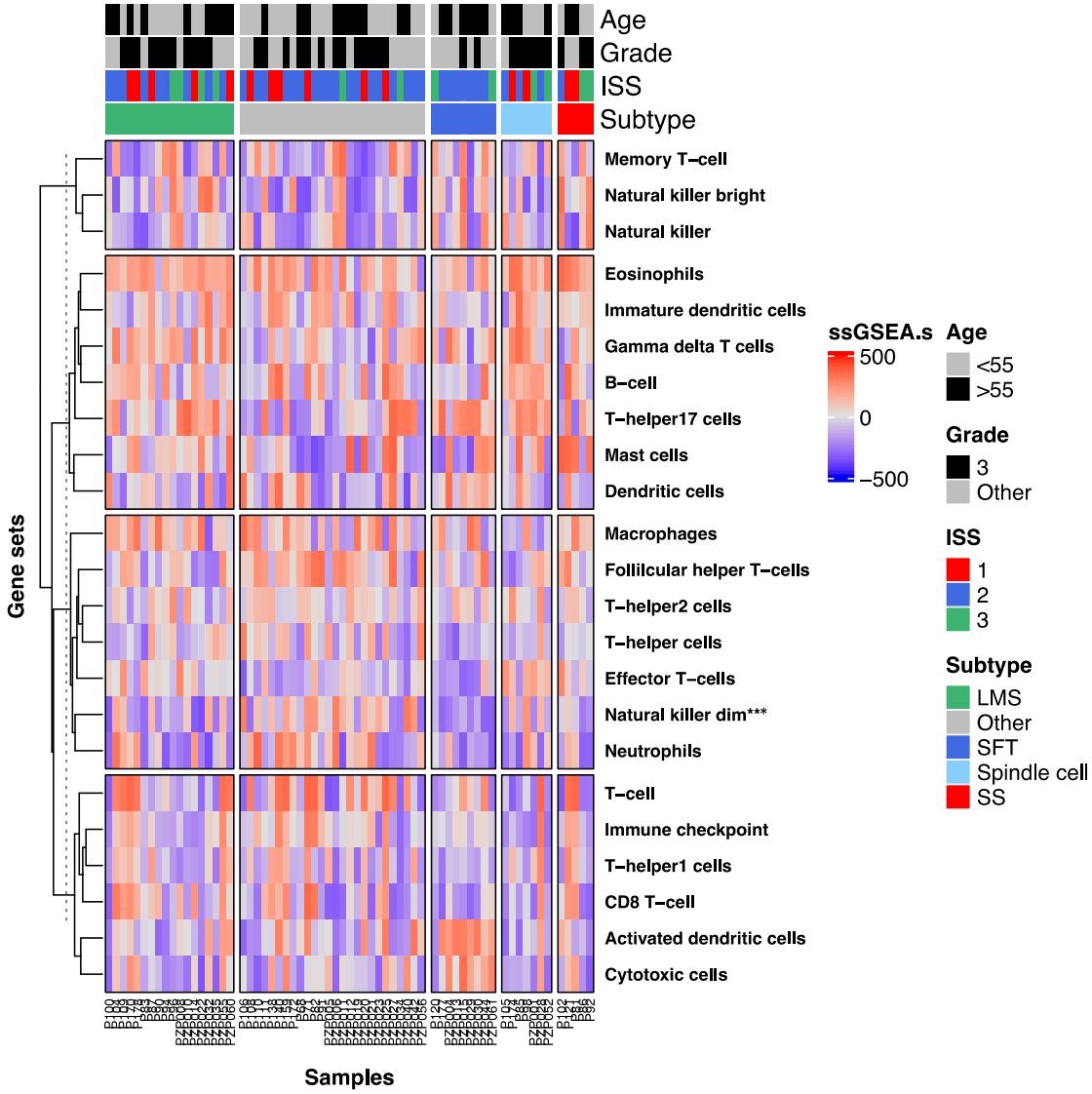

Figure 4.11: Single-sample gene set enrichment analysis (ssGSEA) of the immune cell gene set scores of the combined cohort (n=65), supervised by soft tissue sarcoma subtype. LMS – leiomyosarcoma; SFT – solitary fibrous tumour; SS – synovial sarcoma; ssGSEA.s – single sample gene set enrichment analysis score. *** p<0.001.

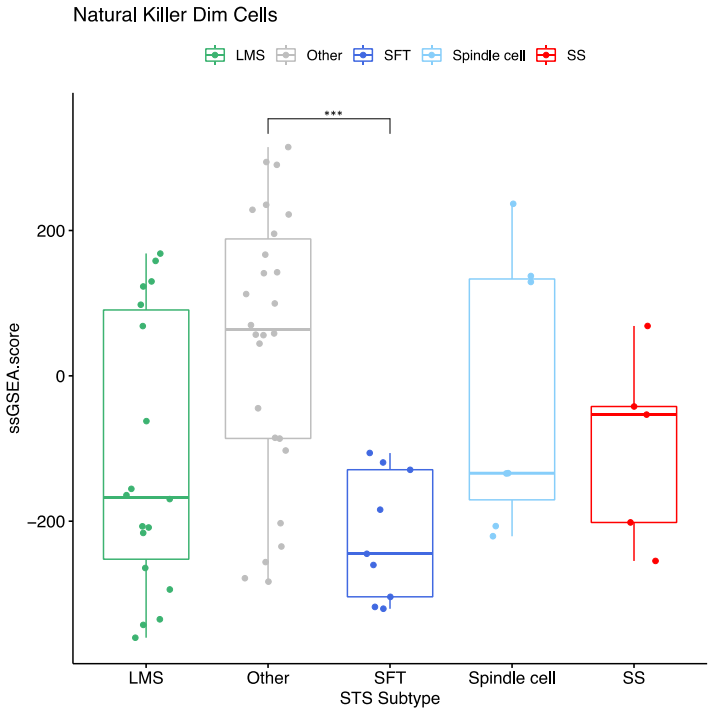

Figure 4.12: Dot and box plot of the combined cohort ssGSEA enrichment scores for natural killer dim cells, comparing different soft tissue sarcoma subtype groups. LMS – leiomyosarcoma, SFT – solitary fibrous tumours, SS – synovial sarcoma. *** p<0.001

4.2.8 Analysing the association between patient age and the immune tumour microenvironment

In the general population, with advancing age the incidence of cancer increases whilst general immunity declines. Indeed, multiple studies have suggested differential immune-related gene expression and immune cell infiltration to the tumour microenvironment based on patient age[374–377]. As such, this cohort of STS was analysed with the aim of identifying any changes in the tumour immune microenvironment associated with increased age. Initially, a heatmap of the entire Nanostring immune codeset supervised by patient age was generated with the aim of identifying any patterns in immune gene expression stratifying patients as either over or under the age of 55 years (**Figure 4.13**). This age was chosen as a number of recent studies analysing the tumour immune microenvironment have utilised age as a binary variable with 55 years of age the cut-off for high/low. For

example, the work by Xu et al. identifying prognostic immune scores in triple-negative breast cancer, the work by Curran et al., identifying differential immune signatures in colon cancer, and the work by Wu et al. identifying stromal infiltration and immune gene expression in colon cancer[378–380]. From this heatmap, in addition to STS subtypes appearing evenly distributed between the two groups, there are no obvious patterns of differential immune gene expression attributable to different patient ages.

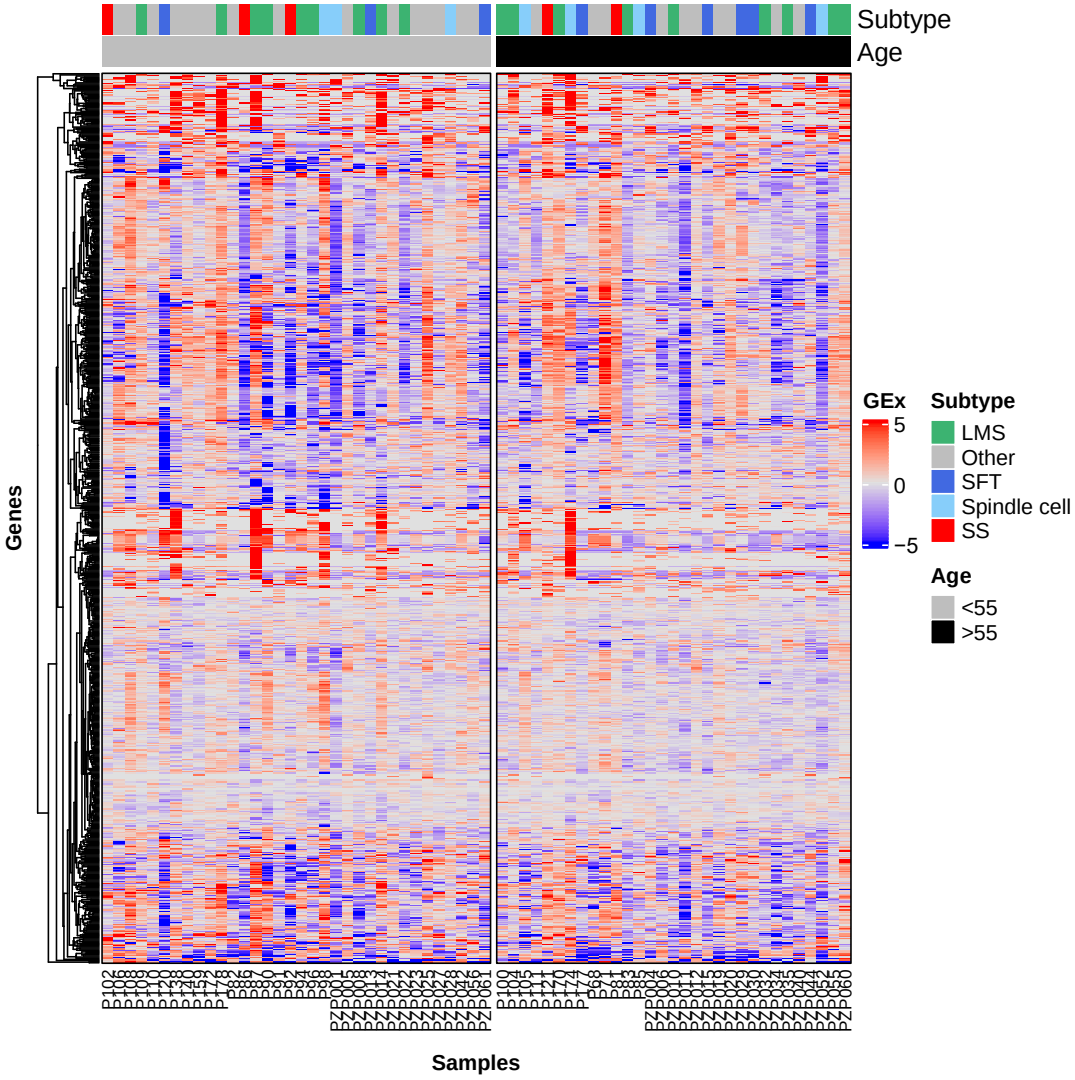

Figure 4.13: Heatmap of gene expression in the combined cohort (n=65) of all 730 immune genes included in the Nanostring codeset, supervised by patient age. LMS – leiomyosarcoma, SFT – solitary fibrous tumours, SS – synovial sarcoma.

In the absence of a clear pattern of differential gene expression, SAM analysis was undertaken to identify significantly differentially expressed genes between different strata based on age, which could then be described and plotted as a heatmap. However, output from the two-class unpaired SAM demonstrated a high false discovery rate when identifying a small number of differentially expressed genes. For example, a delta value of 0.34 would call 33 genes as significantly differentially expressed but with a median false discovery rate of 18%. As such, this analysis was not able to confidently identify any genes significantly differentially expressed between these age-based strata.

Analysis of ssGSEA of immune cell gene sets was also undertaken with the cohort stratified based on patient age. A heatmap of the ssGSEA enrichment scores supervised by patient age was generated with the aim of identifying patterns of differential enrichment for particular immune cells (**Figure 4.14.A**). Based on this heatmap, there is not a clear pattern of global differential enrichment between the two strata. Indeed statistical analysis employing multiple t-tests, with the Bonferroni correction employed to account for multiple tests, shows no significantly differentially enriched immune cells between the over and under-55 age groups (**Figure 4.14.B**).

A

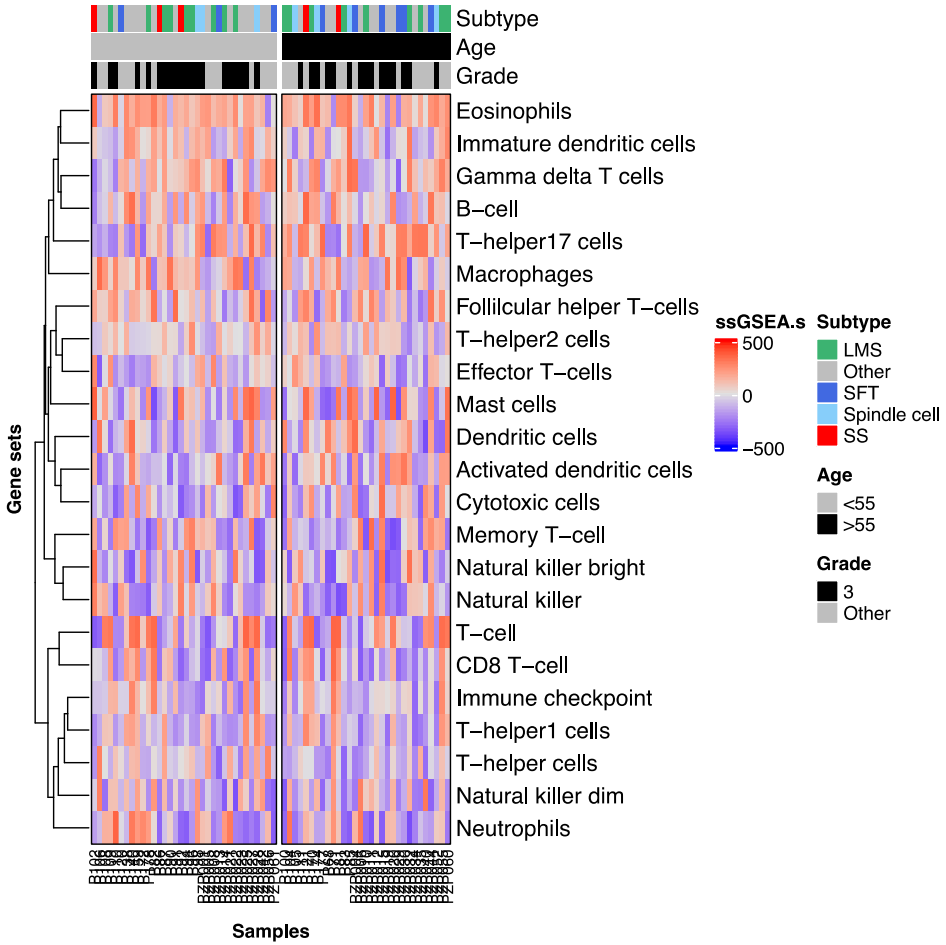

B

Immune cell	T-statistic	df	p-value	Adjusted p-value
Activated dendritic cells	-0.875154	61.03783	0.385	1
B-cell	0.024557	62.94684	0.98	1
CD8 T-cell	0.420847	62.21567	0.675	1
Cytotoxic cells	-1.063374	60.89508	0.292	1
Dendritic cells	-1.131026	59.76902	0.263	1
Effector T-cells	0.207041	62.80478	0.837	1
Eosinophils	0.283433	57.52871	0.778	1
Follilcular helper T-cells	0.465816	60.20934	0.643	1
Gamma delta T cells	0.169936	60.76527	0.866	1
Immature dendritic cells	1.480535	57.77633	0.144	1
Immune checkpoint	0.220087	62.94799	0.827	1
Macrophages	1.001679	62.72744	0.32	1
Mast cells	0.263159	59.30322	0.793	1
Memory T-cell	0.406672	61.79846	0.686	1
Natural killer	0.712366	60.84062	0.479	1
Natural killer bright	0.011368	61.15984	0.991	1
Natural killer dim	0.267234	62.12296	0.79	1
Neutrophils	0.805684	62.95121	0.423	1
T-cell	-0.4877	62.55851	0.627	1
T-helper cells	2.117255	62.9382	0.0382	0.8786
T-helper1 cells	0.307721	61.49599	0.759	1
T-helper17 cells	-2.003961	62.77822	0.0494	1
T-helper2 cells	0.681521	56.51906	0.498	1

Figure 4.14: **A** Heatmap of enrichment scores of single sample enrichment analysis of the combined cohort (n=65), supervised by patient age as a binary variable with patients classed as either over or under 55 years of age. **B** statistical results of multiple t-tests with the Bonferroni correction used to correct for multiple testing. LMS – leiomyosarcoma, SFT – solitary fibrous tumours, SS – synovial sarcoma.

4.2.9 Analysing the association between tumour grade and the immune tumour microenvironment

Within other tumour types, previous studies have shown that high-grade tumours are often characterised by an immune-suppressive microenvironment, with higher levels of regulatory T-cells and myeloid-derived suppressor cells acting to inhibit the activity of anti-tumourigenic immune cells of both the innate and adaptive immune systems[381–384]. As such, this cohort was analysed to assess the association between tumour grade and the immune microenvironment in STS, with cases classed as either grade 3 or “other” based on histology reports. As with previous analyses, the initial analytical step involved plotting the immune gene expression data of all 730 genes included in the Nanostring codeset as a heatmap, in this case supervised by tumour grade (**Figure 4.15**). Based on the heatmap, it appears that the grade 3 tumours appear to be more immune cold relative to the non-grade 3 tumours. In addition, although subtype distribution is reasonably even, there are more spindle cell sarcomas in the grade 3 subgroup.

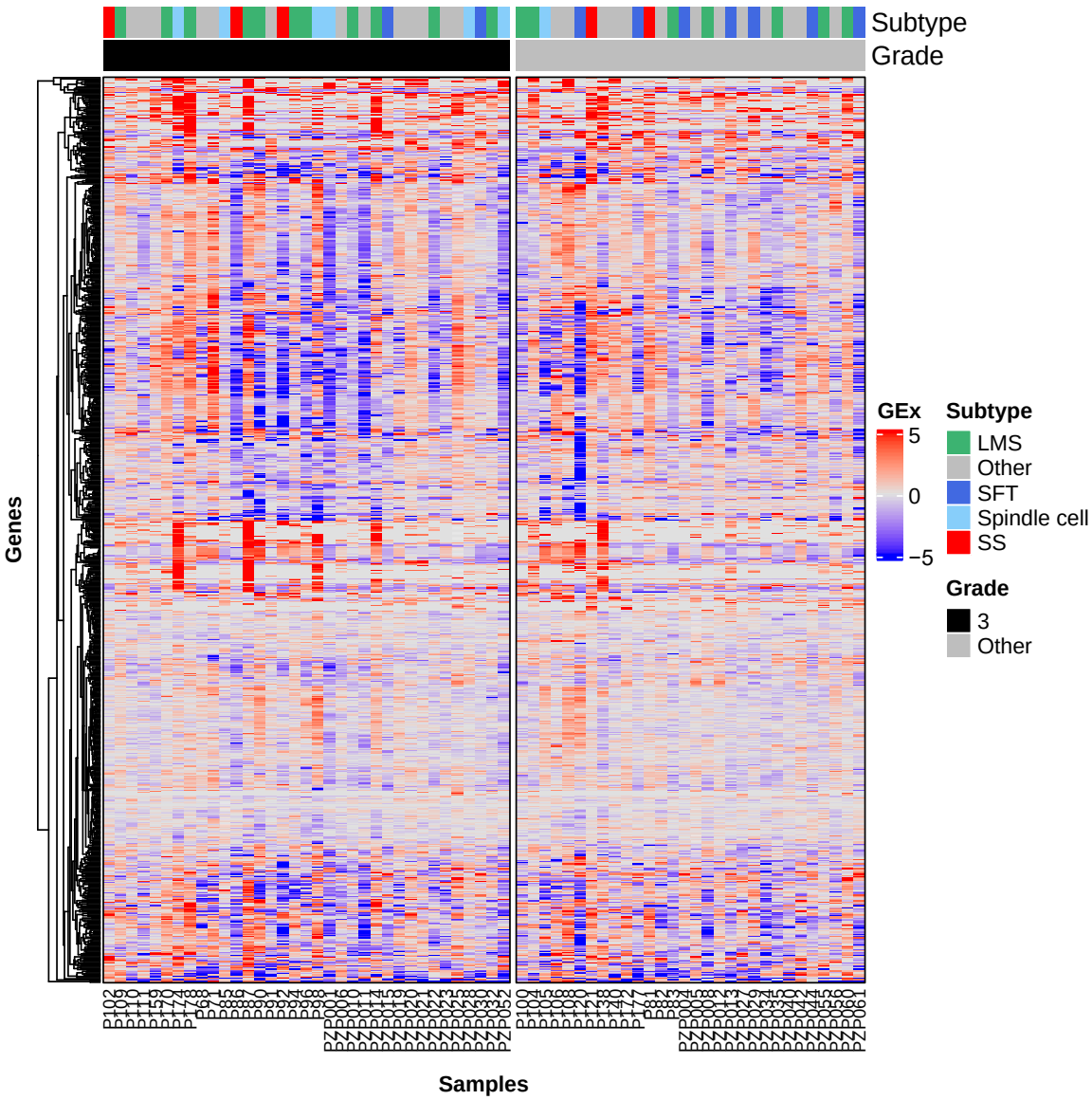

Figure 4.15: Heatmap of gene expression in the combined cohort (n=65) of all 730 immune genes included in the Nanostring codeset, supervised by tumour grade as a binary measure, either as high-grade or “other”. LMS – leiomyosarcoma, SFT – solitary fibrous tumours, SS – synovial sarcoma.

Given the observation of potentially comparatively low immune gene expression in the grade 3 subgroup, two-class unpaired SAM analysis was performed to identify significantly differentially expressed genes between the grade 3 and non-grade 3 tumours. However, as with patient age, the SAM analysis output revealed that selecting any delta value would lead to an unacceptably high false discovery rate, indicating that no genes are robustly differentially expressed between the grade 3 and non-grade 3 subgroups.

Although no individual genes were differentially expressed between the different grade subgroups, it is feasible that immune cell gene sets may be differentially enriched, and as such ssGSEA using the same immune cell gene sets as previously described was undertaken. Initially, a heatmap of the ssGSEA enrichment scores supervised by tumour grade was plotted to assess for any obvious patterns of differential enrichment (**Figure 4.16.A**). However, again no clear pattern of the enrichment scores is visualised to differentiate the grade 3 subgroup from the non-grade 3 subgroup. And indeed, upon multiple t-testing to assess for statistically significant differences, following Bonferroni correction to account for multiple testing, there were no significant differences in any of the immune cell enrichment scores between subgroups (**Figure 4.16.B**).

A

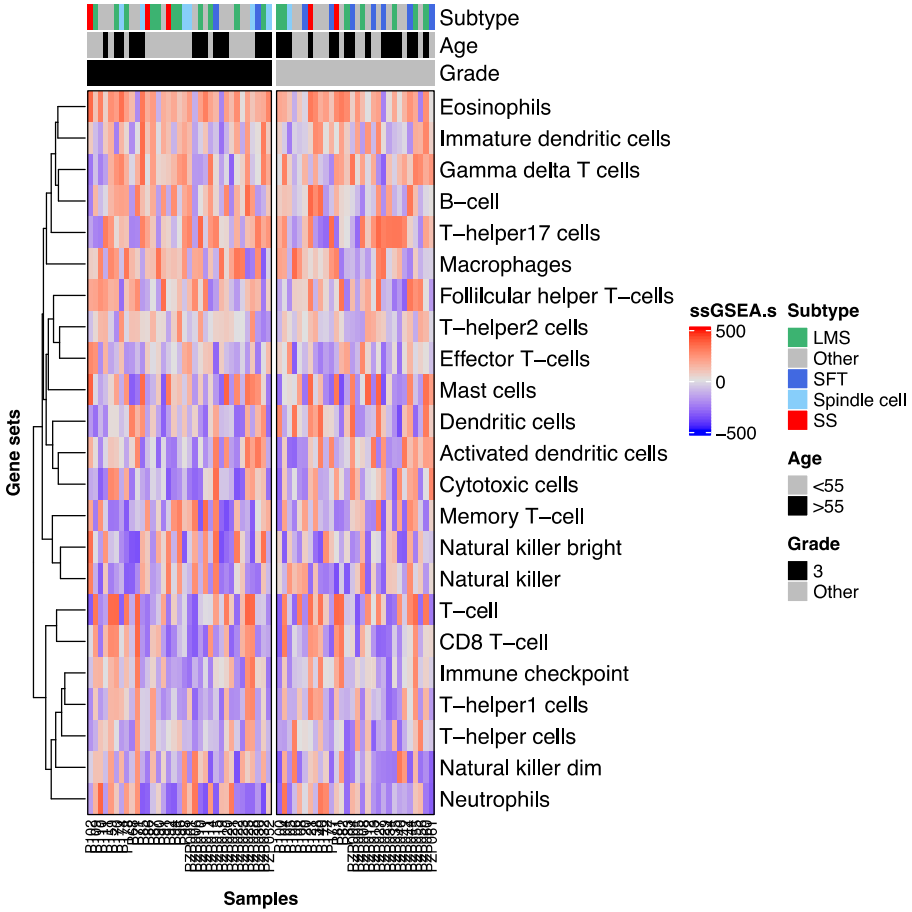

B

Immune cell	T-statistic	df	p	p.adj
Activated dendritic cells	-0.5715481	59.9242223	0.57	1
B-cell	0.7914336	62.226967	0.432	1
CD8 T-cell	-0.0470923	61.944266	0.963	1
Cytotoxic cells	-1.7362152	62.382466	0.0875	1
Dendritic cells	-1.6052896	56.2942792	0.114	1
Effector T-cells	0.47203364	60.2479352	0.639	1
Eosinophils	0.78585463	61.0351471	0.435	1
Follilcular helper T-cells	0.75872124	58.7073367	0.451	1
Gamma delta T cells	-0.4810407	62.5935808	0.632	1
Immature dendritic cells	-0.2255841	61.9314587	0.822	1
Immune checkpoint	-0.3212562	62.960129	0.749	1
Macrophages	1.01611983	62.6317259	0.313	1
Mast cells	0.47638118	59.2309865	0.636	1
Memory T-cell	0.13778176	62.8893821	0.891	1
Natural killer	-0.2729665	62.1381746	0.786	1
Natural killer bright	1.02724274	62.5192756	0.308	1
Natural killer dim	1.52915579	57.5676627	0.132	1
Neutrophils	-0.012897	62.8242887	0.99	1
T-cell	-0.6533234	59.8428809	0.516	1
T-helper cells	0.62442271	56.0082984	0.535	1
T-helper1 cells	-0.3980802	60.8897024	0.692	1
T-helper17 cells	-0.0576479	56.4459044	0.954	1
T-helper2 cells	0.35718474	62.9061533	0.722	1

Figure 4.16: **A** Heatmap of enrichment scores of single sample enrichment analysis of the combined cohort (n=65), supervised by tumour grade as a binary variable with patients classed as either over or under 55 years of age. **B** statistical results of multiple t-tests with the Bonferroni correction used to correct for multiple testing. LMS – leiomyosarcoma, SFT – solitary fibrous tumours, SS – synovial sarcoma.

4.2.10 Summary of results

In this chapter, I set out to undertake immune-based gene expression analysis of pre-treatment tissue on a cohort of patients treated with pazopanib. The ultimate aim was to undertake detailed characterisation and identify differential immune gene expression within the cohort, and associated with clinicopathological variables. Hierarchical clustering was employed to group samples together based on their immune-gene expression, and 3 distinct immune subgroups were identified. These subgroups could broadly be characterised as having an immune hot microenvironment (ISS1), an intermediate immune microenvironment (ISS2) and an immune cold microenvironment (ISS3). Through ssGSEA, these subgroups were then demonstrated to show contrasting enrichment for key cells of both the adaptive and innate immune systems, adding additional granularity to the characterisation of the immune microenvironments associated with each subgroup. Further analysis investigating the association between STS subtype and tumour microenvironment did not yield such significant differential patterns of immune expression, suggesting that the immune microenvironment in STS shows great heterogeneity which is independent of the histological diagnosis. Finally, the association between immune-gene expression and patient age and tumour grade was assessed, but significant differences in the immune microenvironment were not observed.

4.3 Discussion

4.3.1 Immune gene expression defines three groups of patients in the pazopanib-treated combined cohort

In order to describe the immune microenvironment in STS with more depth and granularity, in this chapter I undertook immune-based gene expression analysis on pre-pazopanib tissue from the combined cohort.

Hierarchical clustering of the immune gene expression data for the combined cohort, including all 730 genes in the Nanostring immune gene set, was employed to group samples together based on the similarity of their gene expression profiles. This identified three distinct subgroups within the cohort, with different patterns of immune gene expression, and named ISS1, ISS2 and ISS3. From the heatmap, ISS1 was seen to be characterised by an immune hot tumour microenvironment, with high immune gene expression levels, ISS2 was characterised by an intermediate level of gene expression, whilst ISS3 was characterised as having an immune cold microenvironment with low immune gene expression. Indeed, SAM analysis was undertaken to identify immune genes with significantly differential expression within each of the ISS subgroups. This confirmed that ISS1 demonstrates evidence of being characterised by an anti-tumourigenic immune microenvironment, with significantly higher levels of expression for genes associated with pro-inflammatory cytokines, members of the complement cascade, and anti-tumourigenic immune cells including CD8+ cells, antigen-presenting cells and mature B-cells. Conversely, ISS3 had significantly lower expression levels of genes associated with anti-tumourigenic immune cells, such as modulators of NK and T-cells, and immune system mediators, such as IL-6 and TNF.

When considering the previously published attempts at undertaking descriptive characterisation of STS samples, several similarities with my presented data are noted. The immune-based molecular phenotyping of 206 sarcoma samples carried out by The Cancer Genome Atlas (TCGA) consortium demonstrated heterogenous immune gene expression in their cohort[290]. This is in keeping with the results and patterns I observed in my analysis (**Figure 4.4**). In addition,

Petitprez *et al*.'[293] used publicly available gene expression datasets for a total cohort of 608 samples and developed an immune-based classification assigning STS samples into one of 5 sarcoma immune classes (SIC) denoted as A to E. The SIC A group in this study was characterised as being an 'immune desert' with the lowest expression of immune cell-related genes, whilst SIC E had the highest expression of immune cell-related genes. The remaining SIC subgroups B-D were characterised as having a more bland immune-gene expression profile. Interestingly, looking at the ISS subgroups derived from the combined cohort, similar trends can be observed. ISS1 is characterised by upregulation of immune-related genes and conversely ISS3 by downregulation of these genes. It should be noted however, that the TCGA work is based on primary sarcoma tissue exclusively, whilst Petitprez *et al*. also developed their immune-based classifier on publicly available datasets derived from primary STS tissue. Therefore, direct comparison is not possible given the heterogenous nature of the tissue included in my cohorts. Nonetheless, consistent patterns between previous works and my own confirm that immune gene expression between samples is heterogeneous, and also the ability to identify biological subgroups based upon immune genotyping.

4.3.2 ssGSEA demonstrates contrasting enrichment scores of immune cell gene sets between different immune sarcoma subgroups

To further characterise the immune microenvironment in the ISS subgroups derived from hierarchical clustering, ssGSEA was performed to assess the enrichment of specific gene sets between the subgroups. The heatmap of all of the immune cell gene sets confirmed that ISS1 had a trend for generally higher immune cell enrichment scores compared to the rest of the cohort. However, the heatmap did show that for memory T-cells, NK cells, and NK bright cells, ISS3 had higher enrichment scores, demonstrating the value in undertaking ssGSEA as a complimentary analysis to yield more granularity when compared to single gene analysis alone. Focusing on the gene sets for which there was significantly differential enrichment for specific immune cells, it was observed that ISS1 had significantly higher enrichment scores compared to both ISS2 and ISS3 for CD8+

T-cells and T-helper1 cells (**Figure 4.7**). Given the role of T-helper1 cells to promote the cytotoxic activity of CD8+ cells, the high enrichment scores I observed for ISS1 suggest an immune microenvironment conducive to cytotoxicity and promotion of anti-tumour immune responses[385]. In addition, ISS3 had significantly lower enrichment scores for the global T-cell gene set compared to both ISS1 and ISS2 suggestive of a poorly infiltrated immune microenvironment. It was also observed that ISS1 had significantly higher B-cell ssGSEA scores compared to ISS2. Being responsible for antibody production, B-cells play a key role in the adaptive immune response, including anti-cancer activity[386]. Given the high levels of other effector cells of the immune system which are known to interact and promote B-cell activity, including T-helper1 cells and dendritic cells, this demonstrates further evidence for enrichment of ISS1 with anti-cancer immune cells[269].

For NK cells, I observed that the global NK ssGSEA score was significantly lower in ISS1 compared to ISS3, and this association was also observed when considering NK^{bright} cells (**Figure 4.8**). However, for NK^{dim} cells, there was no significant difference between the ISS subgroups. As such, when considering the composition of the NK population within the ISS subgroups, ISS3 is characterised more predominantly by NK^{bright} cells. NK^{bright} cells are known to function predominantly in the secretion of cytokines, and have previously been shown to contain much lower concentrations of perforin and cytolytic granules compared to NK^{dim} cells[387]. As such, NK^{bright} cells are less actively involved in direct anti-tumour cytotoxic activity and are able to function in both a pro- and anti-immunogenic fashion through either the secretion of cytokines that drive immune response, such as IFN-γ, or immune-regulatory cytokines, such as IL-10[387]. However, given the low expression levels of effector cells of the immune system as described above, T-cells and B-cells, it is more likely that NK^{bright} cells in ISS3 are acting in an immune-modulating role rather than immune-stimulating.

4.3.3 Heterogeneity of the tumour immune microenvironment exists independent of clinicopathological variables

Analysis of the combined cohort was performed to identify any subtype-specific differences in immune gene expression. From the initial heatmap of the 730 genes included in the Nanostring immune gene set, there was no clear pattern of immune gene expression across the 5 subtype categories included for analysis. Although SAM analysis identified differentially expressed immune genes when comparing each subtype to the rest of the cohort, the number of differentially expressed genes for each subtype was small. In addition, insight into the immune-based biology of each subtype was further limited by the contrasting functions of the differentially expressed genes. For example, in the SFT subgroup, *CD207* and *CD40* both had comparatively high expression and are associated with antigen-presenting cells and effector immune cells suggestive of an immune-active microenvironment[295]. In addition, *PRKCD*, associated with TIL infiltration, and IL-11, secreted by tumour-associated macrophages and T-cells, also had higher relative expression[368]. These results would suggest a pro-inflammatory anti-tumourigenic immune microenvironment in SFTs. However, the comparatively high expression of the immune checkpoint *LAG3*, and the low expression of receptors for pro-inflammatory cytokines IL-6 and IL-4 are more suggestive of an immune-suppressed environment. In the LMS subgroup, a similar result is observed with comparatively high expression of genes associated with both pro-inflammatory activity (*CXCL2, IL24, C5* and *A2M*) but also genes associated with immune-suppressive activity (*CDH1, MFGE3*). As such, subtype-specific single gene expression analyses did not clearly define the immune phenotypes of these subtypes within my cohort. In addition, ssGSEA of immune cells did not show clear differential enrichment between subtypes, and upon statistical testing, only NK^{dim} cells had significantly different enrichment scores between different subtypes, with “other” subtypes having higher enrichment scores compared to SFTs.

These results would suggest that within our cohort, there is intra-subtype heterogeneity in immune gene expression and immune cell infiltration. And indeed, these findings are in keeping with a number of published works

demonstrating that many STS subtypes display intra-subtype heterogeneity of the immune microenvironment. For example, work by Toulmonde *et al*. demonstrated that undifferentiated pleomorphic sarcoma can be categorised into immune high/low, with distinct immune gene expression profiles, immune cell infiltration and radiological findings[388]. Indeed a number of studies have demonstrated that subtype-specific expression of putative immune-based biomarkers demonstrates extensive intra-subtype heterogeneity[389]. Furthermore, studies which have leveraged publicly available genomic data sets of a range of STS subtypes to generate immune gene-based molecular subgroups have shown inconsistent subgroup classification of various histological STS subtypes[293,390,391]. As such, although further characterisation of subtype-specific immune microenvironment features may yield markers for clinical course and treatment response, evidence suggests that significant intra-subtype heterogeneity may limit progress.

Given previously reported work suggesting that both tumour grade and patient age are associated with differential immune gene expression and tumour immune microenvironments, the association between tumour grade and age and immune gene expression in the combined cohort was undertaken[374–377,381–384]. However, plotting a heatmap of the immune gene expression data did not show any significant patterns attributable to either factor. In addition, ssGSEA did not show any significantly enriched immune cells based on patient age and tumour grade. As such, within the combined cohort, differences in immune gene expression could not be attributable to either tumour grade or patient age.

4.3.4 Critical assessment of the methods employed and limitations

As previously mentioned, one of the considerations that had to be made when deciding upon analytical techniques in this study was the quantity and quality of tumour material available. Indeed, all of the material was FFPE with many of the samples stored for a number of years prior to extraction of nucleic acid for the purposes of this study. The impact of this preservation and storage method is that it is associated with a significant degree of nucleic acid degradation when

compared to alternative storage methods, such as fresh frozen[392,393]. As such, the platform selected for gene expression analysis had to be capable of generating reliable and robust data for fragmented nucleic acid material, and a number of studies had confirmed Nanostring's ability to achieve that[350–353]. Furthermore, as the goal of this chapter was to focus specifically on the expression of immune-related genes to allow a detailed characterisation of the immune-based biology of STS, the nCounter PanCancer immune profiling panel was ideal for this role. Alternative gene sequencing techniques could have been considered if the quality of extracted nucleic acid had been less problematic. Indeed, complimentary analyses would have provided additional information and granularity to the description of the immune microenvironment in this cohort. For example, whole exome sequencing (WES) could be used to quantify the tumour mutational burden of the samples, whilst RNA-Seq could be used to predict neoantigen immunogenicity or characterise the T-cell receptor repertoire[394–397]. Indeed, any one modality in isolation is insufficient in wholly describing the tumour microenvironment, however, the more information that is acquired and available will help provide a more complete picture. As such, additional next-generation sequencing analyses in the future, such as WES or RNA-Seq would add value to this study in helping to further characterise the immune microenvironment in STS.

4.3.5 Conclusion

In this chapter, analysis of immune gene expression in the combined cohort identified 3 immune subtypes with distinct immune gene expression. I have shown that within the combined cohort, one immune subgroup is characterised by high immune gene expression, one by low immune gene expression, and the final subgroup by intermediate gene expression. Undertaking analysis to identify genes significantly differentially expressed between the subgroups confirmed this finding, whilst ssGSEA identified a number of immune cells which demonstrated significant enrichment based upon ISS category. Analysis of the association between immune gene expression and clinicopathological variables identified genes with differential expression based upon STS subtype. Given the findings in this chapter of distinct immune subgroups, evidence of intra-subtype heterogeneity, and a lack of association between immune gene expression and

both tumour grade and patient age, the next chapter will investigate the potential for an immune-based biomarker to be associated with contrasting survival in the pazopanib-treated combined cohort.

Chapter 5 - Development of a prognostic model in a pazopanib-treated cohort

5.1 Background and objectives

Despite numerous efforts to improve clinical outcomes of patients with advanced soft tissue sarcoma (STS), following failure of first-line therapy, efficacious treatment options are limited and prognosis is generally poor (**Section 1.3.4**)[55,58–63,69]. Pazopanib showed promising results in advanced STS during early clinical trials, and in the PALETTE phase III trial demonstrated improved progression-free survival (PFS) compared to placebo in non-adipocytic STS[128,130,132]. However, the failure to demonstrate a significant overall survival (OS) benefit relative to placebo significantly impacted cost-effectiveness analysis[128,130,132]. Nevertheless, subsequent post-hoc analyses of clinical trial data, as well as published real-word experience, have confirmed that a subset of patients do experience robust and durable clinical benefit following pazopanib therapy[135,140–146]. Indeed, Kasper *et al.*'s analysis of the combined phase II and phase III clinical trial cohorts investigating pazopanib reported 36% of patients having a PFS of greater than 6 months, and 34% having an OS greater than 18 months following initiation of pazopanib[135]. Therefore, one of the greatest challenges in the clinical setting is the lack of clinically relevant biomarkers which are able to stratify patients into those most likely to gain benefit from pazopanib.

In **Chapter 3**, I observed notable survival trends in the pazopanib-treated combined cohort based on stratification by immunohistochemistry (IHC) of tumour infiltrating CD4+ lymphocytes (TILs). In **Chapter 4**, I built on this by undertaking targeted immune gene expression analysis of the combined cohort to better describe the immune tumour microenvironment. This identified that the combined cohort could be split into three immune sarcoma subgroups (ISS) with differential gene expression, and variable immune cell infiltration. Furthermore, different soft tissue sarcoma subtypes also demonstrated differential immune gene expression.

There has been a growing appreciation of the potential for molecular characterisation of tumours to yield clinically meaningful biomarkers able to direct patient care in oncology. Indeed, the Prosigna score in breast cancer is an example of a molecularly-based risk score which is now showing utility in aiding

clinical decision making[199–202]. Furthermore, Beuselinck *et al.* developed a molecular classifier for metastatic clear cell renal cell carcinoma able to predict clinical benefit from the anti-angiogenic tyrosine kinase inhibitors (TKI) sunitinib and pazopanib[311].

However, in STS similar progress has not been made and robust prognostic molecular biomarkers for treatment outcomes are lacking. In addition, given my findings in Chapter 4 which identified differential immune gene expression in the combined cohort, there is a rationale for investigating the potential for an immune-based prognostic model to be built. My hypothesis was that the exploration of a multivariable survival model incorporating immune gene expression data would generate a clinically relevant prognostic model in my pazopanib-treated cohort.

As such, the aims of this chapter are:

1. to analyse the discovery cohort data to assess the significance of immune-gene expression, as well as clinicopathological variables, on survival, and to build a prognostic model based on the discovery cohort
2. to assess the prognostic models built using the discovery cohort data on the independent validation cohort
3. to refine the prognostic model on the combined (discovery plus validation) cohort for a more confident model with better estimates of the risk coefficients.

5.1.1 Contributions

Work of the candidate included:

- Study conception and design in conjunction with the supervisory team.
- Normalisation of discovery and validation cohorts.
- Principal component analysis.
- Cox proportional hazards modelling.
- Forest plot generation.

Advanced statistical analyses were undertaken under the supervision of Dr. Maggie Cheang, team leader at the Institute of Cancer Research's (ICR) Clinical Trials and Statistics Unit.

RNA extraction, quality control, and aliquoting of RNA for subsequent Nanostring analysis of the validation and comparator cohorts was performed by higher scientific officer Nafia Guljar.

Running of the Nanostring assay was performed by Richard Buus, senior scientific officer at the ICR's Ralph Lauren centre.

5.2 Results

5.2.1 Workflow for data analysis

I employed a workflow to incorporate immune gene expression data and clinicopathological variables into a prognostic model initially built from the discovery cohort, before testing against the independent validation cohort, and finally refining the model on the combined discovery plus validation cohort (**Figure 5.1**).

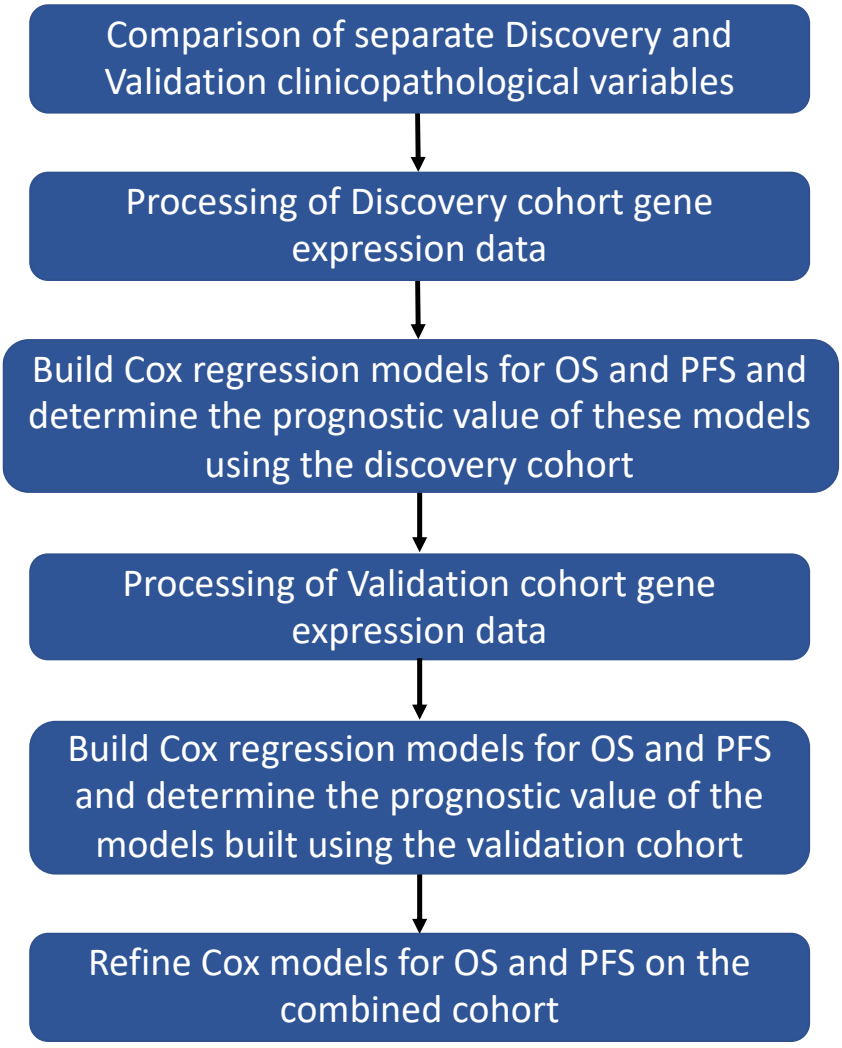

Figure 5.1: Planned workflow for data processing and generation of prognostic models for the combined cohort.

5.2.2 Assessing comparability of the discovery and validation cohorts

The power calculation previously shown in the materials and methods chapter (**Section 2.2.4**) had demonstrated that a minimum of 65 cases would be required for an adequately powered study assessing a single parameter for PFS. As such, the experimental design was to fit Cox regression models initially on a discovery cohort, before then fitting Cox regression models utilising the independent validation cohort. The final prognostic model would then be fit on the combined cohort, because given the larger size this would be more robust, with greater confidence and more accurate estimations of Cox coefficients, and this would be the prognostic model to take forward in future work.

The first stage of analysis to be undertaken involved assessing the comparability of the discovery and validation cohort in terms of clinicopathological variables. Given the aim of building a prognostic model on the discovery cohort, and subsequently testing the model on the independent validation cohort, it was desirable to assess for any biases in variables to ensure comparability. However, given the small cohort sizes, and the heterogeneous nature of the cohorts, some biases were inevitable, but combining them into the combined cohort for the final analyses would negate the biases in these initial cohorts.

Clinicopathological variables of the discovery and validation cohorts were determined (**Tables 5.1** and **5.2**). Between the discovery and validation cohorts, there were no obvious differences in any of the patient or tumour characteristics assessed, including tumour grade, and patient age and performance status at the start of pazopanib therapy.

For data processing, the immune gene data for the discovery cohort were normalised utilising the 'NanostringNorm' R package[325]. Following normalisation, a gene-filtering process was performed in which genes for which 25% or greater of the samples had a value of 0 were removed for subsequent analysis. Following normalisation and filtering, the median immune gene value of the 573 genes for each sample was identified, termed the median gene expression signature (MGES).

In addition, a distribution plot of the MGES values to be employed in the regression models was also plotted (**Figure 5.2**). This demonstrated no obvious differences in the distribution of the MGES values.

Table 5.1: Baseline clinicopathological variables for the discovery and validation cohorts generated for this study. LMS – leiomyosarcoma; LPS - liposarcoma; MPNST – malignant peripheral nerve sheath tumour; NOS – not otherwise specified; SFT – solitary fibrous tumour; UPS – undifferentiated pleomorphic sarcoma.

Cohort	Combined split ino	
	Discovery	Validation
n	37 (%)	28 (%)
Sex		
M	13 (35%)	13 (46%)
F	24 (65%)	15 (54%)
Age (years)		
Median	57.1	54
Range	19.8 - 81.2	18 - 77
Grade		
1	2 (5%)	2 (7%)
2	17 (46%)	4 (14%)
3	18 (49%)	17 (61%)
UNK	0 (0%)	5 (18%)
Performance Status		
0	7 (19%)	12 (43%)
1	17 (46%)	15 (54%)
2	7 (19%)	0 (0%)
UNK	6 (16%)	1 (3%)
Sarcoma Subtype		
LMS	10 (27%)	8 (28%)
SFT	7 (19%)	2 (7%)
UPS	2 (5.5%)	1 (4%)
Chondrosarcoma	2 (5.5%)	0 (0%)
Myxofibrosarcoma	2 (5.5%)	0 (0%)
Myxoid LPS	2 (5.5%)	0 (0%)
Synovial Sarcoma	0 (0%)	5 (18%)
Sarcoma NOS	0 (0%)	5 (18%)
Spindle Cell Sarcoma	3 (8%)	4 (14%)
Other*	9 (24%)	3 (11%)
Prior lines systemic therapy		
0	9 (24%)	3 (11%)
1	8 (22%)	16 (57%)
2	11 (30%)	4 (14%)
3+	9 (24%)	5 (18%)

* other cases include; in the discovery cohort, single cases of alvolear soft part sarcoma, angiosarcoma, clear cell sarcoma, fibromyxoid sarcoma, fibrosarcoma, granular cell tumour, malignant haemangioendothelioma, malignant peripheral nerve sheath tumour, and PEComa; in the validation cohort atypical Ewings, dedifferentiatied liposarcoma and fibromyxoid sarcoma

Table 5.2: Clinicopathological variables including response to therapy and survival data at 18-month censor. Response to therapy was assessed on cross-sectional imaging by response evaluation criteria in solid tumours (RECIST 1.1)[336]. CR – complete response; IQR – interquartile range; OS – overall survival; PD – progressive disease; PFS – progression-free survival; PR – partial response; SD – stable disease; UNK – unknown.

Cohort	Combined split ino	
	Discovery	Validation
n	37 (%)	28 (%)
Sample Type		
Primary	19 (51%)	16 (57%)
Metastasis	11 (30%)	6 (21%)
Local Recurrence	7 (19%)	3 (11%)
UNK	0 (0%)	3 (11%)
Best Response		
PD	7 (19%)	7 (25%)
SD	15 (40.5%)	11 (39%)
PR	5 (13.5%)	7 (25%)
CR	0 (0%)	0 (0%)
UNK	10 (27%)	3 (11%)
PFS (months)		
Median	3.7	4.15
Range	0.27 - 18	0.43 - 18
IQR	1.93 - 7.13	1.96 - 9.14
OS (months)		
Median	9.17	6.48
Range	0.27 - 18	0.43 - 18
IQR	4.07 - 18	3.39 - 13.55

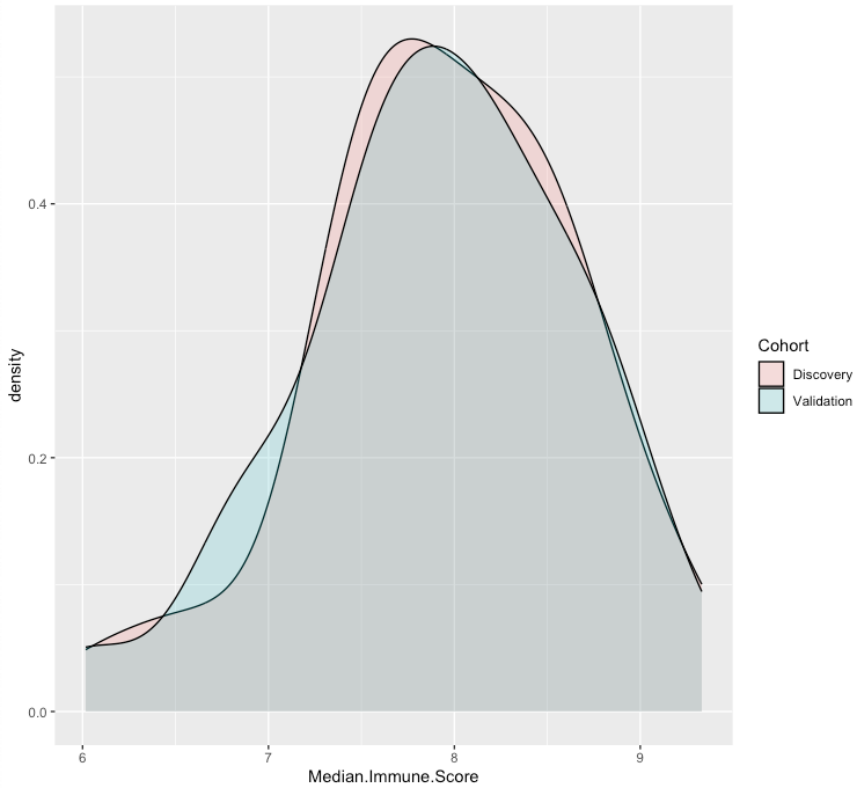

Figure 5.2: Distribution plot of the median gene expression signature (MGES) for the discovery and validation cohorts, showing no obvious differences in distribution.

5.2.3 Fitting Cox regression models to the discovery cohort

5.2.3.1 Overall Survival

Cox regression models incorporating different variables for OS were built using the discovery cohort. Firstly, a univariable Cox regression model for OS was built incorporating the MGES for each sample as the variable of interest. This univariable model was significantly associated with OS (hazard ratio (HR) 2.52, 95% confidence interval (CI) 1.25-5.10; p=0.011), with higher MGES associated with an increased HR and therefore inferior OS.

Subsequently, in order to estimate the prognostic value of the MGES adjusting for other clinicopathological variables, two Cox multivariable regression models for OS were built using the discovery cohort, a full model and a nested model (**Table 5.3** and **Figure 5.3**). For the full model, the clinicopathological features of patient age at the start of pazopanib therapy, patient performance status at the start of pazopanib therapy, tumour grade and MGES were included as co-variables. The nested model included only the standard clinicopathological variables (i.e. without MGES). The aim of this was to determine whether the addition of MGES adds prognostic information when compared to a survival model including only the clinicopathological variables currently used in the clinical setting.

The results of the Cox regression model of the full model for OS show that both higher MGES (p=0.026) and having a high-grade tumour (p=0.027) are significantly associated with inferior OS. Furthermore, the full model itself is statistically significantly associated with OS (p=0.004). In the nested model, a patient performance status of 2 compared to 0, and a high-grade tumour were significantly associated with inferior OS (p=0.034 and 0.023 respectively). The nested model was also significantly associated with OS (p=0.02), however as evidenced by the difference in chi-square between the full and nested models, the full model fits the data significantly better than the nested model (p=0.020).

Therefore, in the discovery cohort, the significant association between higher expression of MGES and inferior survival was observed adjusting for other factors suggesting that MGES could potentially be a prognostic marker.

Table 5.3: Summary of Cox multivariable regression models for overall survival (OS) in the discovery cohort (n=37). The full model was built including the clinicopathological features of tumour grade, patient age and performance, and the median gene expression signature. The nested model excluded MGES as a co-variable. For tumour grade, this was stratified into a binary measure, with category 2 equating to high-grade tumours and category 1 to other grades.

Feature	Groups (#samples)	Full Model - OS		Nested Model - OS	
		HR (95% CI)	P-value	HR (95% CI)	P-value
Median Gene Expression Signature	Continuous (n=37)	2.27 (1.10 – 4.68)	0.0265 *		
Age	Continuous (n=37)	1.00 (0.96 – 1.04)	0.879	0.99 (0.96 – 1.03)	0.6579
Performance Status	0 (n=7)	1	-	1	-
	1 (n=17)	1.43 (0.31 – 6.56)	0.6433	2.74 (0.66 – 11.3)	0.1645
	2 (n=7)	3.53 (0.68 – 18.2)	0.1328	5.91 (1.15 – 30.4)	0.0335 *
	-1 (n=6)	0.45 (0.06 – 3.34)	0.4323	0.72 (0.10 – 5.06)	0.742
Grade	1 (n=19)	1	-	1	-
	2 (n=18)	2.51 (1.11 – 5.70)	0.0276 *	2.49 (1.13 – 5.49)	0.0233 *
Chi-square (Likelihood Ratio)		19.1 (df = 6, p = 0.004*)		13.71 (df = 5, p = 0.02*)	
Chi-square (against ClinPath only model)		5.3913 (p = 0.02024*)			

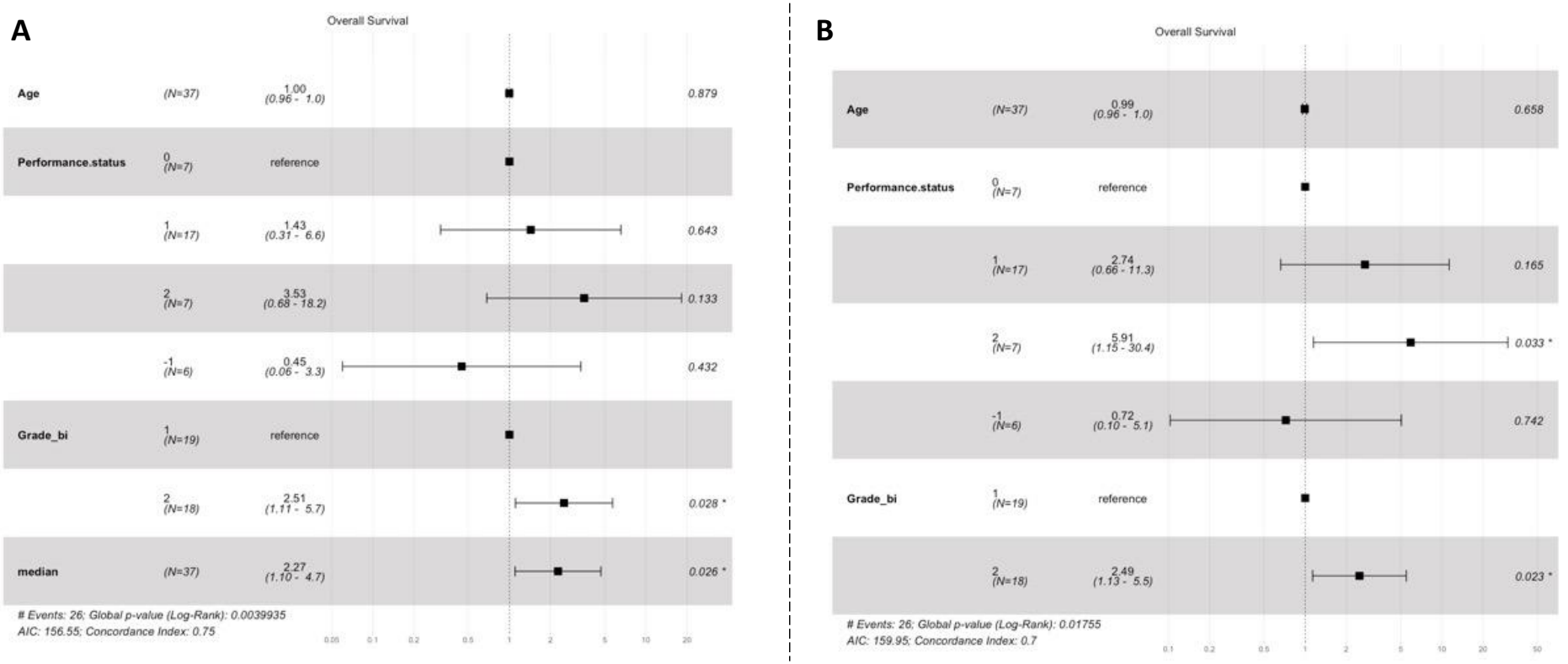

Figure 5.3: Forest plots of Cox multivariable regression models built on the discovery cohort (n=37) for overall survival (OS). **A** Full model – patient age, patient performance status, tumour grade and median gene expression score all included as co-variables **B** Nested model – median gene expression signature excluded from the full mode.

5.2.3.2 Progression-free survival

Cox regression models incorporating different variables were then built to analyse PFS in the discovery cohort. A univariable Cox regression model for PFS, incorporating MGES as the variable of interest, was built. This did not show a significant association between MGES and PFS (HR 1.53, 95% CI 0.89-2.65; p=0.128), although the direction of risk was for increased HR with increased MGES.

Multivariable Cox models were then built to analyse their association with PFS, a full model including MGES and standard clinicopathological features (tumour grade, patient age and performance status), and a nested model in which MGES was not included (**Table 5.4** and **Figure 5.4**). For the full model, there was a significant association with PFS (p=0.03), with high-grade tumours the only co-variable significantly associated with worse PFS (p=0.026). For the nested model, again high-grade tumours were significantly associated with PFS (p=0.033), and the regression model itself was significantly associated with PFS (p=0.03).

When comparing the full model with the nested model for PFS in the discovery cohort, the addition of MGES as a co-variable in the full model adds prognostic value as evidenced by the difference in chi-square between the full and nested models. However, analysis revealed no significant differences between the models in terms of their fit (p=0.202).

Table 5.4: Summary of Cox multivariable regression models for progression-free survival (PFS) in the discovery cohort (n=37). The full model was built including the clinicopathological features of tumour grade, patient age and performance, and the median gene expression signature. The nested model excluded MGES as a co-variable. For tumour grade, this was stratified into a binary measure, with category 2 equating to high-grade tumours and category 1 to other grades.

Feature	Groups (#samples)	Full Model - PFS		Nested Model - PFS	
		HR (95% CI)	P-value	HR (95% CI)	P-value
Median Gene Expression Signature	Continuous (n=37)	1.43 (0.82 – 2.50)	0.206		
Age	Continuous (n=37)	0.99 (0.96 – 1.02)	0.364	0.98 (0.96 – 1.02)	0.3236
Performance Status	0 (n=7)	1	-	1	-
	1 (n=17)	1.87 (0.50 – 7.00)	0.352	2.76 (0.83 – 9.15)	0.0969
	2 (n=7)	1.85 (0.44 – 7.75)	0.399	2.63 (0.67 – 10.4)	0.1662
	-1 (n=6)	0.41 (0.09 – 1.83)	0.243	0.54 (0.13 – 2.24)	0.3928
Grade	1 (n=19)	1	-	1	-
	2 (n=18)	2.34 (1.11 – 4.96)	0.026 *	2.22 (1.07 – 4.61)	0.0327 *
Chi-square (Likelihood Ratio)		13.72 (df = 6, p = 0.03*)		12.1 (df = 5, p = 0.03*)	
Chi-square (against ClinPath only		1.6213 (p = 0.2029)			

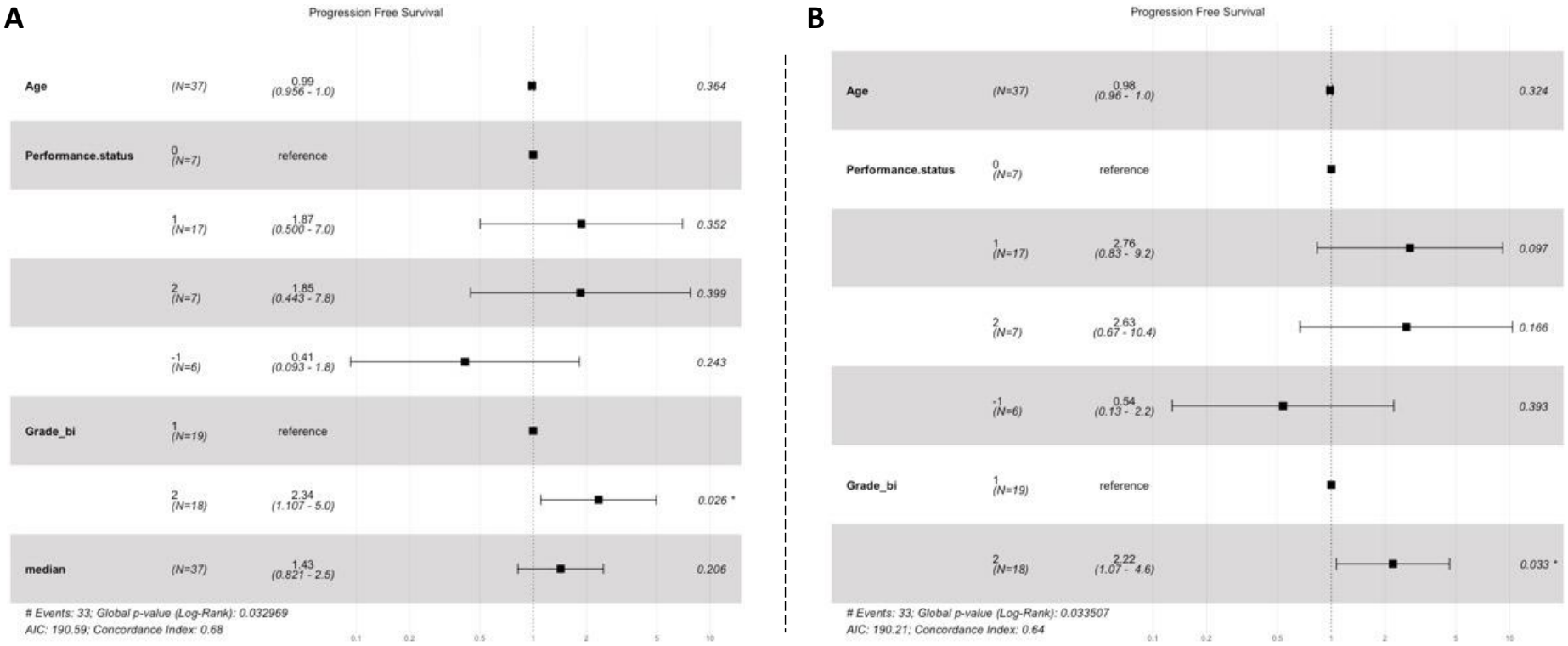

Figure 5.4: Forest plots of Cox multivariable regression models built on the discovery cohort (n=37) for progression-free survival (PFS). **A** Full model – patient age, patient performance status, tumour grade and median gene expression score all included as co-variables **B** Nested model – median gene expression signature excluded from the full model.

5.2.4 Fitting regression models to the validation cohort

After building the Cox regression models on the discovery cohort, samples from the validation cohort were used to validate the clinical prognostic model.

The immune gene expression data generated from samples of the validation cohort were pre-processed with reference to the discovery cohort. Employing the 'NanostringNorm' R package, validation data were normalised with normalisation factors for the geometric means of positive control and housekeeping genes of the discovery cohort used to dictate a normalisation target. Following normalisation, the same 573 genes as previously identified in the discovery cohort were selected to calculate the median gene expression score for each validation sample. Following data normalisation, and identification of the MGES for each sample, Cox regression models were built to assess their prognostic value in the validation cohort.

5.2.4.1 Overall survival

A univariable Cox model for OS was built using MGES alone in the validation cohort. This model demonstrated that higher MGES was associated with a non-significant higher HR for OS (HR 1.21, 95% CI 0.66-2.19; p=0.536). The direction of the association between MGES and higher HR is consistent with findings from the discovery cohort, but not statistically significant likely due to the small sample size.

A multivariable Cox model for OS was then built on the validation cohort including MGES and standard clinicopathological features as co-variables (**Figure 5.5**). Although high-grade tumours were significantly associated with inferior OS (p=0.032), the model itself was not significantly associated with OS (p=0.1).

A

Feature	Groups (#samples)	Full Model - OS	
		HR (95% CI)	P-value
Median Gene Expression Signature	Continuous (n=28)	1.14 (0.59-2.21)	0.6933
Age	Continuous (n=28)	1.00 (0.96 – 1.03)	0.8495
Performance Status	0 (n=12)	1	-
	1 (n=15)	3.69 (0.96 - 14.2)	0.0571
	2 (n=0)	-	-
	-1 (n=1)	48.5 (2.20 - 1069)	0.0139 *
Grade	1 (n=11)	1	-
	2 (n=17)	3.92 (1.13-13.7)	0.0319 *
Chi-square (Likelihood Ratio)		8.68 (df = 5, p = 0.1)	
ΔChi-square (against ClinPath only model)		0.1567 (p = 0.6922)	

B

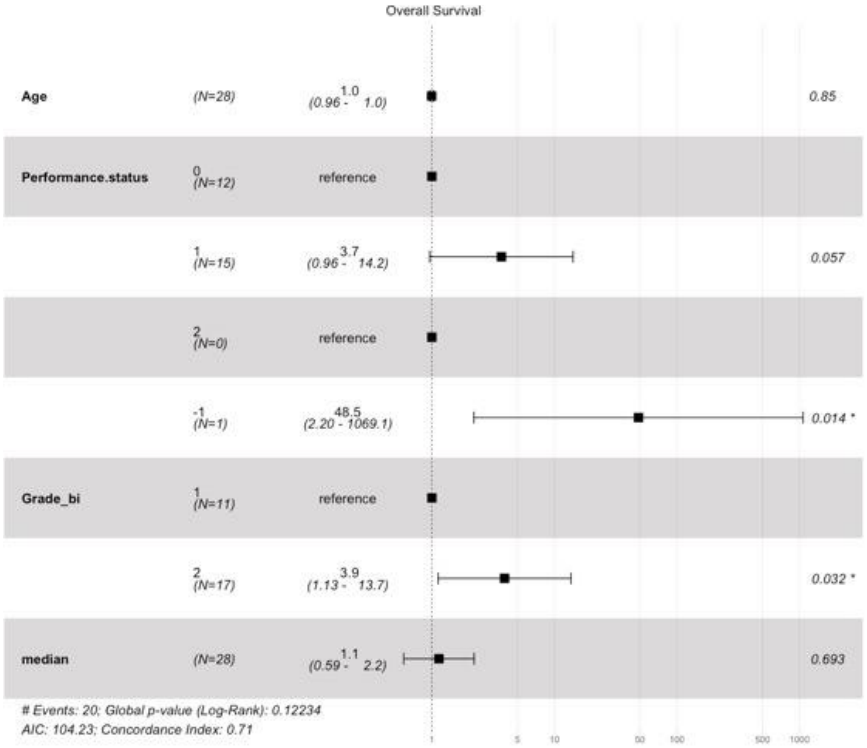

Figure 5.5: **A** Summary of Cox multivariable regression models for overall survival (OS) in the validation cohort (n=28). The model was built including the clinicopathological features of tumour grade, patient age and performance, and the median gene expression signature. For tumour grade, this was stratified into a binary measure, with category 2 equating to high-grade tumours and category 1 to other grades. **B** Forest plot of the multivariable model for OS built on the validation cohort.

5.2.4.2 Progression-free survival

The validation cohort was then analysed by univariable Cox regression modelling for PFS with MGES the variable of interest. As with OS in the validation cohort, this univariable model confirmed a non-significant association between higher MGES and inferior survival in terms of PFS (HR 1.72, 95% CI 0.97-3.05; p=0.064).

Subsequently, a multivariable Cox regression model was built for PFS of the validation cohort, with standard clinicopathological variables and MGES included as co-variables. This regression model was found to be significantly associated with PFS (p=0.05). In this multivariable model, higher MGES is again associated with a non-significant increase in the HR, and therefore inferior PFS.

The association of higher expression of MGES with poor survival was observed adjusting for other factors suggesting that MGES could potentially be a prognostic marker. Furthermore, the direction of the association between MGES and higher HR is consistent with findings from the discovery cohort.

A

Feature	Groups (#samples)	Full Model - PFS	
		HR (95% CI)	P-value
Median Gene Expression Signature	Continuous (n=28)	1.72 (0.93 - 3.16)	0.0825
Age	Continuous (n=28)	1.01 (0.98 - 1.04)	0.5987
Performance Status	0 (n=12)	1	-
	1 (n=15)	2.47 (0.82 - 7.40)	0.1074
	2 (n=0)	-	-
	-1 (n=1)	27.5 (1.55 - 489)	0.0240 *
Grade	1 (n=11)	1	-
	2 (n=17)	2.87 (0.98 - 8.44)	0.055
Chi-square (Likelihood Ratio)		10.85 (df = 5, p = 0.05*)	
Δ Chi-square (against ClinPath only		3.1335 (p = 0.0767)	

B

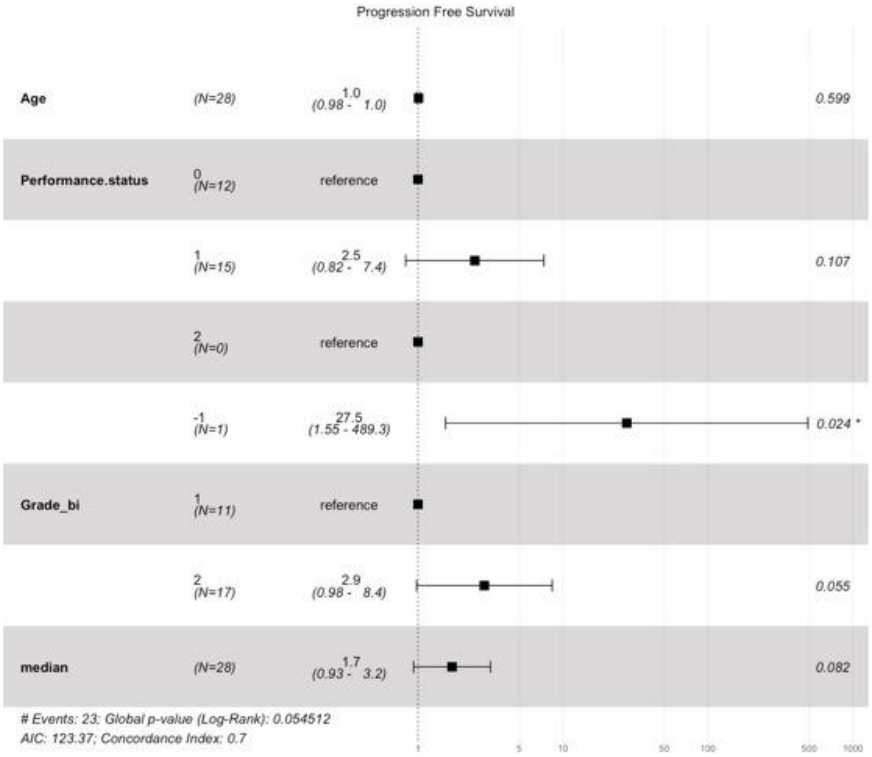

Figure 5.6: **A** Summary of Cox multivariable regression models for progression-free survival (PFS) in the validation cohort (n=28). The model was built including the clinicopathological features of tumour grade, patient age and performance, and the median gene expression signature. For tumour grade, this was stratified into a binary measure, with category 2 equating to high-grade tumours and category 1 to other grades. **B** Forest plot of the multivariable model for PFS built on the validation cohort.

5.2.5 Refining Cox regression models through combined cohort analysis

In this chapter so far, Cox regression models have been built on the discovery cohort which confirmed that a model including standard clinicopathological variables with the addition of the MGES was providing additional prognostic information when compared to one with just standard clinicopathological variables. In addition, analysis of the independent validation cohort confirmed that the direction of the association between MGES and higher HR is consistent between the discovery and validation cohorts.

Therefore, the next step in the analysis was to build prognostic models on the combined cohort. The value of undertaking this step is that it allows refinement of the prognostic model with a better estimate of the coefficients for each variable due to the larger sample size.

5.2.5.1 Overall survival

A univariable Cox regression model was built for OS of the combined cohort, with the MGES value acting as the variable of interest. This demonstrated a significant association between MGES and OS (HR 1.66, 95% CI 1.07-2.58; p=0.024), with higher MGES associated with inferior OS.

Given this result, and with the aim of estimating the prognostic value of the signature adjusting for clinicopathological variables, two multivariable Cox regression models for OS were built. These were a full model incorporating MGES and standard clinicopathological features, and a nested model which did not include MGES as a co-variable (**Table 5.5** and **Figure 5.7**).

Statistical analysis of the full model confirmed that the model was significantly associated with OS (p=0.003). For the co-variables included, higher MGES (p=0.050) and having a high-grade tumour (p=0.005) were significantly associated with inferior OS. In addition, performance status 2 (p=0.012) and performance status 1 (p=0.048) were significantly associated with worse OS.

From analysis of the nested model, again it was determined that there was a significant association between the model and OS (p=0.007). Of the variables included in the nested model, high-grade tumours were significantly associated with inferior OS (p=0.003), whilst patients with performance status 0 had significantly superior OS compared to patients with either performance status 1 (p=0.033) or 2 (p=0.009).

Importantly, when comparing the full model with the nested model, there is a significant difference in the chi-square between the two models for OS (p=0.046). This suggests that the full model fits the data significantly better than the nested model, and as such addition of MGES adds additional prognostic information compared to standard clinicopathological variables alone.

Table 5.5: Summary of Cox multivariable regression models for overall survival (OS) in the combined cohort (n=65). The full model was built including the clinicopathological features of tumour grade, patient age and performance, and the median gene expression signature. The nested model excluded MGES as a co-variable. For tumour grade, this was stratified into a binary measure, with category 2 equating to high-grade tumours and category 1 to other grades.

Feature	Groups (#samples)	Full Model - OS		Nested Model - OS	
		HR (95% CI)	P-value	HR (95% CI)	P-value
Median Gene Expression Signature	Continuous (n=65)	1.57 (1-2.47)	0.0498 *		
Age	Continuous (n=65)	1.00 (0.98-1.02)	0.8991	1.00 (0.98 - 1.02)	0.8967
Performance Status	0 (n=19)	1	-	1	-
	1 (n=32)	2.34 (1.01-5.40)	0.0475 *	2.58 (1.08-6.18)	0.0327 *
	2 (n=7)	4.17 (1.36-12.8)	0.0122 *	4.53 (1.45-14.2)	0.0093 *
	-1 (n=7)	0.92 (0.24-3.61)	0.9064	0.92 (0.23-3.64)	0.9036
Grade	1 (n=30)	1	-	1	-
	2 (n=35)	2.48 (1.33-4.64)	0.0045 *	2.60 (1.38-4.87)	0.0029 *
Chi-square (Likelihood Ratio)		19.96 (df = 6, p = 0.003*)		15.99 (df = 5, p = 0.007*)	
Chi-square (against ClinPath only model)		3.9726 (p = 0.04625*)			

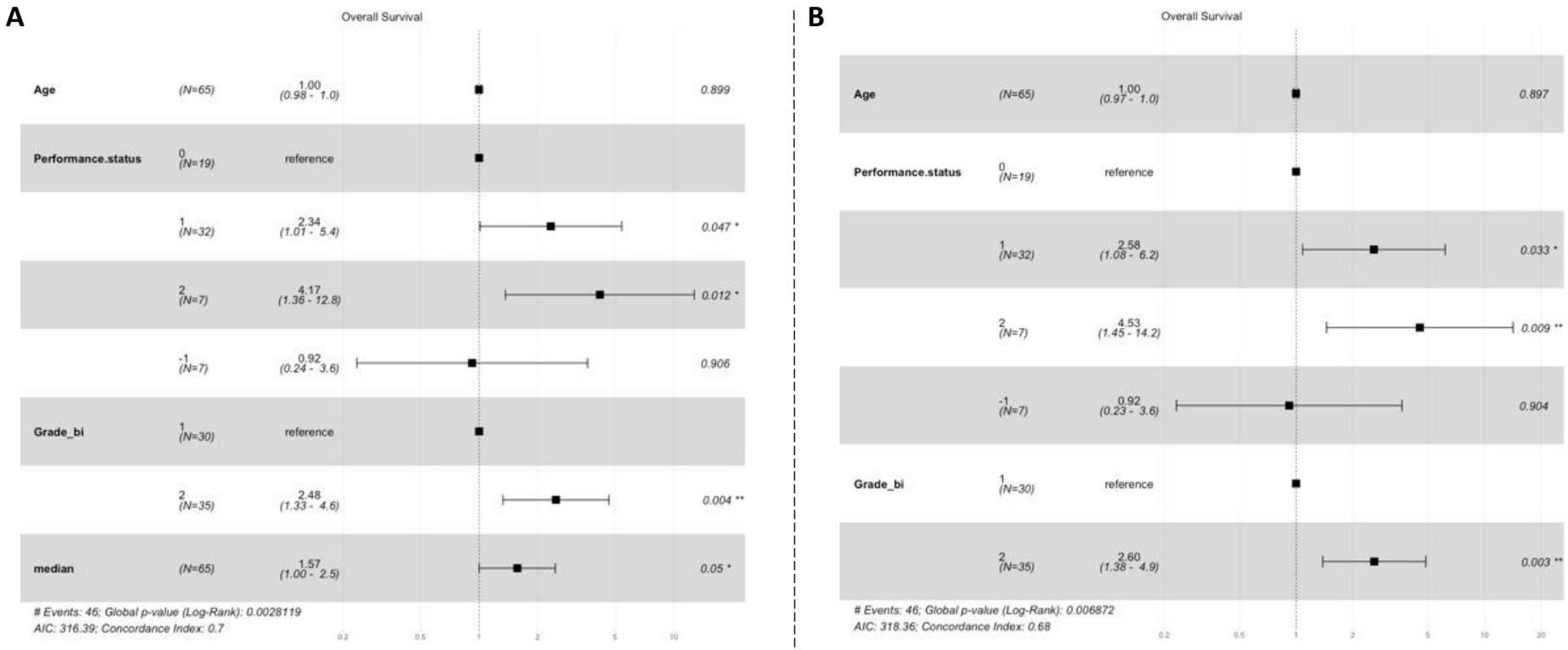

Figure 5.7: Forest plots of Cox multivariable regression models built on the combined cohort (n=65) for overall survival (OS). **A** Full model – patient age, patient performance status, tumour grade and median gene expression score all included as co-variables **B** Nested model – median gene expression signature excluded from the full model.

5.2.5.2 Progression-free survival

A univariable Cox model of PFS was then built for the combined cohort, with MGES as the variable of interest. This demonstrated a significant association between increased MGES and inferior PFS (HR 1.63, 95% CI 1.1-2.42; p=0.016).

Two Cox regression models were then built for PFS, a full model including MGES and clinicopathological features as co-variables, and a nested model which included only standard clinicopathological features as co-variables (**Table 5.6** and **Figure 5.8**). Statistical analysis confirmed that the full model was significantly associated with PFS (p=0.01). In terms of variables, higher MGES was significantly associated with inferior PFS (p=0.025), as was having a high-grade tumour (p=0.015).

Analysis of the nested model also confirmed that the model itself was significantly associated with PFS (p=0.05). From the variables included, high-grade tumours (p=0.013), and performance status 1 compared to 0 (p=0.037) were significantly associated with inferior PFS.

When comparing the full model with the nested model, the difference in chi-square between the two models is significantly different (p=0.024), suggesting a significant improvement of the fit of the full model relative to the nested model. As such, the addition of MGES in the full model adds significant prognostic value compared to clinicopathological variables alone.

Table 5.6: Summary of Cox multivariable regression models for progression-free survival (PFS) in the combined cohort (n=65). The full model was built including the clinicopathological features of tumour grade, patient age and performance, and the median gene expression signature. The nested model excluded MGES as a co-variable. For tumour grade, this was stratified into a binary measure, with category 2 equating to high-grade tumours and category 1 to other grades.

Feature	Groups (#samples)	Full Model - PFS		Nested Model - PFS	
		HR (95% CI)	P-value	HR (95% CI)	P-value
Median Gene Expression Signature	Continuous (n=65)	1.57 (1.06-2.34)	0.0253 *		
Age	Continuous (n=65)	1.00 (0.98-1.02)	0.9736	1.00 (0.98-1.02)	0.8826
Performance Status	0 (n=19)	1	-	1	-
	1 (n=32)	1.92 (0.92-3.99)	0.0815	2.26 (1.05-4.86)	0.0369 *
	2 (n=7)	1.89 (0.681-5.22)	0.222	2.28 (0.81-6.42)	0.1194
	-1 (n=7)	0.72 (0.24-2.12)	0.5459	0.79 (0.26-2.36)	0.67
Grade	1 (n=30)	1	-	1	-
	2 (n=35)	2.04 (1.15-3.64)	0.0154 *	2.09 (1.17-3.75)	0.0130 *
Chi-square (Likelihood Ratio)		16.11 (df = 6, p = 0.01*)		11 (df =5, p = 0.05*)	
Chi-square (against ClinPath only		5.1133 (p = 0.02374*)			

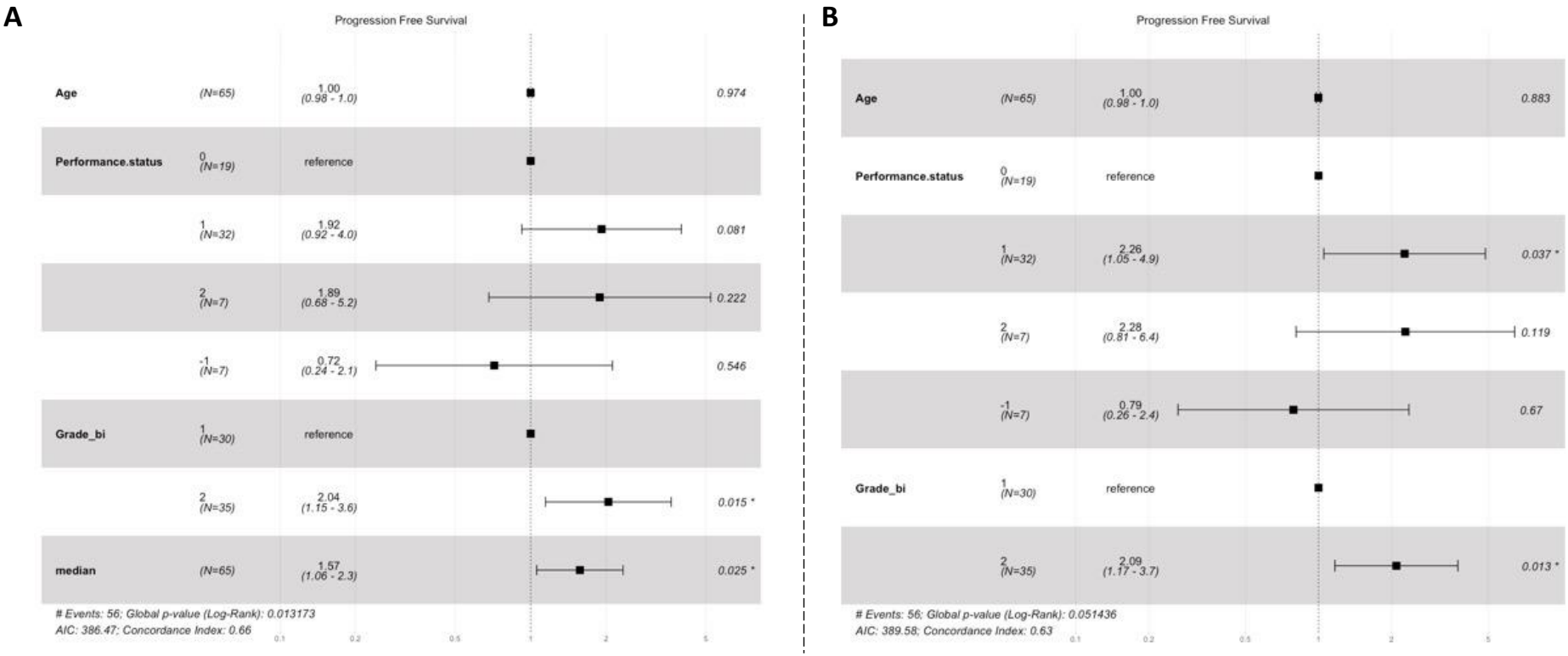

Figure 5.8: Forest plots of Cox multivariable regression models built on the combined cohort (n=65) for progression-free survival (PFS). **A** Full model – patient age, patient performance status, tumour grade and median gene expression score all included as co-variables **B** Nested model – median gene expression signature excluded from the full model.

The final analysis undertaken as part of the development of a prognostic model in the combined cohort was to analyse if STS subtype significantly impacted the prognostic value of the model. As such, STS subtype was added as a co-variable in a multivariable Cox regression model for OS and PFS (**Table 5.7** and **Figure 5.9**). Given the range of STS subtypes, distinct subtype categories were limited to STS subtypes with at least 5 cases, with the remaining STS subtypes categorised as “other”. In this way, 5 categories of STS subtype were included; leiomyosarcoma (LMS), solitary fibrous tumour (SFT), spindle cell sarcoma, synovial sarcoma (SS) and “other” subtypes.

The multivariable Cox regression model built for OS was shown to be significantly associated with OS (p=0.004). For the variables included in building the model, performance status 1 and 2 were significantly associated with inferior OS compared to performance status 0 (p=0.048 and p=0.012 respectively). In addition, high-grade tumours (p=0.005) and increasing MGES (p=0.050) were significantly associated with inferior OS (p=0.050). For STS subtypes, it was noted that spindle cell sarcomas were significantly associated with inferior OS when compared to the “other” STS subtype group (p=0.022). When compared to the model built with clinicopathological variables plus MGES, the addition of STS subtype did increase the prognostic value of the model as evidenced by the increase in chi-square. However, this was not statistically significant, indicating that the addition of STS subtype does not significantly improve the fit of the model (p=0.193).

For PFS, again the multivariable Cox regression model built with clinicopathological variables, MGES and STS subtype, reported a significant association with PFS (p=0.02). For the co-variates included, only high-grade tumours (p=0.015) and increasing MGES (p=0.025) were significantly associated with inferior PFS. As with OS, the addition of STS subtype to the PFS regression model did increase the prognostic value of the model, but this was not a statistically significant increase and therefore addition of STS subtype does not significantly improve the fit of the model (p=0.277).

Table 5.7: Summary of Cox multivariable regression models for overall survival (OS) and progression-free survival (PFS), built using clinicopathological features, median gene expression score and STS subtype of the combined cohort (n=65). The difference in chi-square is relative to the full Cox regression model built on clinicopathological features plus the median gene expression signature. For tumour grade, this was stratified into a b binary measure, with category 2 equating to high-grade tumours and category 1 to other grades.

Feature	Groups (#samples)	OS		PFS	
		HR (95% CI)	P-value	HR (95% CI)	P-value
Median Immune Score	Continuous (n=65)	2.04 (1.19 - 3.51)	0.0099 *	1.78 (1.13 - 2.79)	0.0121 *
Age	Continuous (n=65)	1.00 (0.97 - 1.02)	0.8874	0.99 (0.97 - 1.02)	0.6312
Performance Status	0 (n=19)	1	-	1	-
	1 (n=32)	2.59 (0.97 - 6.93)	0.0584	1.48 (0.68 - 3.22)	0.3232
	2 (n=7)	5.84 (1.71 - 20.0)	0.0050 *	1.73 (0.62 - 4.85)	0.2985
	-1 (n=7)	1.28 (0.30 - 5.43)	0.7363	0.67 (0.22 - 2.07)	0.4901
Grade	1 (n=30)	1	-	1	-
	2 (n=35)	2.12 (1.05 - 4.28)	0.0355 *	1.92 (1.00 - 3.70)	0.0504 *
Subtype	Other (n=30)	1	-	1	-
	LMS (n=14)	1.34 (0.50 - 3.58)	0.5558	1.27 (0.53 - 3.04)	0.5936
	SFT (n=9)	1.10 (0.36 - 3.36)	0.8669	1.07 (0.42 - 2.68)	0.8927
	Spindle cell (n=7)	3.75 (1.21 - 11.6)	0.0223 *	2.71 (0.98 - 7.53)	0.0556
	SS (n=5)	2.71 (0.71 - 10.4)	0.1458	0.52 (0.14 - 1.99)	0.3401
Chi-square (Likelihood Ratio)		26.05 (df = 10, p = 0.004*)		21.22 (df = 10, p = 0.02*)	
Δ Chi-square (against ClinPath plus immune model)		6.0863 (p = 0.1928)		5.1055 (p = 0.2766)	

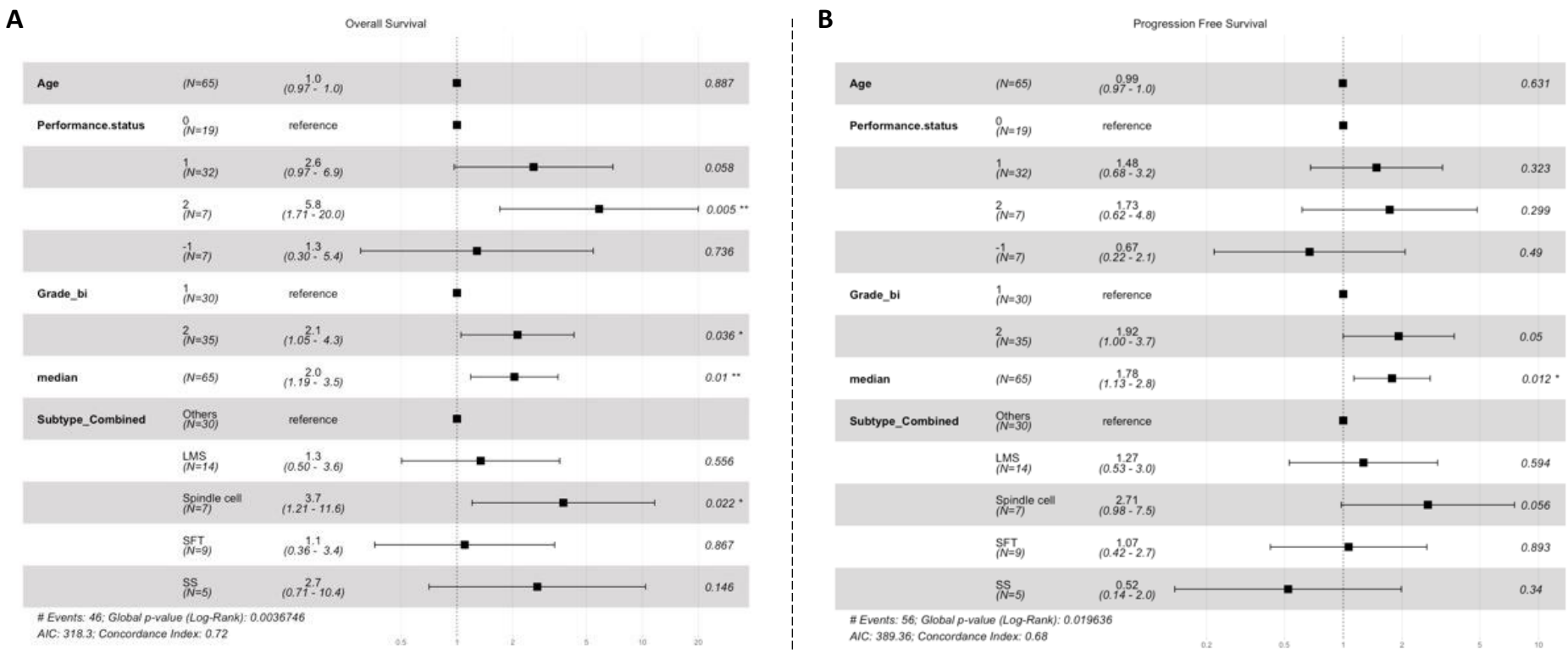

Figure 5.9: Forest plots of Cox multivariable regression models built using clinicopathological features, median gene expression signature and soft tissue sarcoma subtype of the combined cohort (n=65) for **A** overall survival and **B** progression-free survival.

5.2.6 Summary

In this study exploring the potential impact of the immune microenvironment on survival in a cohort of patients with STS treated with pazopanib, I have successfully built a prognostic Cox regression model incorporating a MGES, which is significantly associated with both OS and PFS following pazopanib initiation. Furthermore, the prognostic value of this model was significantly greater when compared to a model which included only the clinicopathological variables of tumour grade, patient age and patient performance status. In addition, including STS subtype as a variable did not significantly improve the prognostic value of the model.

5.3 Discussion

5.3.1 Building a prognostic model associated with clinical outcome following pazopanib therapy

In this study of a heterogenous and retrospectively identified cohort of patients with advanced STS, I have developed, validated and refined a regression model significantly associated with OS and PFS following the initiation of pazopanib therapy. The model incorporates standard clinicopathological variables, in addition to a median gene expression signature. The value of this model is that it would allow clinicians to identify patients most likely to gain benefit from pazopanib therapy. In this way, clinicians will be able to tailor management plans and personalise therapy choices to ensure only patients most likely to gain benefit from pazopanib receive it. Conversely, patients less likely to gain benefit from pazopanib can be managed with alternative therapies which may offer greater clinical benefit for that patient, whilst avoiding the potential side-effects of pazopanib treatment. At present, clinicians will make management decisions on management based on clinicopathological variables, but this study has demonstrated that the addition of the MGES significantly improves the fit of the survival model. As such, incorporation of MGES into clinical decision-making has the potential of improving the identification of patients most likely to gain clinical benefit from pazopanib.

This prognostic model incorporates clinicopathological variables, in addition to MGES, the median immune-gene score from 573 genes included in the nCounter PanCancer immune profiling panel. The association between increased MGES and inferior OS and PFS was confirmed in the univariable analysis of the discovery cohort. Comparing multivariable Cox models including clinicopathological variables with and without MGES demonstrated that the addition of this immune signature significantly increased the fit of the prognostic model, in terms of both OS and PFS, from the start of pazopanib therapy. Subsequent analysis of the independent validation cohort demonstrated that the direction of the association between MGES and higher HR was consistent with

findings from the discovery cohort. In order to refine the model to take forward, the two cohorts were then merged into a single combined cohort of pazopanib-treated patients. From this larger combined cohort, the univariable analysis demonstrated that higher MGES was significantly associated with inferior OS and PFS. Furthermore, upon multivariable analysis, addition of MGES significantly improved the fit of the survival model compared to a model built with clinicopathological variables alone.

Within the field of STS, molecularly defined biomarkers are lacking relative to other cancer types. The aim of prognostic biomarkers in the context of therapy is to allow the identification of patients at increased risk of inferior survival outcomes. In the clinical setting, biomarkers have the power to personalise therapy by identifying those high-risk patients most likely to benefit from a particular treatment. The potential for clinicopathological variables to act as prognostic biomarkers in STS has previously been described, however, immune-based molecular biomarkers are less well developed[398,399].

5.3.2 Critical appraisal of methods employed and limitations of the study

This study has some limitations including the fact these are retrospective cohorts, with a number of variables which are unable to be controlled for. These include the inclusion of tissue from primary lesions, local recurrences and metastatic lesions and a variety of STS subtypes with varying lengths of time from sampling to treatment initiation. In addition, some samples included in both the discovery and validation cohorts were exposed to variable pre-pazopanib therapies. However, this is the scenario facing clinicians in the real world, with pazopanib used in the management of all non-adipocytic STS in the post-first line setting. Therefore, having a biomarker which is robust to this variability is a positive consideration. Furthermore, by building a model on the combined cohort which included STS subtypes, it was demonstrated that the addition of STS subtypes did not significantly increase the prognostic value of the model, suggesting the model was valid across a range of STS subtypes.

In addition, working on a cohort of patients who have received a specific therapy for a group of rare cancers has resulted in a relatively small sample size. Although the power calculation reported this cohort of 65 cases was sufficiently powered for PFS, this would only be for 1 parameter, for example, a continuous variable such as MGES. With this in mind, the analyses in this chapter were designed to generate a prognostic model which could be built upon with additional samples and data in the future, hence the refinement of the model by combining the discovery and validation cohorts into a single combined cohort for the final models.

In terms of the analyses selected for the generation of a prognostic model, alternative approaches could have been employed[400]. For example, splitting the combined cohort based on their survival and employing supervised machine learning techniques would have been one potential strategy to identify a prognostic biomarker[401]. This approach does have limitations in that there is a risk of overfitting and inaccurate biomarker discovery due to inherent biases within the training dataset when stratified by survival outcomes. Indeed, given the small size of this cohort, this increases the chance of these errors occurring. Furthermore, the intention of the study was to define a biomarker in a real-world, unselected cohort, which has been achieved through Cox modelling. Unsupervised or consensus clustering could also have been employed, with analysis of clinical outcomes based on differential gene expression profiles between the subgroups used to drive the identification of gene signatures associated with survival[402]. The potential disadvantage of this approach would be that the biomarker identified is reliant on the subgroups defined in the clustering algorithm, and therefore inaccuracies in subgroup assignment would be propagated to the resultant biomarker signature potentially limiting translatability to the real-world setting. Deep learning techniques could also have been employed, but these methods usually require large volumes of labelled training data and given the size of the cohorts in this study was deemed to be not a feasible approach[403].

5.3.3 Conclusion

In this chapter, our study exploring the immune microenvironment of STS and its relation to clinical outcomes following pazopanib therapy has yielded a prognostic model which includes a median gene expression signature. The model has been shown to fit the survival data significantly better than a model based solely on clinicopathological variables. In addition, STS subtype did not significantly impact the prognostic value, suggesting the utility of the model across a range of subtypes. Moving forward, the final version of the prognostic model can be further validated through the prospective assessment of a new cohort, or as an integral biomarker in a clinical trial.

Chapter 6 - Future directions and conclusions

6.1 Introduction

The current means of classifying soft tissue sarcomas (STS) based on histological subtype inadequately accounts for the heterogeneity of clinical behaviours. Furthermore, the “one size fits all” approach in directing strategies for systemic therapy in patients with advanced STS is no longer appropriate. As technological advances in molecular characterisation techniques become more widespread, and as a community our appreciation of drivers of disease in STS grows, a paradigm shift must occur. As the arsenal of targeted therapies increases, it must be possible to identify those patients most likely to gain benefit from these treatments. This will ensure that each patient only receives a treatment known to be efficacious. To this end, the development of novel predictive biomarkers able to robustly stratify patients into those most likely to acquire clinical benefit from specific therapies, is essential for the advancement of the treatment of patients with advanced STS.

6.2 Summary of key findings

My thesis project has undertaken the characterisation of the immune microenvironment in pre-pazopanib STS tumour samples and developed a prognostic model on a cohort of patients who received pazopanib. Indeed, although a small number of published studies have explored immune-based molecular characterisation in STS, these have sought prognostic biomarkers for clinical utility in the primary setting. As a result, the design and curation of the cohorts described in **Chapter 3** was in itself innovative in the field of STS, in that they were designed to investigate a cohort of patients managed with a specific targeted therapy. As a rare cancer, identification of patients for the curation of clinical cohorts can be challenging. Availability and quality of tumour tissue is also an obstacle, given the degradation bought about by formalin-fixation and paraffin embedding on ribonucleic acid (RNA). Although the Royal Marsden is a leading specialist STS referral centre, and has an extensive archive of tumour tissue from previously treated patients, in order to accumulate a sufficient number of cases for our cohorts, I relied on collaborators from Glasgow and Singapore to increase

the size of the combined cohort. In addition, the curation of a comparator cohort treated with alternative second-line therapies allowed assessment of whether associations of IHC scores with survival in the pazopanib-treated combined cohort were also seen in the comparator cohort.

My initial characterisation of the immune microenvironment employed immunohistochemistry (IHC) of tissue microarrays (TMAs) as a high-throughput and low-cost investigation method. In addition, TMAs containing cores in triplicate offer robust granularity to characterisation of the tumour immune microenvironment, whilst importantly being minimally consumptive of precious tumour tissue[317]. Through a pilot study, I identified that ImageJ was the most robust method for automated cell counting of immune cells. Employing this software, I then quantified the number of tumour infiltrating lymphocytes (TILs) expressing CD3, CD4 and CD8 across the cohorts and analysed the clinical outcomes following stratification based on TIL count and by Cox univariate and multivariable proportional hazards analysis (**Figures 3.9-20**). From these results, I identified a significant association between increased CD4+ counts and inferior OS and PFS. Conversely, in the comparator cohort increased CD4+ count was significantly associated with superior PFS.

To generate more in-depth immune profiles of my discovery cohort, I then analysed the expression of immune-related genes employing the Nanostring nCounter PanCancer immune profiling panel (**Chapter 4**). Following data normalisation and median-centring, a heatmap of the immune gene expression data for the combined cohort was plotted using unsupervised hierarchical clustering to group tumours based on similarities in their expression data. This identified three distinct immune sarcoma subgroups (ISS)(**Figure 4.4**). Significance analysis of microarrays (SAM) identified a number of genes with differential expression between ISS subgroups, with ISS1 characterised as immune ‘hot’ with higher expression of genes associated with inflammation, cytotoxicity and anti-tumourigenic activity. Conversely, ISS3 was characterised by lower expression of genes associated with anti-tumourigenic activity and could be considered immune ‘cold’. ISS2 was characterised by an intermediate pattern of gene expression, with very few differentially expressed genes compared to

ISS1 and 3. Furthermore, single sample gene set enrichment (ssGSEA) demonstrated significant enrichment in ISS1 for CD8 T-cells, T-helper1 cells and dendritic cells, all involved in pro-inflammatory immune responses (**Figure 4.7**). Conversely, ISS3 had significant enrichment for natural killer (NK) cells, predominated by enrichment for NK^{bright} cells which have been shown to be less cytotoxic relative to NK^{dim} cells, and involved in the secretion of both pro- and anti-inflammatory immune modulators[365] (**Figure 4.8**). I also assessed if STS subtype was associated with alterations in the tumour immune microenvironment. This analysis showed that there is substantial intra-subtype heterogeneity in immune profiles in this cohort..

As detailed in **Chapter 5**, I then expanded on this work by building Cox models to identify a model which was prognostic in the pazopanib-treated combined cohort. To achieve this, the combined cohort was initially split into discovery and validation cohorts, to allow training of the model and subsequent validation in an independent cohort. Following normalisation and gene filtering, the median gene score was determined for each sample, called the median gene expression signature (MGES). Univariate analysis of MGES showed a significant association between higher MGES and inferior OS in the discovery cohort, and the prognostic value of the model was improved by the inclusion of other clinicopathological variables. My analysis showed that the positive association between high expression of MGES and inferior OS and PFS was consistent in both the discovery and validation cohorts. Given the small sample sizes in each of the two cohorts, they were then merged into a single combined cohort for refinement into a final prognostic model.

6.3 Further development of the MGES prognostic model

6.3.1 Prospective evaluation of the prognostic value of the MGES model

6.3.1.1 Evaluation in a prospective randomised clinical trial

Following the development of the refined MIS prognostic model, built using the multicentre combined cohort, the next steps in biomarker discovery involve validation within the context of a prospective clinical trial. Updated guidance for the American Society of Clinical Oncology (ASCO) levels of evidence (LOEs) scale related to biomarker evaluation allows for multiple routes to generate level I evidence of clinical utility[177].

Scientifically, the gold standard for assessment of the clinical utility of a biomarker for a particular scenario is considered to be a prospective randomised clinical trial and is considered category A evidence per ASCO guidelines. Such a trial is specifically designed to address the question of tumour marker validity and involves the prospective recruitment of patients, according to a prewritten protocol, and the collection, processing and quantification of the biomarker assay in question in real-time. These studies are prospectively powered to ensure sufficient analytical certainty following the assessment of the results. The benefits of a prospective randomised trial include:

- Tight control on the recruitment of patients suitable for assessment of the biomarker in question.
- Fixed standard operating procedures for the collection, processing and storage of clinical samples.
- Pre-determined protocols related to assessment of the biomarker assay.
- Tight controls of the patient data and clinical end-point data collected for the assessment of biomarker utility.

However, the design and completion of a prospective randomised trial is associated with unavoidable challenges, including the costs and logistics of such an endeavour. These potential obstacles are compounded by the rarity of STS

relative to other tumours, however given the MGES model developed in this thesis was demonstrated to be prognostic across a range of STS subtypes, the inclusion criteria for a trial would be less restrictive than if only specific subtypes were included. The major advantage of the prospective randomised trial is that compelling evidence would be considered definitive, and no further validation of clinical utility would be necessary.

6.3.1.2 Evaluation of archival tissue from a prospective clinical trial

In the original ASCO biomarker guidelines, a prospective randomised trial was the only route for the acquisition of level I data in biomarker discovery. However, the revised guidelines accommodate for the analysis of archived tumour samples collected as part of a prospective clinical trial designed to answer another therapeutic or biomarker question. The study should allow assessment of the current biomarker under consideration, and this is considered a category B study. Analytical robustness states that the biomarker hypothesis in question should be generated independently from any trial results, any trial-associated tissue and data should not be assessed until a new biomarker-specific protocol has been developed. The benefits of adopting this approach over a biomarker-specific randomised clinical trial include:

- Permits the use of previously archived tumour specimens not specifically designed for biomarker validation.
- Use of a pre-determined statistical analysis plan ensures unbiased validity of subsequent biomarker results.
- Patient recruitment, sample standard operating procedures and clinical data curation will adhere to strict procedures ensuring good quality data for analysis.
- Cost and logistics of performing the biomarker arm of a study are reduced relative to a biomarker-specific randomised controlled trial.

A potential limitation of such an approach is the requirement that in order for it to be considered level I evidence, confirmation of clinical utility of a biomarker requires similarly compelling positive results from two category B studies. In

terms of identifying a pazopanib-treated cohort in the management of STS, the PALETTE phase III trial would have been the ideal source on which to undertake the characterisation of the immune microenvironment in STS and the development of survival models in this cohort. Indeed, the analysis of prospective trial material will always be stronger than analyses undertaken on a retrospective cohort. This is due to the controlled nature of a prospective trial, particularly related to the collection, storage and curation of high quality tumour material and clinical data. However, tissue samples for translational research were not collected as part of the PALETTE phase III clinical study, and this represents a missed opportunity to generate a well-curated bank of high-quality tumour material from a large cohort of STS patients. Indeed, following the PALETTE phase III trial, subsequent controlled clinical trials have been infrequent. Therefore, there is limited availability of valuable well-curated tumour specimens from controlled trials of pazopanib in STS.

6.3.2 The role and challenges of retrospective cohort analysis

Although prospective clinical trial material does represent a higher quality basis on which to base translational research, there is still great value in analysing real-world tumour samples. These studies are able to grow the field of knowledge of a particular tumour type or treatment on more readily available tumour samples and in this way direct future research on the precious trial material when it does become available. This maximises the potential clinically relevant yield of limited, well-curated, high-quality trial material.

Indeed, some of the major challenges in undertaking translational research on retrospective cohorts are related to the lack of consistent tissue sampling and storage controls and clinical data which is not prospectively maintained to answer a particular study question. For this thesis, the RM electronic patient record system allowed access to the detailed medical records of patients who met the inclusion criteria for this study. This included histology reports to confirm the histological diagnosis and tumour grade, clinic letters and radiology reports to confirm the date of tumour progression and drug prescription charts to confirm

the start dates of therapies. As such, building well-curated clinical data sets for this study was feasible.

The biggest challenges in this thesis related to cohort size and the quality of tumour material available. Despite engaging collaborators overseas, only 65 patients who met the inclusion and exclusion criteria, and had available pre-treatment tissue of adequate RNA quality to be included for analysis were identified. Indeed, a number of potential samples were lost due to the degree of degradation of RNA following extraction. In terms of improving the quality of the tumour material used as input for translational studies, fresh frozen tissue has been shown to yield significantly higher quality nucleic acids when compared to formalin-fixed paraffin-embedded samples (FFPE)[392,404,405]. Therefore, if fresh frozen tissue was more readily available, that would increase the likelihood that sufficient quality nucleic acids would be extracted to act as input for genotype analysis. The main issue related to fresh frozen tissue is the cost of storage, as samples need to be kept at ultra-low temperatures, whilst FFPE samples, once prepared can be kept at room temperature.

In terms of expanding the cohort sizes, a number of potential solutions could be explored to increase the sample size. Further external collaborators could be sought with the aim of identifying appropriate patients with suitable tumour samples available. Additionally, any future trials of pazopanib in the management of soft tissue sarcoma could present excellent opportunities to prospectively test the prognostic value of the MGES model. Finally, publicly available data sets with matched clinical data could be analysed to generate a cohort of cases on which to prospectively validate the model.

6.3.3 Assessing the value of a predictive test for the clinical setting

Following the development of a predictive test, a number of considerations are required to assess its suitability and utility in the clinical setting. One of the key statistical considerations is the positive predictive value (PPV) of a test – a measure of the probability that a positive test result corresponds to a true positive

outcome calculated as the number of true positives divided by the sum of the true positive and false positives.

In order to be useful to a clinician, a predictive test must have an acceptable PPV to ensure that the treatment the patient is receiving has a good chance of success, and to prevent the administration of a potentially harmful therapy in patients less likely to gain benefit. Therefore, the PPV itself is a balance between the sensitivity of a test, the proportion of true positives successfully identified, and the specificity of a test, the proportion of true negatives a test successfully identifies. An ideal predictive test should have a high sensitivity in identifying patients most likely to gain benefit, whilst maintaining a reasonable level of specificity to ensure people unlikely to benefit are not falsely classified.

In addition, for a predictive test to be of use in the clinical setting, it must be both robust and reproducible. As such, the PPV should ideally remain constant and independent of factors such as clinicopathological features not included as variables within the test. Within the field of STS, this would include STS subtype and it would be important to note if a test was subtype-specific or more generalisable and subtype-agnostic. Furthermore, the test should be reproducible across different research cohorts, to confirm it has practical applicability in the real-world clinical environment. An aspect of this reproducibility is ensuring a predictive test has a robust, tested and finalised standard operating procedure in place to ensure any test results are standardised irrespective of the site at which the test was performed

A further aspect of the clinical utility of a predictive test is that there should be clear and well-communicated guidance on how to interpret and act on results from a predictive test used in the clinic[177]. In addition the predictive test should be well supported through vigorous research and validation to provide clinicians with confidence to employ the test and act upon the result that is formulated. And finally, given the dynamic nature of medical research, the test should be frequently revaluated and refined to ensure it remains up-to-date with new research advances, and can be recalibrated to maximise the PPV of the test.

6.3.4 Quantifying dynamic changes in the immune microenvironment in relation to pazopanib therapy

An additional interesting avenue of translation research to explore is the characterisation of the dynamic changes in the immune microenvironment following treatment with pazopanib. As the cohorts I have curated in the thesis contain exclusively pre-pazopanib tissue, it is not possible to identify changes and trends in immune gene expression associated with pazopanib therapy. At present characterisation of the pre-treatment immune microenvironment has identified interesting trends in terms of enrichment of particular immune cells within the ISS subgroups. However, the characterisation of dynamic changes has the added benefit of allowing a more robust assessment of the influence pazopanib has on the immune microenvironment and may shed light on immune features which increase sensitivity to pazopanib. Furthermore, dynamic immune microenvironmental changes may drive secondary resistance to pazopanib, and there characterising these changes may yield potential treatment strategies when the tumour shows signs of progression. To this end, work has begun within the lab to compile a pilot cohort of patients for whom both pre- and post-pazopanib tumour tissue is available.

6.4 Future perspectives of immunomodulating therapies

Driven by a growing appreciation of the crucial role the immune system plays in cancer development, as well as treatment responses, a number of novel therapies have been developed which aim to enhance anti-cancer immunity to treat cancer.

6.4.1 Immune checkpoint inhibitor monotherapy

The most advanced class of immunomodulating anti-cancer therapies at present are immune checkpoint inhibitors (ICI), monoclonal antibodies which act to block the inhibitory effect of immune checkpoints on the patient's immune system. Although the reported expression levels of immune checkpoints in sarcoma vary in the literature, ICI monotherapy has been investigated in the treatment of STS.

The best described immune checkpoints at present are:

- Programmed cell death receptor-1 (PD-1) and programmed cell death receptor-1 ligand (PD-L1). PD-1 binds to PD-L1 and is upregulated on active T cells, it limits T cell activation via negative costimulatory signals.
- Cytotoxic T lymphocyte-associated protein-4 (CTLA-4) which is upregulated on the surface of active T cells, preventing over stimulation by the T-cell receptor.

To date, the most advanced clinical trial exploring ICI therapy in STS was the multicentre, single-arm, open-label, phase II trial of the anti-PD-1 monoclonal antibody pembrolizumab (Sarcoma Alliance for Research through Collaboration (SARC)028, NCT02301039)[294]. A total of 40 patients with advanced STS were included, with the cohort evenly made up of leiomyosarcoma (LMS), undifferentiated pleomorphic sarcoma (UPS), liposarcoma (LPS) and synovial sarcoma (SS). Disappointingly, the objective response rate (ORR) across the cohort was only 18% (1 complete response and 6 partial responses out of 40 patients). However, high rates of response were observed for UPS and LPS (40% and 10% respectively), and these subtypes were therefore included in an expansion cohort[406]. Following the recruitment of an additional 30 patients to each subtype arm, the final ORR was 23% for UPS (9 out of 40 patients) but only 10% (4 out of 40 patients) for the LPS arm.

Endeavours to correlate PD-L1 with response to pembrolizumab have so far failed to elucidate a robust predictive biomarker. Indeed, analysis of a subset of patients from the SARC208 trial reported PD-L1 positivity in only 4% of cases, all from the UPS strata. However, the work by Petitprez *et al*. is of note[293]. Utilising publicly available gene expression datasets of primary STS, they classified tumours into one of five subgroups based upon immune gene expression. As part of their work, they analysed 47 pre-treatment metastatic samples from the SARC028 trial and assigned them to one of the five immune subgroups they had derived. Notably, their subgroup characterised by immune upregulation, and most characteristically by a high B-cell signature, had the highest ORR to

pembrolizumab of 50%. Conversely their subgroup most associated with reduced immune gene expression had no responses to ICI.

In addition, nivolumab monotherapy is another anti PD-1 monoclonal antibody which has been assessed in STS in the clinical setting. However, clinical trial results have been generally disappointing, with no objective responses to therapy in cohorts of patients with uterine LMS and paediatric solid tumours including STS[407,408]. As a result, further evaluation as a monotherapy in STS is not warranted.

6.4.2 Immune checkpoint inhibitor combination therapies

Following the relatively disappointing results in the limited trials of ICI monotherapy, a number of combinatorial approaches have been adopted and investigated in STS. Given the role for vascular endothelial growth factor (VEGF) to induce an immune suppressive microenvironment (**Section 1.5.2**), there is a rationale for exploring potential synergism in targeting VEGF and the immune checkpoint axis in STS. Indeed a phase II trial of pembrolizumab in combination with the tyrosine kinase inhibitor (TKI) axitinib, which has anti-VEGF activity has been reported (NCT02636725)[409]. A total of 33 patients with advanced STS of multiple subtypes, enriched for cases of alveolar soft part sarcoma (ASPS), were enrolled. Encouraging clinical benefit was reported, with 3-month PFS rate reported to be 65.6%, and highest in cases of ASPS (72.7%).

Additional studies exploring combination approaches involving pembrolizumab have included cytotoxic chemotherapy as the second agent. The rationale behind this being that cytotoxic chemotherapy is postulated to enhance anti-tumour immune responses, through the depletion of suppressive immune cells and increased antigen presentation through tumour cell death. A recent phase II study assessed the combination doxorubicin and pembrolizumab in 37 anthracycline-naïve patients with advanced STS (NCT02888665)[410]. The ORR was disappointing, with only 7 (19%) PRs reported. However, survival outcomes were promising with the study reporting a mPFS of 8.1 months, and a mOS of 27.6 months. However, it should be noted that this cohort was not heavily pre-treated,

with combination doxorubicin plus pembrolizumab representing the first-line of therapy for 28 (76%) patients. As such, although the survival outcomes are reasonable, they are not grossly different from previously published studies of doxorubicin first-line therapy, and the lack of objective results is concerning (**Table 1.3**). Additionally, pembrolizumab has been assessed in combination with metronomic cyclophosphamide, with a phase II study reported by the French Sarcoma Group (FSG) (NCT02406781)[411]. On the whole, the reported efficacy of this combination were disappointing, with a 6-month PFS rate of 0% for the LMS and UPS subgroup, and only 14.3% in the "other" STS subgroup.

Although showing minimal anti-tumour activity in previous studies in STS, nivolumab has been recently explored in an open-label phase II trial comparing nivolumab alone or in combination with the anti-CTLA-4 monoclonal antibody ipilimumab (NCT02500797)[412]. A total of 85 patients with advanced STS of various subtypes following failure of at least 1 line of therapy were eligible. A total of 38 patients were assigned to the nivolumab monotherapy arm, and as with previous studies ORR was poor, with only 2 (5%) confirmed PRs reported. However, in combination with ipilimumab the ORR was 16%, with 6 confirmed responses observed across a range of STS subtypes.

Additional clinical trials exploring combinations of ICIs are ongoing as the STS community attempts to harness the potential for ICIs to improve clinical outcomes, as they have in a number of other solid tumours. However, at the present time the current immune checkpoint targets appear to lack efficacy in STS.

6.4.3 Emerging immune checkpoint targets

Since the emergence of these inhibitory targets, newer immune checkpoints have started to be characterised and explored as potential avenues for anti-cancer therapy.

6.4.3.1 Lymphocyte activation gene-3 (LAG-3)

LAG-3 interacts with major histocompatibility (MHC) class II and is present on activated T cells, leading to downregulation of T-cell cytokine production and T-cell expansion. In addition LAG-3 is over expressed on TILs, and have been associated with tumour growth via the promotion of cellular dysfunction and immune cell exhaustion. Blockage of LAG-3 is therefore hypothesised to drive an anti-tumour immune response.

Several molecular targets for LAG-3 have been developed. LAG525 is a monoclonal antibody that targets LAG-3 and has been investigated in a phase I/II clinical trial in patients with advanced malignancies (NCT02460224)[413]. A total of 240 patients were recruited in the trial, the study arm was either monotherapy LAG525 therapy or combination therapy with the anti-PD-1 monoclonal antibody spartalizumab. Of those receiving LAG525 monotherapy, 79% discontinued due to disease progression versus 67% who discontinued treatment due to disease progression in the combined arm. Early results demonstrated a 10% ORR in the combined group, although it is unclear if this is due to the efficacy of spartalizumab and further evaluation is ongoing. The therapy was reportedly well tolerated, with dose limiting toxicities in 8 patients (4 in each arm), these included pneumonitis, AKI and hepatitis. Although this study did not include patients with STS, a newer phase II open label study of combination spartalizumab and LAG525 is currently recruiting, and includes STS as a cohort to be explored (NCT03365791)[414]. As such, these trial results are awaiting and will hopefully shed light on the potential utility of this combination in patients with advanced STS.

Preclinical models provided anti-tumour evidence for the synergistic activity of LAG-3 and PD-1 molecular blockade. This led to the phase I, first in human study using anti-LAG-3 therapy (REGN3767) with or without the anti-PD-1 monoclonal antibody cemiplimab (REGN2810) in advanced cancers is ongoing (NCT03005782)[415]. Sixty-seven patients with solid organ and haematological malignancies have been recruited. Early results demonstrate combination therapy is superior to monotherapy; 12 patients in the monotherapy group

achieved stable disease and in the combined group 2 patients achieved a PR and 11 had stable disease. Overall the therapy was well tolerated, with 1 patient reaching dose limiting toxicity. At present, patients with STS are not being considered in this trial of this therapeutic combination, but compelling final result data might raise interest in its potential utility. Further evidence is required to establish which immunotherapy agents are best used in combination to achieve best overall outcomes.

Identification of monoclonal antibodies with dual-specificity for anti-PD-1 and anti-LAG-3 blockade have also been developed and are being explored in phase I studies. One example is the phase I study enrolling patients with advanced malignancies to be treated with the bi-specific monoclonal antibody (tebotelimab) alone or with margetuximab (anti HER2 therapy), if they demonstrated HER-2 tumour expression (NCT032198268)[416]. From 207 patients divided into a dose escalation and expansion group, 7 achieved a partial response and 34 achieved stable disease. Although 146 patients (70.5%) reported adverse effects, just 23.2% were grade 3 or greater. Again, recruitment of patients with STS was limited, but depending on trial data may be considered as potential beneficiaries to be considered in future trials.

6.4.3.2 T-cell immunoglobulin-3 (TIM-3)

TIM-3 also represents an interesting immune checkpoint target for drug development. It is expressed on numerous cells, including effector T-cells, B-cells, macrophages, dendritic cells and natural killer (NK) cells. TIM-3 stimulation contributes to T-cell exhaustion and promotes myeloid derived suppressor cell expansion. Both of these factors lead to tumour growth and high levels of TIM-3 have been correlated with poor prognosis across a number of malignancies, including renal cell, colon, cervical cancer[417]. Initial trials suggest that anti-TIM-3 agents may be beneficial when used as adjuvant therapy. A recent a phase I/II clinical trial recruited 173 patients with metastatic solid organ malignancies to receive MBG453, a monoclonal antibody against TIM-3, alone or in combination with spartalizumab (NCT02608268)[418]. Those who received combination therapy

were demonstrated to have improved outcomes and treatment was well tolerated with no grade 3 or 4 toxicities.

6.4 Concluding remarks

In conclusion, this work has characterised the immune microenvironment in patients treated with pazopanib. A multivariable prognostic model has been built on a cohort of pazopanib-treated patients which incorporates both an immune gene-based score and clinicopathological variables. Looking to the future, the era of personalised medicine will rely heavily on molecular tests able to identify patients most likely to gain clinical benefit from specific therapy and the prognostic model presented here is one such example.

Chapter 7 - References

1. W.H.O. Soft tissue and bone tumours in adults. in *Practical Clinical Oncology* 335–346 (2008). doi:10.1017/CBO9780511545375.031

2. Cancer Research UK. Soft tissue sarcoma incidence statistics. Available at: https://www.cancerresearchuk.org/health-professional/cancer-statistics/statistics-by-cancer-type/soft-tissue-sarcoma/incidence#heading-Four. (Accessed: 7th September 2018)

3. Gatta, G. *et al.* Rare cancers are not so rare: The rare cancer burden in Europe. *Eur. J. Cancer* **47**, 2493–2511 (2011).

4. Parikh, R. C. *et al.* Treatment patterns and survival among older adults in the United States with advanced soft-tissue sarcomas. *Clin. Sarcoma Res.* **8**, 8 (2018).

5. Harris, S. J. *et al.* Metastatic soft tissue sarcoma, an analysis of systemic therapy and impact on survival. *J. Clin. Oncol.* **33**, 10545–10545 (2015).

6. Komatsubara, K. M. & Carvajal, R. D. The promise and challenges of rare cancer research. *Lancet Oncol.* **17**, 136–138 (2016).

7. Blay, J. Y., Coindre, J. M., Ducimetière, F. & Ray-Coquard, I. The value of research collaborations and consortia in rare cancers. *The Lancet Oncology* **17**, e62–e69 (2016).

8. Lee, A. T., Huang, P. H. & Jones, R. L. Negative phase III trials announce the need for biomarkers in sarcoma. *Eur. J. Cancer* **123**, 81–82 (2019).

9. Drilon, A. *et al.* Efficacy of Larotrectinib in *TRK* Fusion–Positive Cancers in Adults and Children. *N. Engl. J. Med.* **378**, 731–739 (2018).

10. Wilding, C. P., Loong, H. H., Huang, P. H. & Jones, R. L. Tropomyosin receptor kinase inhibitors in the management of sarcomas. *Current opinion in oncology* **32**, 307–313 (2020).

11. Kelly, C. M., Gutierrez Sainz, L. & Chi, P. The management of metastatic GIST: current standard and investigational therapeutics. *Journal of*

Hematology and Oncology **14**, 1–12 (2021).

12. NICE. Improving outcomes for people with sarcoma | Guidance | NICE.

13. Fujiwara, T. *et al.* Impact of NICE guidelines on the survival of patients with soft-tissue sarcomas. *https://doi.org/10.1302/0301-620X.103B3.BJJ-2020-0743.R1* **103**-**B**, 569–577 (2021).

14. Dangoor, A. *et al.* UK guidelines for the management of soft tissue sarcomas. *Clin. Sarcoma Res.* **6**, 1–26 (2016).

15. Gronchi, A. *et al.* Soft tissue and visceral sarcomas: ESMO-EURACAN-GENTURIS Clinical Practice Guidelines for diagnosis, treatment and follow-up. *Ann. Oncol.* **0**, (2021).

16. Dangoor, A. *et al.* UK guidelines for the management of soft tissue sarcomas. *Clin. Sarcoma Res.* **6**, 20 (2016).

17. Arbiser, Z. K., Folpe, A. L. & Weiss, S. W. Consultative (expert) second opinions in soft tissue pathology: Analysis of problem-prone diagnostic situations. *Am. J. Clin. Pathol.* **116**, 473–476 (2001).

18. Rupani, A., Hallin, M., Jones, R. L., Fisher, C. & Thway, K. Diagnostic Differences in Expert Second-Opinion Consultation Cases at a Tertiary Sarcoma Center. *Sarcoma* **2020**, (2020).

19. Rastogi, S. *et al.* Discordance of histo-pathological diagnosis of patients with soft tissue sarcoma referred to tertiary care center. *J. Clin. Oncol.* **35**, 11064–11064 (2017).

20. Schneider, N. *et al.* The Adequacy of Core Biopsy in the Assessment of Smooth Muscle Neoplasms of Soft Tissues. *Am. J. Surg. Pathol.* **41**, 923–931 (2017).

21. Hornick, J. L. Limited biopsies of soft tissue tumors: the contemporary role of immunohistochemistry and molecular diagnostics. *Modern Pathology* **32**, 27–37 (2019).

22. Sbaraglia, M., Gambarotti, M., Righi, A. & Dei Tos, A. P. Classification of soft tissue lesions and general principles of soft tissue pathology. in *Diagnosis of Musculoskeletal Tumors and Tumor-like Conditions: Clinical, Radiological and Histological Correlations - the Rizzoli Case Archive* 19–22 (Springer, Cham, 2019). doi:10.1007/978-3-030-29676-6_5

23. Schaefer, I. M. & Hornick, J. L. Diagnostic Immunohistochemistry for Soft Tissue and Bone Tumors: An Update. *Adv. Anat. Pathol.* **25**, 400–412 (2018).

24. Schaefer, I. M., Cote, G. M. & Hornick, J. L. Contemporary sarcoma diagnosis, genetics, and genomics. *Journal of Clinical Oncology* **36**, 101–110 (2018).

25. Mariño-Enríquez, A. & Bovée, J. V. M. G. Molecular Pathogenesis and Diagnostic, Prognostic and Predictive Molecular Markers in Sarcoma. *Surgical Pathology Clinics* **9**, 457–473 (2016).

26. Miura, K. *et al.* Usefulness of SS18-SSX antibody as a diagnostic marker for pulmonary metastatic synovial sarcoma. *Diagn. Pathol.* **16**, 1–8 (2021).

27. Reeser, J. W. *et al.* Validation of a Targeted RNA Sequencing Assay for Kinase Fusion Detection in Solid Tumors. *J. Mol. Diagnostics* **19**, 682–696 (2017).

28. Beadling, C. *et al.* A Multiplexed Amplicon Approach for Detecting Gene Fusions by Next-Generation Sequencing. *J. Mol. Diagnostics* **18**, 165–175 (2016).

29. Guillou, L. *et al.* Comparative study of the National Cancer Institute and French Federation of Cancer Centers Sarcoma Group grading systems in a population of 410 adult patients with soft tissue sarcoma. *J. Clin. Oncol.* **15**, 350–362 (1997).

30. AJCC. AJCC Cancer Staging Manual 8th Edition. in *Definitions* 489–539 (2020). doi:10.32388/b30ldk

31. Tanaka, K. & Ozaki, T. New TNM classification (AJCC eighth edition) of bone and soft tissue sarcomas: JCOG Bone and Soft Tissue Tumor Study Group. *Japanese Journal of Clinical Oncology* **49**, 103–107 (2019).

32. Cates, J. M. M. The AJCC 8th edition staging system for soft tissue sarcoma of the extremities or trunk: A Cohort study of the SEER database. *JNCCN J. Natl. Compr. Cancer Netw.* **16**, 144–152 (2018).

33. Bilgeri, A. *et al.* The effect of resection margin on local recurrence and survival in high grade soft tissue sarcoma of the extremities: How far is far enough? *Cancers (Basel).* **12**, 1–13 (2020).

34. Kainhofer, V. *et al.* The width of resection margins influences local recurrence in soft tissue sarcoma patients. *Eur. J. Surg. Oncol.* **42**, 899–906 (2016).

35. Potter, B. K. *et al.* Impact of margin status and local recurrence on soft-tissue sarcoma outcomes. *J. Bone Jt. Surg. - Ser. A* **95**, (2013).

36. Fujiwara, T. *et al.* What is an adequate margin for infiltrative soft-tissue sarcomas? *Eur. J. Surg. Oncol.* **46**, 277–281 (2020).

37. van Schaik, L., Geertzen, J. H. B., Dijkstra, P. U. & Dekker, R. Metabolic costs of activities of daily living in persons with a lower limb amputation: A systematic review and meta-analysis. *PLoS ONE* **14**, e0213256 (2019).

38. Erstad, D. J. *et al.* Amputation for Extremity Sarcoma: Contemporary Indications and Outcomes. *Ann. Surg. Oncol.* **25**, 394–403 (2018).

39. Smith, H. G., Thomas, J. M., Smith, M. J. F., Hayes, A. J. & Strauss, D. C. Major Amputations for Extremity Soft-Tissue Sarcoma. *Ann. Surg. Oncol.* **25**, 387–393 (2018).

40. Hoftiezer, Y. A. J. *et al.* Long-term patient-reported outcome measures following limb salvage with complex reconstruction or amputation in the treatment of upper extremity sarcoma. *J. Surg. Oncol.* **123**, 1328–1335 (2021).

41. Perhavec, A. *et al.* Inoperable Primary Retroperitoneal Sarcomas: Clinical Characteristics and Reasons Against Resection at a Single Referral Institution. *Ann. Surg. Oncol.* **28**, 1151–1157 (2021).

42. Younger, E. *et al.* Health-related quality Of Life In patients with advanced Soft TIssue sarcomas treated with Chemotherapy (The HOLISTIC study): protocol for an international observational cohort study. *BMJ Open* **10**, e035171 (2020).

43. Tan, C. *et al.* Adriamycin-an antitumor antibiotic in the treatment of neoplastic diseases. *Cancer* **32**, 9–17 (1973).

44. Tap, W. D. *et al.* Effect of Doxorubicin Plus Olaratumab vs Doxorubicin Plus Placebo on Survival in Patients with Advanced Soft Tissue Sarcomas: The ANNOUNCE Randomized Clinical Trial. in *JAMA - Journal of the American Medical Association* **323**, 1266–1276 (American Medical Association, 2020).

45. Tap, W. D. *et al.* Olaratumab and doxorubicin versus doxorubicin alone for treatment of soft-tissue sarcoma: an open-label phase 1b and randomised phase 2 trial. *Lancet* **388**, 488–497 (2016).

46. Maurel, J. *et al.* Efficacy of sequential high-dose doxorubicin and ifosfamide compared with standard-dose doxorubicin in patients with advanced soft tissue sarcoma: An open-label randomized phase II study of the Spanish group for research on sarcomas. *J. Clin. Oncol.* **27**, 1893–1898 (2009).

47. Lorigan, P. *et al.* Phase III trial of two investigational schedules of ifosfamide compared with standard-dose doxorubicin in advanced or metastatic soft tissue sarcoma: A European Organisation for Research and Treatment of Cancer Soft Tissue and Bone Sarcoma Group study. *J. Clin. Oncol.* **25**, 3144–3150 (2007).

48. Judson, I. *et al.* Doxorubicin alone versus intensified doxorubicin plus ifosfamide for first-line treatment of advanced or metastatic soft-tissue sarcoma: A randomised controlled phase 3 trial. *Lancet Oncol.* **15**, 415–

423 (2014).

49. Seddon, B. *et al.* A phase II trial to assess the activity of gemcitabine and docetaxel as first line chemotherapy treatment in patients with unresectable leiomyosarcoma. *Clin. Sarcoma Res.* **5**, 1–7 (2015).

50. Seddon, B. *et al.* Gemcitabine and docetaxel versus doxorubicin as first-line treatment in previously untreated advanced unresectable or metastatic soft-tissue sarcomas (GeDDiS): a randomised controlled phase 3 trial. *Lancet Oncol.* **18**, 1397–1410 (2017).

51. Martin-Broto, J. *et al.* Randomized phase II study of trabectedin and doxorubicin compared with doxorubicin alone as first-line treatment in patients with advanced soft tissue sarcomas: A Spanish group for research on sarcoma study. *J. Clin. Oncol.* **34**, 2294–2302 (2016).

52. Bui-Nguyen, B. *et al.* A phase IIb multicentre study comparing the efficacy of trabectedin to doxorubicin in patients with advanced or metastatic untreated soft tissue sarcoma: The TRUSTS trial. *Eur. J. Cancer* **51**, 1312–1320 (2015).

53. Blay, J. Y. *et al.* Randomised phase III trial of trabectedin versus doxorubicin-based chemotherapy as first-line therapy in translocation-related sarcomas. *Eur. J. Cancer* **50**, 1137–1147 (2014).

54. Linch, M., Miah, A. B., Thway, K., Judson, I. R. & Benson, C. Systemic treatment of soft-tissue sarcoma—gold standard and novel therapies. **11**, 187–202 (2014).

55. Nielsen, O. S. *et al.* Effect of high-dose ifosfamide in advanced soft tissue sarcomas. A multicentre phase II study of the EORTC Soft Tissue and Bone Sarcoma Group. *Eur. J. Cancer* **36**, 61–67 (2000).

56. Lee, S. H. *et al.* High-dose ifosfamide as second-or third-line chemotherapy in refractory bone and soft tissue sarcoma patients. *Oncology* **80**, 257–261 (2011).

57. Martin-Liberal, J. *et al.* Clinical activity and tolerability of a 14-day infusional ifosfamide schedule in soft-tissue sarcoma. *Sarcoma* **2013**, (2013).

58. Okuno, S. *et al.* Phase II trial of gemcitabine in advanced sarcomas. *Cancer* **94**, 3225–3229 (2002).

59. Švancárová, L. *et al.* Gemcitabine in advanced adult soft-tissue sarcomas. A phase II study of the EORTC Soft Tissue and Bone Sarcoma Group. *Eur. J. Cancer* **38**, 556–559 (2002).

60. Hensley, M. L. *et al.* Gemcitabine and docetaxel in patients with unresectable leiomyosarcoma: Results of a phase II trial. *J. Clin. Oncol.* **20**, 2824–2831 (2002).

61. Maki, R. G. *et al.* Randomized phase II study of gemcitabine and docetaxel compared with gemcitabine alone in patients with metastatic soft tissue sarcomas. *J. Clin. Oncol.* **25**, 2755–2763 (2007).

62. Pautier, P. *et al.* Randomized Multicenter and Stratified Phase II Study of Gemcitabine Alone Versus Gemcitabine and Docetaxel in Patients with Metastatic or Relapsed Leiomyosarcomas: A Fédération Nationale des Centres de Lutte Contre le Cancer (FNCLCC) French Sarcoma Group . *Oncologist* **17**, 1213–1220 (2012).

63. Losa, R. *et al.* Phase II study with the combination of gemcitabine and DTIC in patients with advanced soft tissue sarcomas. *Cancer Chemother. Pharmacol.* **59**, 251–259 (2007).

64. García-del-Muro, X. *et al.* Randomized phase II study comparing gemcitabine plus dacarbazine versus dacarbazine alone in patients with previously treated soft tissue sarcoma: A Spanish group for research on sarcomas study. *J. Clin. Oncol.* **29**, 2528–2533 (2011).

65. Takahashi, M. *et al.* Efficacy of Trabectedin in Patients with Advanced Translocation-Related Sarcomas: Pooled Analysis of Two Phase II Studies. *Oncologist* **22**, 979–988 (2017).

66. Penel, N. *et al.* Phase II trial of weekly paclitaxel for unresectable angiosarcoma: The ANGIOTAX study. *J. Clin. Oncol.* **26**, 5269–5274 (2008).

67. Schöffski, P. *et al.* Eribulin versus dacarbazine in previously treated patients with advanced liposarcoma or leiomyosarcoma: A randomised, open-label, multicentre, phase 3 trial. in *The Lancet* **387**, 1629–1637 (Elsevier, 2016).

68. OS, N. *et al.* Effect of high-dose ifosfamide in advanced soft tissue sarcomas. A multicentre phase II study of the EORTC Soft Tissue and Bone Sarcoma Group. *Eur. J. Cancer* **36**, 61–67 (2000).

69. Samuels, B. L. *et al.* Clinical outcomes and safety with trabectedin therapy in patients with advanced soft tissue sarcomas following failure of prior chemotherapy: Results of a worldwide expanded access program study. *Ann. Oncol.* **24**, 1703–1709 (2013).

70. Demetri, G. D. *et al.* Efficacy and safety of trabectedin or dacarbazine for metastatic liposarcoma or leiomyosarcoma after failure of conventional chemotherapy: Results of a phase III randomized multicenter clinical trial. *J. Clin. Oncol.* **34**, 786–793 (2016).

71. Register, E. clinical trials. A Randomized & Observational phase II trial assessing the activity of TrabectedIn vs gemCitabine in patients with metastatic or locally advanced LEiomyosarcoma pretreated with conventional chemotherapy. *EU clinical trials register* **34**, 201–203 (2007).

72. ClinicalTrials.gov. Study on Trabectedin in Advanced Rearranged Mesenchymal Chondrosarcoma. *ClinicalTrials.gov* Available at: https://clinicaltrials.gov/ct2/show/NCT04305548. (Accessed: 8th September 2021)

73. Chellappan, D. K. *et al.* The role of pazopanib on tumour angiogenesis and in the management of cancers: A review. *Biomedicine and Pharmacotherapy* **96**, 768–781 (2017).

74. Hanahan, D. & Weinberg, R. A. Hallmarks of Cancer: The Next Generation. *Cell* **144**, 646–674 (2011).

75. Wu, P., Nielsen, T. E. & Clausen, M. H. FDA-approved small-molecule kinase inhibitors. *Trends in Pharmacological Sciences* **36**, 422–439 (2015).

76. Gotink, K. J. & Verheul, H. M. W. Anti-angiogenic tyrosine kinase inhibitors: What is their mechanism of action? *Angiogenesis* **13**, 1–14 (2010).

77. Du, Z. & Lovly, C. M. Mechanisms of receptor tyrosine kinase activation in cancer. *Molecular Cancer* **17**, 1–13 (2018).

78. Lemmon, M. A. & Schlessinger, J. Cell signaling by receptor tyrosine kinases. *Cell* **141**, 1117–1134 (2010).

79. Wu, C. E., Tzen, C. Y., Wang, S. Y. & Yeh, C. N. Clinical diagnosis of gastrointestinal stromal tumor (Gist): From the molecular genetic point of view. *Cancers* **11**, 679 (2019).

80. Yuzawa, S. *et al.* Structural Basis for Activation of the Receptor Tyrosine Kinase KIT by Stem Cell Factor. *Cell* **130**, 323–334 (2007).

81. Asano, N. *et al.* Frequent amplification of receptor tyrosine kinase genes in welldifferentiated/ dedifferentiated liposarcoma. *Oncotarget* **8**, 12941–12952 (2017).

82. Du, Z. *et al.* Structure–function analysis of oncogenic EGFR Kinase Domain Duplication reveals insights into activation and a potential approach for therapeutic targeting. *Nat. Commun.* **12**, 1–15 (2021).

83. Wegert, J. *et al.* Recurrent intragenic rearrangements of EGFR and BRAF in soft tissue tumors of infants. *Nat. Commun.* **9**, 1–6 (2018).

84. Parsons, D. W. *et al.* An integrated genomic analysis of human glioblastoma multiforme. *Science* **321**, 1807–1812 (2008).

85. Horn, L. *et al.* Ensartinib (X-396) in ALK-Positive Non–Small Cell Lung

Cancer: Results from a First-in-Human Phase I/II, Multicenter Study. *Clin. Cancer Res.* **24**, 2771–2779 (2018).

86. Nakajima, K. & Raz, A. Autocrine motility factor and its receptor expression in musculoskeletal tumors. *Journal of Bone Oncology* **24**, 100318 (2020).

87. Hanahan, D. & Weinberg, R. A. The hallmarks of cancer. *Cell* **100**, 57–70 (2000).

88. Kumar, R. *et al.* Pharmacokinetic-pharmacodynamic correlation from mouse to human with pazopanib, a multikinase angiogenesis inhibitor with potent antitumor and antiangiogenic activity. *Mol. Cancer Ther.* **6**, 2012–2021 (2007).

89. Shibuya, M. Vascular Endothelial Growth Factor (VEGF) and Its Receptor (VEGFR) Signaling in Angiogenesis: A Crucial Target for Anti- and Pro-Angiogenic Therapies. *Genes and Cancer* **2**, 1097–1105 (2011).

90. Yoon, S. S. *et al.* Angiogenic Profile of Soft Tissue Sarcomas Based on Analysis of Circulating Factors and Microarray Gene Expression. *J. Surg. Res.* **135**, 282–290 (2006).

91. Hayes, A. J. *et al.* Serum vascular endothelial growth factor as a tumour marker in soft tissue sarcoma. *Br. J. Surg.* **91**, 242–247 (2004).

92. Kilvaer, T. K. *et al.* The VEGF- and PDGF-family of angiogenic markers have prognostic impact in soft tissue sarcomas arising in the extremities and trunk. *BMC Clin. Pathol.* **14**, (2014).

93. Kilvaer, T. K. *et al.* Platelet-derived growth factors in non-GIST soft-tissue sarcomas identify a subgroup of patients with wide resection margins and poor disease-specific survival. *Sarcoma* **2010**, (2010).

94. Yudoh, K. *et al.* Concentration of vascular endothelial growth factor in the tumour tissue as a prognostic factor of soft tissue sarcomas. *Br. J. Cancer* **84**, 1610–1615 (2001).

95. Andrae, J., Gallini, R. & Betsholtz, C. Role of platelet-derived growth factors in physiology and medicine. *Genes and Development* **22**, 1276–1312 (2008).

96. Li, L. *et al.* Platelet-derived growth factor-b (PDGF-B) induced by hypoxia promotes the survival of pulmonary arterial endothelial cells through the PI3K/Akt/stat3 pathway. *Cell. Physiol. Biochem.* **35**, 441–451 (2015).

97. Alvarez, R. H., Kantarjian, H. M. & Cortes, J. E. Biology of platelet-derived growth factor and its involvement in disease. *Mayo Clin. Proc.* **81**, 1241–1257 (2006).

98. Heldin, C. H. & Westermark, B. Mechanism of action and in vivo role of platelet-derived growth factor. *Physiol. Rev.* **79**, 1283–1316 (1999).

99. Raica, M. & Cimpean, A. M. Platelet-derived growth factor (PDGF)/PDGF receptors (PDGFR) axis as target for antitumor and antiangiogenic therapy. *Pharmaceuticals* **3**, 572–599 (2010).

100. Kano, M. R. *et al.* VEGF-A and FGF-2 synergistically promote neoangiogenesis through enhancement of endogenous PDGF-B-PDGFRβ signaling. *J. Cell Sci.* **118**, 3759–3768 (2005).

101. Brahmi, M. *et al.* Expression and prognostic significance of PDGF ligands and receptors across soft tissue sarcomas. *ESMO Open* **6**, (2021).

102. Tammela, T. *et al.* Blocking VEGFR-3 suppresses angiogenic sprouting and vascular network formation. *Nature* **454**, 656–660 (2008).

103. Tomlinson, J. *et al.* Different patterns of angiogenesis in sarcomas and carcinomas. *Clin. Cancer Res.* **5**, 3516–3522 (1999).

104. Hori, Y. *et al.* Functional Characterization of VEGF- And FGF-induced Tumor Blood Vessel Models in Human Cancer Xenografts. *Anticancer Res.* **37**, 6629–6638 (2017).

105. Mossahebi-Mohammadi, M., Quan, M., Zhang, J. S. & Li, X. FGF Signaling

Pathway: A Key Regulator of Stem Cell Pluripotency. *Frontiers in Cell and Developmental Biology* **8**, 79 (2020).

106. Oladipupo, S. S. *et al.* Endothelial cell FGF signaling is required for injury response but not for vascular homeostasis. *Proc. Natl. Acad. Sci. U. S. A.* **111**, 13379–13384 (2014).

107. Zhou, W. Y., Zheng, H., Du, X. L. & Yang, J. L. Characterization of FGFR signaling pathway as therapeutic targets for sarcoma patients. *Cancer Biology and Medicine* **13**, 260–268 (2016).

108. Ishibe, T. *et al.* Disruption of fibroblast growth factor signal pathway inhibits the growth of synovial sarcomas: Potential application of signal inhibitors to molecular target therapy. *Clin. Cancer Res.* **11**, 2702–2712 (2005).

109. Taylor VI, J. G. *et al.* Identification of FGFR4-activating mutations in human rhabdomyosarcomas that promote metastasis in xenotransplanted models. *J. Clin. Invest.* **119**, 3395–3407 (2009).

110. Lemmon, M. A. & Schlessinger, J. Cell signaling by receptor tyrosine kinases. *Cell* **141**, 1117–1134 (2010).

111. Quesada, J. & Amato, R. The Molecular Biology of Soft-Tissue Sarcomas and Current Trends in Therapy. *Sarcoma* **2012**, 849456 (2012).

112. Prior, I. A., Hood, F. E. & Hartley, J. L. The frequency of ras mutations in cancer. *Cancer Res.* **80**, 2669–2974 (2020).

113. Sasaki, K., Hitora, T., Nakamura, O., Kono, R. & Yamamoto, T. The role of MAPK pathway in bone and soft tissue tumors. *Anticancer Res.* **31**, 549–553 (2011).

114. Peng, C. L. *et al.* Sorafenib induces growth inhibition and apoptosis in human synovial sarcoma cells via inhibiting the RAF/MEK/ERK signaling pathway. *Cancer Biol. Ther.* **8**, 1729–1736 (2009).

115. Eger, G., Papadopoulos, N., Lennartsson, J. & Heldin, C. H. NR4A1

promotes PDGF-BB-induced cell colony formation in soft agar. *PLoS One* **9**, e109047 (2014).

116. Todd, J. R., Scurr, L. L., Becker, T. M., Kefford, R. F. & Rizos, H. The MAPK pathway functions as a redundant survival signal that reinforces the PI3K cascade in c-Kit mutant melanoma. *Oncogene* **33**, 236–245 (2014).

117. Xie, Y. *et al.* FGF/FGFR signaling in health and disease. *Signal Transduction and Targeted Therapy* **5**, 1–38 (2020).

118. Porta, C., Paglino, C. & Mosca, A. Targeting PI3K/Akt/mTOR signaling in cancer. *Front. Oncol.* **4 APR**, 1–11 (2014).

119. Yang, J. *et al.* Targeting PI3K in cancer: Mechanisms and advances in clinical trials. *Mol. Cancer* **18**, 1–28 (2019).

120. Hoxhaj, G. & Manning, B. D. The PI3K–AKT network at the interface of oncogenic signalling and cancer metabolism. *Nature Reviews Cancer* **20**, 74–88 (2020).

121. Murugan, A. K. mTOR: Role in cancer, metastasis and drug resistance. *Seminars in Cancer Biology* **59**, 92–111 (2019).

122. Janku, F., Yap, T. A. & Meric-Bernstam, F. Targeting the PI3K pathway in cancer: Are we making headway? *Nature Reviews Clinical Oncology* **15**, 273–291 (2018).

123. Hernando, E. *et al.* The AKT-mTOR pathway plays a critical role in the development of leiomyosarcomas. *Nat. Med.* **13**, 748–753 (2007).

124. Yoon, C., Lu, J., Ryeom, S. W., Simon, M. C. & Yoon, S. S. PIK3R3, part of the regulatory domain of PI3K, is upregulated in sarcoma stem-like cells and promotes invasion, migration, and chemotherapy resistance. *Cell Death Dis.* **12**, 1–11 (2021).

125. Wan, X. & Helman, L. J. The Biology Behind mTOR Inhibition in Sarcoma. *Oncologist* **12**, 1007–1018 (2007).

126. Hosaka, S. *et al.* A novel multi-kinase inhibitor pazopanib suppresses growth of synovial sarcoma cells through inhibition of the PI3K-AKT pathway. *J. Orthop. Res.* **30**, 1493–1498 (2012).

127. Lanzi, C. *et al.* Overactive IGF1/insulin receptors and NRASQ61R mutation drive mechanisms of resistance to pazopanib and define rational combination strategies to treat synovial sarcoma. *Cancers (Basel).* **11**, (2019).

128. Hurwitz, H. I. *et al.* Phase I trial of pazopanib in patients with advanced cancer. *Clin. Cancer Res.* **15**, 4220–4227 (2009).

129. Bender, J. L. G. *et al.* Phase i pharmacokinetic and pharmacodynamic study of pazopanib in children with soft tissue sarcoma and other refractory solid tumors: A children's oncology group phase i consortium report. in *Journal of Clinical Oncology* **31**, 3034–3043 (American Society of Clinical Oncology, 2013).

130. Sleijfer, S. *et al.* Pazopanib, a Multikinase Angiogenesis Inhibitor, in Patients With Relapsed or Refractory Advanced Soft Tissue Sarcoma: A Phase II Study From the European Organisation for Research and Treatment of Cancer–Soft Tissue and Bone Sarcoma Group (EORTC Study 620. *J. Clin. Oncol.* **27**, 3126–3132 (2009).

131. Van Glabbeke, M., Verweij, J., Judson, I. & Nielsen, O. S. Progression-free rate as the principal end-point for phase II trials in soft-tissue sarcomas. *Eur. J. Cancer* **38**, 543–549 (2002).

132. van der Graaf, W. T. *et al.* Pazopanib for metastatic soft-tissue sarcoma (PALETTE): a randomised, double-blind, placebo-controlled phase 3 trial. *Lancet* **379**, 1879–1886 (2012).

133. NHS England » Cancer Drugs Fund. Available at: https://www.england.nhs.uk/cancer/cdf/. (Accessed: 4th August 2019)

134. Amdahl, J. *et al.* Cost-effectiveness of pazopanib in advanced soft tissue

sarcoma in the United kingdom. *Sarcoma* **2014**, 481071 (2014).

135. Kasper, B. *et al.* Long-term responders and survivors on pazopanib for advanced soft tissue sarcomas: subanalysis of two European Organisation for Research and Treatment of Cancer (EORTC) clinical trials 62043 and 62072. *Ann. Oncol.* **25**, 719–724 (2014).

136. Toulmonde, M. *et al.* Retroperitoneal sarcomas: Patterns of care at diagnosis, prognostic factors and focus on main histological subtypes: A multicenter analysis of the French Sarcoma Group. *Ann. Oncol.* **25**, 735–742 (2014).

137. Benson, C. *et al.* Outcome of uterine sarcoma patients treated with pazopanib: A retrospective analysis based on two European -rganisation for Research and Truatment of Cancer (EORTC) Soft Tissue and Bone Sarcoma Group (STBSG) clinical trials 62043 and 62072. *Gynecol. Oncol.* **142**, 89–94 (2016).

138. Cesne, A. Le *et al.* Safety and efficacy of Pazopanib in advanced soft tissue sarcoma: PALETTE (EORTC 62072) subgroup analyses. *BMC Cancer* **19**, 1–7 (2019).

139. Grünwald, V. *et al.* Randomized Comparison of Pazopanib and Doxorubicin as First-Line Treatment in Patients with Metastatic Soft Tissue Sarcoma Age 60 Years or Older: Results of a German Intergroup Study. in *Journal of Clinical Oncology* **38**, 3555–3564 (American Society of Clinical Oncology, 2020).

140. Urakawa, H. *et al.* Phase II trial of pazopanib in patients with metastatic or unresectable chemoresistant sarcomas: A Japanese Musculoskeletal Oncology Group study. *Cancer Sci.* **111**, 3303–3312 (2020).

141. Kim, M. *et al.* A Phase II Trial of Pazopanib in Patients with Metastatic Alveolar Soft Part Sarcoma. *Oncologist* **24**, 20 (2019).

142. Martin-Broto, J. *et al.* Pazopanib for treatment of typical solitary fibrous

tumours: a multicentre, single-arm, phase 2 trial. *Lancet Oncol.* **21**, 456–466 (2020).

143. Martin-Broto, J. *et al.* Pazopanib for treatment of advanced malignant and dedifferentiated solitary fibrous tumour: a multicentre, single-arm, phase 2 trial. *Lancet Oncol.* **20**, 134–144 (2019).

144. Maruzzo, M. *et al.* Pazopanib as first line treatment for solitary fibrous tumours: the Royal Marsden Hospital experience. *Clin. Sarcoma Res.* **5**, 1–7 (2015).

145. Chow, W. *et al.* Results of a prospective phase 2 study of pazopanib in patients with surgically unresectable or metastatic chondrosarcoma. *Cancer* **126**, 105–111 (2020).

146. Stacchiotti, S. *et al.* Pazopanib for treatment of advanced extraskeletal myxoid chondrosarcoma: a multicentre, single-arm, phase 2 trial. *Lancet Oncol.* **20**, 1252–1262 (2019).

147. Gelderblom, H. *et al.* Treatment patterns and clinical outcomes with pazopanib in patients with advanced soft tissue sarcomas in a compassionate use setting: results of the SPIRE study*. *Acta Oncol. (Madr).* **56**, 1769–1775 (2017).

148. Oh, C. R. *et al.* Real-World Outcomes of Pazopanib Treatment in Korean Patients with Advanced Soft Tissue Sarcoma: A Multicenter Retrospective Cohort Study. *Target. Oncol.* **15**, 485–493 (2020).

149. Alshamsan, B. *et al.* Real-world outcome and prognostic factors of pazopanib in advanced soft tissue sarcoma. *Cancer Manag. Res.* **13**, 6755–6766 (2021).

150. Halim, N. A. *et al.* Safety and efficacy of pazopanib as a second-line treatment and beyond for soft tissue sarcomas: A real-life tertiary-center experience in the MENA region. *Cancer Treat. Res. Commun.* **26**, 100275 (2021).

151. Karaağaç, M. *et al.* The real-life outcome of pazopanib in patients with advanced soft tissue sarcoma: A retrospective cross-sectional study of a Turkish cohort. *J. Oncol. Pharm. Pract.* **26**, 1657–1666 (2020).

152. Seto, T. *et al.* Real-World Experiences with Pazopanib in Patients with Advanced Soft Tissue and Bone Sarcoma in Northern California. **7**, 48 (2019).

153. Nakamura, T. *et al.* The clinical outcome of pazopanib treatment in Japanese patients with relapsed soft tissue sarcoma: A Japanese Musculoskeletal Oncology Group (JMOG) study. *Cancer* **122**, 1408–1416 (2016).

154. Yoo, K. H. *et al.* Efficacy of pazopanib monotherapy in patients who had been heavily pretreated for metastatic soft tissue sarcoma: A retrospective case series. *BMC Cancer* **15**, 1–7 (2015).

155. Frezza, A. M. *et al.* Anthracycline, gemcitabine, and pazopanib in epithelioid sarcoma a multi-institutional case series. *JAMA Oncol.* **4**, (2018).

156. Menegaz, B. A. *et al.* Clinical Activity of Pazopanib in Patients with Advanced Desmoplastic Small Round Cell Tumor. *Oncologist* **23**, 360–366 (2018).

157. Kim, H. J., Kim, Y., Lee, S. J., Lee, J. & Park, S. H. Pazopanib monotherapy in the treatment of pretreated, metastatic uterine sarcoma: A single-center retrospective study. *J. Gynecol. Oncol.* **29**, (2018).

158. Lueza, B. *et al.* Difference in restricted mean survival time for cost-effectiveness analysis using individual patient data meta-analysis: Evidence from a case study. *PLoS One* **11**, e0150032 (2016).

159. Wei, Y., Royston, P., Tierney, J. F. & Parmar, M. K. B. Meta-analysis of time-to-event outcomes from randomized trials using restricted mean survival time: Application to individual participant data. *Stat. Med.* **34**,

2881–2898 (2015).

160. Martin-Broto, J. *et al.* Pazopanib for treatment of advanced malignant and dedifferentiated solitary fibrous tumour: a multicentre, single-arm, phase 2 trial. *Lancet Oncol.* **20**, 134–144 (2019).

161. Kim, M. *et al.* A Phase II Trial of Pazopanib in Patients with Metastatic Alveolar Soft Part Sarcoma. *Oncologist* **24**, 20-e29 (2019).

162. Kollár, A. *et al.* Pazopanib in advanced vascular sarcomas: an EORTC Soft Tissue and Bone Sarcoma Group (STBSG) retrospective analysis. *Acta Oncol. (Madr).* **56**, 88–92 (2017).

163. Frezza, A. M. *et al.* Anthracycline, gemcitabine, and pazopanib in epithelioid sarcoma a multi-institutional case series. *JAMA Oncol.* **4**, (2018).

164. Pàez-Ribes, M. *et al.* Antiangiogenic Therapy Elicits Malignant Progression of Tumors to Increased Local Invasion and Distant Metastasis. *Cancer Cell* **15**, 220–231 (2009).

165. Griffioen, A. W. *et al.* Rapid angiogenesis onset after discontinuation of sunitinib treatment of renal cell carcinoma patients. *Clin. Cancer Res.* **18**, 3961–3971 (2012).

166. Mancuso, M. R. *et al.* Rapid vascular regrowth in tumors after reversal of VEGF inhibition. *J. Clin. Invest.* **116**, 2610–2621 (2006).

167. Chaft, J. E. *et al.* Disease flare after tyrosine kinase inhibitor discontinuation in patients with EGFR-mutant lung cancer and acquired resistance to erlotinib or gefitinib: Implications for clinical trial design. *Clin. Cancer Res.* **17**, 6298–6303 (2011).

168. Shin, S.-J. *et al.* The Association Between PD-L1 Expression and the Clinical Outcomes to Vascular Endothelial Growth Factor-Targeted Therapy in Patients With Metastatic Clear Cell Renal Cell Carcinoma. *Oncologist* **20**, 1253–1260 (2015).

169. Tanigawa, T. *et al.* Tumors Sharply Increased after Ceasing Pazopanib Therapy for a Patient with Advanced Uterine Leiomyosarcoma: Experience of Tumor Flare. *Case Rep. Obstet. Gynecol.* **2017**, 1–4 (2017).

170. Mandrekar, S. J. & Sargent, D. J. Clinical trial designs for predictive biomarker validation: One size does not fit all. *J. Biopharm. Stat.* **19**, 530–542 (2009).

171. Taube, S. E., Jacobson, J. W. & Lively, T. G. Cancer diagnostics: Decision criteria for marker utilization in the clinic. *American Journal of PharmacoGenomics* **5**, 357–364 (2005).

172. Henry, N. L. & Hayes, D. F. Cancer biomarkers. *Mol. Oncol.* **6**, 140–146 (2012).

173. Conley, B. A. & Taube, S. E. Prognostic and predictive markers in cancer. *Dis. Markers* **20**, 35–43 (2004).

174. Teutsch, S. M. *et al.* The evaluation of genomic applications in practice and prevention (EGAPP) initiative: Methods of the EGAPP working group. *Genet. Med.* **11**, 3–14 (2009).

175. Hayes, D. F. Biomarker validation and testing. *Molecular Oncology* **9**, 960–966 (2015).

176. Dobbin, K. K. *et al.* Validation of biomarkers to predict response to immunotherapy in cancer: Volume II - clinical validation and regulatory considerations. *J. Immunother. Cancer* **4**, 1–14 (2016).

177. Simon, R. M., Paik, S. & Hayes, D. F. Use of archived specimens in evaluation of prognostic and predictive biomarkers. *Journal of the National Cancer Institute* **101**, 1446–1452 (2009).

178. Simon, R., Radmacher, M. D., Dobbin, K. & McShane, L. M. Pitfalls in the use of DNA microarray data for diagnostic and prognostic classification. *J. Natl. Cancer Inst.* **95**, 14–18 (2003).

179. Ahn, S., Woo, J. W., Lee, K. & Park, S. Y. HER2 status in breast cancer: Changes in guidelines and complicating factors for interpretation. *Journal of Pathology and Translational Medicine* **54**, 34–44 (2020).

180. Hensing, W., Santa-Maria, C. A., Peterson, L. L. & Sheng, J. Y. Landmark trials in the medical oncology management of early stage breast cancer. *Seminars in Oncology* **47**, 278–292 (2020).

181. Reck, M. *et al.* Pembrolizumab versus Chemotherapy for PD-L1–Positive Non–Small-Cell Lung Cancer. *N. Engl. J. Med.* **375**, 1823–1833 (2016).

182. Final appraisal determination-Pembrolizumab for untreated PD-L1-positive metastatic non-small-cell lung cancer Pembrolizumab for untreated PD-L1-positive metastatic non-small-cell lung cancer (CDF review of TA447). (2018).

183. Rossari, F., Minutolo, F. & Orciuolo, E. Past, present, and future of Bcr-Abl inhibitors: From chemical development to clinical efficacy. *Journal of Hematology and Oncology* **11**, 1–14 (2018).

184. Burmeister, T. *et al.* Patients' age and BCR-ABL frequency in adult B-precursor ALL: A retrospective analysis from the GMALL study group. *Blood* **112**, 918–919 (2008).

185. Deininger, M. W. *et al.* Chronic myeloid leukemia, version 2.2021. *JNCCN Journal of the National Comprehensive Cancer Network* **18**, 1385–1415 (2020).

186. Smith, G. *et al.* A British Society for Haematology Guideline on the diagnosis and management of chronic myeloid leukaemia. *Br. J. Haematol.* **191**, 171–193 (2020).

187. Knezevich, S. R., McFadden, D. E., Tao, W., Lim, J. F. & Sorensen, P. H. B. A novel ETV6-NTRK3 gene fusion in congenital fibrosarcoma. *Nat. Genet.* **18**, 184–187 (1998).

188. Haller, F. *et al.* Paediatric and adult soft tissue sarcomas with *NTRK1* gene

fusions: a subset of spindle cell sarcomas unified by a prominent myopericytic/haemangiopericytic pattern. *J. Pathol.* **238**, 700–710 (2016).

189. Chiang, S. *et al.* NTRK Fusions Define a Novel Uterine Sarcoma Subtype with Features of Fibrosarcoma. *Am. J. Surg. Pathol.* **42**, 791–798 (2018).

190. Davis, J. L. *et al.* Expanding the Spectrum of Pediatric NTRK -rearranged Mesenchymal Tumors. *Am. J. Surg. Pathol.* **43**, 435–445 (2019).

191. Marchiò, C. *et al.* ESMO recommendations on the standard methods to detect NTRK fusions in daily practice and clinical research. *Ann. Oncol.* **30**, 1417–1427 (2019).

192. Li, H., van der Merwe, P. A. & Sivakumar, S. Biomarkers of response to PD-1 pathway blockade. *British Journal of Cancer* **126**, 1663–1675 (2022).

193. Snyder, A. *et al.* Genetic Basis for Clinical Response to CTLA-4 Blockade in Melanoma. *N. Engl. J. Med.* **371**, 2189–2199 (2014).

194. Goodman, A. M. *et al.* Tumor Mutational Burden as an Independent Predictor of Response to Immunotherapy in Diverse Cancers. *Mol. Cancer Ther.* **16**, 2598–2608 (2017).

195. Marabelle, A. *et al.* Association of tumour mutational burden with outcomes in patients with advanced solid tumours treated with pembrolizumab: prospective biomarker analysis of the multicohort, open-label, phase 2 KEYNOTE-158 study. *Lancet Oncol.* **21**, 1353–1365 (2020).

196. Jardim, D. L., Goodman, A., de Melo Gagliato, D. & Kurzrock, R. The Challenges of Tumor Mutational Burden as an Immunotherapy Biomarker. *Cancer Cell* **39**, 154–173 (2021).

197. FoundationOne® CDx - P170019/S017 | FDA. Available at: https://www.fda.gov/medical-devices/recently-approved-devices/foundationoner-cdx-p170019s017. (Accessed: 1st June 2023)

198. Perou, C. M. *et al.* Molecular portraits of human breast tumours. *Nature*

406, 747–752 (2000).

199. Bernard, P. S. *et al.* Supervised risk predictor of breast cancer based on intrinsic subtypes. *J. Clin. Oncol.* **27**, 1160–1167 (2009).

200. Wallden, B. *et al.* Development and verification of the PAM50-based Prosigna breast cancer gene signature assay. *BMC Med. Genomics* **8**, 1–14 (2015).

201. NICE. 1 Recommendations | Tumour profiling tests to guide adjuvant chemotherapy decisions in early breast cancer | Guidance | NICE. *Tumour profiling tests2* (2018). Available at: https://www.nice.org.uk/guidance/dg34/chapter/1-recommendations. (Accessed: 22nd October 2021)

202. Rodriguez, C. A. *et al.* Impact of the Prosigna (PAM50) assay on adjuvant clinical decision making in patients with early stage breast cancer: Results of a prospective multicenter public program. *J. Clin. Oncol.* **35**, e12062–e12062 (2017).

203. Lenz, H. J. *et al.* Impact of consensus molecular subtype on survival in patients with metastatic colorectal cancer: Results from CALGB/SWOG 80405 (Alliance). in *Journal of Clinical Oncology* **37**, 1876–1885 (American Society of Clinical Oncology, 2019).

204. Song, B. N. *et al.* Identification of an immunotherapy-responsive molecular subtype of bladder cancer. *EBioMedicine* **50**, 238–245 (2019).

205. Bailey, P. *et al.* Genomic analyses identify molecular subtypes of pancreatic cancer. *Nature* **531**, 47–52 (2016).

206. Van Der Graaf, W. T. A. *et al.* PALETTE: Final overall survival (OS) data and predictive factors for OS of EORTC 62072/GSK VEG110727, a randomized double-blind phase III trial of pazopanib versus placebo in advanced soft tissue sarcoma (STS) patients. *J. Clin. Oncol.* **30**, 10009–10009 (2012).

207. Szkandera, J. *et al.* Pre-Treatment anemia is a poor prognostic factor in soft tissue sarcoma patients. *PLoS One* **9**, (2014).

208. Vincenzi, B. *et al.* Bone metastases in soft tissue sarcoma: a survey of natural history, prognostic value and treatment options. *Clin. Sarcoma Res.* **3**, 1–5 (2013).

209. Duffaud, F. *et al.* Hypertension (HTN) as a potential biomarker of efficacy in pazopanib-treated patients with advanced non-adipocytic soft tissue sarcoma. A retrospective study based on European Organisation for Research and Treatment of Cancer (EORTC) 62043 and 62072 trial. *Eur. J. Cancer* **51**, 2615–2623 (2015).

210. Vos, M. *et al.* Association of pazopanib-induced toxicities with outcome of patients with advanced soft tissue sarcoma; a retrospective analysis based on the European Organisation for Research and Treatment of Cancer (EORTC) 62043 and 62072 clinical trials. *Acta Oncol. (Madr).* **58**, 872–879 (2019).

211. Wang, Y. & Zhang, Y. Prognostic role of interleukin-6 in renal cell carcinoma: a meta-analysis. *Clin. Transl. Oncol.* **22**, 835–843 (2020).

212. Sleijfer, S. *et al.* Cytokine and angiogenic factors associated with efficacy and toxicity of pazopanib in advanced soft-tissue sarcoma: An EORTC-STBSG study. *Br. J. Cancer* **107**, 639–645 (2012).

213. Kobayashi, H. *et al.* Neutrophil-to-lymphocyte ratio after pazopanib treatment predicts response in patients with advanced soft-tissue sarcoma. *Int. J. Clin. Oncol.* **23**, 368–374 (2018).

214. Mirili, C. *et al.* Assessment of potential predictive value of peripheral blood inflammatory indexes in 26 cases with soft tissue sarcoma treated by pazopanib: A retrospective study. *Cancer Manag. Res.* **11**, 3445–3453 (2019).

215. Templeton, A. J. *et al.* Prognostic role of neutrophil-to-lymphocyte ratio in

solid tumors: A systematic review and meta-analysis. *Journal of the National Cancer Institute* **106**, (2014).

216. De Maio, E. *et al.* Evolution in neutrophil-to-lymphocyte ratio (NLR) among advanced soft tissue sarcoma (STS) patients treated with pazopanib within EORTC 62043/62072 trials. *Ann. Oncol.* **28**, v531 (2017).

217. Zhang, L. *et al.* Wild-type p53 suppresses angiogenesis in human leiomyosarcoma and synovial sarcoma by transcriptional suppression of vascular endothelial growth factor expression. *Cancer Res.* **60**, 3655–3661 (2000).

218. Koehler, K., Liebner, D. & Chen, J. L. TP53 mutational status is predictive of pazopanib response in advanced sarcomas. *Ann. Oncol.* **27**, 539–543 (2016).

219. Fu, S. *et al.* Phase I study of pazopanib and vorinostat: A therapeutic approach for inhibiting mutant p53-mediated angiogenesis and facilitating mutant p53 degradation. *Ann. Oncol.* **26**, 1012–1018 (2015).

220. Nassif, E. F. *et al.* TP53 Mutation as a Prognostic and Predictive Marker in Sarcoma: Pooled Analysis of MOSCATO and ProfiLER Precision Medicine Trials. *Cancers (Basel).* **13**, 3362 (2021).

221. D'Arcy, M. E. *et al.* Risk of Rare Cancers among Solid Organ Transplant Recipients. *J. Natl. Cancer Inst.* **113**, 199–207 (2021).

222. Hernández-Ramírez, R. U., Shiels, M. S., Dubrow, R. & Engels, E. A. Cancer risk in HIV-infected people in the USA from 1996 to 2012: a population-based, registry-linkage study. *Lancet HIV* **4**, e495–e504 (2017).

223. Dunn, G. P., Bruce, A. T., Ikeda, H., Old, L. J. & Schreiber, R. D. Cancer immunoediting: From immunosurveillance to tumor escape. *Nature Immunology* **3**, 991–998 (2002).

224. Dunn, G. P., Old, L. J. & Schreiber, R. D. The three Es of cancer immunoediting. *Annual Review of Immunology* **22**, 329–360 (2004).

225. Mittal, D., Gubin, M. M., Schreiber, R. D. & Smyth, M. J. New insights into cancer immunoediting and its three component phases-elimination, equilibrium and escape. *Current Opinion in Immunology* **27**, 16–25 (2014).

226. Schreiber, R. D., Old, L. J. & Smyth, M. J. Cancer immunoediting: Integrating immunity's roles in cancer suppression and promotion. *Science* **331**, 1565–1570 (2011).

227. Zaidi, M. R. The Interferon-Gamma Paradox in Cancer. *J. Interf. Cytokine Res.* **39**, 30–38 (2019).

228. Legut, M., Cole, D. K. & Sewell, A. K. The promise of γδT cells and the γδT cell receptor for cancer immunotherapy. *Cell. Mol. Immunol.* **12**, 656–658 (2015).

229. Kayagaki, N. *et al.* Type I interferons (IFNs) regulate tumor necrosis factor-related apoptosis-inducing ligand (TRAIL) expression on human T cells: A novel mechanism for the antitumor effects of type I IFNs. *J. Exp. Med.* **189**, 1451–1460 (1999).

230. Trapani, J. A. & Smyth, M. J. Functional significance of the perforin/granzyme cell death pathway. *Nature Reviews Immunology* **2**, 735–747 (2002).

231. Koebel, C. M. *et al.* Adaptive immunity maintains occult cancer in an equilibrium state. *Nature* **450**, 903–907 (2007).

232. Wu, X. *et al.* Immune microenvironment profiles of tumor immune equilibrium and immune escape states of mouse sarcoma. *Cancer Lett.* **340**, 124–133 (2013).

233. Yi, M., Niu, M., Xu, L., Luo, S. & Wu, K. Regulation of PD-L1 expression in the tumor microenvironment. *Journal of Hematology and Oncology* **14**, 1–13 (2021).

234. Carlino, M. S., Larkin, J. & Long, G. V. Immune checkpoint inhibitors in melanoma. *The Lancet* **398**, 1002–1014 (2021).

235. Rosenthal, R. *et al.* Neoantigen-directed immune escape in lung cancer evolution. *Nature* **567**, 479–485 (2019).

236. Dhatchinamoorthy, K., Colbert, J. D. & Rock, K. L. Cancer Immune Evasion Through Loss of MHC Class I Antigen Presentation. *Frontiers in Immunology* **12**, 469 (2021).

237. Straten, P. thor & Andersen, M. H. The anti-apoptotic members of the Bcl-2 family are attractive tumor-associated antigens. *Oncotarget* **1**, 239–245 (2010).

238. Zou, S. *et al.* Targeting stat3 in cancer immunotherapy. *Mol. Cancer* **19**, 1–19 (2020).

239. Qin, S. *et al.* Novel immune checkpoint targets: Moving beyond PD-1 and CTLA-4. *Molecular Cancer* **18**, 1–14 (2019).

240. Yang, L., Pang, Y. & Moses, H. L. TGF-β and immune cells: an important regulatory axis in the tumor microenvironment and progression. *Trends in Immunology* **31**, 220–227 (2010).

241. Hirano, T. IL-6 in inflammation, autoimmunity and cancer. *International immunology* **33**, 127–148 (2021).

242. Somarelli, J. A. *et al.* Molecular Biology and Evolution of Cancer: From Discovery to Action. *Mol. Biol. Evol.* **37**, 320–326 (2020).

243. Solary, E. & Lapane, L. The role of host environment in cancer evolution. *Evol. Appl.* **13**, 1756–1770 (2020).

244. Amend, S. R. & Pienta, K. J. Ecology meets cancer biology: The cancer swamp promotes the lethal cancer phenotype. *Oncotarget* **6**, 9669–9678 (2015).

245. Grimes, D. R., Jansen, M., Macauley, R. J., Scott, J. G. & Basanta, D. Evidence for hypoxia increasing the tempo of evolution in glioblastoma. *Br. J. Cancer* **123**, 1562–1569 (2020).

246. Xu, B.-L. *et al.* In vivo growth of subclones derived from Lewis lung carcinoma is determined by the tumor microenvironment. *Am. J. Cancer Res.* **12**, 5255–5270 (2022).

247. Dago, A. E. *et al.* Rapid phenotypic and genomic change in response to therapeutic pressure in prostate cancer inferred by high content analysis of single Circulating Tumor Cells. *PLoS One* **9**, (2014).

248. Zhu, X., Li, S., Xu, B. & Luo, H. Cancer evolution: A means by which tumors evade treatment. *Biomed. Pharmacother.* **133**, 111016 (2021).

249. Espiritu, S. M. G. *et al.* The Evolutionary Landscape of Localized Prostate Cancers Drives Clinical Aggression. *Cell* **173**, 1003-1013.e15 (2018).

250. Raynaud, F., Mina, M., Tavernari, D. & Ciriello, G. Pan-cancer inference of intra-tumor heterogeneity reveals associations with different forms of genomic instability. *PLoS Genet.* **14**, e1007669 (2018).

251. Fortunato, A. *et al.* Natural selection in cancer biology: From molecular snowflakes to trait hallmarks. *Cold Spring Harb. Perspect. Med.* **7**, (2017).

252. Guo, M., Peng, Y., Gao, A., Du, C. & Herman, J. G. Epigenetic heterogeneity in cancer. *Biomark. Res.* **7**, 1–19 (2019).

253. Feinberg, A. P., Koldobskiy, M. A. & Göndör, A. Epigenetic modulators, modifiers and mediators in cancer aetiology and progression. *Nature Reviews Genetics* **17**, 284–299 (2016).

254. You, J. S. & Jones, P. A. Cancer Genetics and Epigenetics: Two Sides of the Same Coin? *Cancer Cell* **22**, 9–20 (2012).

255. Etten, J. L. Van, Dehm, S. M., Van Etten, J. L. & Dehm, S. M. Clonal origin and spread of metastatic prostate cancer. *Endocr. Relat. Cancer* **23**, R207–R217 (2016).

256. Greaves, M. & Maley, C. C. Clonal evolution in cancer. *Nature* **481**, 306–313 (2012).

257. Caswell, D. R. & Swanton, C. The role of tumour heterogeneity and clonal cooperativity in metastasis, immune evasion and clinical outcome. *BMC Medicine* **15**, 1–9 (2017).

258. Tang, Y. J. *et al.* Tracing Tumor Evolution in Sarcoma Reveals Clonal Origin of Advanced Metastasis. *Cell Rep.* **28**, 2837-2850.e5 (2019).

259. Hofvander, J. *et al.* Different patterns of clonal evolution among different sarcoma subtypes followed for up to 25 years. *Nat. Commun.* **9**, 4–11 (2018).

260. Anderson, N. D. *et al.* Lineage-defined leiomyosarcoma subtypes emerge years before diagnosis and determine patient survival. *Nat. Commun.* **12**, 1–14 (2021).

261. Anderson, N. D. *et al.* Rearrangement bursts generate canonical gene fusions in bone and soft tissue tumors. *Science (80-.).* **361**, (2018).

262. Saman, H., Raza, S. S., Uddin, S. & Rasul, K. Inducing angiogenesis, a key step in cancer vascularization, and treatment approaches. *Cancers* **12**, (2020).

263. Bruno, A. *et al.* Orchestration of angiogenesis by immune cells. *Frontiers in Oncology* **4 JUL**, 131 (2014).

264. Zhou, J. *et al.* Tumor-Associated Macrophages: Recent Insights and Therapies. *Frontiers in Oncology* **10**, 188 (2020).

265. Orecchioni, M., Ghosheh, Y., Pramod, A. B. & Ley, K. Macrophage polarization: Different gene signatures in M1(Lps+) vs. Classically and M2(LPS-) vs. Alternatively activated macrophages. *Frontiers in Immunology* **10**, 1084 (2019).

266. Lee, W. S., Yang, H., Chon, H. J. & Kim, C. Combination of anti-angiogenic therapy and immune checkpoint blockade normalizes vascular-immune crosstalk to potentiate cancer immunity. *Experimental and Molecular Medicine* **52**, 1475–1485 (2020).

267. Tripathi, C. *et al.* Macrophages are recruited to hypoxic tumor areas and acquire a Pro-Angiogenic M2-Polarized phenotype via hypoxic cancer cell derived cytokines Oncostatin M and Eotaxin. *Oncotarget* **5**, 5350–5368 (2014).

268. Palucka, K. & Banchereau, J. Cancer immunotherapy via dendritic cells. *Nature Reviews Cancer* **12**, 265–277 (2012).

269. Dhodapkar, M. V., Dhodapkar, K. M. & Palucka, A. K. Interactions of tumor cells with dendritic cells: Balancing immunity and tolerance. *Cell Death and Differentiation* **15**, 39–50 (2008).

270. Seeger, P., Musso, T. & Sozzani, S. The TGF-β superfamily in dendritic cell biology. *Cytokine and Growth Factor Reviews* **26**, 647–657 (2015).

271. Oussa, N. A. E. *et al.* VEGF Requires the Receptor NRP-1 To Inhibit Lipopolysaccharide-Dependent Dendritic Cell Maturation. *J. Immunol.* **197**, 3927–3935 (2016).

272. Tada, Y. *et al.* Targeting VEGFR2 with Ramucirumab strongly impacts effector/ activated regulatory T cells and CD8+ T cells in the tumor microenvironment. *J. Immunother. Cancer* **6**, 1–14 (2018).

273. Voron, T. *et al.* VEGF-A modulates expression of inhibitory checkpoints on CD8++ T cells in tumors. *J. Exp. Med.* **212**, 139–148 (2015).

274. Lanitis, E., Irving, M. & Coukos, G. Targeting the tumor vasculature to enhance T cell activity. *Current Opinion in Immunology* **33**, 55–63 (2015).

275. Bouzin, C., Brouet, A., De Vriese, J., DeWever, J. & Feron, O. Effects of Vascular Endothelial Growth Factor on the Lymphocyte-Endothelium Interactions: Identification of Caveolin-1 and Nitric Oxide as Control Points of Endothelial Cell Anergy. *J. Immunol.* **178**, 1505–1511 (2007).

276. Motz, G. T. *et al.* Tumor endothelium FasL establishes a selective immune barrier promoting tolerance in tumors. *Nat. Med.* **20**, 607–615 (2014).

277. Shetty, S. *et al.* Common Lymphatic Endothelial and Vascular Endothelial Receptor-1 Mediates the Transmigration of Regulatory T Cells across Human Hepatic Sinusoidal Endothelium. *J. Immunol.* **186**, 4147–4155 (2011).

278. Dancsok, A. R. *et al.* Expression of lymphocyte immunoregulatory biomarkers in bone and soft-tissue sarcomas. *Mod. Pathol.* **32**, 1772–1785 (2019).

279. Boxberg, M. *et al.* PD-L1 and PD-1 and characterization of tumor-infiltrating lymphocytes in high grade sarcomas of soft tissue–prognostic implications and rationale for immunotherapy. *Oncoimmunology* **7**, (2018).

280. Shurell, E. *et al.* Characterizing the immune microenvironment of malignant peripheral nerve sheath tumor by PD-L1 expression and presence of CD8+ tumor infiltrating lymphocytes. *Oncotarget* **7**, 64300–64308 (2016).

281. van Erp, A. E. M. *et al.* Expression and clinical association of programmed cell death-1, programmed death-ligand-1 and CD8+ lymphocytes in primary sarcomas is subtype dependent. *Oncotarget* **8**, 71371–71384 (2017).

282. Simard, F. A. *et al.* Description of the immune microenvironment of chondrosarcoma and contribution to progression. *Oncoimmunology* **6**, (2017).

283. D'Angelo, S. P. *et al.* Prevalence of tumor-infiltrating lymphocytes and PD-L1 expression in the soft tissue sarcoma microenvironment. *Hum. Pathol.* **46**, 357–365 (2015).

284. Nowicki, T. S. *et al.* Infiltration of CD8 T cells and expression of PD-1 and PD-L1 in synovial sarcoma. *Cancer Immunol. Res.* **5**, 118–126 (2017).

285. Kostine, M. *et al.* Increased infiltration of M2-macrophages, T-cells and PD-L1 expression in high grade leiomyosarcomas supports immunotherapeutic strategies. *Oncoimmunology* **7**, (2018).

286. Sorbye, S. W. *et al.* Prognostic impact of peritumoral lymphocyte infiltration in soft tissue sarcomas. *BMC Clin. Pathol.* **12**, 1–10 (2012).

287. Oike, N. *et al.* Prognostic impact of the tumor immune microenvironment in synovial sarcoma. *Cancer Sci.* **109**, 3043–3054 (2018).

288. Smolle, M. A. *et al.* Influence of tumor-infiltrating immune cells on local control rate, distant metastasis, and survival in patients with soft tissue sarcoma. *Oncoimmunology* **10**, (2021).

289. Sorbye, S. W. *et al.* Prognostic Impact of Lymphocytes in Soft Tissue Sarcomas. *PLoS One* **6**, e14611 (2011).

290. Abeshouse, A. *et al.* Comprehensive and Integrated Genomic Characterization of Adult Soft Tissue Sarcomas. *Cell* **171**, 950-965.e28 (2017).

291. Hu, C. *et al.* Comprehensive profiling of immune-related genes in soft tissue sarcoma patients. *J. Transl. Med.* **18**, 1–18 (2020).

292. Shen, R. *et al.* Development and validation of an immune gene-set based prognostic signature for soft tissue sarcoma. *BMC Cancer* **21**, 1–14 (2021).

293. Petitprez, F. *et al.* B cells are associated with survival and immunotherapy response in sarcoma. *Nature* **577**, 556–560 (2020).

294. Tawbi, H. A. *et al.* Pembrolizumab in advanced soft-tissue sarcoma and bone sarcoma (SARC028): a multicentre, two-cohort, single-arm, open-label, phase 2 trial. *Lancet Oncol.* **18**, 1493–1501 (2017).

295. Zizzari, I. G. *et al.* TK inhibitor pazopanib primes DCs by downregulation of the β-catenin pathway. *Cancer Immunol. Res.* **6**, 711–722 (2018).

296. Finke, J. H. *et al.* Sunitinib reverses type-1 immune suppression and decreases T-regulatory cells in renal cell carcinoma patients. *Clin. Cancer Res.* **14**, 6674–6682 (2008).

297. Adotevi, O. *et al.* A decrease of regulatory T cells correlates with overall survival after sunitinib-based antiangiogenic therapy in metastatic renal cancer patients. *J. Immunother.* **33**, 991–998 (2010).

298. Chen, M. L. *et al.* Sorafenib relieves cell-intrinsic and cell-extrinsic inhibitions of effector T cells in tumor microenvironment to augment antitumor immunity. *Int. J. Cancer* **134**, 319–331 (2014).

299. Cao, M. *et al.* Kinase inhibitor Sorafenib modulates immunosuppressive cell populations in a murine liver cancer model. *Lab. Investig.* **91**, 598–608 (2011).

300. Kalathil, S. G., Hutson, A., Barbi, J., Iyer, R. & Thanavala, Y. Augmentation of IFN-γ+ CD8+ T cell responses correlates with survival of HCC patients on sorafenib therapy. *JCI Insight* **4**, (2019).

301. Yuan, H. *et al.* Axitinib augments antitumor activity in renal cell carcinoma via STAT3-dependent reversal of myeloid-derived suppressor cell accumulation. *Biomed. Pharmacother.* **68**, 751–756 (2014).

302. Du Four, S. *et al.* Axitinib increases the infiltration of immune cells and reduces the suppressive capacity of monocytic MDSCs in an intracranial mouse melanoma model. *Oncoimmunology* **4**, (2015).

303. Khurana, K. K., Rayman, P. A., Elson, P., Rini, B. I. & Finke, J. Effect of pazopanib on myeloid-derived suppressor cells and T-cell function in patients with metastatic renal cell carcinoma. *J. Clin. Oncol.* **31**, 455–455 (2013).

304. Rinchai, D. *et al.* Integrated transcriptional-phenotypic analysis captures systemic immunomodulation following antiangiogenic therapy in renal cell carcinoma patients. *Clin. Transl. Med.* **11**, e434 (2021).

305. Kim, S. K. *et al.* PD-L1 tumour expression is predictive of pazopanib response in soft tissue sarcoma. *BMC Cancer* **21**, 1–9 (2021).

306. Choueiri, T. K. *et al.* Correlation of PD-L1 tumor expression and treatment

outcomes in patients with renal cell carcinoma receiving sunitinib or pazopanib: Results from COMPARZ, a randomized controlled trial. *Clin. Cancer Res.* **21**, 1071–1077 (2015).

307. Motzer, R. J. *et al.* Pazopanib versus Sunitinib in Metastatic Renal-Cell Carcinoma. *N. Engl. J. Med.* **369**, 722–731 (2013).

308. Shin, S.-J. *et al.* The Association Between PD-L1 Expression and the Clinical Outcomes to Vascular Endothelial Growth Factor-Targeted Therapy in Patients With Metastatic Clear Cell Renal Cell Carcinoma. *Oncologist* **20**, 1253–1260 (2015).

309. Hakimi, A. A. *et al.* Transcriptomic profiling of the tumor microenvironment reveals distinct subgroups of clear cell renal cell cancer: Data from a randomized phase III trial. *Cancer Discov.* **9**, 510–525 (2019).

310. Yoshihara, K. *et al.* Inferring tumour purity and stromal and immune cell admixture from expression data. *Nat. Commun.* **4**, (2013).

311. Beuselinck, B. *et al.* Molecular subtypes of clear cell renal cell carcinoma are associated with sunitinib response in the metastatic setting. *Clin. Cancer Res.* **21**, 1329–1339 (2015).

312. Verbiest, A. *et al.* Molecular Subtypes of Clear Cell Renal Cell Carcinoma Are Associated With Outcome During Pazopanib Therapy in the Metastatic Setting. *Clin. Genitourin. Cancer* **16**, e605–e612 (2018).

313. Epaillard, N. *et al.* BIONIKK: A phase 2 biomarker driven trial with nivolumab and ipilimumab or VEGFR tyrosine kinase inhibitor (TKI) in naïve metastatic kidney cancer. *Bull. Cancer* **107**, eS22–eS27 (2020).

314. ESMO 2020. Results from the Phase 2 Biomarker Driven Trial with Nivolumab and Ipilimumab or VEGFR Tyrosine Kinase Inhibitor in Naïve Metastatic Kidney Cancer Patients: The BIONIKK Trial. Available at: https://www.urotoday.com/conference-highlights/esmo-2020/kidney-cancer/124676-esmo-virtual-congress-2020-results-from-the-phase-2-

biomarker-driven-trial-with-nivolumab-and-ipilimumab-or-vegfr-tyrosine-kinase-inhibitor-in-naive-metastatic-kidney-cancer-pat. (Accessed: 22nd October 2021)

315. CRAN - Package pmsampsize. Available at: https://cran.r-project.org/web/packages/pmsampsize/index.html.

316. Riley, R. D. *et al.* Minimum sample size for developing a multivariable prediction model: PART II - binary and time-to-event outcomes. *Stat. Med.* **38**, 1276–1296 (2019).

317. Lee, A. T. J. *et al.* The adequacy of tissue microarrays in the assessment of inter- and intra-tumoural heterogeneity of infiltrating lymphocyte burden in leiomyosarcoma. *Sci. Rep.* **9**, 14602 (2019).

318. Schindelin, J. *et al.* Fiji: an open-source platform for biological-image analysis. *Nat. Methods* **9**, 676–682 (2012).

319. Bankhead, P. *et al.* QuPath: Open source software for digital pathology image analysis. *Sci. Rep.* **7**, 1–7 (2017).

320. Schindelin, J. *et al.* Fiji: an open-source platform for biological-image analysis. *Nat. Methods* **9**, 676–682 (2012).

321. Bland, J. M. & Altman, D. G. Measuring agreement in method comparison studies. *Stat. Methods Med. Res.* **8**, 135–160 (1999).

322. Bland, J. M. & Altman, D. G. Survival probabilities (the Kaplan-Meier method). *BMJ (Clinical research ed.)* **317**, 1572 (1998).

323. Bland, J. M. & Altman, D. G. The logrank test. *BMJ* **328**, 1073 (2004).

324. Cox, D. R. Regression Models and Life-Tables. *J. R. Stat. Soc. Ser. B* **34**, 187–202 (1972).

325. Waggott, D. *et al.* NanoStringNorm: An extensible R package for the pre-processing of nanostring mRNA and miRNA data. *Bioinformatics* **28**, 1546–

1548 (2012).

326. Jollife, I. T. & Cadima, J. Principal component analysis: A review and recent developments. *Philosophical Transactions of the Royal Society A: Mathematical, Physical and Engineering Sciences* **374**, (2016).

327. Blighe K & A, L. GitHub - kevinblighe/PCAtools: PCAtools: everything Principal Components Analysis. *R package version 2.0.0* (2020). Available at: https://github.com/kevinblighe/PCAtools. (Accessed: 6th December 2021)

328. Horn, J. L. A rationale and test for the number of factors in factor analysis. *Psychometrika* **30**, 179–185 (1965).

329. Thorndike, R. L. Who belongs in the family? *Psychometrika* **18**, 267–276 (1953).

330. Gu, Z., Eils, R. & Schlesner, M. Complex heatmaps reveal patterns and correlations in multidimensional genomic data. *Bioinformatics* **32**, 2847–2849 (2016).

331. CRAN - Package samr. Available at: https://cran.r-project.org/web/packages/samr/index.html.

332. Javanmard, A. & Montanari, A. Online rules for control of false discvoery rate and False Discovery Exceedance. *Ann. Stat.* **46**, 526–554 (2018).

333. Subramanian, A. *et al.* Gene set enrichment analysis: A knowledge-based approach for interpreting genome-wide expression profiles. *Proc. Natl. Acad. Sci. U. S. A.* **102**, 15545–15550 (2005).

334. Buus, R. *et al.* Development and validation for research assessment of Oncotype DX® Breast Recurrence Score, EndoPredict® and Prosigna®. *npj Breast Cancer* **7**, (2021).

335. Lee, A. T. J. *et al.* The adequacy of tissue microarrays in the assessment of inter- and intra-tumoural heterogeneity of infiltrating lymphocyte burden

in leiomyosarcoma. *Sci. Rep.* **9**, 1–12 (2019).

336. Eisenhauer, E. A. *et al.* New response evaluation criteria in solid tumours: Revised RECIST guideline (version 1.1). *Eur. J. Cancer* **45**, 228–247

337. Yoshida, N. *et al.* A High RORγT/CD3 Ratio is a Strong Prognostic Factor for Postoperative Survival in Advanced Colorectal Cancer: Analysis of Helper T Cell Lymphocytes (Th1, Th2, Th17 and Regulatory T Cells). *Ann. Surg. Oncol.* **23**, 919–927 (2016).

338. Miksch, R. C. *et al.* Development of a reliable and accurate algorithm to quantify the tumor immune stroma (QTiS) across tumor types. *Oncotarget* **8**, 114935–114944 (2017).

339. Berben, L. *et al.* Computerised scoring protocol for identification and quantification of different immune cell populations in breast tumour regions by the use of QuPath software. *Histopathology* **77**, 79–91 (2020).

340. Loughrey, M. B. *et al.* Validation of the systematic scoring of immunohistochemically stained tumour tissue microarrays using QuPath digital image analysis. *Histopathology* **73**, 327–338 (2018).

341. Watson, P. F. & Petrie, A. Method agreement analysis: A review of correct methodology. *Theriogenology* **73**, 1167–1179 (2010).

342. Stefanovski, P. D. *et al.* Prognostic factors in soft tissue sarcomas: a study of 395 patients. *Eur. J. Surg. Oncol.* **28**, 153–164 (2002).

343. Penel, N. *et al.* Performance status is the most powerful risk factor for early death among patients with advanced soft tissue sarcomaThe European Organisation for Research and Treatment of Cancer- Soft Tissue and Bone Sarcoma Group (STBSG) and French Sarcoma Group (FSG) s. *Br. J. Cancer* **104**, 1544–1550 (2011).

344. Boxberg, M. *et al.* PD-L1 and PD-1 and characterization of tumor-infiltrating lymphocytes in high grade sarcomas of soft tissue–prognostic implications and rationale for immunotherapy. *Oncoimmunology* **7**, (2018).

345. Schroeder, B. A. *et al.* CD4+ T cell and M2 macrophage infiltration predict dedifferentiated liposarcoma patient outcomes. *J. Immunother. Cancer* **9**, (2021).

346. Aoki, T. *et al.* Single-Cell Transcriptome Analysis Reveals Disease-Defining T-cell Subsets in the Tumor Microenvironment of Classic Hodgkin Lymphoma. *Cancer Discov.* **10**, 406–421 (2020).

347. Kawai, O. *et al.* Predominant infiltration of macrophages and CD8 $^{+}$ T Cells in cancer nests is a significant predictor of survival in stage IV nonsmall cell lung cancer. *Cancer* **113**, 1387–1395 (2008).

348. Goytain, A. & Ng, T. NanoString nCounter Technology: High-Throughput RNA Validation. in *Methods in Molecular Biology* **2079**, 125–139 (Humana, New York, NY, 2020).

349. David, L. E., Fowler, C. B., Cunningham, B. R., Mason, J. T. & O'Leary, T. J. The effect of formaldehyde fixation on RNA: Optimization of formaldehyde adduct removal. *J. Mol. Diagnostics* **13**, 282–288 (2011).

350. Veldman-Jones, M. H. *et al.* Evaluating robustness and sensitivity of the nanostring technologies ncounter platform to enable multiplexed gene expression analysis of clinical samples. *Cancer Res.* **75**, 2587–2593 (2015).

351. Scott, D. W. *et al.* Gene expression-based model using formalin-fixed paraffin-embedded biopsies predicts overall survival in advanced-stage classical hodgkin lymphoma. *J. Clin. Oncol.* **31**, 692–700 (2013).

352. Saba, N. F. *et al.* Mutation and Transcriptional Profiling of Formalin-Fixed Paraffin Embedded Specimens as Companion Methods to Immunohistochemistry for Determining Therapeutic Targets in Oropharyngeal Squamous Cell Carcinoma (OPSCC): A Pilot of Proof of Principle. *Head Neck Pathol.* **9**, 223–235 (2015).

353. Talla, S. B. *et al.* Immuno-oncology gene expression profiling of formalin-

fixed and paraffin-embedded clear cell renal cell carcinoma: Performance comparison of the NanoString nCounter technology with targeted RNA sequencing. *Genes Chromosom. Cancer* **59**, 406–416 (2020).

354. Cesano, A. nCounter® PanCancer Immune Profiling Panel (NanoString Technologies, Inc., Seattle, WA). *J. Immunother. Cancer* **3**, 1–3 (2015).

355. Jollife, I. T. & Cadima, J. Principal component analysis: A review and recent developments. *Philosophical Transactions of the Royal Society A: Mathematical, Physical and Engineering Sciences* **374**, (2016).

356. Li, Z. *et al.* CD83: Activation marker for antigen presenting cells and its therapeutic potential. *Frontiers in Immunology* **10**, (2019).

357. Chu, P. G. & Arber, D. A. CD79: A Review. *Appl. Immunohistochem. Mol. Morphol.* **9**, 97–106 (2001).

358. Chistiakov, D. A., Killingsworth, M. C., Myasoedova, V. A., Orekhov, A. N. & Bobryshev, Y. V. CD68/macrosialin: Not just a histochemical marker. *Lab. Investig.* **97**, 4–13 (2017).

359. Feuerer, M., Hill, J. A., Mathis, D. & Benoist, C. Foxp3+ regulatory T cells: Differentiation, specification, subphenotypes. *Nature Immunology* **10**, 689–695 (2009).

360. Cai, G. *et al.* CD160 inhibits activation of human CD4+ T cells through interaction with herpesvirus entry mediator. *Nat. Immunol.* **9**, 176–185 (2008).

361. Fabriek, B. O. *et al.* The macrophage scavenger receptor CD163 functions as an innate immune sensor for bacteria. *Blood* **113**, 887–892 (2009).

362. Xia, F. *et al.* TCR and CD28 Concomitant Stimulation Elicits a Distinctive Calcium Response in Naive T Cells. *Front. Immunol.* **9**, 428198 (2018).

363. Yeung, L. *et al.* Leukocyte Tetraspanin CD53 Restrains α3 Integrin Mobilization and Facilitates Cytoskeletal Remodeling and Transmigration

in Mice. *J. Immunol.* **205**, 521–532 (2020).

364. Georgiev, H., Ravens, I., Papadogianni, G. & Bernhardt, G. Coming of age: CD96 emerges as modulator of immune responses. *Frontiers in Immunology* **9**, 369169 (2018).

365. Jacobs, R. *et al.* CD56bright cells differ in their KIR repertoire and cytotoxic features from CD56dim NK cells. *Eur. J. Immunol.* **31**, 3121–3126 (2001).

366. Laplante, P. *et al.* MFG-E8 Reprogramming of Macrophages Promotes Wound Healing by Increased bFGF Production and Fibroblast Functions. *J. Invest. Dermatol.* **137**, 2005–2013 (2017).

367. Fan, T. *et al.* CDH1 overexpression predicts bladder cancer from early stage and inversely correlates with immune infiltration. *BMC Urol.* **22**, 1–18 (2022).

368. Abdelatty, A. *et al.* Pan-Cancer Study on Protein Kinase C Family as a Potential Biomarker for the Tumors Immune Landscape and the Response to Immunotherapy. *Front. Cell Dev. Biol.* **9**, (2022).

369. Chen, D. *et al.* Pan-cancer analysis of the prognostic and immunological role of PSMB8. *Sci. Rep.* **11**, 1–19 (2021).

370. Kalaora, S. *et al.* Immunoproteasome expression is associated with better prognosis and response to checkpoint therapies in melanoma. *Nat. Commun.* **11**, 1–12 (2020).

371. Wu, H. *et al.* An Integrative Pan-Cancer Analysis of Kinesin Family Member C1 (KIFC1) in Human Tumors. *Biomedicines* **10**, 755911 (2022).

372. De Andrade, L. F. *et al.* Inhibition of MICA and MICB shedding elicits NK-cell-mediated immunity against tumors resistant to cytotoxic T cells. *Cancer Immunol. Res.* **8**, 769–780 (2020).

373. Li, L. *et al.* Integrative Pan-Cancer Analysis Confirmed that FCGR3A is a Candidate Biomarker Associated With Tumor Immunity. *Front. Pharmacol.*

13, 900699 (2022).

374. Zhao, B. *et al.* Aging microenvironment and antitumor immunity for geriatric oncology: the landscape and future implications. *J. Hematol. Oncol. 2023 161* **16**, 1–34 (2023).

375. Zhou, Z., Wei, J. H. & Jiang, W. Characterization of aging tumor microenvironment with drawing implications in predicting the prognosis and immunotherapy response in low-grade gliomas. *Sci. Reports 2022 121* **12**, 1–16 (2022).

376. Erbe, R. *et al.* Aging interacts with tumor biology to produce major changes in the immune tumor microenvironment. *bioRxiv* 2020.06.08.140764 (2020). doi:10.1101/2020.06.08.140764

377. Erbe, R. *et al.* Evaluating the impact of age on immune checkpoint therapy biomarkers. *Cell Rep.* **36**, 109599 (2021).

378. Xu, M. *et al.* Immune and Stroma Related Genes in Breast Cancer: A Comprehensive Analysis of Tumor Microenvironment Based on the Cancer Genome Atlas (TCGA) Database. *Front. Med.* **7**, 490729 (2020).

379. Curran, T. *et al.* Differential immune signatures in the tumor microenvironment are associated with colon cancer racial disparities. *Cancer Med.* **10**, 1805–1814 (2021).

380. Wu, Y. *et al.* Immune and stromal related genes in colon cancer: Analysis of tumour microenvironment based on the cancer genome atlas (TCGA) and gene expression omnibus (GEO) databases. *Scand. J. Immunol.* **95**, e13119 (2022).

381. Grabowski, M. M. *et al.* Immune suppression in gliomas. *Journal of Neuro-Oncology* **151**, 3–12 (2021).

382. Geissler, K. *et al.* Immune signature of tumor infiltrating immune cells in renal cancer. *Oncoimmunology* **4**, 985082 (2015).

383. Gonzalez, V. D. *et al.* High-grade serous ovarian tumor cells modulate NK cell function to create an immune-tolerant microenvironment. *Cell Rep.* **36**, 109632 (2021).

384. Hendry, S. *et al.* Assessing Tumor-Infiltrating Lymphocytes in Solid Tumors. *Adv. Anat. Pathol.* **24**, 311–335 (2017).

385. Hoekstra, M. E., Vijver, S. V. & Schumacher, T. N. Modulation of the tumor micro-environment by CD8+ T cell-derived cytokines. *Curr. Opin. Immunol.* **69**, 65 (2021).

386. Laumont, C. M., Banville, A. C., Gilardi, M., Hollern, D. P. & Nelson, B. H. Tumour-infiltrating B cells: immunological mechanisms, clinical impact and therapeutic opportunities. *Nat. Rev. Cancer 2022 227* **22**, 414–430 (2022).

387. Poli, A. *et al.* CD56bright natural killer (NK) cells: An important NK cell subset. *Immunology* **126**, 458–465 (2009).

388. Toulmonde, M. *et al.* High throughput profiling of undifferentiated pleomorphic sarcomas identifies two main subgroups with distinct immune profile, clinical outcome and sensitivity to targeted therapies. *EBioMedicine* **62**, 103131 (2020).

389. Zhu, M. M. T., Shenasa, E. & Nielsen, T. O. Sarcomas: Immune biomarker expression and checkpoint inhibitor trials. *Cancer Treat. Rev.* **91**, 102115 (2020).

390. Weng, W. *et al.* The immune subtypes and landscape of sarcomas. *BMC Immunol.* **23**, 1–19 (2022).

391. Wu, C. *et al.* Identification of Tumor Antigens and Immune Subtypes for the Development of mRNA Vaccines and Individualized Immunotherapy in Soft Tissue Sarcoma. *Cancers (Basel).* **14**, 448 (2022).

392. De Paoli-Iseppi, R. *et al.* Comparison of whole-exome sequencing of matched fresh and formalin fixed paraffin embedded melanoma tumours: Implications for clinical decision making. *Pathology* **48**, 261–266 (2016).

393. Fujii, T. *et al.* Evaluation of DNA and RNA quality from archival formalin-fixed paraffin-embedded tissue for next-generation sequencing – Retrospective study in Japanese single institution. *Pathol. Int.* **70**, 602–611 (2020).

394. Vilimas, T. Measuring Tumor Mutational Burden Using Whole-Exome Sequencing. *Methods Mol. Biol.* **2055**, 63–91 (2020).

395. Roudko, V., Greenbaum, B. & Bhardwaj, N. Computational Prediction and Validation of Tumor-Associated Neoantigens. *Front. Immunol.* **11**, 493366 (2020).

396. Zhigalova, E. A. *et al.* RNA-Seq-Based TCR Profiling Reveals Persistently Increased Intratumoral Clonality in Responders to Anti-PD-1 Therapy. *Front. Oncol.* **10**, 385 (2020).

397. Karasaki, T. *et al.* Prediction and prioritization of neoantigens: integration of RNA sequencing data with whole-exome sequencing. *Cancer Sci.* **108**, 170 (2017).

398. Yu, C. & Zhang, Y. Development and validation of a prognostic nomogram for early-onset colon cancer. *Biosci. Rep.* **39**, 346 (2019).

399. Tu, Q. H. *et al.* Development and Validation of Novel Nomograms for Predicting Specific Distant Metastatic Sites and Overall Survival of Patients With Soft Tissue Sarcoma. *Technol. Cancer Res. Treat.* **20**, (2021).

400. Al-Tashi, Q. *et al.* Machine Learning Models for the Identification of Prognostic and Predictive Cancer Biomarkers: A Systematic Review. *Int. J. Mol. Sci.* **24**, 7781 (2023).

401. Arora, C., Kaur, D., Naorem, L. D. & Raghava, G. P. S. Prognostic biomarkers for predicting papillary thyroid carcinoma patients at high risk using nine genes of apoptotic pathway. *PLoS One* **16**, e0259534 (2021).

402. Cheong, J. H. *et al.* Development and validation of a prognostic and predictive 32-gene signature for gastric cancer. *Nat. Commun.* **13**, 1–9

(2022).

403. Bychkov, D. *et al.* Outcome and biomarker supervised deep learning for survival prediction in two multicenter breast cancer series. *J. Pathol. Inform.* **13**, 9 (2022).

404. Robbe, P. *et al.* Clinical whole-genome sequencing from routine formalin-fixed, paraffin-embedded specimens: pilot study for the 100,000 Genomes Project. *Genet. Med.* **20**, 1196–1205 (2018).

405. Esteve-Codina, A. *et al.* A Comparison of RNA-Seq Results from Paired Formalin-Fixed Paraffin-Embedded and Fresh-Frozen Glioblastoma Tissue Samples. *PLoS One* **12**, e0170632 (2017).

406. Burgess, M. A. *et al.* Clinical activity of pembrolizumab (P) in undifferentiated pleomorphic sarcoma (UPS) and dedifferentiated/pleomorphic liposarcoma (LPS): Final results of SARC028 expansion cohorts. *J. Clin. Oncol.* **37**, 11015–11015 (2019).

407. Ben-Ami, E. *et al.* Immunotherapy with single agent nivolumab for advanced leiomyosarcoma of the uterus: Results of a phase 2 study. *Cancer* **123**, 3285–3290 (2017).

408. Davis, K. L. *et al.* ADVL1412: Initial results of a phase I/II study of nivolumab and ipilimumab in pediatric patients with relapsed/refractory solid tumors—A COG study. *J. Clin. Oncol.* **35**, 10526–10526 (2017).

409. Wilky, B. A. *et al.* A phase II trial of axitinib plus pembrolizumab for patients with advanced alveolar soft part sarcoma (ASPS) and other soft tissue sarcomas (STS). *J. Clin. Oncol.* **36**, 11547–11547 (2018).

410. Pollack, S. M. *et al.* Assessment of Doxorubicin and Pembrolizumab in Patients with Advanced Anthracycline-Naive Sarcoma: A Phase 1/2 Nonrandomized Clinical Trial. in *JAMA Oncology* **6**, 1778–1782 (American Medical Association, 2020).

411. Toulmonde, M. *et al.* Combination of pembrolizumab and metronomic

cyclophosphamide in patients with advanced sarcomas and GIST: A French Sarcoma Group phase II trial. *J. Clin. Oncol.* **35**, 11053–11053 (2017).

412. D'Angelo, S. P. *et al.* Nivolumab with or without ipilimumab treatment for metastatic sarcoma (Alliance A091401): two open-label, non-comparative, randomised, phase 2 trials. *Lancet Oncol.* **19**, 416–426 (2018).

413. Hong, D. S. *et al.* Phase I/II study of LAG525 ± spartalizumab (PDR001) in patients (pts) with advanced malignancies. *J. Clin. Oncol.* **36**, 3012–3012 (2018).

414. Piha-Paul, S. A. *et al.* A phase 2, open-label study of the combination of spartalizumab (PDR001) and LAG525 for patients with advanced solid tumors and hematologic malignancies. *J. Clin. Oncol.* **36**, TPS2616–TPS2616 (2018).

415. Papadopoulos, K. P. *et al.* First-in-human study of REGN3767 (R3767), a human LAG-3 monoclonal antibody (mAb), ± cemiplimab in patients (pts) with advanced malignancies. *J. Clin. Oncol.* **37**, 2508–2508 (2019).

416. Luke, J. J. *et al.* A phase I, first-in-human, open-label, dose-escalation study of MGD013, a bispecific DART molecule binding PD-1 and LAG-3, in patients with unresectable or metastatic neoplasms. *J. Clin. Oncol.* **38**, 3004–3004 (2020).

417. Du, W. *et al.* Tim-3 as a target for cancer immunotherapy and mechanisms of action. *International Journal of Molecular Sciences* **18**, (2017).

418. Curigliano, G. *et al.* Abstract CT183: Phase (Ph) I/II study of MBG453± spartalizumab (PDR001) in patients (pts) with advanced malignancies. in *Cancer Research* **79**, CT183–CT183 (American Association for Cancer Research, 2019).

1. W.H.O. Soft tissue and bone tumours in adults. in *Practical Clinical Oncology* 335–346 (2008). doi:10.1017/CBO9780511545375.031

2. Cancer Research UK. Soft tissue sarcoma incidence statistics. Available at: https://www.cancerresearchuk.org/health-professional/cancer-statistics/statistics-by-cancer-type/soft-tissue-sarcoma/incidence#heading-Four. (Accessed: 7th September 2018)

3. Gatta, G. *et al.* Rare cancers are not so rare: The rare cancer burden in Europe. *Eur. J. Cancer* **47**, 2493–2511 (2011).

4. Parikh, R. C. *et al.* Treatment patterns and survival among older adults in the United States with advanced soft-tissue sarcomas. *Clin. Sarcoma Res.* **8**, 8 (2018).

5. Harris, S. J. *et al.* Metastatic soft tissue sarcoma, an analysis of systemic therapy and impact on survival. *J. Clin. Oncol.* **33**, 10545–10545 (2015).

6. Komatsubara, K. M. & Carvajal, R. D. The promise and challenges of rare cancer research. *Lancet Oncol.* **17**, 136–138 (2016).

7. Blay, J. Y., Coindre, J. M., Ducimetière, F. & Ray-Coquard, I. The value of research collaborations and consortia in rare cancers. *The Lancet Oncology* **17**, e62–e69 (2016).

8. Lee, A. T., Huang, P. H. & Jones, R. L. Negative phase III trials announce the need for biomarkers in sarcoma. *Eur. J. Cancer* **123**, 81–82 (2019).

9. Drilon, A. *et al.* Efficacy of Larotrectinib in *TRK* Fusion–Positive Cancers in Adults and Children. *N. Engl. J. Med.* **378**, 731–739 (2018).

10. Wilding, C. P., Loong, H. H., Huang, P. H. & Jones, R. L. Tropomyosin receptor kinase inhibitors in the management of sarcomas. *Current opinion in oncology* **32**, 307–313 (2020).

11. Kelly, C. M., Gutierrez Sainz, L. & Chi, P. The management of metastatic GIST: current standard and investigational therapeutics. *Journal of Hematology and Oncology* **14**, 1–12 (2021).

12. NICE. Improving outcomes for people with sarcoma | Guidance | NICE.

13. Fujiwara, T. *et al.* Impact of NICE guidelines on the survival of patients with soft-tissue sarcomas. *https://doi.org/10.1302/0301-620X.103B3.BJJ-2020-0743.R1* **103**-**B**, 569–577 (2021).

14. Dangoor, A. *et al.* UK guidelines for the management of soft tissue sarcomas. *Clin. Sarcoma Res.* **6**, 1–26 (2016).

15. Gronchi, A. *et al.* Soft tissue and visceral sarcomas: ESMO-EURACAN-GENTURIS Clinical Practice Guidelines for diagnosis, treatment and follow-up. *Ann. Oncol.* **0**, (2021).

16. Dangoor, A. *et al.* UK guidelines for the management of soft tissue sarcomas. *Clin. Sarcoma Res.* **6**, 20 (2016).

17. Arbiser, Z. K., Folpe, A. L. & Weiss, S. W. Consultative (expert) second opinions in soft tissue pathology: Analysis of problem-prone diagnostic situations. *Am. J. Clin. Pathol.* **116**, 473–476 (2001).

18. Rupani, A., Hallin, M., Jones, R. L., Fisher, C. & Thway, K. Diagnostic Differences in Expert Second-Opinion Consultation Cases at a Tertiary Sarcoma Center. *Sarcoma* **2020**, (2020).

19. Rastogi, S. *et al.* Discordance of histo-pathological diagnosis of patients with soft tissue sarcoma referred to tertiary care center. *J. Clin. Oncol.* **35**, 11064–11064 (2017).

20. Schneider, N. *et al.* The Adequacy of Core Biopsy in the Assessment of Smooth Muscle Neoplasms of Soft Tissues. *Am. J. Surg. Pathol.* **41**, 923–931 (2017).

21. Hornick, J. L. Limited biopsies of soft tissue tumors: the contemporary role of immunohistochemistry and molecular diagnostics. *Modern Pathology* **32**, 27–37 (2019).

22. Sbaraglia, M., Gambarotti, M., Righi, A. & Dei Tos, A. P. Classification of soft tissue lesions and general principles of soft tissue pathology. in *Diagnosis of Musculoskeletal Tumors and Tumor-like Conditions: Clinical,*

Radiological and Histological Correlations - the Rizzoli Case Archive 19–22 (Springer, Cham, 2019). doi:10.1007/978-3-030-29676-6_5

23. Schaefer, I. M. & Hornick, J. L. Diagnostic Immunohistochemistry for Soft Tissue and Bone Tumors: An Update. *Adv. Anat. Pathol.* **25**, 400–412 (2018).

24. Schaefer, I. M., Cote, G. M. & Hornick, J. L. Contemporary sarcoma diagnosis, genetics, and genomics. *Journal of Clinical Oncology* **36**, 101–110 (2018).

25. Mariño-Enríquez, A. & Bovée, J. V. M. G. Molecular Pathogenesis and Diagnostic, Prognostic and Predictive Molecular Markers in Sarcoma. *Surgical Pathology Clinics* **9**, 457–473 (2016).

26. Miura, K. *et al.* Usefulness of SS18-SSX antibody as a diagnostic marker for pulmonary metastatic synovial sarcoma. *Diagn. Pathol.* **16**, 1–8 (2021).

27. Reeser, J. W. *et al.* Validation of a Targeted RNA Sequencing Assay for Kinase Fusion Detection in Solid Tumors. *J. Mol. Diagnostics* **19**, 682–696 (2017).

28. Beadling, C. *et al.* A Multiplexed Amplicon Approach for Detecting Gene Fusions by Next-Generation Sequencing. *J. Mol. Diagnostics* **18**, 165–175 (2016).

29. Guillou, L. *et al.* Comparative study of the National Cancer Institute and French Federation of Cancer Centers Sarcoma Group grading systems in a population of 410 adult patients with soft tissue sarcoma. *J. Clin. Oncol.* **15**, 350–362 (1997).

30. AJCC. AJCC Cancer Staging Manual 8th Edition. in *Definitions* 489–539 (2020). doi:10.32388/b30ldk

31. Tanaka, K. & Ozaki, T. New TNM classification (AJCC eighth edition) of bone and soft tissue sarcomas: JCOG Bone and Soft Tissue Tumor Study Group. *Japanese Journal of Clinical Oncology* **49**, 103–107 (2019).

32. Cates, J. M. M. The AJCC 8th edition staging system for soft tissue sarcoma of the extremities or trunk: A Cohort study of the SEER database. *JNCCN J. Natl. Compr. Cancer Netw.* **16**, 144–152 (2018).

33. Bilgeri, A. *et al.* The effect of resection margin on local recurrence and survival in high grade soft tissue sarcoma of the extremities: How far is far enough? *Cancers (Basel).* **12**, 1–13 (2020).

34. Kainhofer, V. *et al.* The width of resection margins influences local recurrence in soft tissue sarcoma patients. *Eur. J. Surg. Oncol.* **42**, 899–906 (2016).

35. Potter, B. K. *et al.* Impact of margin status and local recurrence on soft-tissue sarcoma outcomes. *J. Bone Jt. Surg. - Ser. A* **95**, (2013).

36. Fujiwara, T. *et al.* What is an adequate margin for infiltrative soft-tissue sarcomas? *Eur. J. Surg. Oncol.* **46**, 277–281 (2020).

37. van Schaik, L., Geertzen, J. H. B., Dijkstra, P. U. & Dekker, R. Metabolic costs of activities of daily living in persons with a lower limb amputation: A systematic review and meta-analysis. *PLoS ONE* **14**, e0213256 (2019).

38. Erstad, D. J. *et al.* Amputation for Extremity Sarcoma: Contemporary Indications and Outcomes. *Ann. Surg. Oncol.* **25**, 394–403 (2018).

39. Smith, H. G., Thomas, J. M., Smith, M. J. F., Hayes, A. J. & Strauss, D. C. Major Amputations for Extremity Soft-Tissue Sarcoma. *Ann. Surg. Oncol.* **25**, 387–393 (2018).

40. Hoftiezer, Y. A. J. *et al.* Long-term patient-reported outcome measures following limb salvage with complex reconstruction or amputation in the treatment of upper extremity sarcoma. *J. Surg. Oncol.* **123**, 1328–1335 (2021).

41. Perhavec, A. *et al.* Inoperable Primary Retroperitoneal Sarcomas: Clinical Characteristics and Reasons Against Resection at a Single Referral Institution. *Ann. Surg. Oncol.* **28**, 1151–1157 (2021).

42. Younger, E. *et al.* Health-related quality Of Life In patients with advanced Soft TIssue sarcomas treated with Chemotherapy (The HOLISTIC study): protocol for an international observational cohort study. *BMJ Open* **10**, e035171 (2020).

43. Tan, C. *et al.* Adriamycin-an antitumor antibiotic in the treatment of neoplastic diseases. *Cancer* **32**, 9–17 (1973).

44. Tap, W. D. *et al.* Effect of Doxorubicin Plus Olaratumab vs Doxorubicin Plus Placebo on Survival in Patients with Advanced Soft Tissue Sarcomas: The ANNOUNCE Randomized Clinical Trial. in *JAMA - Journal of the American Medical Association* **323**, 1266–1276 (American Medical Association, 2020).

45. Tap, W. D. *et al.* Olaratumab and doxorubicin versus doxorubicin alone for treatment of soft-tissue sarcoma: an open-label phase 1b and randomised phase 2 trial. *Lancet* **388**, 488–497 (2016).

46. Maurel, J. *et al.* Efficacy of sequential high-dose doxorubicin and ifosfamide compared with standard-dose doxorubicin in patients with advanced soft tissue sarcoma: An open-label randomized phase II study of the Spanish group for research on sarcomas. *J. Clin. Oncol.* **27**, 1893–1898 (2009).

47. Lorigan, P. *et al.* Phase III trial of two investigational schedules of ifosfamide compared with standard-dose doxorubicin in advanced or metastatic soft tissue sarcoma: A European Organisation for Research and Treatment of Cancer Soft Tissue and Bone Sarcoma Group study. *J. Clin. Oncol.* **25**, 3144–3150 (2007).

48. Judson, I. *et al.* Doxorubicin alone versus intensified doxorubicin plus ifosfamide for first-line treatment of advanced or metastatic soft-tissue sarcoma: A randomised controlled phase 3 trial. *Lancet Oncol.* **15**, 415–423 (2014).

49. Seddon, B. *et al.* A phase II trial to assess the activity of gemcitabine and docetaxel as first line chemotherapy treatment in patients with unresectable

leiomyosarcoma. *Clin. Sarcoma Res.* **5**, 1–7 (2015).

50. Seddon, B. *et al.* Gemcitabine and docetaxel versus doxorubicin as first-line treatment in previously untreated advanced unresectable or metastatic soft-tissue sarcomas (GeDDiS): a randomised controlled phase 3 trial. *Lancet Oncol.* **18**, 1397–1410 (2017).

51. Martin-Broto, J. *et al.* Randomized phase II study of trabectedin and doxorubicin compared with doxorubicin alone as first-line treatment in patients with advanced soft tissue sarcomas: A Spanish group for research on sarcoma study. *J. Clin. Oncol.* **34**, 2294–2302 (2016).

52. Bui-Nguyen, B. *et al.* A phase IIb multicentre study comparing the efficacy of trabectedin to doxorubicin in patients with advanced or metastatic untreated soft tissue sarcoma: The TRUSTS trial. *Eur. J. Cancer* **51**, 1312–1320 (2015).

53. Blay, J. Y. *et al.* Randomised phase III trial of trabectedin versus doxorubicin-based chemotherapy as first-line therapy in translocation-related sarcomas. *Eur. J. Cancer* **50**, 1137–1147 (2014).

54. Linch, M., Miah, A. B., Thway, K., Judson, I. R. & Benson, C. Systemic treatment of soft-tissue sarcoma—gold standard and novel therapies. **11**, 187–202 (2014).

55. Nielsen, O. S. *et al.* Effect of high-dose ifosfamide in advanced soft tissue sarcomas. A multicentre phase II study of the EORTC Soft Tissue and Bone Sarcoma Group. *Eur. J. Cancer* **36**, 61–67 (2000).

56. Lee, S. H. *et al.* High-dose ifosfamide as second-or third-line chemotherapy in refractory bone and soft tissue sarcoma patients. *Oncology* **80**, 257–261 (2011).

57. Martin-Liberal, J. *et al.* Clinical activity and tolerability of a 14-day infusional ifosfamide schedule in soft-tissue sarcoma. *Sarcoma* **2013**, (2013).

58. Okuno, S. *et al.* Phase II trial of gemcitabine in advanced sarcomas. *Cancer*

94, 3225–3229 (2002).

59. Švancárová, L. *et al.* Gemcitabine in advanced adult soft-tissue sarcomas. A phase II study of the EORTC Soft Tissue and Bone Sarcoma Group. *Eur. J. Cancer* **38**, 556–559 (2002).

60. Hensley, M. L. *et al.* Gemcitabine and docetaxel in patients with unresectable leiomyosarcoma: Results of a phase II trial. *J. Clin. Oncol.* **20**, 2824–2831 (2002).

61. Maki, R. G. *et al.* Randomized phase II study of gemcitabine and docetaxel compared with gemcitabine alone in patients with metastatic soft tissue sarcomas. *J. Clin. Oncol.* **25**, 2755–2763 (2007).

62. Pautier, P. *et al.* Randomized Multicenter and Stratified Phase II Study of Gemcitabine Alone Versus Gemcitabine and Docetaxel in Patients with Metastatic or Relapsed Leiomyosarcomas: A Fédération Nationale des Centres de Lutte Contre le Cancer (FNCLCC) French Sarcoma Group . *Oncologist* **17**, 1213–1220 (2012).

63. Losa, R. *et al.* Phase II study with the combination of gemcitabine and DTIC in patients with advanced soft tissue sarcomas. *Cancer Chemother. Pharmacol.* **59**, 251–259 (2007).

64. García-del-Muro, X. *et al.* Randomized phase II study comparing gemcitabine plus dacarbazine versus dacarbazine alone in patients with previously treated soft tissue sarcoma: A Spanish group for research on sarcomas study. *J. Clin. Oncol.* **29**, 2528–2533 (2011).

65. Takahashi, M. *et al.* Efficacy of Trabectedin in Patients with Advanced Translocation-Related Sarcomas: Pooled Analysis of Two Phase II Studies. *Oncologist* **22**, 979–988 (2017).

66. Penel, N. *et al.* Phase II trial of weekly paclitaxel for unresectable angiosarcoma: The ANGIOTAX study. *J. Clin. Oncol.* **26**, 5269–5274 (2008).

67. Schöffski, P. *et al.* Eribulin versus dacarbazine in previously treated patients with advanced liposarcoma or leiomyosarcoma: A randomised, open-label, multicentre, phase 3 trial. in *The Lancet* **387**, 1629–1637 (Elsevier, 2016).

68. OS, N. *et al.* Effect of high-dose ifosfamide in advanced soft tissue sarcomas. A multicentre phase II study of the EORTC Soft Tissue and Bone Sarcoma Group. *Eur. J. Cancer* **36**, 61–67 (2000).

69. Samuels, B. L. *et al.* Clinical outcomes and safety with trabectedin therapy in patients with advanced soft tissue sarcomas following failure of prior chemotherapy: Results of a worldwide expanded access program study. *Ann. Oncol.* **24**, 1703–1709 (2013).

70. Demetri, G. D. *et al.* Efficacy and safety of trabectedin or dacarbazine for metastatic liposarcoma or leiomyosarcoma after failure of conventional chemotherapy: Results of a phase III randomized multicenter clinical trial. *J. Clin. Oncol.* **34**, 786–793 (2016).

71. Register, E. clinical trials. A Randomized & Observational phase II trial assessing the activity of TrabectedIn vs gemCitabine in patients with metastatic or locally advanced LEiomyosarcoma pretreated with conventional chemotherapy. *EU clinical trials register* **34**, 201–203 (2007).

72. ClinicalTrials.gov. Study on Trabectedin in Advanced Rearranged Mesenchymal Chondrosarcoma. *ClinicalTrials.gov* Available at: https://clinicaltrials.gov/ct2/show/NCT04305548. (Accessed: 8th September 2021)

73. Chellappan, D. K. *et al.* The role of pazopanib on tumour angiogenesis and in the management of cancers: A review. *Biomedicine and Pharmacotherapy* **96**, 768–781 (2017).

74. Hanahan, D. & Weinberg, R. A. Hallmarks of Cancer: The Next Generation. *Cell* **144**, 646–674 (2011).

75. Wu, P., Nielsen, T. E. & Clausen, M. H. FDA-approved small-molecule kinase inhibitors. *Trends in Pharmacological Sciences* **36**, 422–439 (2015).

76. Gotink, K. J. & Verheul, H. M. W. Anti-angiogenic tyrosine kinase inhibitors: What is their mechanism of action? *Angiogenesis* **13**, 1–14 (2010).

77. Du, Z. & Lovly, C. M. Mechanisms of receptor tyrosine kinase activation in cancer. *Molecular Cancer* **17**, 1–13 (2018).

78. Lemmon, M. A. & Schlessinger, J. Cell signaling by receptor tyrosine kinases. *Cell* **141**, 1117–1134 (2010).

79. Wu, C. E., Tzen, C. Y., Wang, S. Y. & Yeh, C. N. Clinical diagnosis of gastrointestinal stromal tumor (Gist): From the molecular genetic point of view. *Cancers* **11**, 679 (2019).

80. Yuzawa, S. *et al.* Structural Basis for Activation of the Receptor Tyrosine Kinase KIT by Stem Cell Factor. *Cell* **130**, 323–334 (2007).

81. Asano, N. *et al.* Frequent amplification of receptor tyrosine kinase genes in welldifferentiated/ dedifferentiated liposarcoma. *Oncotarget* **8**, 12941–12952 (2017).

82. Du, Z. *et al.* Structure–function analysis of oncogenic EGFR Kinase Domain Duplication reveals insights into activation and a potential approach for therapeutic targeting. *Nat. Commun.* **12**, 1–15 (2021).

83. Wegert, J. *et al.* Recurrent intragenic rearrangements of EGFR and BRAF in soft tissue tumors of infants. *Nat. Commun.* **9**, 1–6 (2018).

84. Parsons, D. W. *et al.* An integrated genomic analysis of human glioblastoma multiforme. *Science* **321**, 1807–1812 (2008).

85. Horn, L. *et al.* Ensartinib (X-396) in ALK-Positive Non–Small Cell Lung Cancer: Results from a First-in-Human Phase I/II, Multicenter Study. *Clin. Cancer Res.* **24**, 2771–2779 (2018).

86. Nakajima, K. & Raz, A. Autocrine motility factor and its receptor expression in musculoskeletal tumors. *Journal of Bone Oncology* **24**, 100318 (2020).

87. Hanahan, D. & Weinberg, R. A. The hallmarks of cancer. *Cell* **100**, 57–70 (2000).

88. Kumar, R. *et al.* Pharmacokinetic-pharmacodynamic correlation from mouse to human with pazopanib, a multikinase angiogenesis inhibitor with potent antitumor and antiangiogenic activity. *Mol. Cancer Ther.* **6**, 2012–2021 (2007).

89. Shibuya, M. Vascular Endothelial Growth Factor (VEGF) and Its Receptor (VEGFR) Signaling in Angiogenesis: A Crucial Target for Anti- and Pro-Angiogenic Therapies. *Genes and Cancer* **2**, 1097–1105 (2011).

90. Yoon, S. S. *et al.* Angiogenic Profile of Soft Tissue Sarcomas Based on Analysis of Circulating Factors and Microarray Gene Expression. *J. Surg. Res.* **135**, 282–290 (2006).

91. Hayes, A. J. *et al.* Serum vascular endothelial growth factor as a tumour marker in soft tissue sarcoma. *Br. J. Surg.* **91**, 242–247 (2004).

92. Kilvaer, T. K. *et al.* The VEGF- and PDGF-family of angiogenic markers have prognostic impact in soft tissue sarcomas arising in the extremities and trunk. *BMC Clin. Pathol.* **14**, (2014).

93. Kilvaer, T. K. *et al.* Platelet-derived growth factors in non-GIST soft-tissue sarcomas identify a subgroup of patients with wide resection margins and poor disease-specific survival. *Sarcoma* **2010**, (2010).

94. Yudoh, K. *et al.* Concentration of vascular endothelial growth factor in the tumour tissue as a prognostic factor of soft tissue sarcomas. *Br. J. Cancer* **84**, 1610–1615 (2001).

95. Andrae, J., Gallini, R. & Betsholtz, C. Role of platelet-derived growth factors in physiology and medicine. *Genes and Development* **22**, 1276–1312 (2008).

96. Li, L. *et al.* Platelet-derived growth factor-b (PDGF-B) induced by hypoxia promotes the survival of pulmonary arterial endothelial cells through the PI3K/Akt/stat3 pathway. *Cell. Physiol. Biochem.* **35**, 441–451 (2015).

97. Alvarez, R. H., Kantarjian, H. M. & Cortes, J. E. Biology of platelet-derived growth factor and its involvement in disease. *Mayo Clin. Proc.* **81**, 1241–1257 (2006).

98. Heldin, C. H. & Westermark, B. Mechanism of action and in vivo role of platelet-derived growth factor. *Physiol. Rev.* **79**, 1283–1316 (1999).

99. Raica, M. & Cimpean, A. M. Platelet-derived growth factor (PDGF)/PDGF receptors (PDGFR) axis as target for antitumor and antiangiogenic therapy. *Pharmaceuticals* **3**, 572–599 (2010).

100. Kano, M. R. *et al.* VEGF-A and FGF-2 synergistically promote neoangiogenesis through enhancement of endogenous PDGF-B-PDGFRβ signaling. *J. Cell Sci.* **118**, 3759–3768 (2005).

101. Brahmi, M. *et al.* Expression and prognostic significance of PDGF ligands and receptors across soft tissue sarcomas. *ESMO Open* **6**, (2021).

102. Tammela, T. *et al.* Blocking VEGFR-3 suppresses angiogenic sprouting and vascular network formation. *Nature* **454**, 656–660 (2008).

103. Tomlinson, J. *et al.* Different patterns of angiogenesis in sarcomas and carcinomas. *Clin. Cancer Res.* **5**, 3516–3522 (1999).

104. Hori, Y. *et al.* Functional Characterization of VEGF- And FGF-induced Tumor Blood Vessel Models in Human Cancer Xenografts. *Anticancer Res.* **37**, 6629–6638 (2017).

105. Mossahebi-Mohammadi, M., Quan, M., Zhang, J. S. & Li, X. FGF Signaling Pathway: A Key Regulator of Stem Cell Pluripotency. *Frontiers in Cell and Developmental Biology* **8**, 79 (2020).

106. Oladipupo, S. S. *et al.* Endothelial cell FGF signaling is required for injury

response but not for vascular homeostasis. *Proc. Natl. Acad. Sci. U. S. A.* **111**, 13379–13384 (2014).

107. Zhou, W. Y., Zheng, H., Du, X. L. & Yang, J. L. Characterization of FGFR signaling pathway as therapeutic targets for sarcoma patients. *Cancer Biology and Medicine* **13**, 260–268 (2016).

108. Ishibe, T. *et al.* Disruption of fibroblast growth factor signal pathway inhibits the growth of synovial sarcomas: Potential application of signal inhibitors to molecular target therapy. *Clin. Cancer Res.* **11**, 2702–2712 (2005).

109. Taylor VI, J. G. *et al.* Identification of FGFR4-activating mutations in human rhabdomyosarcomas that promote metastasis in xenotransplanted models. *J. Clin. Invest.* **119**, 3395–3407 (2009).

110. Lemmon, M. A. & Schlessinger, J. Cell signaling by receptor tyrosine kinases. *Cell* **141**, 1117–1134 (2010).

111. Quesada, J. & Amato, R. The Molecular Biology of Soft-Tissue Sarcomas and Current Trends in Therapy. *Sarcoma* **2012**, 849456 (2012).

112. Prior, I. A., Hood, F. E. & Hartley, J. L. The frequency of ras mutations in cancer. *Cancer Res.* **80**, 2669–2974 (2020).

113. Sasaki, K., Hitora, T., Nakamura, O., Kono, R. & Yamamoto, T. The role of MAPK pathway in bone and soft tissue tumors. *Anticancer Res.* **31**, 549–553 (2011).

114. Peng, C. L. *et al.* Sorafenib induces growth inhibition and apoptosis in human synovial sarcoma cells via inhibiting the RAF/MEK/ERK signaling pathway. *Cancer Biol. Ther.* **8**, 1729–1736 (2009).

115. Eger, G., Papadopoulos, N., Lennartsson, J. & Heldin, C. H. NR4A1 promotes PDGF-BB-induced cell colony formation in soft agar. *PLoS One* **9**, e109047 (2014).

116. Todd, J. R., Scurr, L. L., Becker, T. M., Kefford, R. F. & Rizos, H. The MAPK

pathway functions as a redundant survival signal that reinforces the PI3K cascade in c-Kit mutant melanoma. *Oncogene* **33**, 236–245 (2014).

117. Xie, Y. *et al.* FGF/FGFR signaling in health and disease. *Signal Transduction and Targeted Therapy* **5**, 1–38 (2020).

118. Porta, C., Paglino, C. & Mosca, A. Targeting PI3K/Akt/mTOR signaling in cancer. *Front. Oncol.* **4 APR**, 1–11 (2014).

119. Yang, J. *et al.* Targeting PI3K in cancer: Mechanisms and advances in clinical trials. *Mol. Cancer* **18**, 1–28 (2019).

120. Hoxhaj, G. & Manning, B. D. The PI3K–AKT network at the interface of oncogenic signalling and cancer metabolism. *Nature Reviews Cancer* **20**, 74–88 (2020).

121. Murugan, A. K. mTOR: Role in cancer, metastasis and drug resistance. *Seminars in Cancer Biology* **59**, 92–111 (2019).

122. Janku, F., Yap, T. A. & Meric-Bernstam, F. Targeting the PI3K pathway in cancer: Are we making headway? *Nature Reviews Clinical Oncology* **15**, 273–291 (2018).

123. Hernando, E. *et al.* The AKT-mTOR pathway plays a critical role in the development of leiomyosarcomas. *Nat. Med.* **13**, 748–753 (2007).

124. Yoon, C., Lu, J., Ryeom, S. W., Simon, M. C. & Yoon, S. S. PIK3R3, part of the regulatory domain of PI3K, is upregulated in sarcoma stem-like cells and promotes invasion, migration, and chemotherapy resistance. *Cell Death Dis.* **12**, 1–11 (2021).

125. Wan, X. & Helman, L. J. The Biology Behind mTOR Inhibition in Sarcoma. *Oncologist* **12**, 1007–1018 (2007).

126. Hosaka, S. *et al.* A novel multi-kinase inhibitor pazopanib suppresses growth of synovial sarcoma cells through inhibition of the PI3K-AKT pathway. *J. Orthop. Res.* **30**, 1493–1498 (2012).

127. Lanzi, C. *et al.* Overactive IGF1/insulin receptors and NRASQ61R mutation drive mechanisms of resistance to pazopanib and define rational combination strategies to treat synovial sarcoma. *Cancers (Basel).* **11**, (2019).

128. Hurwitz, H. I. *et al.* Phase I trial of pazopanib in patients with advanced cancer. *Clin. Cancer Res.* **15**, 4220–4227 (2009).

129. Bender, J. L. G. *et al.* Phase i pharmacokinetic and pharmacodynamic study of pazopanib in children with soft tissue sarcoma and other refractory solid tumors: A children's oncology group phase i consortium report. in *Journal of Clinical Oncology* **31**, 3034–3043 (American Society of Clinical Oncology, 2013).

130. Sleijfer, S. *et al.* Pazopanib, a Multikinase Angiogenesis Inhibitor, in Patients With Relapsed or Refractory Advanced Soft Tissue Sarcoma: A Phase II Study From the European Organisation for Research and Treatment of Cancer–Soft Tissue and Bone Sarcoma Group (EORTC Study 620. *J. Clin. Oncol.* **27**, 3126–3132 (2009).

131. Van Glabbeke, M., Verweij, J., Judson, I. & Nielsen, O. S. Progression-free rate as the principal end-point for phase II trials in soft-tissue sarcomas. *Eur. J. Cancer* **38**, 543–549 (2002).

132. van der Graaf, W. T. *et al.* Pazopanib for metastatic soft-tissue sarcoma (PALETTE): a randomised, double-blind, placebo-controlled phase 3 trial. *Lancet* **379**, 1879–1886 (2012).

133. NHS England » Cancer Drugs Fund. Available at: https://www.england.nhs.uk/cancer/cdf/. (Accessed: 4th August 2019)

134. Amdahl, J. *et al.* Cost-effectiveness of pazopanib in advanced soft tissue sarcoma in the United kingdom. *Sarcoma* **2014**, 481071 (2014).

135. Kasper, B. *et al.* Long-term responders and survivors on pazopanib for advanced soft tissue sarcomas: subanalysis of two European Organisation

for Research and Treatment of Cancer (EORTC) clinical trials 62043 and 62072. *Ann. Oncol.* **25**, 719–724 (2014).

136. Toulmonde, M. *et al.* Retroperitoneal sarcomas: Patterns of care at diagnosis, prognostic factors and focus on main histological subtypes: A multicenter analysis of the French Sarcoma Group. *Ann. Oncol.* **25**, 735–742 (2014).

137. Benson, C. *et al.* Outcome of uterine sarcoma patients treated with pazopanib: A retrospective analysis based on two European -rganisation for Research and Truatment of Cancer (EORTC) Soft Tissue and Bone Sarcoma Group (STBSG) clinical trials 62043 and 62072. *Gynecol. Oncol.* **142**, 89–94 (2016).

138. Cesne, A. Le *et al.* Safety and efficacy of Pazopanib in advanced soft tissue sarcoma: PALETTE (EORTC 62072) subgroup analyses. *BMC Cancer* **19**, 1–7 (2019).

139. Grünwald, V. *et al.* Randomized Comparison of Pazopanib and Doxorubicin as First-Line Treatment in Patients with Metastatic Soft Tissue Sarcoma Age 60 Years or Older: Results of a German Intergroup Study. in *Journal of Clinical Oncology* **38**, 3555–3564 (American Society of Clinical Oncology, 2020).

140. Urakawa, H. *et al.* Phase II trial of pazopanib in patients with metastatic or unresectable chemoresistant sarcomas: A Japanese Musculoskeletal Oncology Group study. *Cancer Sci.* **111**, 3303–3312 (2020).

141. Kim, M. *et al.* A Phase II Trial of Pazopanib in Patients with Metastatic Alveolar Soft Part Sarcoma. *Oncologist* **24**, 20 (2019).

142. Martin-Broto, J. *et al.* Pazopanib for treatment of typical solitary fibrous tumours: a multicentre, single-arm, phase 2 trial. *Lancet Oncol.* **21**, 456–466 (2020).

143. Martin-Broto, J. *et al.* Pazopanib for treatment of advanced malignant and

dedifferentiated solitary fibrous tumour: a multicentre, single-arm, phase 2 trial. *Lancet Oncol.* **20**, 134–144 (2019).

144. Maruzzo, M. *et al.* Pazopanib as first line treatment for solitary fibrous tumours: the Royal Marsden Hospital experience. *Clin. Sarcoma Res.* **5**, 1–7 (2015).

145. Chow, W. *et al.* Results of a prospective phase 2 study of pazopanib in patients with surgically unresectable or metastatic chondrosarcoma. *Cancer* **126**, 105–111 (2020).

146. Stacchiotti, S. *et al.* Pazopanib for treatment of advanced extraskeletal myxoid chondrosarcoma: a multicentre, single-arm, phase 2 trial. *Lancet Oncol.* **20**, 1252–1262 (2019).

147. Gelderblom, H. *et al.* Treatment patterns and clinical outcomes with pazopanib in patients with advanced soft tissue sarcomas in a compassionate use setting: results of the SPIRE study*. *Acta Oncol. (Madr).* **56**, 1769–1775 (2017).

148. Oh, C. R. *et al.* Real-World Outcomes of Pazopanib Treatment in Korean Patients with Advanced Soft Tissue Sarcoma: A Multicenter Retrospective Cohort Study. *Target. Oncol.* **15**, 485–493 (2020).

149. Alshamsan, B. *et al.* Real-world outcome and prognostic factors of pazopanib in advanced soft tissue sarcoma. *Cancer Manag. Res.* **13**, 6755–6766 (2021).

150. Halim, N. A. *et al.* Safety and efficacy of pazopanib as a second-line treatment and beyond for soft tissue sarcomas: A real-life tertiary-center experience in the MENA region. *Cancer Treat. Res. Commun.* **26**, 100275 (2021).

151. Karaağaç, M. *et al.* The real-life outcome of pazopanib in patients with advanced soft tissue sarcoma: A retrospective cross-sectional study of a Turkish cohort. *J. Oncol. Pharm. Pract.* **26**, 1657–1666 (2020).

152. Seto, T. *et al.* Real-World Experiences with Pazopanib in Patients with Advanced Soft Tissue and Bone Sarcoma in Northern California. **7**, 48 (2019).

153. Nakamura, T. *et al.* The clinical outcome of pazopanib treatment in Japanese patients with relapsed soft tissue sarcoma: A Japanese Musculoskeletal Oncology Group (JMOG) study. *Cancer* **122**, 1408–1416 (2016).

154. Yoo, K. H. *et al.* Efficacy of pazopanib monotherapy in patients who had been heavily pretreated for metastatic soft tissue sarcoma: A retrospective case series. *BMC Cancer* **15**, 1–7 (2015).

155. Frezza, A. M. *et al.* Anthracycline, gemcitabine, and pazopanib in epithelioid sarcoma a multi-institutional case series. *JAMA Oncol.* **4**, (2018).

156. Menegaz, B. A. *et al.* Clinical Activity of Pazopanib in Patients with Advanced Desmoplastic Small Round Cell Tumor. *Oncologist* **23**, 360–366 (2018).

157. Kim, H. J., Kim, Y., Lee, S. J., Lee, J. & Park, S. H. Pazopanib monotherapy in the treatment of pretreated, metastatic uterine sarcoma: A single-center retrospective study. *J. Gynecol. Oncol.* **29**, (2018).

158. Lueza, B. *et al.* Difference in restricted mean survival time for cost-effectiveness analysis using individual patient data meta-analysis: Evidence from a case study. *PLoS One* **11**, e0150032 (2016).

159. Wei, Y., Royston, P., Tierney, J. F. & Parmar, M. K. B. Meta-analysis of time-to-event outcomes from randomized trials using restricted mean survival time: Application to individual participant data. *Stat. Med.* **34**, 2881–2898 (2015).

160. Martin-Broto, J. *et al.* Pazopanib for treatment of advanced malignant and dedifferentiated solitary fibrous tumour: a multicentre, single-arm, phase 2

trial. *Lancet Oncol.* **20**, 134–144 (2019).

161. Kim, M. *et al.* A Phase II Trial of Pazopanib in Patients with Metastatic Alveolar Soft Part Sarcoma. *Oncologist* **24**, 20-e29 (2019).

162. Kollár, A. *et al.* Pazopanib in advanced vascular sarcomas: an EORTC Soft Tissue and Bone Sarcoma Group (STBSG) retrospective analysis. *Acta Oncol. (Madr).* **56**, 88–92 (2017).

163. Frezza, A. M. *et al.* Anthracycline, gemcitabine, and pazopanib in epithelioid sarcoma a multi-institutional case series. *JAMA Oncol.* **4**, (2018).

164. Pàez-Ribes, M. *et al.* Antiangiogenic Therapy Elicits Malignant Progression of Tumors to Increased Local Invasion and Distant Metastasis. *Cancer Cell* **15**, 220–231 (2009).

165. Griffioen, A. W. *et al.* Rapid angiogenesis onset after discontinuation of sunitinib treatment of renal cell carcinoma patients. *Clin. Cancer Res.* **18**, 3961–3971 (2012).

166. Mancuso, M. R. *et al.* Rapid vascular regrowth in tumors after reversal of VEGF inhibition. *J. Clin. Invest.* **116**, 2610–2621 (2006).

167. Chaft, J. E. *et al.* Disease flare after tyrosine kinase inhibitor discontinuation in patients with EGFR-mutant lung cancer and acquired resistance to erlotinib or gefitinib: Implications for clinical trial design. *Clin. Cancer Res.* **17**, 6298–6303 (2011).

168. Shin, S.-J. *et al.* The Association Between PD-L1 Expression and the Clinical Outcomes to Vascular Endothelial Growth Factor-Targeted Therapy in Patients With Metastatic Clear Cell Renal Cell Carcinoma. *Oncologist* **20**, 1253–1260 (2015).

169. Tanigawa, T. *et al.* Tumors Sharply Increased after Ceasing Pazopanib Therapy for a Patient with Advanced Uterine Leiomyosarcoma: Experience of Tumor Flare. *Case Rep. Obstet. Gynecol.* **2017**, 1–4 (2017).

170. Mandrekar, S. J. & Sargent, D. J. Clinical trial designs for predictive biomarker validation: One size does not fit all. *J. Biopharm. Stat.* **19**, 530–542 (2009).

171. Taube, S. E., Jacobson, J. W. & Lively, T. G. Cancer diagnostics: Decision criteria for marker utilization in the clinic. *American Journal of PharmacoGenomics* **5**, 357–364 (2005).

172. Henry, N. L. & Hayes, D. F. Cancer biomarkers. *Mol. Oncol.* **6**, 140–146 (2012).

173. Conley, B. A. & Taube, S. E. Prognostic and predictive markers in cancer. *Dis. Markers* **20**, 35–43 (2004).

174. Teutsch, S. M. *et al.* The evaluation of genomic applications in practice and prevention (EGAPP) initiative: Methods of the EGAPP working group. *Genet. Med.* **11**, 3–14 (2009).

175. Hayes, D. F. Biomarker validation and testing. *Molecular Oncology* **9**, 960–966 (2015).

176. Dobbin, K. K. *et al.* Validation of biomarkers to predict response to immunotherapy in cancer: Volume II - clinical validation and regulatory considerations. *J. Immunother. Cancer* **4**, 1–14 (2016).

177. Simon, R. M., Paik, S. & Hayes, D. F. Use of archived specimens in evaluation of prognostic and predictive biomarkers. *Journal of the National Cancer Institute* **101**, 1446–1452 (2009).

178. Simon, R., Radmacher, M. D., Dobbin, K. & McShane, L. M. Pitfalls in the use of DNA microarray data for diagnostic and prognostic classification. *J. Natl. Cancer Inst.* **95**, 14–18 (2003).

179. Ahn, S., Woo, J. W., Lee, K. & Park, S. Y. HER2 status in breast cancer: Changes in guidelines and complicating factors for interpretation. *Journal of Pathology and Translational Medicine* **54**, 34–44 (2020).

180. Hensing, W., Santa-Maria, C. A., Peterson, L. L. & Sheng, J. Y. Landmark trials in the medical oncology management of early stage breast cancer. *Seminars in Oncology* **47**, 278–292 (2020).

181. Reck, M. *et al.* Pembrolizumab versus Chemotherapy for PD-L1–Positive Non–Small-Cell Lung Cancer. *N. Engl. J. Med.* **375**, 1823–1833 (2016).

182. Final appraisal determination-Pembrolizumab for untreated PD-L1-positive metastatic non-small-cell lung cancer Pembrolizumab for untreated PD-L1-positive metastatic non-small-cell lung cancer (CDF review of TA447). (2018).

183. Rossari, F., Minutolo, F. & Orciuolo, E. Past, present, and future of Bcr-Abl inhibitors: From chemical development to clinical efficacy. *Journal of Hematology and Oncology* **11**, 1–14 (2018).

184. Burmeister, T. *et al.* Patients' age and BCR-ABL frequency in adult B-precursor ALL: A retrospective analysis from the GMALL study group. *Blood* **112**, 918–919 (2008).

185. Deininger, M. W. *et al.* Chronic myeloid leukemia, version 2.2021. *JNCCN Journal of the National Comprehensive Cancer Network* **18**, 1385–1415 (2020).

186. Smith, G. *et al.* A British Society for Haematology Guideline on the diagnosis and management of chronic myeloid leukaemia. *Br. J. Haematol.* **191**, 171–193 (2020).

187. Knezevich, S. R., McFadden, D. E., Tao, W., Lim, J. F. & Sorensen, P. H. B. A novel ETV6-NTRK3 gene fusion in congenital fibrosarcoma. *Nat. Genet.* **18**, 184–187 (1998).

188. Haller, F. *et al.* Paediatric and adult soft tissue sarcomas with *NTRK1* gene fusions: a subset of spindle cell sarcomas unified by a prominent myopericytic/haemangiopericytic pattern. *J. Pathol.* **238**, 700–710 (2016).

189. Chiang, S. *et al.* NTRK Fusions Define a Novel Uterine Sarcoma Subtype

with Features of Fibrosarcoma. *Am. J. Surg. Pathol.* **42**, 791–798 (2018).

190. Davis, J. L. *et al.* Expanding the Spectrum of Pediatric NTRK -rearranged Mesenchymal Tumors. *Am. J. Surg. Pathol.* **43**, 435–445 (2019).

191. Marchiò, C. *et al.* ESMO recommendations on the standard methods to detect NTRK fusions in daily practice and clinical research. *Ann. Oncol.* **30**, 1417–1427 (2019).

192. Li, H., van der Merwe, P. A. & Sivakumar, S. Biomarkers of response to PD-1 pathway blockade. *British Journal of Cancer* **126**, 1663–1675 (2022).

193. Snyder, A. *et al.* Genetic Basis for Clinical Response to CTLA-4 Blockade in Melanoma. *N. Engl. J. Med.* **371**, 2189–2199 (2014).

194. Goodman, A. M. *et al.* Tumor Mutational Burden as an Independent Predictor of Response to Immunotherapy in Diverse Cancers. *Mol. Cancer Ther.* **16**, 2598–2608 (2017).

195. Marabelle, A. *et al.* Association of tumour mutational burden with outcomes in patients with advanced solid tumours treated with pembrolizumab: prospective biomarker analysis of the multicohort, open-label, phase 2 KEYNOTE-158 study. *Lancet Oncol.* **21**, 1353–1365 (2020).

196. Jardim, D. L., Goodman, A., de Melo Gagliato, D. & Kurzrock, R. The Challenges of Tumor Mutational Burden as an Immunotherapy Biomarker. *Cancer Cell* **39**, 154–173 (2021).

197. FoundationOne® CDx - P170019/S017 | FDA. Available at: https://www.fda.gov/medical-devices/recently-approved-devices/foundationoner-cdx-p170019s017. (Accessed: 1st June 2023)

198. Perou, C. M. *et al.* Molecular portraits of human breast tumours. *Nature* **406**, 747–752 (2000).

199. Bernard, P. S. *et al.* Supervised risk predictor of breast cancer based on intrinsic subtypes. *J. Clin. Oncol.* **27**, 1160–1167 (2009).

200. Wallden, B. *et al.* Development and verification of the PAM50-based Prosigna breast cancer gene signature assay. *BMC Med. Genomics* **8**, 1–14 (2015).

201. NICE. 1 Recommendations | Tumour profiling tests to guide adjuvant chemotherapy decisions in early breast cancer | Guidance | NICE. *Tumour profiling tests2* (2018). Available at: https://www.nice.org.uk/guidance/dg34/chapter/1-recommendations. (Accessed: 22nd October 2021)

202. Rodriguez, C. A. *et al.* Impact of the Prosigna (PAM50) assay on adjuvant clinical decision making in patients with early stage breast cancer: Results of a prospective multicenter public program. *J. Clin. Oncol.* **35**, e12062–e12062 (2017).

203. Lenz, H. J. *et al.* Impact of consensus molecular subtype on survival in patients with metastatic colorectal cancer: Results from CALGB/SWOG 80405 (Alliance). in *Journal of Clinical Oncology* **37**, 1876–1885 (American Society of Clinical Oncology, 2019).

204. Song, B. N. *et al.* Identification of an immunotherapy-responsive molecular subtype of bladder cancer. *EBioMedicine* **50**, 238–245 (2019).

205. Bailey, P. *et al.* Genomic analyses identify molecular subtypes of pancreatic cancer. *Nature* **531**, 47–52 (2016).

206. Van Der Graaf, W. T. A. *et al.* PALETTE: Final overall survival (OS) data and predictive factors for OS of EORTC 62072/GSK VEG110727, a randomized double-blind phase III trial of pazopanib versus placebo in advanced soft tissue sarcoma (STS) patients. *J. Clin. Oncol.* **30**, 10009–10009 (2012).

207. Szkandera, J. *et al.* Pre-Treatment anemia is a poor prognostic factor in soft tissue sarcoma patients. *PLoS One* **9**, (2014).

208. Vincenzi, B. *et al.* Bone metastases in soft tissue sarcoma: a survey of

natural history, prognostic value and treatment options. *Clin. Sarcoma Res.* **3**, 1–5 (2013).

209. Duffaud, F. *et al.* Hypertension (HTN) as a potential biomarker of efficacy in pazopanib-treated patients with advanced non-adipocytic soft tissue sarcoma. A retrospective study based on European Organisation for Research and Treatment of Cancer (EORTC) 62043 and 62072 trial. *Eur. J. Cancer* **51**, 2615–2623 (2015).

210. Vos, M. *et al.* Association of pazopanib-induced toxicities with outcome of patients with advanced soft tissue sarcoma; a retrospective analysis based on the European Organisation for Research and Treatment of Cancer (EORTC) 62043 and 62072 clinical trials. *Acta Oncol. (Madr).* **58**, 872–879 (2019).

211. Wang, Y. & Zhang, Y. Prognostic role of interleukin-6 in renal cell carcinoma: a meta-analysis. *Clin. Transl. Oncol.* **22**, 835–843 (2020).

212. Sleijfer, S. *et al.* Cytokine and angiogenic factors associated with efficacy and toxicity of pazopanib in advanced soft-tissue sarcoma: An EORTC-STBSG study. *Br. J. Cancer* **107**, 639–645 (2012).

213. Kobayashi, H. *et al.* Neutrophil-to-lymphocyte ratio after pazopanib treatment predicts response in patients with advanced soft-tissue sarcoma. *Int. J. Clin. Oncol.* **23**, 368–374 (2018).

214. Mirili, C. *et al.* Assessment of potential predictive value of peripheral blood inflammatory indexes in 26 cases with soft tissue sarcoma treated by pazopanib: A retrospective study. *Cancer Manag. Res.* **11**, 3445–3453 (2019).

215. Templeton, A. J. *et al.* Prognostic role of neutrophil-to-lymphocyte ratio in solid tumors: A systematic review and meta-analysis. *Journal of the National Cancer Institute* **106**, (2014).

216. De Maio, E. *et al.* Evolution in neutrophil-to-lymphocyte ratio (NLR) among

advanced soft tissue sarcoma (STS) patients treated with pazopanib within EORTC 62043/62072 trials. *Ann. Oncol.* **28**, v531 (2017).

217. Zhang, L. *et al.* Wild-type p53 suppresses angiogenesis in human leiomyosarcoma and synovial sarcoma by transcriptional suppression of vascular endothelial growth factor expression. *Cancer Res.* **60**, 3655–3661 (2000).

218. Koehler, K., Liebner, D. & Chen, J. L. TP53 mutational status is predictive of pazopanib response in advanced sarcomas. *Ann. Oncol.* **27**, 539–543 (2016).

219. Fu, S. *et al.* Phase I study of pazopanib and vorinostat: A therapeutic approach for inhibiting mutant p53-mediated angiogenesis and facilitating mutant p53 degradation. *Ann. Oncol.* **26**, 1012–1018 (2015).

220. Nassif, E. F. *et al.* TP53 Mutation as a Prognostic and Predictive Marker in Sarcoma: Pooled Analysis of MOSCATO and ProfiLER Precision Medicine Trials. *Cancers (Basel).* **13**, 3362 (2021).

221. D'Arcy, M. E. *et al.* Risk of Rare Cancers among Solid Organ Transplant Recipients. *J. Natl. Cancer Inst.* **113**, 199–207 (2021).

222. Hernández-Ramírez, R. U., Shiels, M. S., Dubrow, R. & Engels, E. A. Cancer risk in HIV-infected people in the USA from 1996 to 2012: a population-based, registry-linkage study. *Lancet HIV* **4**, e495–e504 (2017).

223. Dunn, G. P., Bruce, A. T., Ikeda, H., Old, L. J. & Schreiber, R. D. Cancer immunoediting: From immunosurveillance to tumor escape. *Nature Immunology* **3**, 991–998 (2002).

224. Dunn, G. P., Old, L. J. & Schreiber, R. D. The three Es of cancer immunoediting. *Annual Review of Immunology* **22**, 329–360 (2004).

225. Mittal, D., Gubin, M. M., Schreiber, R. D. & Smyth, M. J. New insights into cancer immunoediting and its three component phases-elimination, equilibrium and escape. *Current Opinion in Immunology* **27**, 16–25 (2014).

226. Schreiber, R. D., Old, L. J. & Smyth, M. J. Cancer immunoediting: Integrating immunity's roles in cancer suppression and promotion. *Science* **331**, 1565–1570 (2011).

227. Zaidi, M. R. The Interferon-Gamma Paradox in Cancer. *J. Interf. Cytokine Res.* **39**, 30–38 (2019).

228. Legut, M., Cole, D. K. & Sewell, A. K. The promise of γδT cells and the γδT cell receptor for cancer immunotherapy. *Cell. Mol. Immunol.* **12**, 656–658 (2015).

229. Kayagaki, N. *et al.* Type I interferons (IFNs) regulate tumor necrosis factor-related apoptosis-inducing ligand (TRAIL) expression on human T cells: A novel mechanism for the antitumor effects of type I IFNs. *J. Exp. Med.* **189**, 1451–1460 (1999).

230. Trapani, J. A. & Smyth, M. J. Functional significance of the perforin/granzyme cell death pathway. *Nature Reviews Immunology* **2**, 735–747 (2002).

231. Koebel, C. M. *et al.* Adaptive immunity maintains occult cancer in an equilibrium state. *Nature* **450**, 903–907 (2007).

232. Wu, X. *et al.* Immune microenvironment profiles of tumor immune equilibrium and immune escape states of mouse sarcoma. *Cancer Lett.* **340**, 124–133 (2013).

233. Yi, M., Niu, M., Xu, L., Luo, S. & Wu, K. Regulation of PD-L1 expression in the tumor microenvironment. *Journal of Hematology and Oncology* **14**, 1–13 (2021).

234. Carlino, M. S., Larkin, J. & Long, G. V. Immune checkpoint inhibitors in melanoma. *The Lancet* **398**, 1002–1014 (2021).

235. Rosenthal, R. *et al.* Neoantigen-directed immune escape in lung cancer evolution. *Nature* **567**, 479–485 (2019).

236. Dhatchinamoorthy, K., Colbert, J. D. & Rock, K. L. Cancer Immune Evasion Through Loss of MHC Class I Antigen Presentation. *Frontiers in Immunology* **12**, 469 (2021).

237. Straten, P. thor & Andersen, M. H. The anti-apoptotic members of the Bcl-2 family are attractive tumor-associated antigens. *Oncotarget* **1**, 239–245 (2010).

238. Zou, S. *et al.* Targeting stat3 in cancer immunotherapy. *Mol. Cancer* **19**, 1–19 (2020).

239. Qin, S. *et al.* Novel immune checkpoint targets: Moving beyond PD-1 and CTLA-4. *Molecular Cancer* **18**, 1–14 (2019).

240. Yang, L., Pang, Y. & Moses, H. L. TGF-β and immune cells: an important regulatory axis in the tumor microenvironment and progression. *Trends in Immunology* **31**, 220–227 (2010).

241. Hirano, T. IL-6 in inflammation, autoimmunity and cancer. *International immunology* **33**, 127–148 (2021).

242. Somarelli, J. A. *et al.* Molecular Biology and Evolution of Cancer: From Discovery to Action. *Mol. Biol. Evol.* **37**, 320–326 (2020).

243. Solary, E. & Lapane, L. The role of host environment in cancer evolution. *Evol. Appl.* **13**, 1756–1770 (2020).

244. Amend, S. R. & Pienta, K. J. Ecology meets cancer biology: The cancer swamp promotes the lethal cancer phenotype. *Oncotarget* **6**, 9669–9678 (2015).

245. Grimes, D. R., Jansen, M., Macauley, R. J., Scott, J. G. & Basanta, D. Evidence for hypoxia increasing the tempo of evolution in glioblastoma. *Br. J. Cancer* **123**, 1562–1569 (2020).

246. Xu, B.-L. *et al.* In vivo growth of subclones derived from Lewis lung carcinoma is determined by the tumor microenvironment. *Am. J. Cancer*

Res. **12**, 5255–5270 (2022).

247. Dago, A. E. *et al.* Rapid phenotypic and genomic change in response to therapeutic pressure in prostate cancer inferred by high content analysis of single Circulating Tumor Cells. *PLoS One* **9**, (2014).

248. Zhu, X., Li, S., Xu, B. & Luo, H. Cancer evolution: A means by which tumors evade treatment. *Biomed. Pharmacother.* **133**, 111016 (2021).

249. Espiritu, S. M. G. *et al.* The Evolutionary Landscape of Localized Prostate Cancers Drives Clinical Aggression. *Cell* **173**, 1003-1013.e15 (2018).

250. Raynaud, F., Mina, M., Tavernari, D. & Ciriello, G. Pan-cancer inference of intra-tumor heterogeneity reveals associations with different forms of genomic instability. *PLoS Genet.* **14**, e1007669 (2018).

251. Fortunato, A. *et al.* Natural selection in cancer biology: From molecular snowflakes to trait hallmarks. *Cold Spring Harb. Perspect. Med.* **7**, (2017).

252. Guo, M., Peng, Y., Gao, A., Du, C. & Herman, J. G. Epigenetic heterogeneity in cancer. *Biomark. Res.* **7**, 1–19 (2019).

253. Feinberg, A. P., Koldobskiy, M. A. & Göndör, A. Epigenetic modulators, modifiers and mediators in cancer aetiology and progression. *Nature Reviews Genetics* **17**, 284–299 (2016).

254. You, J. S. & Jones, P. A. Cancer Genetics and Epigenetics: Two Sides of the Same Coin? *Cancer Cell* **22**, 9–20 (2012).

255. Etten, J. L. Van, Dehm, S. M., Van Etten, J. L. & Dehm, S. M. Clonal origin and spread of metastatic prostate cancer. *Endocr. Relat. Cancer* **23**, R207–R217 (2016).

256. Greaves, M. & Maley, C. C. Clonal evolution in cancer. *Nature* **481**, 306–313 (2012).

257. Caswell, D. R. & Swanton, C. The role of tumour heterogeneity and clonal

cooperativity in metastasis, immune evasion and clinical outcome. *BMC Medicine* **15**, 1–9 (2017).

258. Tang, Y. J. *et al.* Tracing Tumor Evolution in Sarcoma Reveals Clonal Origin of Advanced Metastasis. *Cell Rep.* **28**, 2837-2850.e5 (2019).

259. Hofvander, J. *et al.* Different patterns of clonal evolution among different sarcoma subtypes followed for up to 25 years. *Nat. Commun.* **9**, 4–11 (2018).

260. Anderson, N. D. *et al.* Lineage-defined leiomyosarcoma subtypes emerge years before diagnosis and determine patient survival. *Nat. Commun.* **12**, 1–14 (2021).

261. Anderson, N. D. *et al.* Rearrangement bursts generate canonical gene fusions in bone and soft tissue tumors. *Science (80-.).* **361**, (2018).

262. Saman, H., Raza, S. S., Uddin, S. & Rasul, K. Inducing angiogenesis, a key step in cancer vascularization, and treatment approaches. *Cancers* **12**, (2020).

263. Bruno, A. *et al.* Orchestration of angiogenesis by immune cells. *Frontiers in Oncology* **4 JUL**, 131 (2014).

264. Zhou, J. *et al.* Tumor-Associated Macrophages: Recent Insights and Therapies. *Frontiers in Oncology* **10**, 188 (2020).

265. Orecchioni, M., Ghosheh, Y., Pramod, A. B. & Ley, K. Macrophage polarization: Different gene signatures in M1(Lps+) vs. Classically and M2(LPS-) vs. Alternatively activated macrophages. *Frontiers in Immunology* **10**, 1084 (2019).

266. Lee, W. S., Yang, H., Chon, H. J. & Kim, C. Combination of anti-angiogenic therapy and immune checkpoint blockade normalizes vascular-immune crosstalk to potentiate cancer immunity. *Experimental and Molecular Medicine* **52**, 1475–1485 (2020).

267. Tripathi, C. *et al.* Macrophages are recruited to hypoxic tumor areas and acquire a Pro-Angiogenic M2-Polarized phenotype via hypoxic cancer cell derived cytokines Oncostatin M and Eotaxin. *Oncotarget* **5**, 5350–5368 (2014).

268. Palucka, K. & Banchereau, J. Cancer immunotherapy via dendritic cells. *Nature Reviews Cancer* **12**, 265–277 (2012).

269. Dhodapkar, M. V., Dhodapkar, K. M. & Palucka, A. K. Interactions of tumor cells with dendritic cells: Balancing immunity and tolerance. *Cell Death and Differentiation* **15**, 39–50 (2008).

270. Seeger, P., Musso, T. & Sozzani, S. The TGF-β superfamily in dendritic cell biology. *Cytokine and Growth Factor Reviews* **26**, 647–657 (2015).

271. Oussa, N. A. E. *et al.* VEGF Requires the Receptor NRP-1 To Inhibit Lipopolysaccharide-Dependent Dendritic Cell Maturation. *J. Immunol.* **197**, 3927–3935 (2016).

272. Tada, Y. *et al.* Targeting VEGFR2 with Ramucirumab strongly impacts effector/ activated regulatory T cells and CD8+ T cells in the tumor microenvironment. *J. Immunother. Cancer* **6**, 1–14 (2018).

273. Voron, T. *et al.* VEGF-A modulates expression of inhibitory checkpoints on CD8++ T cells in tumors. *J. Exp. Med.* **212**, 139–148 (2015).

274. Lanitis, E., Irving, M. & Coukos, G. Targeting the tumor vasculature to enhance T cell activity. *Current Opinion in Immunology* **33**, 55–63 (2015).

275. Bouzin, C., Brouet, A., De Vriese, J., DeWever, J. & Feron, O. Effects of Vascular Endothelial Growth Factor on the Lymphocyte-Endothelium Interactions: Identification of Caveolin-1 and Nitric Oxide as Control Points of Endothelial Cell Anergy. *J. Immunol.* **178**, 1505–1511 (2007).

276. Motz, G. T. *et al.* Tumor endothelium FasL establishes a selective immune barrier promoting tolerance in tumors. *Nat. Med.* **20**, 607–615 (2014).

277. Shetty, S. *et al.* Common Lymphatic Endothelial and Vascular Endothelial Receptor-1 Mediates the Transmigration of Regulatory T Cells across Human Hepatic Sinusoidal Endothelium. *J. Immunol.* **186**, 4147–4155 (2011).

278. Dancsok, A. R. *et al.* Expression of lymphocyte immunoregulatory biomarkers in bone and soft-tissue sarcomas. *Mod. Pathol.* **32**, 1772–1785 (2019).

279. Boxberg, M. *et al.* PD-L1 and PD-1 and characterization of tumor-infiltrating lymphocytes in high grade sarcomas of soft tissue–prognostic implications and rationale for immunotherapy. *Oncoimmunology* **7**, (2018).

280. Shurell, E. *et al.* Characterizing the immune microenvironment of malignant peripheral nerve sheath tumor by PD-L1 expression and presence of CD8+ tumor infiltrating lymphocytes. *Oncotarget* **7**, 64300–64308 (2016).

281. van Erp, A. E. M. *et al.* Expression and clinical association of programmed cell death-1, programmed death-ligand-1 and CD8+ lymphocytes in primary sarcomas is subtype dependent. *Oncotarget* **8**, 71371–71384 (2017).

282. Simard, F. A. *et al.* Description of the immune microenvironment of chondrosarcoma and contribution to progression. *Oncoimmunology* **6**, (2017).

283. D'Angelo, S. P. *et al.* Prevalence of tumor-infiltrating lymphocytes and PD-L1 expression in the soft tissue sarcoma microenvironment. *Hum. Pathol.* **46**, 357–365 (2015).

284. Nowicki, T. S. *et al.* Infiltration of CD8 T cells and expression of PD-1 and PD-L1 in synovial sarcoma. *Cancer Immunol. Res.* **5**, 118–126 (2017).

285. Kostine, M. *et al.* Increased infiltration of M2-macrophages, T-cells and PD-L1 expression in high grade leiomyosarcomas supports immunotherapeutic strategies. *Oncoimmunology* **7**, (2018).

286. Sorbye, S. W. *et al.* Prognostic impact of peritumoral lymphocyte infiltration in soft tissue sarcomas. *BMC Clin. Pathol.* **12**, 1–10 (2012).

287. Oike, N. *et al.* Prognostic impact of the tumor immune microenvironment in synovial sarcoma. *Cancer Sci.* **109**, 3043–3054 (2018).

288. Smolle, M. A. *et al.* Influence of tumor-infiltrating immune cells on local control rate, distant metastasis, and survival in patients with soft tissue sarcoma. *Oncoimmunology* **10**, (2021).

289. Sorbye, S. W. *et al.* Prognostic Impact of Lymphocytes in Soft Tissue Sarcomas. *PLoS One* **6**, e14611 (2011).

290. Abeshouse, A. *et al.* Comprehensive and Integrated Genomic Characterization of Adult Soft Tissue Sarcomas. *Cell* **171**, 950-965.e28 (2017).

291. Hu, C. *et al.* Comprehensive profiling of immune-related genes in soft tissue sarcoma patients. *J. Transl. Med.* **18**, 1–18 (2020).

292. Shen, R. *et al.* Development and validation of an immune gene-set based prognostic signature for soft tissue sarcoma. *BMC Cancer* **21**, 1–14 (2021).

293. Petitprez, F. *et al.* B cells are associated with survival and immunotherapy response in sarcoma. *Nature* **577**, 556–560 (2020).

294. Tawbi, H. A. *et al.* Pembrolizumab in advanced soft-tissue sarcoma and bone sarcoma (SARC028): a multicentre, two-cohort, single-arm, open-label, phase 2 trial. *Lancet Oncol.* **18**, 1493–1501 (2017).

295. Zizzari, I. G. *et al.* TK inhibitor pazopanib primes DCs by downregulation of the β-catenin pathway. *Cancer Immunol. Res.* **6**, 711–722 (2018).

296. Finke, J. H. *et al.* Sunitinib reverses type-1 immune suppression and decreases T-regulatory cells in renal cell carcinoma patients. *Clin. Cancer Res.* **14**, 6674–6682 (2008).

297. Adotevi, O. *et al.* A decrease of regulatory T cells correlates with overall survival after sunitinib-based antiangiogenic therapy in metastatic renal cancer patients. *J. Immunother.* **33**, 991–998 (2010).

298. Chen, M. L. *et al.* Sorafenib relieves cell-intrinsic and cell-extrinsic inhibitions of effector T cells in tumor microenvironment to augment antitumor immunity. *Int. J. Cancer* **134**, 319–331 (2014).

299. Cao, M. *et al.* Kinase inhibitor Sorafenib modulates immunosuppressive cell populations in a murine liver cancer model. *Lab. Investig.* **91**, 598–608 (2011).

300. Kalathil, S. G., Hutson, A., Barbi, J., Iyer, R. & Thanavala, Y. Augmentation of IFN-γ+ CD8+ T cell responses correlates with survival of HCC patients on sorafenib therapy. *JCI Insight* **4**, (2019).

301. Yuan, H. *et al.* Axitinib augments antitumor activity in renal cell carcinoma via STAT3-dependent reversal of myeloid-derived suppressor cell accumulation. *Biomed. Pharmacother.* **68**, 751–756 (2014).

302. Du Four, S. *et al.* Axitinib increases the infiltration of immune cells and reduces the suppressive capacity of monocytic MDSCs in an intracranial mouse melanoma model. *Oncoimmunology* **4**, (2015).

303. Khurana, K. K., Rayman, P. A., Elson, P., Rini, B. I. & Finke, J. Effect of pazopanib on myeloid-derived suppressor cells and T-cell function in patients with metastatic renal cell carcinoma. *J. Clin. Oncol.* **31**, 455–455 (2013).

304. Rinchai, D. *et al.* Integrated transcriptional-phenotypic analysis captures systemic immunomodulation following antiangiogenic therapy in renal cell carcinoma patients. *Clin. Transl. Med.* **11**, e434 (2021).

305. Kim, S. K. *et al.* PD-L1 tumour expression is predictive of pazopanib response in soft tissue sarcoma. *BMC Cancer* **21**, 1–9 (2021).

306. Choueiri, T. K. *et al.* Correlation of PD-L1 tumor expression and treatment

outcomes in patients with renal cell carcinoma receiving sunitinib or pazopanib: Results from COMPARZ, a randomized controlled trial. *Clin. Cancer Res.* **21**, 1071–1077 (2015).

307. Motzer, R. J. *et al.* Pazopanib versus Sunitinib in Metastatic Renal-Cell Carcinoma. *N. Engl. J. Med.* **369**, 722–731 (2013).

308. Shin, S.-J. *et al.* The Association Between PD-L1 Expression and the Clinical Outcomes to Vascular Endothelial Growth Factor-Targeted Therapy in Patients With Metastatic Clear Cell Renal Cell Carcinoma. *Oncologist* **20**, 1253–1260 (2015).

309. Hakimi, A. A. *et al.* Transcriptomic profiling of the tumor microenvironment reveals distinct subgroups of clear cell renal cell cancer: Data from a randomized phase III trial. *Cancer Discov.* **9**, 510–525 (2019).

310. Yoshihara, K. *et al.* Inferring tumour purity and stromal and immune cell admixture from expression data. *Nat. Commun.* **4**, (2013).

311. Beuselinck, B. *et al.* Molecular subtypes of clear cell renal cell carcinoma are associated with sunitinib response in the metastatic setting. *Clin. Cancer Res.* **21**, 1329–1339 (2015).

312. Verbiest, A. *et al.* Molecular Subtypes of Clear Cell Renal Cell Carcinoma Are Associated With Outcome During Pazopanib Therapy in the Metastatic Setting. *Clin. Genitourin. Cancer* **16**, e605–e612 (2018).

313. Epaillard, N. *et al.* BIONIKK: A phase 2 biomarker driven trial with nivolumab and ipilimumab or VEGFR tyrosine kinase inhibitor (TKI) in naïve metastatic kidney cancer. *Bull. Cancer* **107**, eS22–eS27 (2020).

314. ESMO 2020. Results from the Phase 2 Biomarker Driven Trial with Nivolumab and Ipilimumab or VEGFR Tyrosine Kinase Inhibitor in Naïve Metastatic Kidney Cancer Patients: The BIONIKK Trial. Available at: https://www.urotoday.com/conference-highlights/esmo-2020/kidney-cancer/124676-esmo-virtual-congress-2020-results-from-the-phase-2-

biomarker-driven-trial-with-nivolumab-and-ipilimumab-or-vegfr-tyrosine-kinase-inhibitor-in-naive-metastatic-kidney-cancer-pat. (Accessed: 22nd October 2021)

315. CRAN - Package pmsampsize. Available at: https://cran.r-project.org/web/packages/pmsampsize/index.html.

316. Riley, R. D. *et al.* Minimum sample size for developing a multivariable prediction model: PART II - binary and time-to-event outcomes. *Stat. Med.* **38**, 1276–1296 (2019).

317. Lee, A. T. J. *et al.* The adequacy of tissue microarrays in the assessment of inter- and intra-tumoural heterogeneity of infiltrating lymphocyte burden in leiomyosarcoma. *Sci. Rep.* **9**, 14602 (2019).

318. Schindelin, J. *et al.* Fiji: an open-source platform for biological-image analysis. *Nat. Methods* **9**, 676–682 (2012).

319. Bankhead, P. *et al.* QuPath: Open source software for digital pathology image analysis. *Sci. Rep.* **7**, 1–7 (2017).

320. Schindelin, J. *et al.* Fiji: an open-source platform for biological-image analysis. *Nat. Methods* **9**, 676–682 (2012).

321. Bland, J. M. & Altman, D. G. Measuring agreement in method comparison studies. *Stat. Methods Med. Res.* **8**, 135–160 (1999).

322. Bland, J. M. & Altman, D. G. Survival probabilities (the Kaplan-Meier method). *BMJ (Clinical research ed.)* **317**, 1572 (1998).

323. Bland, J. M. & Altman, D. G. The logrank test. *BMJ* **328**, 1073 (2004).

324. Cox, D. R. Regression Models and Life-Tables. *J. R. Stat. Soc. Ser. B* **34**, 187–202 (1972).

325. Waggott, D. *et al.* NanoStringNorm: An extensible R package for the pre-processing of nanostring mRNA and miRNA data. *Bioinformatics* **28**, 1546–

1548 (2012).

326. Jollife, I. T. & Cadima, J. Principal component analysis: A review and recent developments. *Philosophical Transactions of the Royal Society A: Mathematical, Physical and Engineering Sciences* **374**, (2016).

327. Blighe K & A, L. GitHub - kevinblighe/PCAtools: PCAtools: everything Principal Components Analysis. *R package version 2.0.0* (2020). Available at: https://github.com/kevinblighe/PCAtools. (Accessed: 6th December 2021)

328. Horn, J. L. A rationale and test for the number of factors in factor analysis. *Psychometrika* **30**, 179–185 (1965).

329. Thorndike, R. L. Who belongs in the family? *Psychometrika* **18**, 267–276 (1953).

330. Gu, Z., Eils, R. & Schlesner, M. Complex heatmaps reveal patterns and correlations in multidimensional genomic data. *Bioinformatics* **32**, 2847–2849 (2016).

331. CRAN - Package samr. Available at: https://cran.r-project.org/web/packages/samr/index.html.

332. Javanmard, A. & Montanari, A. Online rules for control of false discvoery rate and False Discovery Exceedance. *Ann. Stat.* **46**, 526–554 (2018).

333. Subramanian, A. *et al.* Gene set enrichment analysis: A knowledge-based approach for interpreting genome-wide expression profiles. *Proc. Natl. Acad. Sci. U. S. A.* **102**, 15545–15550 (2005).

334. Buus, R. *et al.* Development and validation for research assessment of Oncotype DX® Breast Recurrence Score, EndoPredict® and Prosigna®. *npj Breast Cancer* **7**, (2021).

335. Lee, A. T. J. *et al.* The adequacy of tissue microarrays in the assessment of inter- and intra-tumoural heterogeneity of infiltrating lymphocyte burden

in leiomyosarcoma. *Sci. Rep.* **9**, 1–12 (2019).

336. Eisenhauer, E. A. *et al.* New response evaluation criteria in solid tumours: Revised RECIST guideline (version 1.1). *Eur. J. Cancer* **45**, 228–247

337. Yoshida, N. *et al.* A High RORγT/CD3 Ratio is a Strong Prognostic Factor for Postoperative Survival in Advanced Colorectal Cancer: Analysis of Helper T Cell Lymphocytes (Th1, Th2, Th17 and Regulatory T Cells). *Ann. Surg. Oncol.* **23**, 919–927 (2016).

338. Miksch, R. C. *et al.* Development of a reliable and accurate algorithm to quantify the tumor immune stroma (QTiS) across tumor types. *Oncotarget* **8**, 114935–114944 (2017).

339. Berben, L. *et al.* Computerised scoring protocol for identification and quantification of different immune cell populations in breast tumour regions by the use of QuPath software. *Histopathology* **77**, 79–91 (2020).

340. Loughrey, M. B. *et al.* Validation of the systematic scoring of immunohistochemically stained tumour tissue microarrays using QuPath digital image analysis. *Histopathology* **73**, 327–338 (2018).

341. Watson, P. F. & Petrie, A. Method agreement analysis: A review of correct methodology. *Theriogenology* **73**, 1167–1179 (2010).

342. Stefanovski, P. D. *et al.* Prognostic factors in soft tissue sarcomas: a study of 395 patients. *Eur. J. Surg. Oncol.* **28**, 153–164 (2002).

343. Penel, N. *et al.* Performance status is the most powerful risk factor for early death among patients with advanced soft tissue sarcomaThe European Organisation for Research and Treatment of Cancer- Soft Tissue and Bone Sarcoma Group (STBSG) and French Sarcoma Group (FSG) s. *Br. J. Cancer* **104**, 1544–1550 (2011).

344. Boxberg, M. *et al.* PD-L1 and PD-1 and characterization of tumor-infiltrating lymphocytes in high grade sarcomas of soft tissue–prognostic implications and rationale for immunotherapy. *Oncoimmunology* **7**, (2018).

345. Schroeder, B. A. *et al.* CD4+ T cell and M2 macrophage infiltration predict dedifferentiated liposarcoma patient outcomes. *J. Immunother. Cancer* **9**, (2021).

346. Aoki, T. *et al.* Single-Cell Transcriptome Analysis Reveals Disease-Defining T-cell Subsets in the Tumor Microenvironment of Classic Hodgkin Lymphoma. *Cancer Discov.* **10**, 406–421 (2020).

347. Kawai, O. *et al.* Predominant infiltration of macrophages and CD8 $^{+}$ T Cells in cancer nests is a significant predictor of survival in stage IV nonsmall cell lung cancer. *Cancer* **113**, 1387–1395 (2008).

348. Goytain, A. & Ng, T. NanoString nCounter Technology: High-Throughput RNA Validation. in *Methods in Molecular Biology* **2079**, 125–139 (Humana, New York, NY, 2020).

349. David, L. E., Fowler, C. B., Cunningham, B. R., Mason, J. T. & O'Leary, T. J. The effect of formaldehyde fixation on RNA: Optimization of formaldehyde adduct removal. *J. Mol. Diagnostics* **13**, 282–288 (2011).

350. Veldman-Jones, M. H. *et al.* Evaluating robustness and sensitivity of the nanostring technologies ncounter platform to enable multiplexed gene expression analysis of clinical samples. *Cancer Res.* **75**, 2587–2593 (2015).

351. Scott, D. W. *et al.* Gene expression-based model using formalin-fixed paraffin-embedded biopsies predicts overall survival in advanced-stage classical hodgkin lymphoma. *J. Clin. Oncol.* **31**, 692–700 (2013).

352. Saba, N. F. *et al.* Mutation and Transcriptional Profiling of Formalin-Fixed Paraffin Embedded Specimens as Companion Methods to Immunohistochemistry for Determining Therapeutic Targets in Oropharyngeal Squamous Cell Carcinoma (OPSCC): A Pilot of Proof of Principle. *Head Neck Pathol.* **9**, 223–235 (2015).

353. Talla, S. B. *et al.* Immuno-oncology gene expression profiling of formalin-

fixed and paraffin-embedded clear cell renal cell carcinoma: Performance comparison of the NanoString nCounter technology with targeted RNA sequencing. *Genes Chromosom. Cancer* **59**, 406–416 (2020).

354. Cesano, A. nCounter® PanCancer Immune Profiling Panel (NanoString Technologies, Inc., Seattle, WA). *J. Immunother. Cancer* **3**, 1–3 (2015).

355. Jollife, I. T. & Cadima, J. Principal component analysis: A review and recent developments. *Philosophical Transactions of the Royal Society A: Mathematical, Physical and Engineering Sciences* **374**, (2016).

356. Li, Z. *et al.* CD83: Activation marker for antigen presenting cells and its therapeutic potential. *Frontiers in Immunology* **10**, (2019).

357. Chu, P. G. & Arber, D. A. CD79: A Review. *Appl. Immunohistochem. Mol. Morphol.* **9**, 97–106 (2001).

358. Chistiakov, D. A., Killingsworth, M. C., Myasoedova, V. A., Orekhov, A. N. & Bobryshev, Y. V. CD68/macrosialin: Not just a histochemical marker. *Lab. Investig.* **97**, 4–13 (2017).

359. Feuerer, M., Hill, J. A., Mathis, D. & Benoist, C. Foxp3+ regulatory T cells: Differentiation, specification, subphenotypes. *Nature Immunology* **10**, 689–695 (2009).

360. Cai, G. *et al.* CD160 inhibits activation of human CD4+ T cells through interaction with herpesvirus entry mediator. *Nat. Immunol.* **9**, 176–185 (2008).

361. Fabriek, B. O. *et al.* The macrophage scavenger receptor CD163 functions as an innate immune sensor for bacteria. *Blood* **113**, 887–892 (2009).

362. Xia, F. *et al.* TCR and CD28 Concomitant Stimulation Elicits a Distinctive Calcium Response in Naive T Cells. *Front. Immunol.* **9**, 428198 (2018).

363. Yeung, L. *et al.* Leukocyte Tetraspanin CD53 Restrains α3 Integrin Mobilization and Facilitates Cytoskeletal Remodeling and Transmigration

in Mice. *J. Immunol.* **205**, 521–532 (2020).

364. Georgiev, H., Ravens, I., Papadogianni, G. & Bernhardt, G. Coming of age: CD96 emerges as modulator of immune responses. *Frontiers in Immunology* **9**, 369169 (2018).

365. Jacobs, R. *et al.* CD56bright cells differ in their KIR repertoire and cytotoxic features from CD56dim NK cells. *Eur. J. Immunol.* **31**, 3121–3126 (2001).

366. Laplante, P. *et al.* MFG-E8 Reprogramming of Macrophages Promotes Wound Healing by Increased bFGF Production and Fibroblast Functions. *J. Invest. Dermatol.* **137**, 2005–2013 (2017).

367. Fan, T. *et al.* CDH1 overexpression predicts bladder cancer from early stage and inversely correlates with immune infiltration. *BMC Urol.* **22**, 1–18 (2022).

368. Abdelatty, A. *et al.* Pan-Cancer Study on Protein Kinase C Family as a Potential Biomarker for the Tumors Immune Landscape and the Response to Immunotherapy. *Front. Cell Dev. Biol.* **9**, (2022).

369. Chen, D. *et al.* Pan-cancer analysis of the prognostic and immunological role of PSMB8. *Sci. Rep.* **11**, 1–19 (2021).

370. Kalaora, S. *et al.* Immunoproteasome expression is associated with better prognosis and response to checkpoint therapies in melanoma. *Nat. Commun.* **11**, 1–12 (2020).

371. Wu, H. *et al.* An Integrative Pan-Cancer Analysis of Kinesin Family Member C1 (KIFC1) in Human Tumors. *Biomedicines* **10**, 755911 (2022).

372. De Andrade, L. F. *et al.* Inhibition of MICA and MICB shedding elicits NK-cell-mediated immunity against tumors resistant to cytotoxic T cells. *Cancer Immunol. Res.* **8**, 769–780 (2020).

373. Li, L. *et al.* Integrative Pan-Cancer Analysis Confirmed that FCGR3A is a Candidate Biomarker Associated With Tumor Immunity. *Front. Pharmacol.*

13, 900699 (2022).

374. Zhao, B. *et al.* Aging microenvironment and antitumor immunity for geriatric oncology: the landscape and future implications. *J. Hematol. Oncol. 2023 161* **16**, 1–34 (2023).

375. Zhou, Z., Wei, J. H. & Jiang, W. Characterization of aging tumor microenvironment with drawing implications in predicting the prognosis and immunotherapy response in low-grade gliomas. *Sci. Reports 2022 121* **12**, 1–16 (2022).

376. Erbe, R. *et al.* Aging interacts with tumor biology to produce major changes in the immune tumor microenvironment. *bioRxiv* 2020.06.08.140764 (2020). doi:10.1101/2020.06.08.140764

377. Erbe, R. *et al.* Evaluating the impact of age on immune checkpoint therapy biomarkers. *Cell Rep.* **36**, 109599 (2021).

378. Xu, M. *et al.* Immune and Stroma Related Genes in Breast Cancer: A Comprehensive Analysis of Tumor Microenvironment Based on the Cancer Genome Atlas (TCGA) Database. *Front. Med.* **7**, 490729 (2020).

379. Curran, T. *et al.* Differential immune signatures in the tumor microenvironment are associated with colon cancer racial disparities. *Cancer Med.* **10**, 1805–1814 (2021).

380. Wu, Y. *et al.* Immune and stromal related genes in colon cancer: Analysis of tumour microenvironment based on the cancer genome atlas (TCGA) and gene expression omnibus (GEO) databases. *Scand. J. Immunol.* **95**, e13119 (2022).

381. Grabowski, M. M. *et al.* Immune suppression in gliomas. *Journal of Neuro-Oncology* **151**, 3–12 (2021).

382. Geissler, K. *et al.* Immune signature of tumor infiltrating immune cells in renal cancer. *Oncoimmunology* **4**, 985082 (2015).

383. Gonzalez, V. D. *et al.* High-grade serous ovarian tumor cells modulate NK cell function to create an immune-tolerant microenvironment. *Cell Rep.* **36**, 109632 (2021).

384. Hendry, S. *et al.* Assessing Tumor-Infiltrating Lymphocytes in Solid Tumors. *Adv. Anat. Pathol.* **24**, 311–335 (2017).

385. Hoekstra, M. E., Vijver, S. V. & Schumacher, T. N. Modulation of the tumor micro-environment by CD8+ T cell-derived cytokines. *Curr. Opin. Immunol.* **69**, 65 (2021).

386. Laumont, C. M., Banville, A. C., Gilardi, M., Hollern, D. P. & Nelson, B. H. Tumour-infiltrating B cells: immunological mechanisms, clinical impact and therapeutic opportunities. *Nat. Rev. Cancer 2022 227* **22**, 414–430 (2022).

387. Poli, A. *et al.* CD56bright natural killer (NK) cells: An important NK cell subset. *Immunology* **126**, 458–465 (2009).

388. Toulmonde, M. *et al.* High throughput profiling of undifferentiated pleomorphic sarcomas identifies two main subgroups with distinct immune profile, clinical outcome and sensitivity to targeted therapies. *EBioMedicine* **62**, 103131 (2020).

389. Zhu, M. M. T., Shenasa, E. & Nielsen, T. O. Sarcomas: Immune biomarker expression and checkpoint inhibitor trials. *Cancer Treat. Rev.* **91**, 102115 (2020).

390. Weng, W. *et al.* The immune subtypes and landscape of sarcomas. *BMC Immunol.* **23**, 1–19 (2022).

391. Wu, C. *et al.* Identification of Tumor Antigens and Immune Subtypes for the Development of mRNA Vaccines and Individualized Immunotherapy in Soft Tissue Sarcoma. *Cancers (Basel).* **14**, 448 (2022).

392. De Paoli-Iseppi, R. *et al.* Comparison of whole-exome sequencing of matched fresh and formalin fixed paraffin embedded melanoma tumours: Implications for clinical decision making. *Pathology* **48**, 261–266 (2016).

393. Fujii, T. *et al.* Evaluation of DNA and RNA quality from archival formalin-fixed paraffin-embedded tissue for next-generation sequencing – Retrospective study in Japanese single institution. *Pathol. Int.* **70**, 602–611 (2020).

394. Vilimas, T. Measuring Tumor Mutational Burden Using Whole-Exome Sequencing. *Methods Mol. Biol.* **2055**, 63–91 (2020).

395. Roudko, V., Greenbaum, B. & Bhardwaj, N. Computational Prediction and Validation of Tumor-Associated Neoantigens. *Front. Immunol.* **11**, 493366 (2020).

396. Zhigalova, E. A. *et al.* RNA-Seq-Based TCR Profiling Reveals Persistently Increased Intratumoral Clonality in Responders to Anti-PD-1 Therapy. *Front. Oncol.* **10**, 385 (2020).

397. Karasaki, T. *et al.* Prediction and prioritization of neoantigens: integration of RNA sequencing data with whole-exome sequencing. *Cancer Sci.* **108**, 170 (2017).

398. Yu, C. & Zhang, Y. Development and validation of a prognostic nomogram for early-onset colon cancer. *Biosci. Rep.* **39**, 346 (2019).

399. Tu, Q. H. *et al.* Development and Validation of Novel Nomograms for Predicting Specific Distant Metastatic Sites and Overall Survival of Patients With Soft Tissue Sarcoma. *Technol. Cancer Res. Treat.* **20**, (2021).

400. Al-Tashi, Q. *et al.* Machine Learning Models for the Identification of Prognostic and Predictive Cancer Biomarkers: A Systematic Review. *Int. J. Mol. Sci.* **24**, 7781 (2023).

401. Arora, C., Kaur, D., Naorem, L. D. & Raghava, G. P. S. Prognostic biomarkers for predicting papillary thyroid carcinoma patients at high risk using nine genes of apoptotic pathway. *PLoS One* **16**, e0259534 (2021).

402. Cheong, J. H. *et al.* Development and validation of a prognostic and predictive 32-gene signature for gastric cancer. *Nat. Commun.* **13**, 1–9

(2022).

403. Bychkov, D. *et al.* Outcome and biomarker supervised deep learning for survival prediction in two multicenter breast cancer series. *J. Pathol. Inform.* **13**, 9 (2022).

404. Robbe, P. *et al.* Clinical whole-genome sequencing from routine formalin-fixed, paraffin-embedded specimens: pilot study for the 100,000 Genomes Project. *Genet. Med.* **20**, 1196–1205 (2018).

405. Esteve-Codina, A. *et al.* A Comparison of RNA-Seq Results from Paired Formalin-Fixed Paraffin-Embedded and Fresh-Frozen Glioblastoma Tissue Samples. *PLoS One* **12**, e0170632 (2017).

406. Burgess, M. A. *et al.* Clinical activity of pembrolizumab (P) in undifferentiated pleomorphic sarcoma (UPS) and dedifferentiated/pleomorphic liposarcoma (LPS): Final results of SARC028 expansion cohorts. *J. Clin. Oncol.* **37**, 11015–11015 (2019).

407. Ben-Ami, E. *et al.* Immunotherapy with single agent nivolumab for advanced leiomyosarcoma of the uterus: Results of a phase 2 study. *Cancer* **123**, 3285–3290 (2017).

408. Davis, K. L. *et al.* ADVL1412: Initial results of a phase I/II study of nivolumab and ipilimumab in pediatric patients with relapsed/refractory solid tumors—A COG study. *J. Clin. Oncol.* **35**, 10526–10526 (2017).

409. Wilky, B. A. *et al.* A phase II trial of axitinib plus pembrolizumab for patients with advanced alveolar soft part sarcoma (ASPS) and other soft tissue sarcomas (STS). *J. Clin. Oncol.* **36**, 11547–11547 (2018).

410. Pollack, S. M. *et al.* Assessment of Doxorubicin and Pembrolizumab in Patients with Advanced Anthracycline-Naive Sarcoma: A Phase 1/2 Nonrandomized Clinical Trial. in *JAMA Oncology* **6**, 1778–1782 (American Medical Association, 2020).

411. Toulmonde, M. *et al.* Combination of pembrolizumab and metronomic

cyclophosphamide in patients with advanced sarcomas and GIST: A French Sarcoma Group phase II trial. *J. Clin. Oncol.* **35**, 11053–11053 (2017).

412. D'Angelo, S. P. *et al.* Nivolumab with or without ipilimumab treatment for metastatic sarcoma (Alliance A091401): two open-label, non-comparative, randomised, phase 2 trials. *Lancet Oncol.* **19**, 416–426 (2018).

413. Hong, D. S. *et al.* Phase I/II study of LAG525 ± spartalizumab (PDR001) in patients (pts) with advanced malignancies. *J. Clin. Oncol.* **36**, 3012–3012 (2018).

414. Piha-Paul, S. A. *et al.* A phase 2, open-label study of the combination of spartalizumab (PDR001) and LAG525 for patients with advanced solid tumors and hematologic malignancies. *J. Clin. Oncol.* **36**, TPS2616–TPS2616 (2018).

415. Papadopoulos, K. P. *et al.* First-in-human study of REGN3767 (R3767), a human LAG-3 monoclonal antibody (mAb), ± cemiplimab in patients (pts) with advanced malignancies. *J. Clin. Oncol.* **37**, 2508–2508 (2019).

416. Luke, J. J. *et al.* A phase I, first-in-human, open-label, dose-escalation study of MGD013, a bispecific DART molecule binding PD-1 and LAG-3, in patients with unresectable or metastatic neoplasms. *J. Clin. Oncol.* **38**, 3004–3004 (2020).

417. Du, W. *et al.* Tim-3 as a target for cancer immunotherapy and mechanisms of action. *International Journal of Molecular Sciences* **18**, (2017).

418. Curigliano, G. *et al.* Abstract CT183: Phase (Ph) I/II study of MBG453± spartalizumab (PDR001) in patients (pts) with advanced malignancies. in *Cancer Research* **79**, CT183–CT183 (American Association for Cancer Research, 2019).